DISSERTATION

USING GENE EXPRESSION AND MUTATIONAL PROFILING TO CHARACTERIZE CANINE ACUTE MYELOID LEUKEMIA AND ASSESS THEIR COMPARATIVE FEATURES WITH HUMAN ACUTE MYELOID LEUKEMIA

Submitted by

Adam Harris

Department of Microbiology, Immunology and Pathology

In partial fulfillment of the requirements

For the Degree of Doctor of Philosophy

Colorado State University

Fort Collins, Colorado

Summer 2023

Doctoral Committee:
Advisor: Anne Avery

Paul Avery
Steven Dow
Dawn Duval

ABSTRACT

USING GENE EXPRESSION AND MUTATIONAL PROFILING TO CHARACTERIZE CANINE ACUTE MYELOID LEUKEMIA AND ASSESS THEIR COMPARATIVE FEATURES WITH HUMAN ACUTE MYELOID LEUKEMIA

Acute myeloid leukemia (AML) is an aggressive heterogenous hematopoietic neoplasm that afflicts both dogs and people. Over 10,000 individuals (about the seating capacity of Cameron basketball stadium at Duke University) in the United States succumb to AML-related deaths every year. Treatment options for AML have made little progress in the past few decades and prognosis for both human and canine AML (cAML) remains dismal. However, there are large ongoing multi-institutional studies devoted to advancing medical management for human AML (hAML) by providing targeted therapeutics to patients based on their molecular characteristics. A preclinical model for testing novel therapies could accelerate the development of better treatments in people. We hypothesize that cAML will have similar underlying molecular features as human AML and dogs could be a translational model for developing therapeutics focused on treating AML.

The goals of this thesis were to assess the gene expression programs and mutational profiles of cAML and compare our findings with available human AML data. First, we established diagnostic criteria for defining cAML using flow cytometry. Next, we globally assessed normal hematopoiesis in dogs using single cell transcriptomics to generate a hematopoietic tree for defining the cellular composition of cAML. Additionally, we investigated the mRNA expression and genetic variants in cAML to ultimately compare the molecular features with pediatric and adult AML subtypes. We hope this work advances our knowledge of

cAML molecular characteristics and adds further credentials to the dog as spontaneous model for human AML.

ACKNOWLEDGEMENTS

First, I would like to acknowledge all the members of the Clinical Hematopathology Laboratory and the Clinical Pathology Laboratory at Colorado State University. I would specifically like to acknowledge Dr. Anne Avery's mentorship and guidance over the last few years. Her passion, determination, leadership skills, and wit are all qualities I aspire to have as a veterinary researcher. She has served as a role model for many individuals, and I genuinely appreciate her for pushing me to become the scientist I am today. I am grateful for the Clinical Hematopathology team and their patience for training me in countless laboratory skills. None of the work in this proposal would be possible without their support and commitment to veterinary diagnostics and research.

Thank you to the Clinical Pathology team, for helping me navigate my residency. Your positive attitude and diligence in the laboratory setting are very much appreciated and I always looked forward to my weeks in the laboratory with everyone. My experience in the residency program would never have been the same without your support. I would like to thank the clinical pathology faculty for seeing my potential and supporting me through this journey. I want to particularly thank my residency mentor, Dr. Russell Moore, for his support and the opportunities he has allotted me. I hope to echo his drive and ambition in my own projects as I move forward.

Thank you to the members of my doctoral committee: Drs. Paul Avery, Steven Dow, and Dawn Duval. I appreciate the time and interest you invested in my project, and the insightful questions and guidance you provided. Thank you to the NIH T32 and TL1 training programs for funding support and training. The resources and opportunities both programs have awarded me will always be remembered as I progress through my career. Thank you to my friends and family for your support and commitment to me during this long journey. I appreciate my partner, who

has been with me through this entire experience. Additionally, I value the insightful discussions that I've had with the collaborators and met along the way. I would like to acknowledge Dylan Ammons, Evan Conaway, and Emily Rout, all of which I have appreciated your friendship and guidance through my PhD projects. I would also like to thank the veterinarians and clients, for which none of this work would be possible. Finally, I would like to recognize the patients. They are the reason for this work, which, I hope, will improve our understanding of this disease for future veterinary patients.

TABLE OF CONTENTS

INTRODUCTION

Acute myeloid leukemia at a glance

Acute myeloid leukemia (AML) is an aggressive hematopoietic neoplasm that claims over 10,000 lives in the United States every year.[1] Survivorship of both human and canine acute myeloid leukemia remains dismal, despite modern therapeutics.[2–4] AML is heterogeneous, with over 20 different subclassifications of adult AML (aAML) recognized by the World Health Organization.[5] This complexity contributes to poor outcomes, with different therapies required for treating different subtypes (e.g. FLT3 inhibitors for AML patients with *FLT3* mutations).[2,6] Most of the subclassifications are based on the molecular alterations (e.g., somatic mutations and translocations) these tumors develop.[5,7] Substantial breakthroughs in targeted therapeutics for AML have been slow to develop and only 20% of adult AML patients experience durable remission.[2,8] Not only are there substantial differences in disease biology associated with AML subtypes, but there are even unique features between age groups. For instance, pediatric AML (pAML) is characterized by fusion genes and somatic mutations not seen in the adult counterpart, making finding a cure even more challenging.[9–11] A large animal model that spontaneously develops AML could recapitulate the natural pathogenesis of this neoplasm and help bridge gaps in clinical translation of experimental therapeutics.

Approximately 20,000 new cases of AML are diagnosed yearly in the United States, the majority of which appear to arise de novo.[1,12] Secondary and therapy-related myeloid neoplasms are reported to occur in ~25% and ~8% of adult AML patients, respectively, and both entities are associated with a worse outcome, compared to de novo AML.[13,14] In people, AML accounts for ~80% of acute leukemias in adults and ~20% in pediatric acute leukemias.[10,11] The incidence of AML gradually increases as humans age, and most cases are identified in populations over 65 years old, a trend that is also seen in companion dogs (Figure 1).[1,15] Despite therapeutic advances, over 50% of patients older than 65 years will succumb in a years' time of diagnosis, and only one in four patients survive more than 5 years.[1,16,17] Pediatric and young adults have a

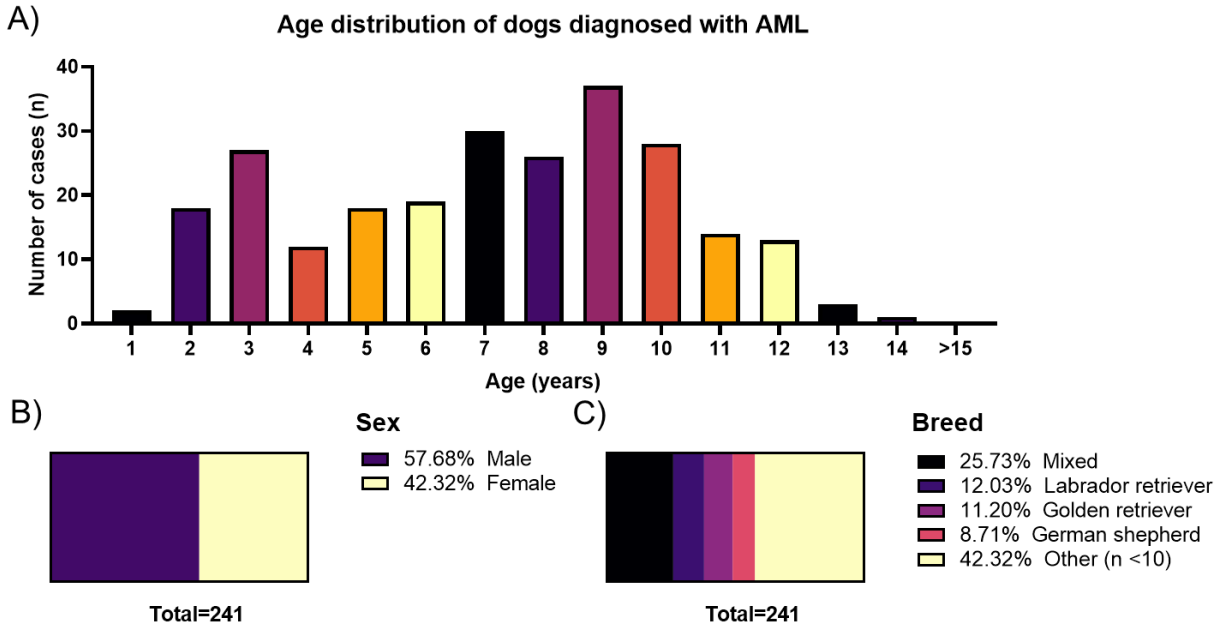

Figure 1: Signalment data from dogs diagnosed with AML since January 2021. The Colorado State University's Clinical Hematopathology laboratory database was queried for canine AML cases diagnosed in the peripheral blood or bone marrow samples post implementation of a diagnostic algorithm to distinguish acute leukemia lineage. Data represent the 241 AML cases that were diagnosed with AML since January 2021 to November 2022. Subfigures A, B, and C are bar plots of the age distribution, sex and breed proportions of dogs diagnosed with AML. The median age at diagnosis for this cohort is 7.6 years old (interquartile range (IQR): 5.1-9.5 years) and there is a slightly higher proportion of males. The top four breeds, i.e., Mixed breed, Labrador retrievers, Golden retrievers, and German shepherds, are represented, as well as the proportion of other dog breeds with less than 10 individuals.

better median survival time, comparatively.[16–19] Part of this could be related to fewer therapy-related mortality events and higher primary induction remission rates observed in pediatric AML patients.[11,20–22] Nevertheless, the proportion of pediatric AML cases that relapse remains high, between 30-40%, indicating that therapeutic advances are still needed.[11,18,23,24] Novel therapies to treat the spectrum of human AML malignancies are slow to develop and, as mentioned previously, clinical prognosis remains dismal.[2,6] To combat this, there are two large ongoing multi-institutional studies, one devoted to pediatric AML (pAML) and the other to adult AML (aAML), to understand the underlying molecular features that affect therapeutic responses.[25,26] Characterizing the transcriptome and somatic mutations of canine AML (cAML) could add further credentials to the dog as a model for human AML and aid in the development of novel therapeutics.

Pathophysiology of leukemogenesis in context of acute myeloid leukemia

Irrespective of the underlying initiating cause (i.e., de novo vs. secondary vs. therapy-related) of AML in people, the result is an abnormal clonal proliferation of malignant myeloid progenitors/stem cells. Patients often present with clinical sequalae secondary to the disease process and subsequent bone marrow failure.[12] These myeloid stem cells expand and typically replace hematopoietic stem cells and disrupt normal hematopoiesis. Not all AMLs biologically behave the same, as some can maintain a degree of differentiation, while others display a failure of maturation.[5,7] Peripheral blood cytopenias are often present at the time of diagnosis as well as an accompanying leukocytosis, characterized by an expansion of neoplastic myeloid cells (Figure 2). Extramedullary tissue involvement with infiltration of neoplastic myeloid cells can occur (Figure 4). Both dogs and people with AML clinically present with fatigue, lethargy, anorexia, and/or weight loss.[12,27] The disease progression of AML is quick, as the neoplastic

cells typically exhibit rapid proliferation, and if left untreated, death typically follows in a few weeks to months post diagnosis.[28]

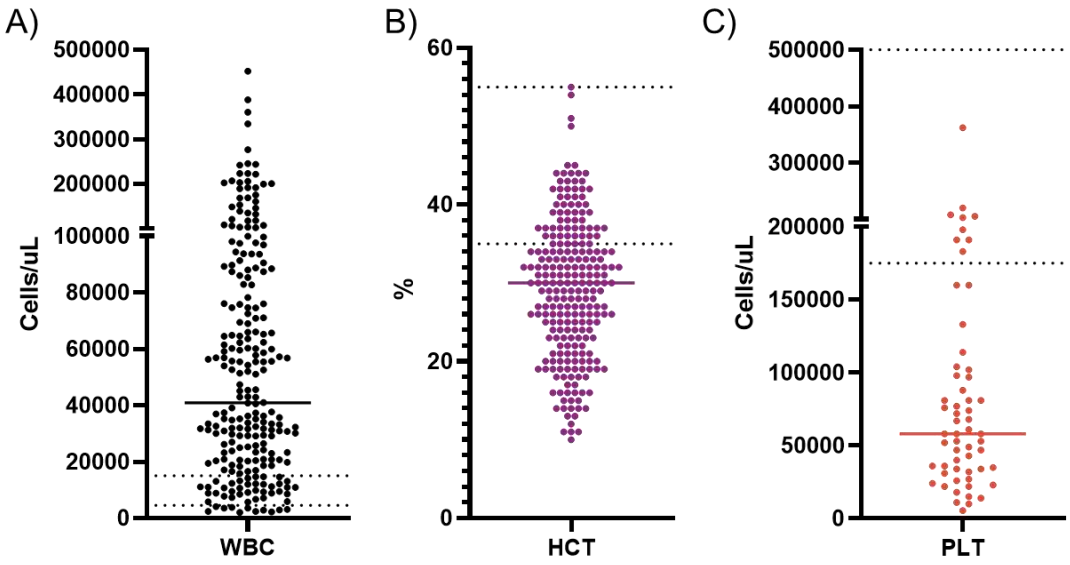

Figure 2: Hematologic data from dogs diagnosed with AML since January 2021. Dot plots represent CBC data concurrently submitted at the time of diagnosis. Subfigures A), B), and C) show white blood cell concentrations (WBC), hematocrit (HCT), or platelet concentrations (PLT), respectively. WBC and HCT data were available in 237 dogs and PLT data without clumping reported were available in 58 dogs. The solid lines in each subfigure represents the median value for the cAML samples. The dashed lines represent the upper and lower reference intervals expected in normal dogs. Most dogs were anemic (72.6%), thrombocytopenic (84.5%), and/or had a leukocytosis (79.7%).

Genetic aberrations, including, but not limited to, tandem duplications, point mutations, small insertions/deletions (indels), and/or chromosomal translocations, all appear to contribute to the pathogenesis of AML.[6,29–31] Hundreds of genetic mutations have been identified, but functional data investigating their biologic impact has primarily been focused on the most common molecular lesions. [6,29–31] In general, the most frequently identified genetic mutations of human AML are broken down into these categories: epigenetic modifiers (e.g. *DNMT3A, TET2,* or *IDH2*), activating signalers (e.g. *NRAS/KRAS, KIT,* or *FLT3*), chromatin-cohesins/modifiers (e.g. *ASXL1, STAG2,* or *EZH2)* , chromatin-spliceosomes (e.g. *SRSF2, SF3B1,* or *U2AF1*), myeloid transcription factors (e.g. *RUNX1, GATA2,* or *CEBPA*), tumor suppressors (e.g. *TP53* or

WT1), or other (e.g. *NPM1,* loss/gain of chromosomes, or complex karyotypes).[30,32] Interestingly, the median somatic mutational frequency (i.e. tumor mutational burden (TMB)) of AMLs tends to be lower compared to other cancer types including chronic lymphocytic leukemias, multiple myelomas, diffuse large B cell lymphomas, and even solid tumor types.[33] An exception to this occurs in AML patients who have acquired a TP53 mutation, because in those individuals their TMB is considerably higher.[34] The general observation that the TMB in AMLs tends to be low compared to other tumor types also speaks to the role of structural variants and/or epigenetic modification in leukemogenesis.

Recurrent genetic translocations are a common phenomenon that contribute to the underlying pathogenesis of human AML. Structural variants are reportedly higher in pediatric patients compared to adults, and only ~20% of pediatric AML patients have a normal karyotype at diagnosis compared to over 50% in adults (Figure 3).[11,30,35] Certain chromosomal translocations are well-characterized and result in the transcription of chimeric proteins that either promote cell proliferation or inhibit differentiation. For instance, the retinoic acid signaling pathways is required for granulocytic differentiation. *PML-RARα* translocations, which results in the fusion of the *PML* gene, from chromosome 15, with the retinoic acid receptor-alpha (*RARA*), from chromosome 17, results in inhibition of retinoic acid signaling pathways and multimerization, via the PML portion, with other proteins including transcription and epigenetic modifiers.[36–38] This altered signaling pathway prevents myeloid differentiation and promotes survival, resulting in leukemic cells that proliferate and have a pause in maturation at the myelocytic stage.[39,40] Other examples include the core binding factor (CBF) AMLs, which comprise either the *RUNX1-RUNX1T1* or the *CBFB-MYH11* fusion genes. The *RUNX1-RUNX1T1* fusion oncogene results in formation of a transcription regulatory complex that

triggers chromatin remodeling and abnormal gene expression, ultimately culminating in enhanced self-renewal capacity and differentiation blockade.[41–43] Additionally, the *CBFB-MYH11* fusion product appears to result in a similar obstruction of normal hematopoiesis progression by repressing RUNX1 and CBFB activities.[44] Although these examples provide insight into the contributory role of fusion oncoproteins in the pathogenesis of AML, it appears that other mutations are also instrumental and contribute to leukemic transformation and therapy resistance.

Traditionally, the mutations implicated in AML have been divided into classes (i.e. Class I, Class II, Class III, etc.) based on their biological function.[32,45] In the early 2000s, a two-hit model was originally proposed in which class I mutations consisted of activating signalers (e.g. tyrosine kinases) and class II comprised mutations that affected transcription factors.[46] Activating signalers (i.e. Class I mutations) appear to occur at the latest time points in AML development, whereas Class II mutations are considered founding events.[46] Also, class II mutations are typically mutually exclusive and do not co-occur. Later additions to this two-hit model incorporated class III (i.e. epigenetic modifiers) and class IV mutations (i.e. tumor suppressors).[47] This classification scheme was based on previous animal models devoted to understanding the contributory roles of recurrent mutations in leukemia pathogenesis.[39,44,48,49] However, investigational studies have revealed that AML pathogenesis is highly complex and involves a multi-step process beyond original hypotheses.

The clonal evolution that leads to development of AML is a stepwise process and multiple studies have reported the chronological order of mutations that occur based on their variant allele fractions (i.e., variant allele reads/total allele reads) at the time of diagnosis. Initiating mutations are often found in epigenetic modifiers, such as *DNMT3A, TET2,*

ASXL1.[29,31,50] Interestingly, mutations in these genes are also found in the peripheral blood of one in ten "healthy" elderly individuals over the age of 65, a process referred to as clonal hematopoiesis of indeterminate potential or age-related clonal hematopoiesis.[51–53] These mutations confer a survival advantage and/or increase responsiveness of hematopoietic stem cells (HSC) to external cytokine stimulation, which can have greater expansion capabilities compared to non-mutated HSC.[54] Although the proportion of CHIP+ individuals that develop fulminant hematopoietic neoplasia is low, there is evidence that these mutations are critical for leukemic cell evolution. These mutations alone do not appear sufficient to cause leukemia however: instead, activating signaling mutations, particularly in the RAS/RTK signaling pathway, are common (>50% of AML patients) and appear to be important for transitioning of pre-malignant clones into fulminant neoplasia.[51–53] Other leukemogenic-potential events include mutations in *NPMI* or genetic translocations.[55] In essence, the constellation of mutations that are acquired contribute uniquely to each patient's development of AML and even to the clonal heterogeneity of their neoplasm.[55–57]

Overview of the mutational landscape of human acute myeloid leukemias

Approximately 95% of adult AML cases have at least one driver mutation identified at the time of diagnosis.[29,30] In one study, 76 different genes contained over 5,000 driver mutations in 1,540 patients.[30] Mutations in only 7 of the 76 genes accounted for nearly 40% of the driver mutations identified in this cohort and *FLT3, NPM1,* and *DNMT3A* mutations were the most common recurrently mutated.[30] However, mutations found in secondary AML tend to be different than mutations reported in de novo AML, which include genes such as: *SRSF2, SF3B1, U2AF1, ZRSR2, ASXL1, EZH2, BCOR, and STAG2*.[58] Also adding to the complexity of human AMLs' genetic diversity, the mutational landscape, including the frequency and positions of

mutations, differs between age groups (Figure 3).[9,59,60] For instance, somatic mutations in *DNMT3A* or *TP53* are not readily identified in pediatric AML patients and, in general, cytogenetic alterations occur more often in pediatric patients compared to adults. Approximately 70-75% of pediatric AML patients can be classified based on a recurrent translocation or cytogenetic abnormality, whereas most adult AML patients have a cytogenetically normal profile (Figure 3). [6,9] Also, certain translocations appear to be age restricted or more frequently in younger patients. For instance, the *RBM15-MKL1* translocation only appears in individuals younger than 3 years old and *KMT2A* translocations commonly occur in children (up to 20% of pediatric AML) but are rarely observed (<4% of adult AML) in adults.[9] Activating mutations in the RAS/RTK signaling pathway (i.e. *NRAS, KIT,* and *FLT3)* are considered to be common occurrences between the two age groups.[9] Mutations in *MYC* and *WT1* appear more often in pediatric AML, which may suggest that these genes have a role in leukemogenesis for younger patients.[9] In essence, although AML is used as an umbrella term for a group of heterogeneous neoplasms, there is mounting evidence that the underlying molecular mechanisms determine clinical outcomes and prognosis, even between age groups. Future investigations are needed to develop targeted therapies to combat the broad spectrum of AML based on their unique features.[2,6] Although major strides are underway to tackle these challenges, additional research is necessary for understanding the underlying pathogenesis and providing therapeutics for patients based on their constellations of mutations.[28]

Gene expression profiling of human acute myeloid leukemias

Scientific investigations are revealing more and more the biological impacts of aberrant gene expression on therapy resistance and prognosis. Absolute quantitative measurements of mRNA are beginning to be implemented into diagnostic laboratory workflows. Gene expression

profiling of AML is no exception, and AML research has been leading the way for stratifying this heterogeneous neoplasm based on their transcriptomic programs.[61–63] One of the first manuscripts that described gene expression profiling of acute leukemias was performed by Golub et al. in 1999, where this group was able to distinguish acute lymphoid leukemias (ALL) from AML by gene expression.[64] This work was one of the first publications in leukemia research that revealed that one could differentiate AML from other acute leukemia subtypes with gene expression alone. Since then, additional work has been devoted to studying the transcriptomic programs of AML subtypes and their relationship with clinical outcome.

Refractoriness to chemotherapeutics is suspected to be due to the underlying biology of the leukemic stem cells (LSC), a low-frequency quiescent cell type capable of self-renewal of the

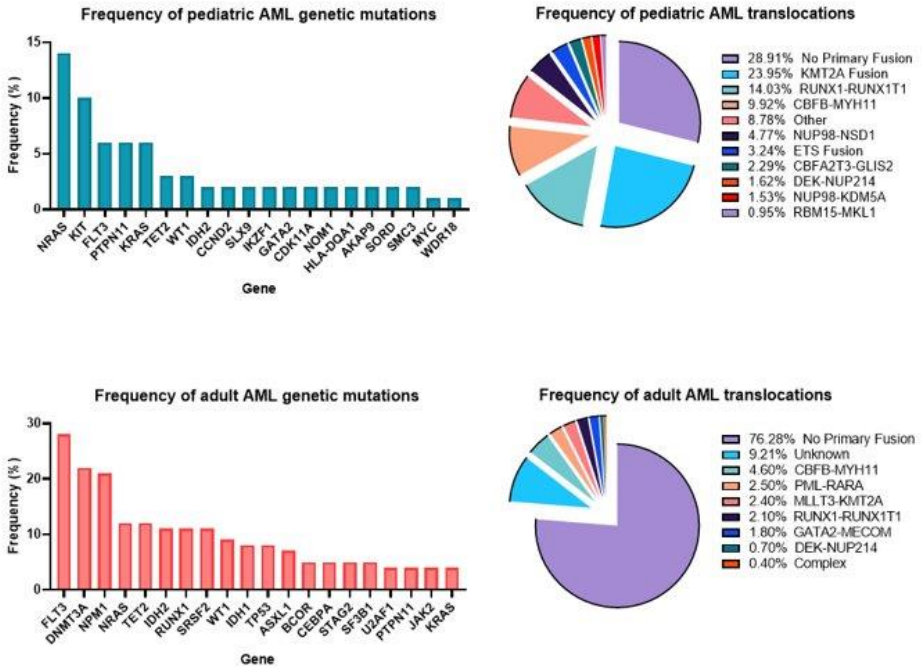

Figure 3: Frequency of genetic mutations between pediatric and adult AML. Bar plots for the top 20 most frequently mutated genes are provided for both pediatric (top) and adult (bottom) AML. Results are from either whole genome or whole exome sequencing datasets, available via cBioPortal, from either pediatric (TARGET, n = 150) or adult (BEAT, n =622) AML cohorts.[25,26] Pie charts represent the frequency of recurrent cytogenetic abnormalities detected between pediatric (top) and adult (bottom) AML patients.

bulk tumor, and one of the first gene expression panels to be developed for AML was the LSC17

scoring system using nCounter technology.[65,66] For decades, measurement of LSC in AML samples has remained challenging, as their patterns of antigen expression are often too ambiguous for immunophenotyping methodologies alone. To combat this, S. Ng, et. al, developed a panel of 17 genes that confer stemness.[65] They found that the LSC17 score was predictive of overall survival in multiple independent AML cohorts, and even performed better than other biomarkers available.[65] Additionally, their work revealed that the LSC17 score was a strong prognostic factor irrespective of the numerous AML genotypes, which they hypothesized could be the result of multiple driver mutations coalescing into stemness properties despite their downstream effects.[65] Since then, a pediatric LSC gene list, comprised of 6 genes, has also been proposed and found to correlate with outcome, highlighting that gene expression profiling could be impactful in the clinical setting for the spectrum of AML cases.[67]

Additional evidence has revealed that gene expression patterns correlate with outcomes and drug responses. For instance, one of the aims of the BEAT AML project is to integrate mutational and gene expression programs with ex vivo drug sensitivity analysis. Since the project's launch, this consortium has enrolled over 800 patients and collected more than 900 specimens.[26] In their first publication, they assessed the correlations between mutational status or gene expression and ex vivo drug sensitivity results from over 70 compounds.[6] Differential gene expression analysis between samples deemed to be sensitive versus resistant for each drug were summarized and their work highlighted gene expression networks that are involved in drug responses.[6] With the advent of single cell sequencing and the capability to predict cell type compositions within bulk RNA-sequencing data, their second iteration revealed that deconvolution of transcriptomic data to predict AML cell types (e.g. HSC-like, progenitor-like, monocyte-like, etc.) correlated with drug family responses and survival.[2] For example, samples

with a higher HSC-like cell type score were associated with shorter overall survival and, pending on their mutational status, sensitivity, or resistance to drug families, such as phosphoninositide kinase inhibitors.[2] They also found that the expression of a single gene, *PEAR1,* was highly predictive of patient survival, and the authors hypothesized that PEAR1 inhibition may aid in treating AML patients; although, no small molecule inhibitors for PEAR1 are currently approved for the treatment of AML.[2] With the upcoming era of personalized medicine, investigational studies devoted to the development, safety, and efficacy of novel therapeutics will be required to improve clinical outcome for AML patients.[28]

Classification and known prognostic factors of acute myeloid leukemia

The French-American-British (FAB) classification system was established in the 1970s and was the first international scheme for subtyping AMLs based on cellular morphology and characteristics (i.e. cytochemical properties).[68] Early iterations included six different subtypes (M1-M6). Later revisions added M0 (AML with minimal differentiation), M4Eo (Acute myelomonocytic leukemia with eosinophilia), and M7 (Acute megakaryoblastic leukemia) subtypes, bringing the total cytomorphology distinct categories recognized to 9.[69] In human AML, the FAB classification scheme has been shown to correlate with molecular characteristics and are important for therapeutic decisions. For instance, the M3 subtype (i.e. acute promyelocytic leukemia (APL)) is most often associated with the PML-RARα translocations (see above).[70] AML patients with the M3 subtype (i.e. PML-RARα translocation) are typically responsive with initial treatment with all-trans retinoic acid, as it forces neoplastic cell differentiation.[71–73] Additionally, M3 subtypes or APL patients are at a high risk for development of disseminated intravascular coagulation and a life-threatening hemorrhagic event. [71–73] The risk of an early death from a coagulopathy-related event is reported at ~30% in APL patients, making

a quick diagnosis and alerting the clinician crucial for patient survival. [71–73] A presumptive diagnosis of APL can be achieved with morphology and cytochemical staining, and is a good example of why morphologic assessment is still relied upon to this day, despite diagnostic recommendations shifting to more objective testing methodologies for subtyping AMLs (i.e. flow cytometry and molecular sequencing).[45]

To date, AML subtypes are defined by two categories.[5,7] AML patients that have an established genetic abnormality are placed within the first tier according to the World Health Organization's (WHO) recognized entities.[5,7] If AML patients do not have a recurrent genetic abnormality, then patients are classified based on their degree of differentiation (proportion of maturing leukocytes) and/or maturation proclivity (e.g. monocytic vs. erythroid vs. megakaryocytic).[5,7] This second-tier grouping is based on the previous FAB classification scheme. For context, nearly 50% of patients cannot be mapped to a defining genetic class using the 2016 WHO classification scheme, thus highlighting the need for additional studies focusing on characterizing the cytogenetic features of AML and their translation into the clinical setting.[74]

The diagnostic testing scheme recommended by the WHO for subtyping AMLs consists of bone marrow or peripheral blood cytologic and histologic review, accompanied with immunophenotyping via flow cytometry, cytogenetic analysis, and mutational analysis.[5,7] All these results must be taken considering the full clinical picture and patient history.[5,7] Until recently, a hallmark for distinguishing acute myeloid leukemia from other myeloproliferative disorders in people was based on the proportion of myeloblasts in the peripheral blood and/or bone marrow. A bone marrow or peripheral blood sample composition with over 20% (decreased from 30% in 2001) myeloblasts is the current cutoff point for distinguishing AML from similar diseases, such as myelodysplasia.[5,7] However, as more clinical data has become available, that

strict cutoff of 20% for differentiating AML from myelodysplasia might not be optimal, as high-grade myelodysplastic neoplasms present similarly and are diagnostic conundrums.[75,76] Current recommendations for distinguishing the two entities are still evolving and the WHO has noted that the 20% blast threshold is not a mandate but must always be considered in context of the clinical information available.[5,7]

As previously mentioned, more objective diagnostic tests have revolutionized the clinical management and decisions for AML patients. For instance, multiparametric approaches for immunophenotyping via flow cytometry are highly sensitive for detection of neoplastic cells.[77,78] Immunophenotyping is widely implemented, considered efficient, and the gold standard for stratifying acute leukemias by lineage (i.e. lymphoid vs. myeloid).[7] Despite the complex intra- and inter- tumor heterogeneity of AML, their lineage is most often identified by the expression of myeloid specific proteins, such as CD11c, CD13, CD14, CD33, lysozyme, and/or myeloperoxidase.[7,79] However, diagnostic challenges for defining lineage do occur and cross-lineage expression of lymphoid markers in myeloid neoplasms are reported, and vice versa.[79] This phenomenon, referred to as mixed phenotype acute leukemias, is suspected to be due to either a leukemic stem cell clone differentiating down two lineages (i.e. bilineal) or antigen expression of both lineages on the same cells.[80–82] The true occurrence of mixed phenotype acute leukemias are rare in people and are yet to be fully investigated in dogs.[80] Regardless of the challenges for classifying acute leukemias, immunophenotyping via flow cytometry is considered essential and is utilized for monitoring AML patients for minimal residual disease that can't be detected microscopically.[77,78]

According to recent publications, there are over 16 recurrent fusion genes and 60 recurrent somatic mutations in adult AML alone.[2,6,29,30] To test for this wide breadth of

mutations, next generation sequencing (NGS) testing panels for hallmark mutations and fusion genes are being incorporated into clinical diagnostic laboratories. NGS is rapidly replacing more traditional methodologies like polymerase chain reactions (PCR) and fluorescence in-situ hybridization, due to their increased sensitivity and ease for testing mutations in multiple genes at once. Despite diagnostic advances and increased availability of molecular testing, there are still challenges for decreasing turnaround times and improving precision medicine for molecular AML subtypes.[28] For example, as previously mentioned, the shortest turnaround time possible for diagnosing acute promyelocytic leukemia (APL) is essential as clinical decisions need to be made within hours of initial presentation. This timeframe is different than current protocols utilized for molecular diagnostics.[45,73] Additionally, nearly 1/3 of AML patients have a driver mutation considered to be individually rare and supportive data for such mutations and their associated prognostic information is deficient, highlighting the necessity to expand molecular diagnostic panels.[50]

All this clinical and diagnostic data can cumulatively provide prognostic insight and help physicians decide treatment regimens and intensity. Clinical factors such as an advanced age (>60 years old) at diagnosis, high white blood cell (WBC) counts, platelet counts, central nervous system involvement, are all poor prognostic indicators.[83,84] Poor performance status at diagnosis have been correlated with worse outcomes.[84] Additionally, biochemical parameters such as an elevated creatinine, elevated lactic dehydrogenase, or hypoalbuminemia at diagnosis are all reported to be adverse prognostic factors.[85–88] Of the previously mentioned variables, age appears to be predictive of treatment response, as elderly patients have the highest treatment-related mortality rates and shortest overall survival times and 5-15% of patients over 60 years of age will have achieved durable remission.[16,84,89]

Cytogenetic and mutational profiling can stratify AML cases even further into favorable, intermediate, or adverse risk groups.[12,90,91] For instance, patients identified as having a complex karyotype (three or more chromosomal abnormalities without a recurrent translocation) often are associated with the highest risk of treatment failure and death.[12,90,91] However, patients with particular translocations, such as t(8:21)(q22;q22) or t(15;17)(q22;q12) , have a favorable prognosis, comparatively.[12,90,91] Gene mutation status offers even more dimensionality to risk stratification. Cytogenetically normal AMLs (CN-AML) make up over half of the de novo AML cases, and their constellation of gene mutations will define their prognostic risk category.[12,90,91] Mutations such as those in *DNMT3A*, *FLT3*-ITD, and *KMT2A*-PTD all are classified as an adverse risk group compared to mutations in *NPM1* or *CEBPA*, both of which are considered favorable.[12,90,91] However, there is still a substantial number of somatic mutations that lack clinical data and their impact on the disease biology is still unknown.[50] Adding even more complexity to this heterogeneous disease, leukemias typically have multiple clones cooccurring, some of which contain unique mutations, which could confer a survival advantage (i.e. treatment resistance) compared to other clones.[55,56,92]

Canine acute myeloid leukemia (cAML): what we know

Like people, dogs spontaneously develop acute leukemia, yet the underlying risk factors for developing acute leukemia in dogs is unknown. There is some evidence that there may be a breed predilection, but true occurrence in subsets of dog breeds is yet to be determined (Figure 1). Additionally, the spectrum of canine acute leukemias' clinical and diagnostic features isn't entirely clear, as there aren't any defined consensus criteria in veterinary medicine for distinguishing acute leukemia lineages (i.e. myeloid vs. lymphoid) in dogs. Lineage assignment is the first step for optimizing future research investigations, as disease biology and treatment

options for ALL vs. AML are vastly different in people. As we will show in Chapter 2 of this thesis, diagnostic laboratories, including the Clinical Hematopathology laboratory, are preferentially relying on flow cytometry for immunophenotyping and classifying AMLs from ALLs.[27,93–96] Overexpression of myeloid associated antigens appears to be concordant with myeloid lineage between the two species.[96] Antigens that have been proposed as being indicative of myeloid lineage commitment in dogs include expression of CD14, CD11b, CD11c, myeloperoxidase, MAC387, CD4 (without expression of lymphoid associated antigens), and CD61 (megakaryocytic).[27,96–98] Cytochemical staining or immunohistochemistry are also available for distinguishing lineage, but in the author's opinion these techniques can be cumbersome and/or cost ineffective compared to flow cytometry. However, these methodologies do offer additional antigen detection that might not be currently available by flow cytometry and should be used in cases that have equivocal immunophenotyping results.

One hurdle still facing veterinary medicine is a universal classification scheme for diagnosing AML versus other acute leukemia lineages (e.g. lymphoid or mixed phenotypes) and a significant proportion of cases remain unclassifiable, due to the limited availability of species-specific or cross-reactive reagents.[96] Because of this, the true incidence of AML in dogs is unknown, yet the veterinary literature considers AML to be a rare entity.[27,93,99] Using published assignment criteria described in Chapter 2, The Clinical Hematopathology laboratory at Colorado State University receives on average of ~170 cAML cases/per year. Many cases appear to occur de novo and, to the author's knowledge, secondary and therapy-related myeloid neoplasms resulting from receiving chemo- or radiation-therapeutics are rarely reported in dogs.[100,101]

Veterinary medicine adopted the FAB scheme for subtyping cAMLs in the 1990s, which is currently the only method for subtyping cAML and has not been correlated with outcome.[102] Since being implemented into veterinary medicine, acute myelomonocytic leukemias (M4) and acute monocytic leukemias (M5) are reported to occur at the highest frequencies in dogs.[27,93,98] Moreover, the human equivalent of acute promyelocytic leukemia (M3) has not been reported to occur in animals.[102] However, larger studies devoted to subtyping acute myeloid leukemias are needed to determine the true frequencies of these cAML subtypes and their clinical significance. Median survival times for canine acute leukemia, regardless of lineage, are reported between 9-19 days, which only slightly improves by a few weeks-months with chemotherapeutics.[27,94] Therapeutic options in veterinary medicine are limited to supportive care, steroids, and/or in combination with cytotoxic chemotherapeutics. While good strides have been made in human medicine for the treatment of AML, veterinary medicine has yet to incorporate small molecular inhibitors and/or immunotherapies into the treatment regimen of cAML. No institutional studies specifically devoted to the treatment of cAML have been published and supportive evidence for the effectiveness of novel therapies is lacking.

Comparative and unique features of acute myeloid leukemias between species: into the unknown

A PubMed query for dog or canine acute myeloid leukemia yielded an average of 1.3 publications/per year over the last 10 years, the majority of which are case reports or retrospective case series.[27,96,97,103-111] The largest retrospective study available consisted of 35 dogs with AML, which likely doesn't capture the spectrum of this neoplasm.[27] Saying that there is a "knowledge gap" between the features of dog AML and human AML would be an understatement. Regardless, the clinical presentation, clinical course, cytomorphology, and

patterns of antigen expression all appear similar between human and dog AML. However, larger studies are still required to further assess the spectrum of cAMLs' clinical features.

A query of the Clinical Hematopathology's database for clinical signs reported by the veterinarians at the time of diagnosis for dogs with AML is summarized in Figure 4. In addition to the peripheral blood leukocytosis and cytopenias (Figure 2), dogs often have detectable abnormalities in their viscera. Similar clinical signs and findings are also reported to occur in people, although, there are notable differences in the frequency of clinical signs reported at presentation. For instance, mediastinal masses are reported by our survey in nearly one in every 5 dogs, whereas mediastinal involvement is considered exceptionally rare as a presenting sign in human AML.[112] Also, hepatosplenic involvement appears to be common in dogs, yet evidence for extramedullary disease is only reported between 2.5-30% of human patients.[83,113] Interestingly, skin and gingiva are common extramedullary sites afflicted in human patients, which is not a feature readily recognized in cAML.

Given the overlapping clinical features shared between the two species, it is conceivable that they also share overlapping molecular features. One study provided evidence that there are mutations in common genes mutated in human and shared with dog AML, including *RAS, KIT*, and *FLT3*.[114] A separate study found that a subset of cAML samples typically have abnormal DNA methylation patterns compared to normal controls, which is a hallmark feature of human AML patients with *DNMT3A* mutations.[110] This group also identified missense mutations in the methyltransferase gene, *DNMT3L*, by performing targeted next generation sequencing.[110] Mutations in *DNMT3A* or *DNMT3B* were not identified.[110] Additional publications investigating the molecular characteristics of cAML are needed to assess the comparative features more comprehensively between human AML and dog AML.

Finally, it is important to mention the differences in treatment options existing between the two medical fields. Treatments that are currently available for human AML have been reviewed elsewhere and the author refers the reader to this collection of articles.[12,115,116] Historically, AML induction treatment has relied on the '7+3' drug regimen since the 1970s, which consists of 7 days of cytarabine followed by 3 days of anthracycline.[12,116] Combinational therapies using venetoclax and azacytidine have emerged as alternative therapies within the last decade.[117] It wasn't until molecular characterization and development of targeted therapeutics (e.g. FLT3 inhibitors, IDH1/2 inhibitors, Gemtuzumab ozogamicin (CD33 antibody-toxin conjugate)) did novel drugs start to be implemented into patient management.[12,116] Additionally,

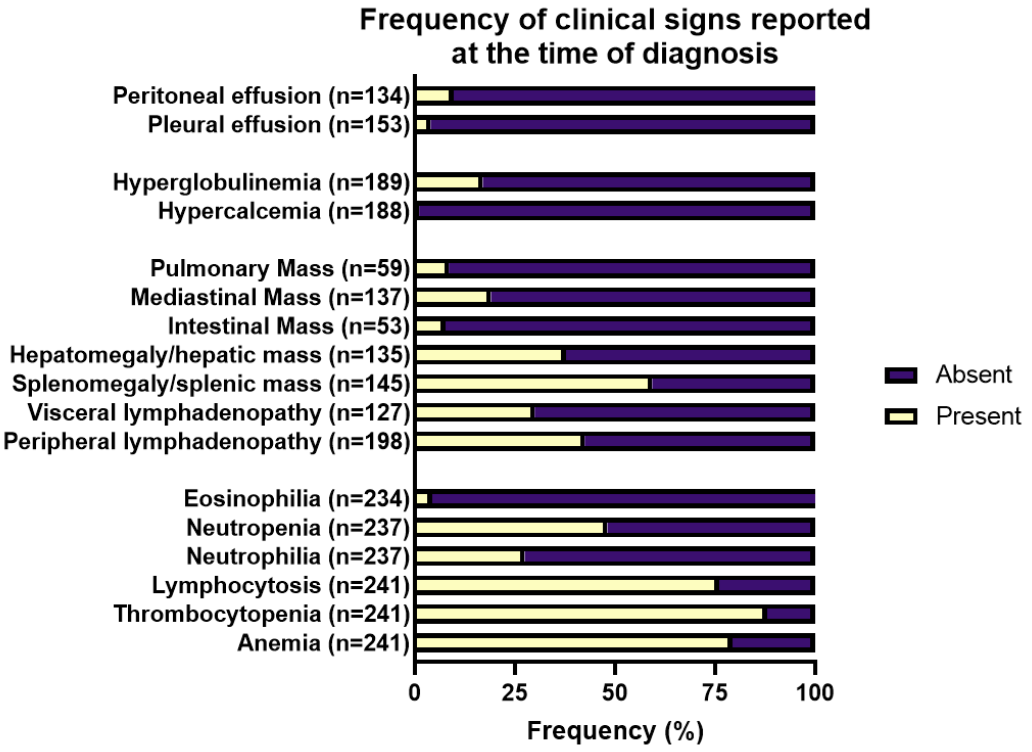

Figure 4: Clinical signs reported by the submitting clinic in dogs diagnosed with AML since January 2021. Stacked bar plots represent the frequency at which each of the reported clinical signs as being present of absent. The total number of patients (n) with data available for each of the clinical signs is reported along the y-axis. Clinical signs data with less than 10 dogs available (i.e., cutaneous mass) or data reported as being unknown at the time of diagnosis are excluded.

allogenic hematopoietic cell transplantation is often performed in human medicine and was

considered the only curative option for AML patients with primary refractory disease in 2017.[116] Treatment options for cAML have remained stagnant over the last few decades, and achieving durable remission is unprecedented.[27,94,99] Cytoreductive chemotherapies are the first route for treating canine AML, which includes a combination of anthracyclines or cytosine arabinoside (Ara-C) with or without prednisone.[118] Bone marrow transplants are one possible solution previously reported, but these techniques are not widely available, cost prohibitive, and carry significant risks.[119] Therefore, future medical management for cAML will likely rely on a combination of chemotherapeutics, targeted small molecule inhibitors, and/or immunotherapies. In essence, overlapping features shared between cAML and hAML could be targeted in the dog and provide translational insight for narrowing prospective therapeutic candidates and improve treatment options for both species.

Conclusions

Although human and dog AML share overlapping microscopic and biologic features, further work is needed to investigate the dog as a model for human AML. If cAML reveals similar molecular features as human AML, then studies investigating environmental or genetic risk factors, disease pathogenesis, and targeted therapeutics could be initiated. Given that dogs already share similar environments as people, they may better recapitulate the natural development of AML compared to genetically engineered mouse models. Additionally, cAML currently carries a grave prognosis and has a rapid disease progression. This rapid clinical course could be leveraged for testing therapeutic safety and effectiveness, as a clinical response would be evident quickly.

CHAPTER 1: Generating a single cell transcriptional map of canine hematopoiesis to aid in the investigation of hematopoietic neoplasms

Summary

Hematopoiesis is a complex process, which starts with hematopoietic stem cells that progressively differentiate to mature leukocytes, erythrocytes, and platelets. Numerous cell states exist along this continuum and alterations from normal can lead to disorders, including hematopoietic neoplasms. While dogs are a model for several human diseases, comparative studies investigating the transcriptomic programs of normal canine hematopoiesis are lacking. The goals of this study are to summarize the gene expression of each cell type identified in canine bone marrow, identify marker genes and transcription factors that define cell states, and summarize gene expression changes during cell differentiation. We performed single cell RNA-sequencing on whole bone marrow and fluorescence activated cell sorted CD34+ hematopoietic precursor cell types. Using unsupervised clustering methodologies, we predicted 28 and 13 transcriptomically unique cell populations in whole bone marrow and CD34+ sorted cells, respectively. First, we focused on identifying the genes that define each cluster. Next, we utilized trajectory analysis to highlight how gene expression programs progress during differentiation of major leukocyte and erythrocyte populations. Taken together, our data provides insight into transcripts that define major hematopoietic populations, which can serve as a reference and can be applied to investigate the cell of origin in canine hematopoietic malignancies.

Introduction

Hematopoiesis is a complex biologic process that involves numerous diverse cell types. This process is essential for replenishing aged mature leukocytes, red blood cells, and platelets, and providing support during disease states, e.g., fighting infections and wound healing.[120,121]

Traditionally, hematopoiesis has been viewed as a step-wise model, where each cell type differentiates along a linear axis starting from progenitor cells that progress towards mature well-differentiated cells.[122–125] However, recent models have proposed that numerous cell states exist on a continuum of the hematopoietic differentiation scheme.[126–128] This makes it challenging to define the cell-of-origin and pinpoint diseases, particularly in non-traditional model species that have limited commercialized reagents for phenotyping.

Hematopoiesis starts with hematopoietic stem cells (HSC), which are rare cell types that primarily reside in the bone marrow and undergo asynchronous cell division to generate multipotent progenitors, which then begin differentiating into lineage-committed progeny.[126,129] HSC differentiation is highly regulated by cell signaling pathways that induce differentiation and division towards mature blood cells. These pathways are responsive to external stimuli, which influence their lineage commitment to granulocytic, monocytic, erythrocytic, megakaryocytic or lymphocytic cell types.[130,131] Disturbances in normal hematopoietic processes can occur anywhere along this hematopoietic tree, which can result in a wide breadth of diseases that are systemically impactful (e.g., neoplasia, immunodeficiencies, and red blood cell and primary hemostatic disorders). Regardless of the overarching disease process, a baseline understanding is required to recognize deviations from health and investigate underlying pathogeneses. Gene expression profiling has been utilized for these situations to address questions pertaining to gene expression dysregulation in disease states.[132,133] With the advent of singe cell RNA-sequencing (scRNA-seq), gene expression programs from individual cells can be defined at high resolution, even those cell types that are in a continuum.[128,134–138] In fact, there are multiple single cell transcriptomic atlases of normal tissues available for humans and mice, which support studies

investigating perturbations from healthy cellular processes.[120,139–141] To date, none have been published devoted to the dog.

There is growing evidence that the dog is a model for human diseases, particularly in the immuno-oncology field. However, very few publications have employed scRNA-seq to investigate canine cell populations, and it is unclear if dog hematopoietic cell transcriptomes are universally similar or different than humans.[142–150] Here, we perform scRNA-seq to assess the gene expression programs of canine hematopoietic cell types in the bone marrow. The goals of this study are to summarize the gene expression of each cell type identified in canine bone marrow, identify marker genes and transcription factors that define cell states, and summarize gene expression changes during cell differentiation. We aimed to generate a single cell transcriptomic atlas to aid in future investigations focused on defining cell type annotation and composition in diseases that involve hematopoiesis, including lymphomas/leukemias.

Methods

Study Population and Sample Collection:

Samples were collected from three reportedly healthy dogs provided by the contract research organization, Inotiv co. Peripheral blood was collected in ethylenediaminetetraacetic acid tubes and submitted for complete blood counts at Colorado State University's Veterinary Diagnostic Laboratory to assess hematologic status. Whole bones were stored on ice within 30 minutes post collection. Single cell suspensions were collected by flushing the bone marrow cavity with asterile Hank's balanced salt solution. Red blood cells were lysed with ammonium-chloride-potassium lysis buffer prior to immunophenotyping, cytologic review of single cell suspensions, and 10x Genomics GEM creation. Whole bone marrow sections were submitted for histologic evaluation.

Immunophenotyping and Fluorescence Activated Cell Sorting:

Immunophenotyping of bone marrow samples was completed using a Beckman Coulter three laser Gallios flow cytometer or a Sony ID7000 spectral flow cytometer (Supplemental Table 1). Viable (propidium iodide negative) CD34+ cells were enriched from 2 of the 3 bone marrow samples via a Sony SH800 cell sorter, then post sort purity was evaluated prior to GEM generation (Supplemental Table 1). For the 3 whole bone marrow samples prepared for GEM generation, we performed a viability check using propidium iodide and assessed neutrophil (CD4+CD3-CD5-CD18+ cells) proportions. All whole bone marrow samples that had a viability >70% and contained <25% neutrophils were used for sequencing.

Generation and preprocessing of single cell transcriptomic data:

Cells from 3 whole bone marrow samples and 2 CD34+ cell sorted populations were resuspended in phosphate-buffered saline and 0.04% molecular grade bovine serum albumin. We targeted 5,000 cells for capture using a Chromium iX instrument (10x Genomics). Post GEM generation, standard Illumina libraries were generated using a Chromium Next GEM Single Cell 3′ Kit v3.1 dual index (10x Genomics) following manufacture recommended protocols. Completed libraries were sequenced via Novogene Corporation on an Illumina NovaSeq 6000 sequencer targeting 100,000 reads/cell with 150 bp paired-end sequencing. Raw FASTQ files were aligned to the *Canis lupus familiaris* genome (Ensembl v.104 canfam3.1) using a standard Cell Ranger (v. 7.1.0, 10x Genomics) analysis pipeline with include-introns = FALSE. The Cell Ranger cell barcode x feature (column x row) count matrices were imported into R to complete downstream analysis.

Gene counts matrix files were analyzed with the Seurat R package.[151] Prior to cluster annotation, low quality cells were removed using standard cutoffs, such as the number of unique

features identified <200 or >5,500, RNA counts <100 or >50,000, and mitochondrial transcript abundance >25%. Doublets were inspected and eliminated using DoubletFinder.[152] After processing individual data files from each sample, we respectively concatenated each sample type (i.e., whole bone marrow or CD34+ sorted cells) for data visualization and cell type annotation. We utilized the R package clustree, to determine the optimal number of clusters predicted in each sample type.[153] Post clustree analysis, the total number of dimensions and the final shared nearest neighbor (snn) resolution was determined based on visual inspection. Optimal clustering parameters for the integrated bone marrow samples revealed to be 45 total dimensions at a snn = 0.8. Likewise, parameters for the integrated CD34 samples revealed to be 35 total dimensions at a snn = 0.3.

Data analysis, visualization, and statistical analysis:

First, the Seurat FindNeighbors() command was implemented for each sample type using the default settings and using dims = 1:45 or 1:35, for bone marrow or CD34+ samples, respectively. Next, Seurat cluster prediction of the integrated samples for each sample type was performed with smart local moving (SLM) algorithm using the FindClusters() command and the final resolution = 0.8 for the integrated bone marrow samples and 0.3 for the integrated CD34+ cell samples.[151,154] Default UMAP parameters were used, in addition to min_dist=0.6, with n.neighbors = 75, and the number of dimensions incorporated using dims = 1:45 or 1:35, for bone marrow or CD34+ samples, respectively.

Cell types were annotated using a combination of manual review, automated cell type prediction, and gene set enrichment analysis. Once cell clusters were predicted, we utilized Seurat's FindMarkers() function using the non-parametric Wilcoxon Rank Sum test to identify genes that defined each subgroup based on differentially expressed genes.[151] Specific cell

markers were visualized using the DotPlot() and FeaturePlot() functions. The reference-based annotation package, singleR, was used to assign identities based on five human immune cell databases (ref1 = HumanPrimaryCellAtlasData (), ref2 = BlueprintEncodeData (), ref3 = DatabaseImmuneCellExpressionData (), ref4 = NovershternHematopoieticData (), ref5 = MonacoImmuneData ()).[155] Cell identities were further investigated using gene set enrichment analysis with enrichR and the publicly available HAY_BONE_MARROW cell type gene sets available through the Molecular Signature Databases' (MSigDB) collection 8.[139,156,157] Final cell type annotations were determined by reviewing the marker genes that defined each cluster, the automated cell types predicted, and reviewing the literature for expected gene expression patterns for individual cell types. Additionally, we performed differential gene expression analysis using pseudo-bulk conversion followed by DESeq2 to determine differentially expressed genes between granulocyte cell types.[151,158]

Table 1: Clinical data from healthy control samples used for generating the single cell transcriptomic atlas

Sample ID	154801	157848	165596
Signalment			
Sex	Female	Female	Female
Age at sample acquisition (years)	0.8	0.7	0.6
Hematologic data			
WBC concentration (cells/uL)	7,700	7,600	10,100
HCT (%)	42	40	42
PLT (cells/uL)	372,000	184,000	364,000
Estimated single cell count based on UMI			
Bone Marrow	7,896	5,033	5,201
CD34+ cells	N/A	4,943	4,880

Abbreviations: Single cell RNA-sequencing, scRNA-seq; White blood cell, WBC; Hematocrit, HCT; Platelet, PLT.

Trajectory analysis was performed using the Monocle 3 R package.[159] We excluded poor-quality clusters and cycling populations from trajectory analysis. Cell populations were identified as cycling if cycling genes, such as *TOP2A* or *MKI67,* were amongst the top 100 genes that

defined that cluster.[160] Next, the data was subcategorized by major cell type identity and extracted cell clusters to investigate each cellular lineage. We implemented independent re-clustering and converted the new Seurat object into a CellDataSet object prior to performing the standard Monocle 3 pipeline. The starting node was selected based on biological knowledge and identification of markers associated with hematopoietic stem or progenitor cells (Supplemental Tables 2 & 3). Differentially expressed genes were identified if they had a q value < 0.05 and a Moran's I > 0.25.

Statistically significant observations for this study were defined as p values, adjusted p values, or q values < 0.05. P values were corrected for multiple testing using the Benjamini-Hochberg approach, unless otherwise specified.

Results

Overview of Sample Characteristics:

An overview of the study design is provided in Supplemental Figure 1. Briefly, bone marrow was collected from three reportedly healthy dogs, which were all <1 year old reproductively intact mixed breed females (Table 1). Cellularity and cellular compositions of the histologic and cytologic specimens evaluated were appropriate for the given age of the dogs (Supplemental Figure 3A). Complete blood count data was within normal limits and no overt hematologic disturbances were noted (Table 1). All bone marrow samples were considered viable (% viable range = 90.1-91.8%) and contained <25% mature neutrophils (CD4+CD5-CD18+ cells: range = 16.2-23.7) by flow cytometry (Table 2). To highlight early hematopoietic cell transcriptomic programs, we performed fluorescence activated cell sorting (FACS) to enrich for CD34+ cells, which comprised < 5% of the total viable cell population in the whole bone

marrow samples. CD34+ cells were sorted in two of the bone marrow samples and post sort CD34+ purity was 94.6% and 98.7%, respectively.

Overview of scRNA-seq data:

In total, 18,130 bone marrow cells were captured and sequenced at a mean depth of 115,850 reads/cell across 3 samples. The distribution of the number of features, gene counts, and mitochondrial transcript abundance are provided (Supplemental Figure 2). Post removal of poor-quality cells, unsupervised clustering using uniform manifold approximation and projection (UMAP) revealed 28 different cell types within the whole bone marrow collection. An additional 9,823 CD34+ cells were captured and sequenced at a mean depth of 125,047 reads/cell across 2 samples. After processing similarly to the bone marrow samples, 13 transcriptomically unique cell clusters were identified in the CD34+ collection. The contribution from each of the samples and the distribution of relative proportions of each cell cluster identified are provided in Supplemental Figure 3.

Table 2: Summarized immunophenotyping data from bone marrow samples

	Average % (range)
Tissue	Bone Marrow
N	3
Immunophenotyping data	
Hematopoietic Precursors (CD34+)	2.9 (2.5-3.2)
T cells (CD3+CD5+)	2.7 (1.8-3.7)
CD4+ T cells	0.6 (0.3-1.0)
CD8+ T cells	1.4 (0.9-1.8)
B cells (CD21+CD22+)	3.6 (2.8-4.7)
Monocytes (CD14+MHCII+)	6.1 (3.2-10.2)
Neutrophils (CD4+CD5-)	19.7 (16.2-23.7)
Myeloid other (CD18+MHCII-)	39.6 (35.2-42.2)
Possible erythroid/megakaryocytic ($CD45^{neg\text{-}low}$)	7.0 (5.0-9.7)

We used a combination of manual and automated methods to tentatively annotate cell clusters. First, differentially expressed genes (DEG) were identified for each cluster, via

Wilcoxon's rank sum test. The top 100 DEG with gene symbols for each cluster from each sample type are reported in Supplemental Tables 2 and 3. These DEG were cross-referenced with known hematopoietic markers in humans and dogs. Automated annotations were achieved using the SingleR package with five human data references.[155] Additionally, we also performed gene set enrichment analysis using the human bone marrow cell gene sets provided by Hay et. al. and available through the MSigDB's C8 gene set collections.[139,157]

Hematopoietic transcriptomic programs in dogs are similar to humans:

Our datasets featured numerous hematopoietic cell types. The unique cell clusters predicted for the CD34+ sorted cell data and the whole bone marrow samples are provided in Figure 5A and Figure 6A, respectively. Given that cell cluster proportions were equally distributed between samples, we concluded that there were no overt batch effects identified in these data sets (Supplemental Figure 3). Hematopoietic stem cells (HSC) and early multipotential progenitors (MPP) were readily identified by overexpression of immature markers such as *HOXA6, NRIP1,* and *TAL1* (Figure 5A, C and Supplemental Table 2).[139,161] Committed lymphoid progenitors, particularly B cell progenitors, overexpressed canonical markers such as *DNTT, FOXO1, BLNK, CD19,* and *RAG1* (Figure 5A-C and Supplemental Table 2).[162,163] Two clusters(Clusters 4 and 10) of the cycling cells were identified based on their expression of *TOP2A, MKI67,* and multiple cyclin family genes. Delineating the progression from late MPP and their differentiation towards common myeloid progenitors (CMPs) was challenging because they overexpressed both immature hematopoietic markers and myeloid markers and clustered with other myeloid progenitors (Supplemental Table 2). As such, these two cell types were tentatively classified together (LateMPP-CMP). Other myeloid progenitors, including the granulocyte-monocyte progenitors (GMP) and megakaryocytic-erythroid progenitors (MEP),

clustered together. Granulocytic and monocytic markers (e.g., *MPO, SPI1, CEBPE, BPI, NPMI)* and erythroid specific markers (e.g., *GATA1 and KLF1)* were overexpressed in clusters annotated as GMP and MEP, respectively.[139,164] One cluster overexpressed markers associated with both monocytic-dendritic cell progenitor (MDP) and early lymphoid cell types (e.g. *RUNX2*, *IRF8, IL7R, ITGB7*), and was tentatively annotated as CD34pos_MLP-MDP-like.[165–167] A small cluster of cells overexpressed endothelial markers (e.g. *LYVE1, CD93, ID1*), which we suspect were inadvertently enriched during FACS as endothelial cells express CD34.[168–170]

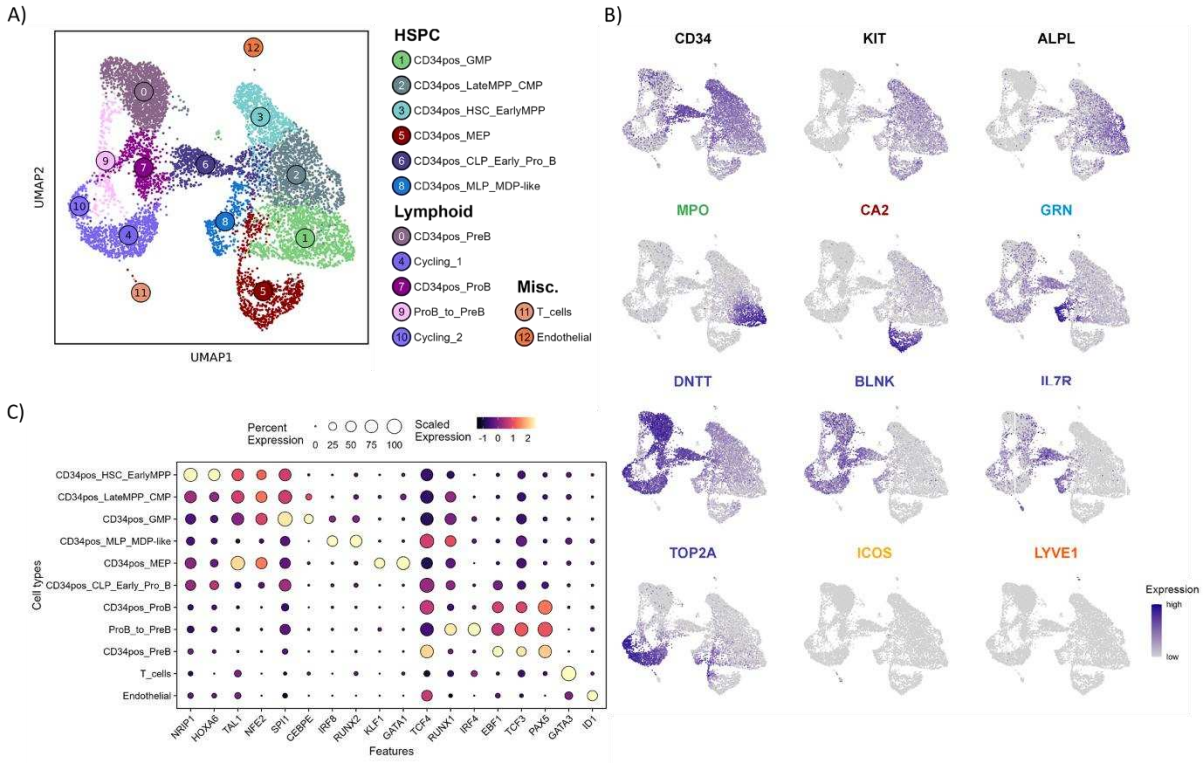

Figure 5: Unsupervised clustering of sorted CD34+ canine leukocytes revealed 13 unique clusters. A) UMAP projection of sorted CD34+ cells. Clusters are identified by major cell types. B) Canonical hematopoietic genes and cell differentiation markers depicted as feature plots. Gene names are color-coded to depict specific features in subpopulations. Genes highlighted in black are expressed over multiple populations. The level of expression is color-coded according to the scale. C) Dot plot of transcription factors expressed between cell types. The size and color of each dot corresponds to the percentage of cells that express that gene and the scaled expression, respectively. Abbreviations: HSPC, Hematopoietic stem and progenitor cells; pos, positive, GMP, Granulocyte-monocyte precursor; MPP, Multipotent progenitor; MEP, Megakaryocytic-erythroid progenitor; CLP, Common lymphoid progenitor; MLP, Multi-lymphoid progenitor; MDP, Monocyte-dendritic precursor.

Altogether, 28 unique clusters were identified in the whole bone marrow data set (Figure 6A). All cell populations, except for cluster 7, were universally represented and equally distributed in the three healthy marrow samples (Supplemental Figure 3). Therefore, we concluded that no overt batch effects were present. The top 100 markers with gene symbols that were used to define and tentatively annotate each cell cluster in the whole bone marrow are provided in Supplemental Table 3. We observed multiple branches of developing and mature leukocytes extending from a centralized cluster of hematopoietic stem and progenitor cells (HSPC), which were enriched for *CD34, KIT,* and *ALPL* (Figure 6B). Each branch represented major leukocyte lineages such as granulocytes (*MPO+, LYZ+, BPI+*), monocytes (*LYZ+, BPI+, MNDA+*), developing erythrocytes (*HBM+, GYPA+*), and a disconnected branch of developing B cells (*IGHM+, PAX5+, LTB+*) (Figures 6B-C). Mature neutrophils in dogs express CD4 and we noted a population at the tip of the developing granulocytes that coincided with this observation.[171] Discrete clusters of resident macrophages (*MSR1+, MRC1+*), T cells (*CD3E+*), and plasma cells (*JCHAIN+*) were also readily identified.[139] One cluster of poor-quality cells and one cluster with ambiguous features were noted and removed from down-stream analysis (Supplemental Table 3).

We noted two branches (clusters 9, 5, 10 and clusters 2, 0, 1) of developing granulocytes/ neutrophils. When we performed differential gene expression analysis using a pseudobulk approach and compared the gene expression between cluster 10 and cluster 1, we found a single gene that was differentially expressed between them, *ENSCAFG00000030793* (Log2 fold change = 3.38, adjusted p value = < 0.001). Previous publications have indicated that *ENSCAFG00000030793* is an interferon-induced transmembrane protein.[147] Given the lack of other defining features that distinguished these two arms of the developing granulocytes, we

utilized clusters 0, 1, and 2 for downstream analysis as these comprised most of the developing neutrophil data points.

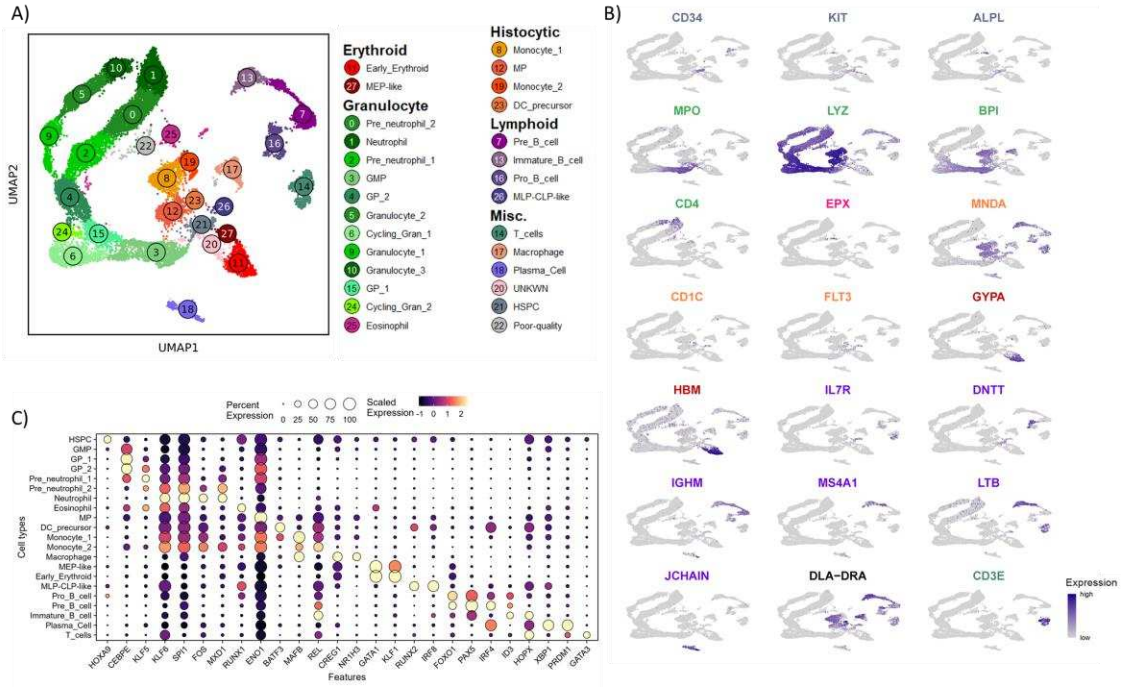

Figure 6: Unsupervised clustering of whole bone marrow canine leukocytes revealed 28 unique clusters. A) UMAP projection of whole bone marrow cells. Major cell types are labeled. B) Canonical hematopoietic genes and cell differentiation markers depicted as feature plots. Gene names are color-coded to depict specific features in subpopulations. Genes highlighted in black are expressed over multiple populations. The level of expression is color-coded according to the scale. C) Dot plot of transcription factors expressed between cell types. The size and color of each dot corresponds to the percentage of cells that express that gene and the scaled expression, respectively. Abbreviations: MEP, Megakaryocytic-erythroid progenitor; GMP, Granulocyte-monocyte precursor; Gran, Granulocyte; MP, Monocyte precursor; DC, Dendritic cell; MLP, Multi-lymphoid progenitor; CLP, Common lymphoid progenitor; Misc., Miscellaneous; UNKWN, Unknown; HSPC, Hematopoietic stem and progenitor cells.

Gene expression programs that govern human hematopoiesis are similar in dogs:

Amongst the top markers that defined each cell cluster were canonical transcription factors and cell differentiation markers that have previously been validated in other species. For instance, transcription factors involved in maintaining stem cell properties, including the HOX genes, *NRIP1,* and *TAL1*, were all enriched in the HSC/early MPP cluster compared to others (Figure 5C).[139,161] *SPI1* expression, which is required for myeloid cell differentiation, was

maintained throughout multiple granulocytic and monocytic populations (Figures 5C and 6C).[172] Furthermore, *BAFT3, MAFB,* and *ENO1* all appear to be involved in monocyte and dendritic cell development, as is similar to people (Figure 6C).[166,173,174] Additionally, both *GATA1* and *KLF1* are influential in erythroid development and co-expression of these markers was noted in the developing erythroid cell clusters (Figures 5C and 6C).[175] *TCF3 (E2A), EBF1, PAX5*, *IRF4* are all instrumental in B cell development and expressed at various levels in the committed B cell progenitors (Figures 5C and 6C).[163]

Trajectory analysis of canine hematopoiesis:

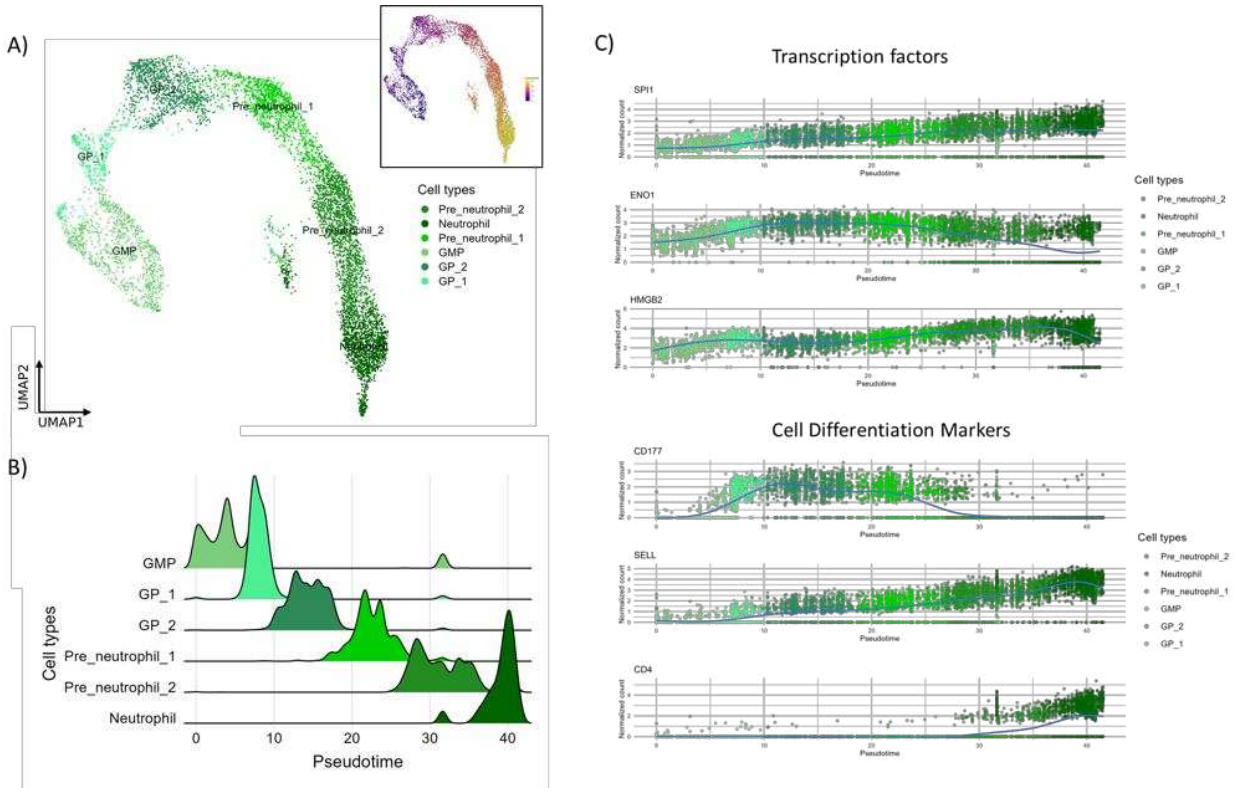

Figure 7: Trajectory analysis of dog granulocytic/neutrophilic lineage. A) UMAP projection of granulocytic/neutrophilic cell types post-reclustering. Overlaid pseudotime inference for each data point along the granulocytic lineage (inlet). B) Ridgeplot of each of the granulocytic/neutrophilic cell types over pseudotime. C) Dot plot of highlighted transcription factors and cell differentiation markers expressed between cell types. The blue line represents the average expression detected. Abbreviations: Granulocyte-monocyte precursor; GP, Granulocyte precursor.

To highlight the changes in gene expression patterns over differentiating cell populations, we performed trajectory analysis for each of the major leukocyte lineages (i.e., granulocytes/neutrophils, monocytes/dendritic cells, B cells, and erythrocytes). First, we extracted the cell populations of interest then performed independent re-clustering. We excluded overtly apparent cycling populations to limit the influence of cell cycling genes (e.g. *TOP2A, MKI67, etc.*), which included the two clusters of cycling granulocytes and the "unknown" cell population. Post-re-clustering, we noted that the cell populations of each lineage maintained their spatial relationships as observed in the original UMAP relatively well (Figures 7A, 8A, 9A, and 10A). Results from our trajectory analysis are provided for each of the major lineages (Supplemental Tables 4-7).

Next, we highlighted the comparable features between human and dog hematopoietic transcriptomic programs in each of the major leukocyte populations. For example, within the developing granulocytic lineage, we noted that critical myeloid-specific transcription factors are maintained throughout differentiation in dogs, like people (Figure 3C, Supplemental Table 4). Expression of transcription factors such as *SPI1* and *HMGB2* appear to steadily increase from early granulocytic precursors through neutrophil development. We also highlighted comparable cell differentiation markers that correspond with the development of human granulocytes/neutrophils. For instance, *CD177* encodes for a glycosylphosphatidylinositol (GPI) – anchored protein, which is typically expressed in developing neutrophils and modulates neutrophil activation.[176,177] At the transcriptomic level in dogs, it appears that *CD177* expression is first initiated in the granulocytic progenitors (Figure 7C). We noted a similar pattern with other canonical granulocyte transcripts, like *MPO* (Figure 5B, 6B & Supplemental Table 4).[139] It is conceivable that the messenger RNA is first detected at these earliest stages and the protein is

stable throughout differentiation, and additional transcripts are not required for maintenance in later stages of development. On the other hand, we noted that *CD4* transcripts appear to be isolated to later stages in neutrophil development, which corresponds with previous observations.[171]

Like the granulocytic lineage, *SPI1* expression is maintained in developing monocytic/dendritic cell types (Figure 6C & 8C).[178] Both *MAFB* and *FOS* are important for myeloid cell differentiation and monocyte development in humans and transcripts were detected at similar cell stages in our cohort (Figure 8C).[179,180] The DC precursor cell type overexpressed

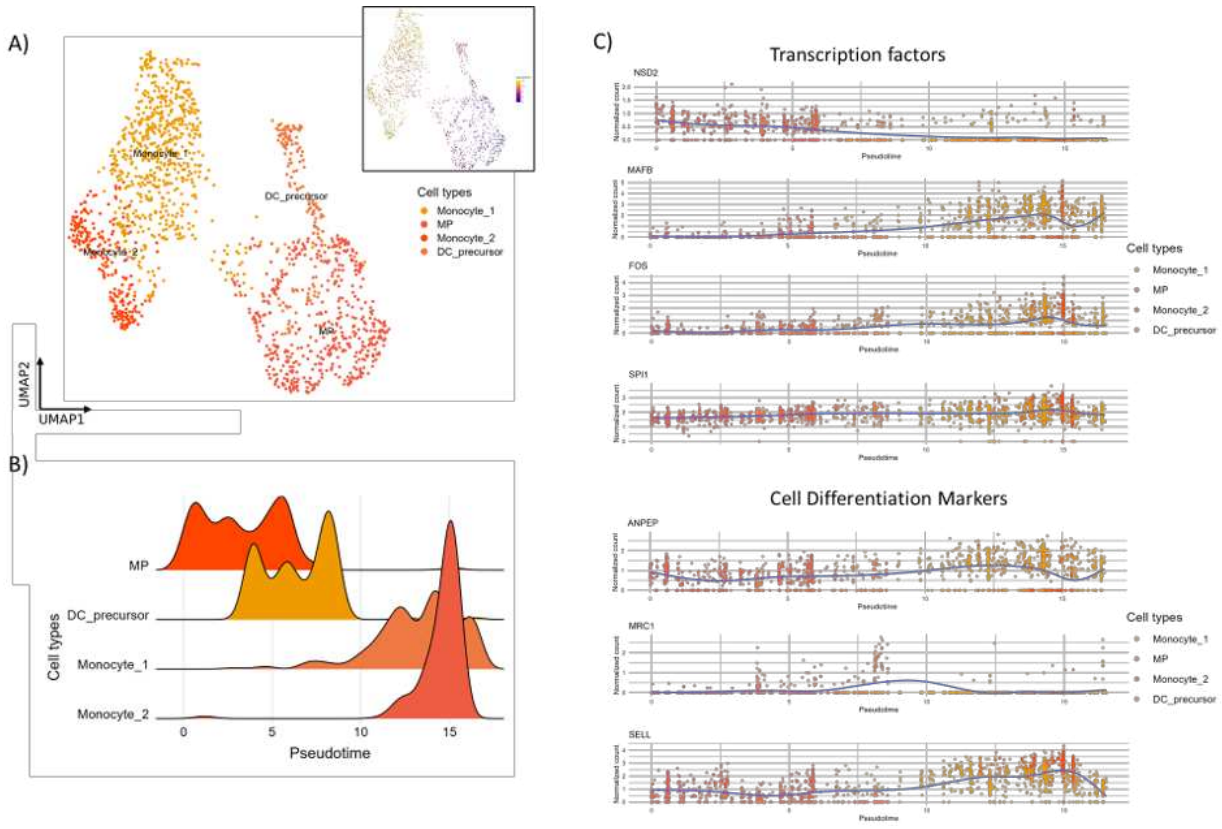

Figure 8: Trajectory analysis of dog monocytic/dendritic cell lineage. A) UMAP projection of monocytic and dendritic cell types post-reclustering. Overlaid pseudotime inference for each data point along the monocytic/dendritic cell lineage (inlet). B) Ridgeplot of each of the monocytic/dendritic cell types over pseudotime. C) Dot plot of highlighted transcription factors and cell differentiation markers expressed between cell types. The blue line represents the average expression detected. Abbreviations: MP, Monocyte precursor; DC, Dendritic cell.

MRC1, which has previously been shown to be a marker for immature dendritic cells.[181] They also overexpressed *BATF3* and *IRF4*, which are required for dendritic cell differentiation into subsets (Figure 8C, Supplemental Table 5).[173,182] Additionally, transcripts for myeloid specific cell-differentiation markers, such as *ANPEP* (CD13), were maintained throughout monocytic differentiation, yet others, such as antimicrobial peptides (e.g. *CAMP*) and mature cell differentiation markers (e.g. *SELL* and *CD74*), had the highest transcript abundance at the latest stages (Supplemental Table 5).

Commitment of developing hematopoietic precursors to the lymphoid lineage in people is an early decision event along the hematopoietic axis.[139] In our dataset, we detected cell types that resembled MLP/CLP in humans. There was strong evidence that this cluster represented a

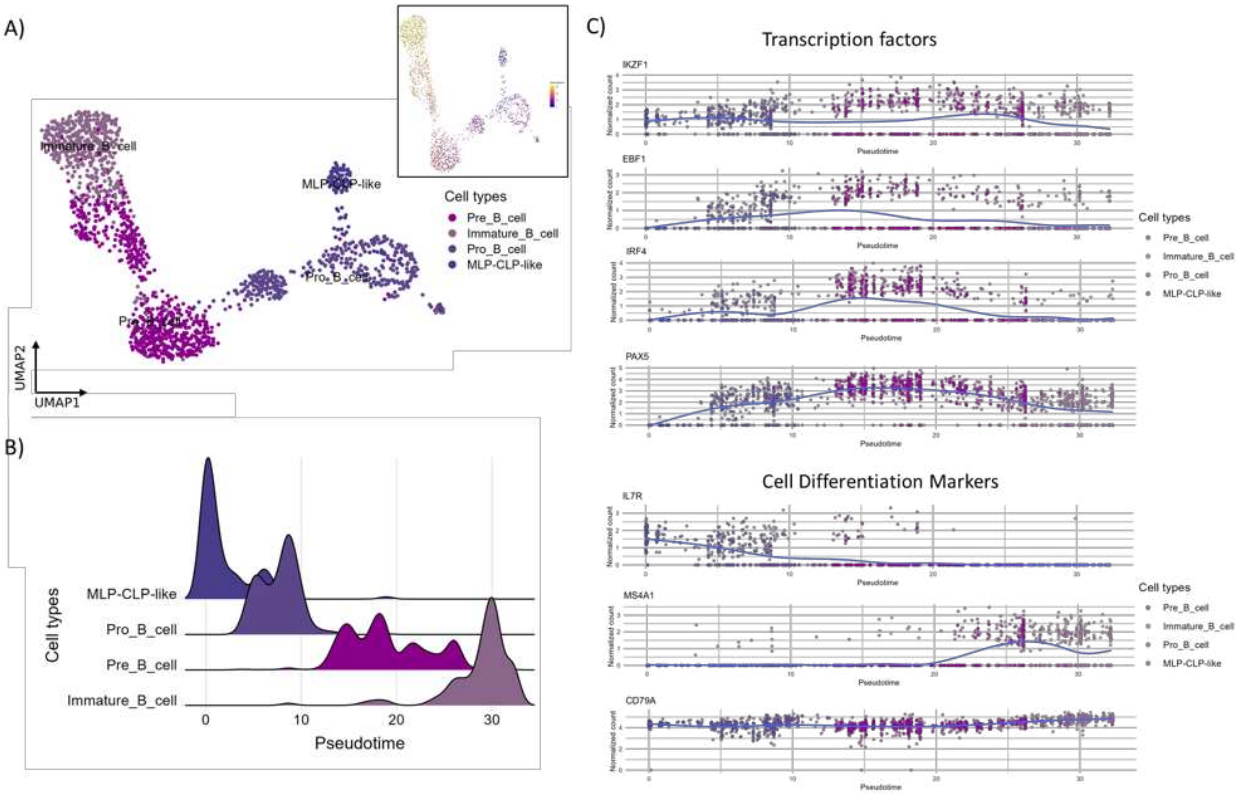

Figure 9: Trajectory analysis of dog B cell lineage. A) UMAP projection of B cell cell types post-reclustering. Overlaid pseudotime inference for each data point along the developing B cell lineage (inlet). B) Ridgeplot of each of the B cell cell types over pseudotime. C) Dot plot of highlighted transcription factors and cell differentiation markers expressed between cell types. The blue line represents the average expression detected. Abbreviations: MLP, Multi-lymphoid progenitor; CLP, Common lymphoid progenitor.

MLP/CLP cell types based on their enrichment of transcription factors such as *IKZF1* (IKAROS) and cell differentiation markers, like *IL7R*, which are both regulators of early lymphoid differentiation (Figure 6C & 9C).[163,167,183] After the CLP stage, early T cell precursors leave the bone marrow and migrate to the thymus, which were not readily detectable in either the bulk bone marrow or CD34+ sorted cell data sets.[139,184]

B cells continue to develop in the bone marrow and we noted multiple stages of B cell development that in general progressed from pro-B cells to pre-B cells, and finally immature/naive B cells.[163] Intermediate stages exist between these major B cell groups, but these were not identifiable in our dataset. Similar to humans, it appears that transcription factors like *EBF1, PAX5,* and *IRF4,* are involved in B cell commitment and lymphopoiesis.[163] Transcript abundance for these progressively changed over the cell stages (Supplemental Table 6). For instance, *IRF4* appeared to be co-expressed with *PAX5,* a characteristic of Pro- and Pre-B cells in people, but steadily declined as the B cells progressed to the immature B cells. *PAX5* expression was maintained in the immature B cells, which also coincided with detection of *MS4A1 (CD20)* transcripts. Although we noted that *CD79A* was maintained throughout the spectrum of B cell development, this marker was not unique to B cells and *CD79A* transcripts were detected in numerous cell clusters.

Developing megakaryocytic-erythroid progenitors are identifiable by upregulation of GATA1 and KLF1 in people, and we observed a similar pattern in the CD34+ MEP population, the MEP-like cells, and early erythroid progenitors (Figures 5C, 6C & 10C).[175] Additionally, *MYB* is important for lineage fate decision between megakaryocytic versus erythroid and preferentially shifts differentiation toward the erythroid lineage.[179] In our dataset, the transcript level of *MYB* appears to rapidly decrease once commitment to the erythroid lineage is initiated (Figure 10C and Supplemental Table 7). As we demonstrate, once commitment to the erythroid lineage is underway, canonical erythroid differentiation markers are quickly expressed (e.g. *GYPA*) and *HBM* transcription is initiated.

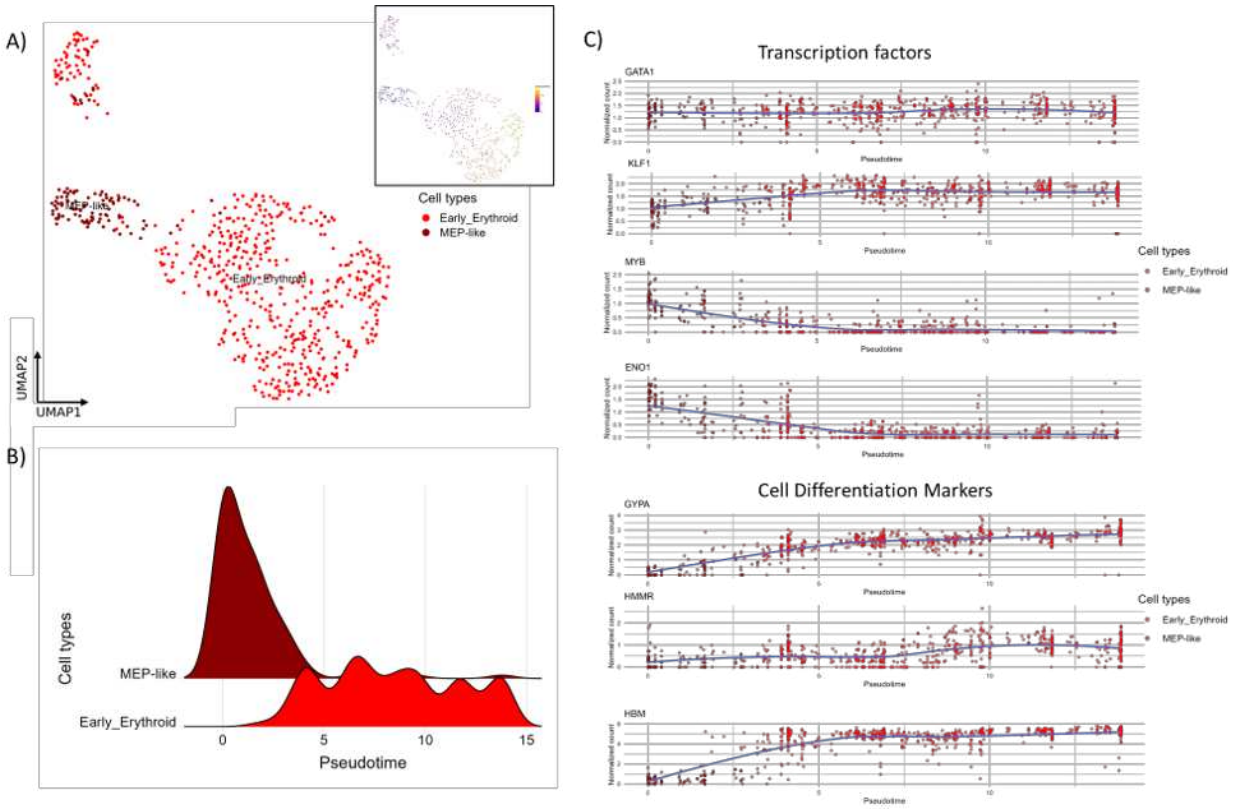

Figure 10: Trajectory analysis of dog erythroid lineage. A) UMAP projection of erythroid cell types post-reclustering. Overlaid pseudotime inference for each data point along the developing erythroid lineage (inlet). B) Ridgeplot of each of the erythroid cell types over pseudotime. C) Dot plot of highlighted transcription factors and cell differentiation markers expressed between cell types. The blue line represents the median expression detected. Abbreviations: MEP, Megakaryocytic-erythroid progenitor.

Discussion

We robustly identified major cell types within canine bone marrow tissue, including transcriptomically unique subtypes not identifiable with traditional methodologies (i.e., flow cytometry). Here, we identified similar gene expression programs between dog and human hematopoietic cells. Canonical transcription factors and cell differentiation markers that define cell types in humans were readily identified in similar cell populations in the dog. Pseudotemporal (trajectory) analysis also allowed us to characterize the maturation and development gene expression programs in each major leukocyte population.

Our data did yield some unexpected results. For instance, the two branches of tentatively annotated developing neutrophils/granulocytes were surprising. *ENSCAFG00000030793* was the only distinguishing marker that separated these two branches. At this point, the authors currently do not have any supportive data to explain this observation. One theory is that the smaller granulocyte/neutrophil branch (clusters 9, 5, and 10) could be a population of neutrophils that have been in circulation in the peripheral blood and were inadvertently sampled during processing. Another possible explanation is that there truly are two developing branches of developing neutrophils in dogs. The latter is considered unlikely, but additional experimentation, including assessment of peripheral blood neutrophil gene expression profiles, is needed.

This study is not without limitations. Previous studies have described the weakness of scRNA-seq, which are also present here. One of which is the level of 3' annotation in the canine genome compared to that of humans or mice. We noted that important transcription factors and cell differentiation markers were missing from our data set. For instance, *CEBPA* is a critical gene involved in commitment to and the development of the myeloid lineage. However, it is poorly annotated in the CanFam 3.1 genome, and we were unable to evaluate its role in cell

differentiation in the dog. Transcripts of other markers were also absent, which in part could be due to the limitations of the annotated genome or the methodology used to capture transcripts from single cells (i.e. dropout).[185] Regardless of this current limitation, the data generated here exceeds what has been previously shown for canine hematopoiesis in health, which could enhance focused hematopathology studies utilizing the dog as a translational model.

A few cell types were not overtly apparent in our data set. For instance, we did not identify a clear population of developing megakaryocytes and later stage erythrocytes. The population of "unknown" cells were initially suspected to be of megakaryocytic lineage based on their proximity to other erythroid clusters, but this was not obvious from their list of enriched genes. Additionally, post-re-clustering of the erythroid lineage from the bulk bone marrow sample a discrete population of cells, all of which were previously annotated as early erythroid appeared. Pseudobulk analysis comparing this new cluster to the early erythroid cluster did not yield any obvious indication that these were megakaryocytes (data not shown). We suspect that later stage erythrocytes (e.g. metarubricytes) were missing because of our sample processing technique, which was evidenced by the cytologic review prior to performing scRNA-seq (Supplemental Figure 3A).

Lastly, while these initial investigations offer a general overview of canine hematopoietic pathways, our study only included a three young dogs. Focused investigations on individual lineages, complemented with functional assays, and including a higher number of samples would offer more insight and strengthen our observations. One could do this by invoking cell differentiation of isolated HSC under various cytokines/growth factors on solid growth media and performing single cell gene expression profiling concurrently with proteomic analysis of developing colony forming units. This methodology could answer questions pertaining to lineage

decision regulatory networks and enrich for cell types that were not apparent in our current study.

In conclusion, the data presented here provides a detailed molecular framework of the gene expression profiles in major leukocyte populations in the canine bone marrow. This resource could complement ongoing investigations that utilize the dog as a translational model, particularly in the immuno-oncology field.

CHAPTER 2: Using digital RNA counting to establish flow cytometry diagnostic criteria for subtypes of CD34+ canine acute leukaemia[1]

Summary

Canine acute leukaemia is a heterogeneous neoplasm with multiple phenotypes. Criteria to subtype acute leukaemia by flow cytometry have not been validated. The goal of this study was to develop a panel of antibodies and objective antigen expression criteria for the assignment of lymphoid or myeloid lineage by flow cytometry. We isolated mRNA from the blood of 45 CD34+ acute leukaemia cases and measured expression of 43 genes that represent lymphoid and myeloid lineages using NanoString technology. We determined differentially expressed genes between major groups identified by unsupervised hierarchical clustering. We then evaluated the expression of antigens by flow cytometry to determine if cases could be assigned to a lineage. Two groups were identified by gene expression. Group 1/LYMPH overexpressed lymphoid-associated genes (ex. DNTT) and had a higher percentage of CD5 + CD3- cells by flow cytometry. Group 2/MYELO overexpressed myeloid-associated genes (ex. ANPEP/CD13) and had a higher percentage of class II major histocompatibility complex (MHCII)- CD14+ and/or CD18 + CD4- cells. We proposed that >12.5% CD5 + CD3- cells in the blood was indicative of lymphoid lineage, and > 3.0% CD14 + MHCII- cells or > 18% CD18 + MHCII-CD4- cells was indicative of myeloid lineage. 15/15 cases that met the proposed criteria for acute lymphocytic leukaemia were in LYMPH group and 12/15 cases that met the proposed criteria for acute myeloid leukaemia were in MYELO group. The majority of CD34+ cases that did not meet

either immunophenotyping lineage criterion (12/13) clustered within the LYMPH group. In conclusion, currently available antibodies can be useful for determining canine acute leukaemia subtypes.

Introduction

Acute leukemia (AL) is a group of heterogeneous, clinically aggressive hematopoietic neoplasms that arise from precursor lymphoid or myeloid cells that have not completed their program of differentiation. In human medicine, a combination of diagnostic tests, including cytology, histology, flow cytometry, and molecular genetics/mutational analysis are commonly used to characterize the neoplasm and assign lineage. Acute leukemias typically express antigens associated with immature hematopoietic cells, including the stem cell antigen CD34.[186,187] However, the expression of CD34 can be variable and lack of CD34 expression does not rule out AL as a diagnosis.[94,188] Acute myeloid leukemias (AML) in humans are initially identified using immunophenotyping and are characterized by expression of CD14, CD11c, and/or myeloperoxidase expressed by neoplastic cells.[7] Acute lymphocytic leukemias (ALL) are subdivided into B cell lineage (B-ALL) and T cell lineage (T-ALL) and typically express surface CD19 and/or cytoplasmic CD79a and CD22 or surface or cytoplasmic CD3, respectively.[7] CD5 expression in human T-ALL is variable.[189,190] Acute unclassifiable leukemias (AUL) lack lineage specific antigens whereas mixed phenotype acute leukemias (MPAL) express two or more lineage associated antigens.[7]

The diagnosis of AL in dogs begins with the identification of immature leukocytes in the blood and/or bone marrow. Some reports use >20% circulating blasts in the blood or >30% in the marrow as diagnostic criteria for AL in the dog.[3,93] The expression of CD34, as assessed by flow cytometry, can further help distinguish immature or precursor cells from lymphoproliferative

disorders of mature leukocytes and has been used independently of blast count as an indicator of AL.[191] Determination of lineage (myeloid versus lymphoid) requires additional tools. Adam et al used expression of cell surface CD14, intracellular MAC387, and myeloperoxidase to diagnose AML, and lack of expression of these together with positive intracellular expression of CD79a to indicate B-ALL and intracellular expression of CD3 and surface expression of CD5 to indicate T-ALL.[93] Similar criteria for identifying AMLs were employed by Stokol et al, who also demonstrated the use of alkaline phosphatase staining as an indicator of myeloid lineage.[97]

While the use of these antibodies to define lineage is consistent with practices in human hematopathology, species differences in antigen expression raise the possibility that different criteria for lineage assignment may be necessary in dogs. Furthermore, while CD79a expression has been used as an indicator of B cell lineage, it is expressed on precursor myeloid cells in people and mature myeloid cells in dogs and therefore does not reliably identify precursor B cells.[192–194] Other groups have relied on additional antigens such as CD21, and/or CD22 to identify B-cell lineage AL by flow cytometry.[8,11] In this study we attempt to address some gaps in our ability to determine the lineage of CD34+ canine AL.

In human medicine, gene expression profiling reliably classifies leukemia subclasses and mRNA and DNA sequencing have revealed numerous genetic abnormalities that are critical for prognosis and prediction of treatment response.[64,195] Differentiation between tumor subclasses is imperative in human medicine because of disease-specific therapeutic options.[196] Similar clinical significances likely exist in veterinary medicine but have not been fully explored. The utility of microarray and digital RNA technology in a diagnostic setting is limited in veterinary medicine, partially attributed to cost and lack of supportive data. However, gene expression profiles of hematopoietic neoplasms can be used to design flow cytometry criteria to distinguish tumor

subtypes. The goal of this study was to use gene expression to classify CD34+ AL as myeloid or lymphoid, and then correlate that classification with the immunophenotype observed by flow cytometry. We focused on CD34+ AL cases because, in the authors' experience, CD34+ AL cases are typically difficult to assign to a lineage, given their ambiguous protein expression and biological behavior. This study allowed us to assign lineage to AL based on commercially available directly conjugated cell surface antibodies. Currently, outcomes in canine AL are poor and improving classification of canine AL may allow for more targeted therapy and improve clinical outcomes.

Methods

Case selection:

Samples included EDTA peripheral blood samples from dogs (n=45) diagnosed with AL by flow cytometry through the Colorado State University's (CSU) Clinical Hematopathology Laboratory between August 2015 to May 2017. Samples were not solicited for this study. These cases were not breed or age restricted. A diagnosis of acute leukemia was made using a combination of laboratory abnormalities and protein expression assessed by flow cytometry. AL were considered CD34+ if >10% of total leukocytes expressed CD34 or there was >1000 CD34+ cells/uL. Some B cell lymphomas can express CD34 but these cases are readily identified by expression of class II MHC (MHCII) and the B cell antigen CD21, and were excluded from analysis.[197,198] Rarely plasma cell tumors can express CD34, but IRF4 (MUM1) was included in the gene expression panel to try to identify and exclude potential plasma cell cases.[199] AL cases were chosen to represent samples that were tentatively classified as lymphoid, myeloid, unclassified, or mixed phenotype based on subjective flow cytometric criteria. Blood samples from two dogs with no suspicion of hematopoietic neoplasia were used as controls.

Immunophenotyping:

Routine CBCs were performed and submitted concurrently with the patient's sample. CBCs were either performed in the submitting clinic with a bench top analyzer, by a veterinary diagnostic reference laboratory, or performed at the Clinical Pathology Laboratory at the CSU-Veterinary Diagnostic Laboratory. Samples (n=14) submitted to CSU Clinical Pathology Laboratory were submitted for automated cell counts (Advia 120 Hematology Analyzer, Siemans, Tarrytown, NY), blood smear evaluation, and a manual white blood cell differential count. For CSU CBC cases, a leukocytosis was defined as >15,000 cells/uL, neutropenia as <2,600 neutrophils/uL, neutrophilia as >11,000 neutrophils/uL. Additionally, patients were considered thrombocytopenic and anemic if they had a platelet count less than 200,000/uL without platelet clumps and a hematocrit less than 40%, respectively. For all other CBC data provided by the clinic, we interpreted those results using the reported analyzers' reference interval. A manual review of the blood film was not available in a subset (n=14) of these cases.

Flow cytometry was performed as previously described and analyzed using Kaluza software (Beckman Coulter, www.beckmancoulter.com).[200] Samples were acquired over 21 months and the staining panel was changed during this time. The two panels are provided in Supplemental Table 8. The panel does not detect intracellular antigens. Diagnosis of AL was based on CD34+ expression as noted above. All neoplasms expressed the pan-leukocyte marker, CD45. Cases were selected for further study based on subjective flow cytometric criteria with the goal of having a mixture of lineages (Figure 11). These included cases with a population of cells expressing CD5 but no other T cell antigens (surface CD3, CD4, or CD8) (n=12), cases with a population of CD14+MHCII- cells (n=19), cases where neoplastic cells expressed no lineage-specific antigens (n=11), and cases with mixed phenotypes (CD5+ population and

CD14+MHCII- population) (n=3). These cases had variable expression of CD18 and none of these cases had surface expression of CD21 or surface CD3. The CD18 antibody used in this study is a cross-reactive anti-human CD18. This is used because of the wider variety of fluorochromes available. A prior study demonstrated that this antibody binds primarily to canine

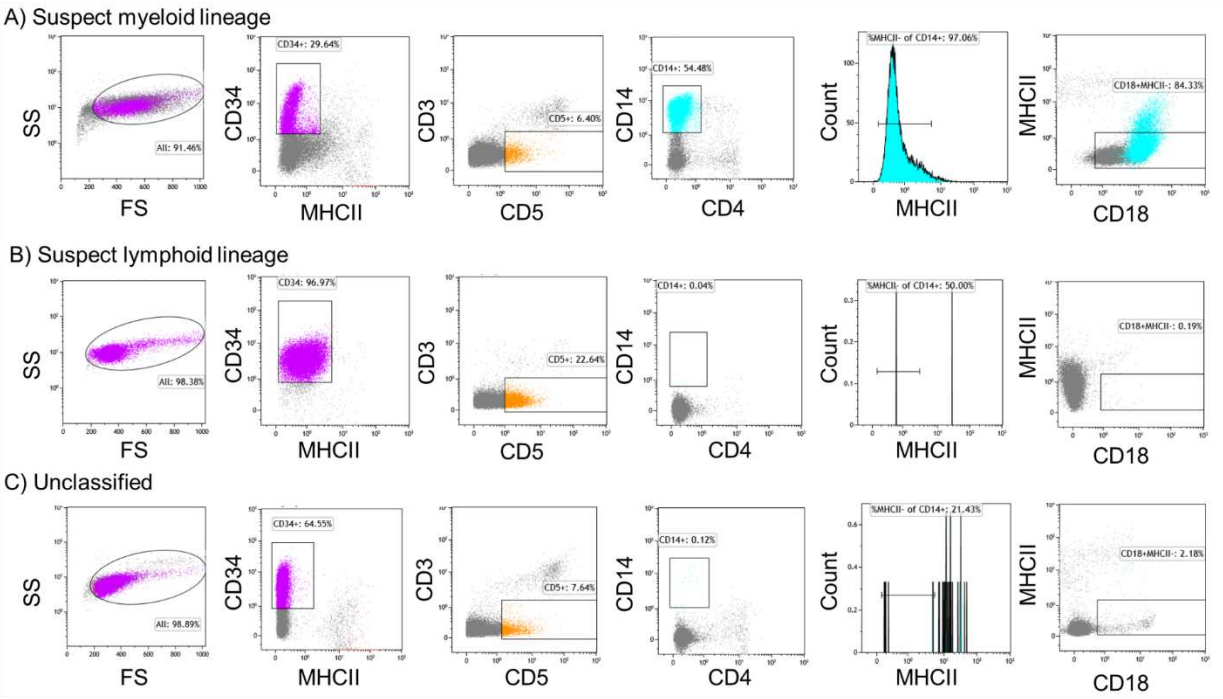

Figure 11: Flow cytometric plots for acute leukemia subtypes. These are the most common subtypes of acute leukemia seen by the CSU Clinical Hematopathology laboratory. A) Suspected myeloid lineage neoplasms often have either CD14+CD4- cells that lack MHCII expression and/or a CD18+ population that is also MHCII- and lacks CD4 expression (indicating they are not mature neutrophils). B) Suspected lymphoid lineages express CD5 and typically lack surface CD3 expression. C) Lineage unclassified acute leukemias do not express lineage associated antigens, including CD5, and lack CD14+MHCII- cells. CD18 expression is often variable in these cases. FS, linear forward light scatter. SS, log side light scatter.

neutrophils and monocytes, and only at low levels to lymphocytes.[201]

Gene expression profiling:

Red blood cells were lysed with ACK lysis buffer using the same protocol as used for preparing cells for flow cytometry. After red cell lysis, leukocytes were pelleted and total RNA was isolated from the leukocyte pellet using the PureLink RNA Mini kit (ThermoFisher,

Waltham, MA) as previously described.[202] RNA samples were analyzed for concentration and integrity using a Nanodrop 2000c (ThermoFisher, Waltham, MA) and Agilent RNA ScreenTape assay (Agilent Technologies, Santa Clara, CA), respectively. Samples had concentrations ranging from 15-2,177 ng/μL (median, 221 ng/μL; interquartile range (IQR), 99-370 ng/μL) and RNA integrity numbers (RINs) ranging from 3.1 to 8.4 (median: 6.0; IQR: 4.5-7.3) (Supplemental Table 9). mRNA counts were obtained through the University of Arizona's Genetics Core using an nCounter Digital Analyzer (Nanostring Technologies, Seattle, WA) with a custom-built panel of genes. We compiled a list of 43 genes to represent hematopoietic lineages, including genes commonly expressed by myeloid, T cell, and B cell lineages, by reviewing available literature for human and dog (Table 3 and Supplemental Table 8). Additional genes were included that are expressed in hematopoietic precursors. Seven of the genes selected were previously shown to be differentially expressed between AML and ALL in humans.[64] Six housekeeping genes were originally included as internal normalization controls. Probes were designed by NanoString based on proprietary algorithms designed to provide the most efficient detection of mRNA using the known *Canine lupus familiaris* annotated gene sequences using the CanFam3.1 assembly (Supplemental Table 10).

Table 3: Gene list used for investigating AL subtypes.

Gene symbol§	Alternative symbol	Gene name§	Probe category ‡
CD19	CD19	CD19 Molecule	B cell
CD22	CD22	CD22 Molecule	B cell
CD79A	CD79a	CD79a Molecule	B cell
CR2	CD21	Complement C3d Receptor 2	B cell
IGHG	IgG	Immunoglobulin Heavy Constant Gamma	B cell
IGHM	IgM	Immunoglobulin Heavy Constant Mu	B cell

MS4A1	CD20	Membrane Spanning 4-Domains A1	B cell
PAX5	Pax5	Paired Box 5	B cell
CD2	CD2	CD2 Molecule	T cell
CD3E	CD3e	CD3e Molecule	T cell
CD5	CD5	CD5 Molecule	T cell
CD7	CD7	CD7 Molecule	T cell
LYL1	LYL1	LYL1, Basic Helix-Loop-Helix Family Member	T cell
TRBC	TCR beta	T Cell Receptor Beta Locus	T cell
TRGC2	TCR gamma	T Cell Receptor Gamma Locus	T cell
TRGC3	TCR gamma	T Cell Receptor Gamma Locus	T cell
TRGC8	TCR gamma	T Cell Receptor Gamma Locus	T cell
CFD	Adipsin	Complement factor D	Myeloid
LGALS3	Lectin	Galaectin 3	Myeloid
MCL1	MCL1	BCL2 family apoptosis regulator	Myeloid
SQSTM1	P62	Sequestosome 1	Myeloid
ZYX	Zyxin	Zyxin	Myeloid
ANPEP	CD13	Alanyl Aminopeptidase, Membrane	Myeloid
CD14	CD14	CD14 Molecule	Myeloid
CD33	CD33	CD33 Molecule	Myeloid
ITGAM	CD11b	Integrin Subunit Alpha M	Myeloid
ITGAX	CD11c	Integrin Subunit Alpha X	Myeloid
LYZ	Lysozyme	Lysozyme	Myeloid
MPO	MPO	Myeloperoxidase	Myeloid
NPM1	NPM	Nucleophosmin	Myeloid
CD34	CD34	CD34 Molecule	Other
MPL	CD110	MPL Proto-Oncogene, Thrombopoietin Receptor	Other
IL3RA	CD123	Interleukin 3 Receptor Subunit Alpha	Other
ITGB2	CD18	Integrin Subunit Beta 2	Other
PROM1	CD133	Prominin 1	Other
CIITA	MHC2TA/CIITA	Class II, Major Histocompatibility Complex, Transactivator	Other

DLA-DQA1	MHC class II/DLA-DQA1, dog ortholog of HLA-DQA2	Major Histocompatibility Complex, Class II, DQ Alpha 2	Other
DLA-DRA	MHC class II/DLA-DRA, dog ortholog of HLA-DRA	Major Histocompatibility Complex, Class II, DR Alpha	Other
DNTT	Tdt	DNA Nucleotidylexotransferase	Other
GATA3	GATA3	GATA Binding Protein 3	Other
HLA-DRB1	MHC class II/HLA-DRB1	Major Histocompatibility Complex, Class II, DR Beta 1	Other
IRF4	MUM1	Interferon Regulatory Factor 4	Other
KIT	CD117	KIT Proto-Oncogene Receptor Tyrosine Kinase	Other
EEF1G	EEF1G	Eukaryotic Translation Elongation Factor 1 Gamma	Housekeeping
GUSB	GUSB	Glucuronidase Beta	Housekeeping
HPRT1	HPRT1	Hypoxanthine Phosphoribosyltransferase 1	Housekeeping
POLR2A	POLR2A	RNA Polymerase II Subunit A	Housekeeping
RPL19	RPL19	Ribosomal Protein L19	Housekeeping
SDHA	SDHA	Succinate Dehydrogenase Complex Flavoprotein Subunit A	Housekeeping

§ Gene symbols and gene names are provided for the 49 genes used in this study to determine AL lineages.

‡ The probe category and the associated hematopoietic lineage were labeled accordingly as B cell, T cell, Myeloid, Other, and the housekeeping genes.

Table 4: Descriptive statistics for each group.

	%CD5+		%CD14+MHCII-		%CD18+MHCII-CD4-		%CD34+	
Gene Expression Group	1/LYMPH	2/MYELO	1/LYMPH	2/MYELO	1/LYMPH	2/MYELO	1/LYMPH	2/MYELO
n	31	14	31	14	31	14	31	14
Minimum	4.4	4.1	0.0	0.4	0.6	1.9	15.4	8.8
Maximum	57.5	18.8	7.9	52.4	27.1	90.8	96.9	75.1
Median	15.5	7.9	0.2	6.1	5.6	35.9	72.4	58.2
IQR of Median	6.5-25.6	7.1-10.5	0.0-1.4	2.7-20.6	2.4-11.9	16.7-77.5	47.1-90.9	15.8-66.6
Mean	19.0	9.0	1.2	12.1	7.7	43.4	67.6	45.1
Std. Deviation of Mean	14.5	3.5	2.0	14.1	6.4	31.2	22.7	25.8
Lower 95% CI of mean §	13.5	6.9	0.5	4.0	5.4	25.4	57.9	27.6
Upper 95% CI of mean §	24.3	10.8	2.0	20.3	10.1	61.5	77.2	62.6

§ Criteria for subtyping acute leukemia cases were generated by using the half-way point between each group's 95% confidence intervals of the mean for each category.

Statistical analysis:

Results were analyzed using nSolver 4.0 software (NanoString Technologies, Seattle, WA). No quality control flags were identified by the nSolver software for any of the probes in our panel. Gene counts were normalized using the four housekeeping genes that had the lowest variance (*SDHA, RPL19, POLR2A, HPRT1*). Gene counts were transformed into log2 for further analysis. Genes were first clustered using Pearson's correlation. To prevent bias in the expression profiles, multi-loci genes were removed if they clustered together (see below). Unsupervised hierarchical clustering of the normalized transformed log2 gene counts separated AL cases into two groups (Supplemental Figure 7). Differential gene expression was determined between the two AL groups, excluding controls, using a cutoff of false discovery rate (FDR) < 0.05. Due to the fewer number of genes left post differential gene expression analysis, Spearman's correlation was then used to recluster AL samples, excluding controls, to generate a new heatmap (Figure 12). nCounter normalized gene counts were visually inspected between the controls and AL cases and a student's T test was performed between selected genes. For each of these groups defined by gene expression, the flow cytometry immunophenotyping data were summarized and descriptive statistics were generated in Prism (Graphpad, La Jolla, California) to determine new diagnostic criteria. nCounter normalized gene counts and median fluorescence intensity (MFI) of expression of the corresponding cell surface protein by flow cytometry for five different antigens were chosen for a comparative analysis using Spearman's correlation. Spearman's correlation was chosen because the MFI of all AL samples had a nonparametric distribution. Statistically significant (p value < 0.05) correlation coefficients were determined.

Eliminating co-regulated genes:

A subset of genes chosen in the panel included genes that are co-regulated. For example, the initial gene set included multiple class II MHC, immunoglobulin, and T cell receptor genes. Class II MHC genes are under the control of the CIITA protein and their expression is controlled as a group.[203] Similarly, IgG and IgM are under common transcriptional control.[204] To prevent overrepresenting these groups of genes that are co-regulated, we restricted our analysis to prevent overrepresenting each of these families of genes. To do this, we assessed how the genes we chose clustered together to identify potential bias. We first used Pearson's correlation to cluster the genes. Multi-locus probes for genes encoding MHCII (*DLA-DQA1, DLA-DRA,* and *HLA-DRB1*) and immunoglobulin heavy chains (*IGHG* and *IGHM*) clustered with their respective groups and were considered highly correlated (Pearson's r = 0.55-0.94). The genes that had the highest coefficients of variations (CV) (*DLA-DRA* CV = 240%; *IGHM* CV = 157%) were left to represent those families of genes for further analysis. Interestingly, the TRGC genes (*TRG2*, *TRG3*, and *TRG8*) did not cluster together, which could potentially be explained by the difference in expression of TRG-related genes seen between human ALL and AML.[205] Therefore, all TCR loci (*TRG2*, *TRG3*, and *TRG8*) were included for downstream analysis.

Results

Patient population and clinical presentation:

Digital RNA quantification was performed on peripheral blood from 45 cases and two healthy controls. Patient information, white blood cell concentrations, and flow cytometry data are available in Supplemental Table 11. Ages of the 45 newly diagnosed AL patients ranged from 1.1 to 15.85 (median 8.7) years. There were 22 spayed females, 19 castrated males, and two intact males. Cases included mixed breed dogs (n=10), Labrador Retrievers (n=10), Golden Retrievers (n=6), German Shepherds (n=3), Australian Shepherds (n=2), Labradoodles (n=2), Pit

bull terriers (n=2), and one each of Belgian Shepherd, Bullmastiff, Portuguese Water dog, Keeshond, Boxer, Irish Setter, Greyhound, Maltese, and Beagle. Control samples were from one intact male English Bulldog and one castrated male Golden Retriever. Date of birth and sex status were not available for two samples and breed information was not available for one of the samples. 42/45 (93%) AL cases presented with a leukocytosis (median: 77,300 leukocytes/µl; IQR: 35,540 – 171,650 cells/µl, range: 11,300-417,220 cells/uL), 29/45 (64%) were neutropenic, and 3/45 (6.6%) had a neutrophilia. AL cases had a median platelet count of 60,000/µl (range: 10,000 – 216,000/µl) and 40/45 (88.8%) were thrombocytopenic. Additionally, they had a median hematocrit of 28% (range, 12-46%) and 41/45 (91%) were considered anemic.

Validating and reviewing the nCounter probe gene set:

We first determined that the samples were consistent with immature hematopoietic neoplasms. The normalized mRNA counts for genes expressed in precursor cells (*CD34, KIT,* and *DNTT*(TdT)) were compared between all the leukemic samples and the normal controls. Genes specific for early hematopoietic precursors were significantly increased compared to controls: *CD34* was upregulated 73-fold (p value <0.01), *KIT* was upregulated 187-fold (p value < 0.01), and *DNTT* was upregulated 168-fold (p value = 0.02). We evaluated the correlation between gene expression and flow cytometry by comparing the gene count and antigen expression MFI for CD34, CD5, CD18, CD14 and MHCII (Supplemental Figure 6). Gene counts and protein expression of CD34, CD5, CD18 and MHC class II correlated (r = 0.38-0.68, p value <0.05), but CD14 gene counts and protein were not correlated (r = 0.04, p value = 0.75). A possible explanation for this is that the NanoString CD14 probe was designed against the CanFam3.1 assembly, but more recent canine genome builds have a discordant CD14 sequence. Therefore, it is possible this probe did not bind well to CD14 transcripts.

Differential gene expression between AL groups:

The average normalized gene counts for the control samples and each of the two groups are provided in Supplemental Table 12. Nine of the 43 genes were significantly differentially expressed (FDR<0.05) between the two groups. Six of these differentially expressed genes were myeloid-associated (*SQSTM1, LGALS3, ITAGX, LYZ, ANPEP, CFD)* and three were lymphoid-associated (*IGHM, DNTT, CD79A)*. Cases were clustered using these nine genes and a heat map was generated (Figure 12). Cases overexpressing the lymphoid-associated genes were assigned to a LYMPH group (n=31 cases) and cases overexpressing myeloid-associated genes were assigned to a MYELO group (n=14 cases).

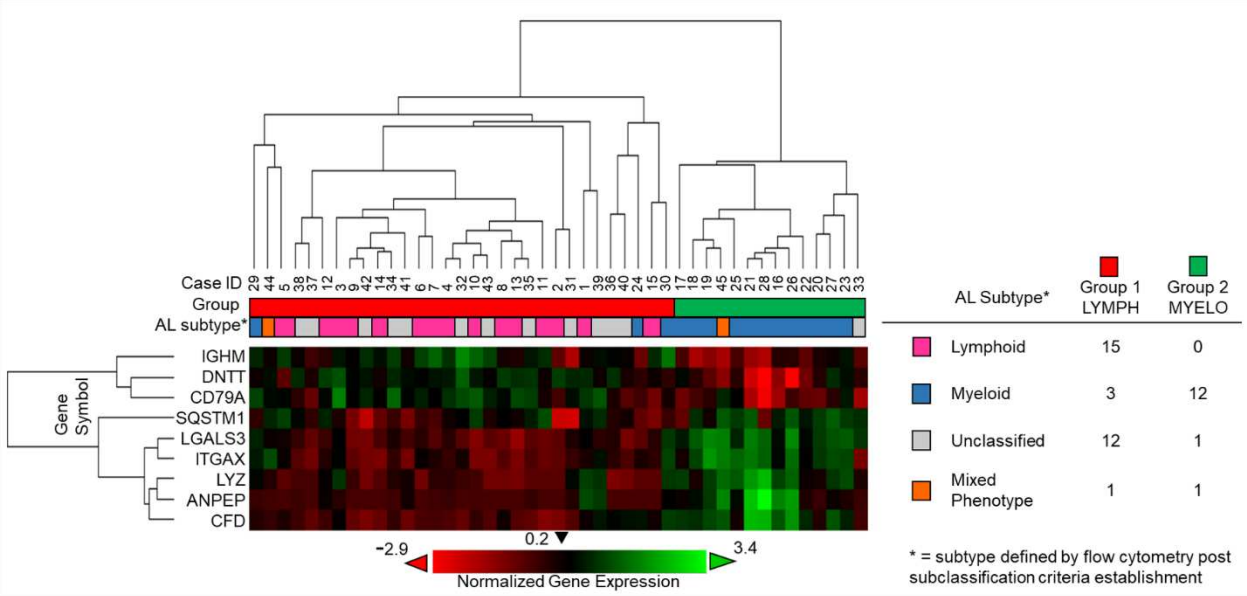

Figure 12: Hierarchical clustering of genes and cases. Samples were reclustered using the nine differentially expressed genes (FDR<0.05) identified by unsupervised hierarchical clustering. By gene expression, cases were clustered into two groups: Group 1/LYMPH (red bar) overexpressed lymphoid genes and Group 2/MYELO (green bar) overexpressed myeloid genes. By flow cytometry, each case was retroactively classified as lymphoid, myeloid, unclassified or mixed phenotype using the developed immunophenotyping guidelines. The majority of CD5+ cases (lymphoid, pink) and CD14+/CD18+ MHCII- cases (myeloid, blue) separated into gene expression groups 1/LYMPH and 2/MYELO, respectively. Additionally, the majority of cases that did not express lineage specific antigens (unclassified, grey) also clustered with group 1/LYMPH. (Flow cytometry classified groups: lymphoid = pink, myeloid = blue, unclassified = grey, mixed phenotype = orange).

Two genes were included in the expression panel that are considered defining for the T cell and B cell lineage: *CD3* and *PAX5*. *CD3* was considered highly expressed in the LYMPH group compared to the MYELO group (Supplemental Table 13), being 3.4 log2 fold change times higher in the LYMPH group. It was also 1.7 log2 fold change higher than in the control peripheral blood. The comparison in *CD3* expression between the two AL groups was significant

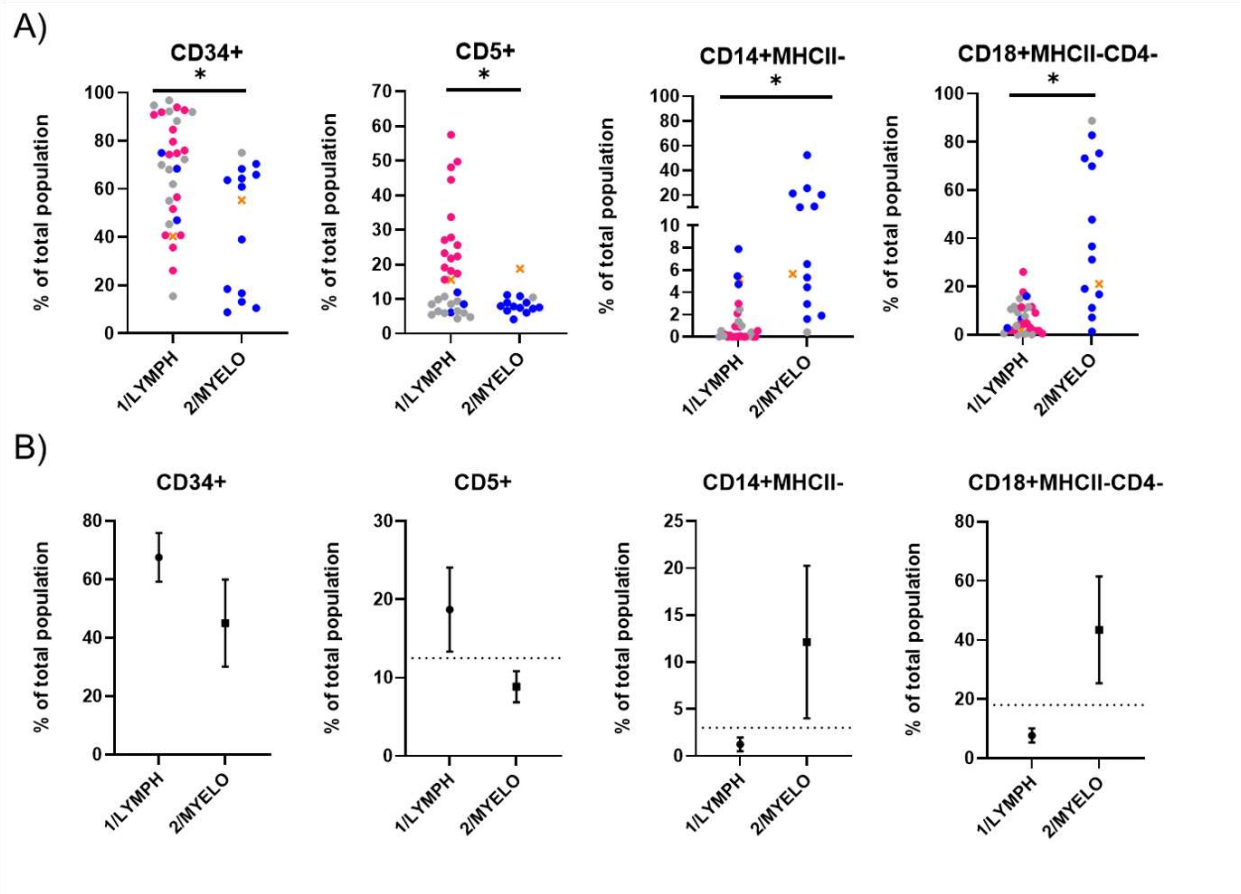

Figure 13: Comparison of flow cytometric data between groups. A) The percentage of positive cells for each surface marker assessed was statistically different (* = p value < 0.05) between gene expression groups 1/LYMPH and 2/MYELO. Each dot is an individual case, colored by the flow cytometry subtype determined retroactively using the developed immunophenotyping classification scheme (myeloid = blue dots, lymphoid = pink dots, unclassified = grey dots, mixed phenotype = orange X). B) The 95% confidence interval (CI) of the mean for the percentages of CD5+ cells, CD14+MHCII- cells, and CD18+MHCII-CD4- cells are shown. The dashed line represents the proposed cutoff for subtyping acute leukemias into lymphoid, myeloid, or unclassified. Note that even though the percentage of CD34+ cells was statistically different, the %CD34+ cells was highly variable, and the 95% CI overlapped substantially between the groups, so a cutoff was not established.

(p = .005) but because of the variability in expression, the FDR was greater than 0.05, and this gene was not included in the lineage-defining gene list. *PAX5* is the defining B cell lineage gene and was expressed at higher levels in the two control peripheral blood samples than either the LYMPH or MYELO group.

Flow cytometric features of each group:

Flow cytometric data from each of the groups were compared using a Mann-Whitney U test for each of the following: %CD34+, %CD5+, %CD14+MHCII-, and %CD18+MHCII-CD4- (Figure 13A). Expression of all surface proteins, as determined by MFI, were statistically different between the groups. Descriptive statistics for each group were used to establish flow cytometric diagnostic guidelines for myeloid, lymphoid, unclassified, and mixed phenotype AL (Table 4). The LYMPH group had higher percentages of CD34+ cells ($p < 0.01$) and CD5+ (surface CD3-/CD4-/CD8-) cells ($p < 0.03$). The MYELO group had higher percentages of CD14+CD4- cells ($p < 0.01$). The percentage of CD18+MHCII-CD4- cells was also statistically higher (p value < 0.01) in the MYELO group. Even though the percentage of CD34+ cells was significantly different between the two groups, CD34 expression was not used in establishing the guidelines as the 95% confidence interval (CI) of the mean overlapped between the two groups.

Establishing immunophenotypic criteria for lineage assignment:

We established flow cytometry criteria to differentiate lymphoid from myeloid leukemias based on the total percentage of CD5+ cells, CD14+MHCII- cells, and CD18+MHCII-CD4- cells in the two groups defined by gene expression (Figure 13B). We calculated the upper and lower limits of the 95% CI of the mean for each group and defined the diagnostic cutoff as the halfway point between the upper 95% CI of one group and the lower 95% of the other group (rounding to the nearest 0.5% for a practical diagnostic cutoff percentage). For example, the

lower 95% CI of %CD5+ cells for the LYMPH group was 13.6% and the upper 95% CI for %CD5+ cells in the MYELO group was 11.0% (Figure 13B & Table 4). The point halfway between them was chosen as the diagnostic cutoff: 12.5% (rounded to the nearest 0.5). The %CD5+ and %CD14+MHCII- were considered primary diagnostic criteria. If cases did not meet the primary criteria, then the total %CD18+MHCII-CD4- cells was considered a secondary criterion. For instance, if a sample had <3.0% CD14+MHCII- cells and <12.5 CD5+ cells, we would then consider CD18 expression as the final diagnostic criteria cutoff. In these cases, samples with >18% CD18+MHCII-CD4- cells were identified as AML and those with <18% CD18+MHCII-CD4- cells were considered AUL. A proposed algorithm for subtyping canine AL into ALL, AML, AUL and MPAL is provided in Figure 14.

After developing the flow cytometry diagnostic criteria, the 45 AL cases were classified as ALL, AML, AUL or MPAL based on flow cytometry immunophenotyping (Figure 12 & Figure 13A). By flow cytometry, there were 15 ALL cases, 15 AML cases, 13 AUL cases and 2 MPAL cases. All ALL cases segregated into the LYMPH group by gene expression and 12/15 AML cases segregated into the MYELO group by gene expression. Most of the cases classified as AUL (12/13) by flow cytometry segregated into the LYMPH gene expression group. In total, the LYMPH gene expression group contained all 15 ALL cases, 12 AUL cases, 3 AML, and 1 MPAL case (Figure 14C). The MYELO gene expression group contained 12 AML cases, 1 AUL cases and 1 MPAL case.

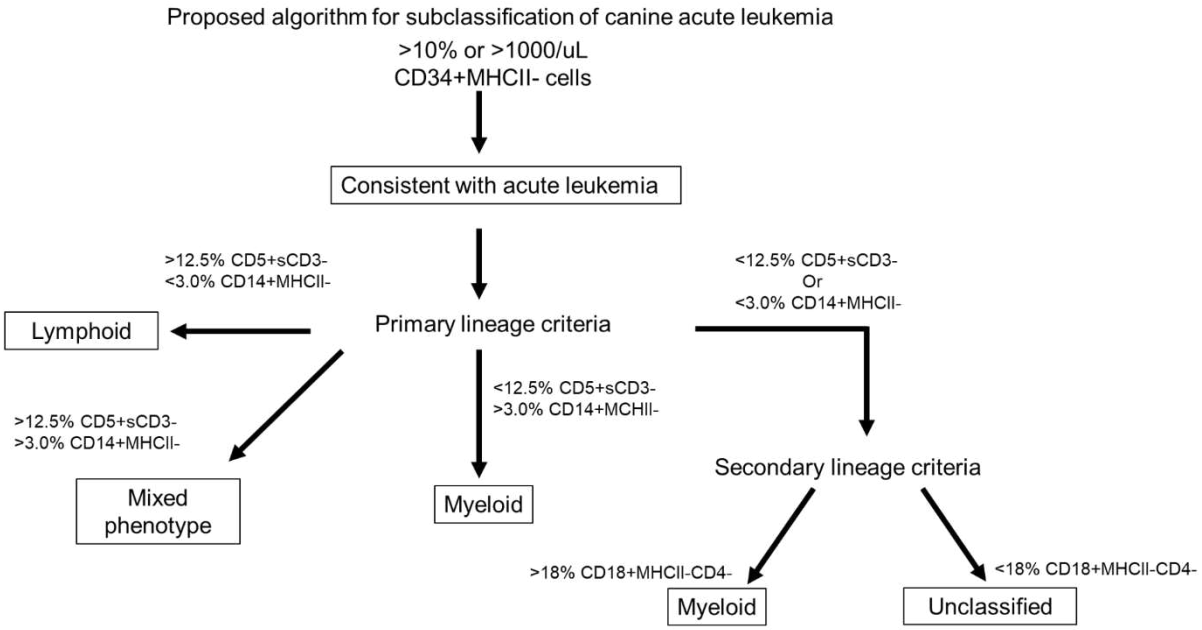

Figure 14: Algorithm for subclassification of canine acute leukemia by flow cytometry. A lineage classification scheme was developed using the cutoffs established in Figure 3B. Lineage is first determined based on the percentages of CD5+CD3- cells and CD14+MHCII- cells. Cases not defined by these primary lineage criteria are further evaluated for a CD18+MHCII-CD4- population to differentiate myeloid and unclassified acute leukemia cases.

Evaluating gene expression between flow cytometry-defined AL subtypes:

Normalized mRNA counts are provided for the controls and each AL subtype as defined by flow cytometry (Supplemental Table 12). In our probe list, 11 genes were differentially expressed (FDR < 0.05) between flow cytometry defined lymphoid and myeloid cases (Supplemental Figure 8). Lymphoid associated genes were upregulated in the CD5+ cases compared to CD14+MHCII-/CD18+MHCII-CD4- cases. Myeloid genes, including *ITGAX* and *LGALS3,* were overexpressed in CD14+MHCII-/CD18+MHCII-CD4- cases compared to both CD5+ and unclassified cases. CD5 was the only gene differentially expressed between CD5+ cases and unclassified cases.

Discussion

In this study, we used gene expression profiling to assign myeloid or lymphoid lineage to canine AL. We then determined the immunophenotypic features of these groups using

commercially available, directly conjugated antibodies and developed an algorithm for lineage assignment of CD34+ AL by flow cytometry. Lymphoid lineage AL were identified by expression of CD5 and myeloid lineage AL were identified by expression of CD14+MHCII- and CD18+MHCII-CD4- cells. The lineage of some cases could not be determined because they did not express any of these antigens or expressed both lymphoid and myeloid lineage antigens. Most unclassified cases clustered by gene expression with CD5+ AL cases and it is likely that some of these are of lymphoid origin.

After determining the differentially expressed genes between the two groups originally identified by unsupervised clustering, a heat map was generated to further classify the groups based on the differentially expressed genes of all the samples. The new groups identified (LYMPH vs. MYELO) were used to establish flow cytometric criteria. Nine genes defined the two clusters, the majority of which are associated with myeloid lineage (*SQSTM1, LGALS3, ITAGX, LYZ, ANPEP, CFD). DNTT*, *CD79A*, and *IGHM* are genes associated with lymphoid lineages. Once CD5+ and CD14+MHCII-/CD18+MHCII-CD4- AL were separated using the flow cytometric diagnostic criteria, the CD5+ neoplasms overexpressed lymphoid associated genes (*DNTT*, *CD2*, *CD5*, *CD79A*, and *IGHM*) compared to myeloid defined cases (Supplemental Figure 6). The overexpression of B cell associated genes, including *CD79A* and *IGHM,* is surprising on initial examination.

The lineage (B vs. T cell) of the ALL was not determined in this study. While two of the three lymphoid-defining genes are *CD79A* and *IGHM*, which are expressed by mature B cells but not mature T cells, neither of these genes exhibits lineage fidelity in immature hematopoietic cells or AL. In particular, CD79a is considered nonspecific for distinguishing B-ALL from T-ALL in humans.[189,193,206] CD79a is expressed in normal canine monocytes and T cells.[194] It is

important to note that, at least in human hematopoietic progenitors, committed T cell lineage progenitors express antigens in the following order of development: CD7, CD2, CD5, and lastly surface CD3.[6] The authors hypothesize that the CD5+ ALL are a derivative of a T cell precursor neoplasm and along this biological spectrum. For instance, several T cell specific genes, including *CD2*, *CD3*, *CD7* and *GATA3* were upregulated in the LYMPH group of leukemias compared to the MYELO group, reaching statistical significance in individual comparisons, but not at the level of multiple comparisons (Supplemental Table 12). By contrast, none of the B cell lineage-specific genes (*PAX5*, *CD19*, *CD20*, *CD21* or *CD22*) were significantly different between the groups. The conflicting gene expression data does not allow us to draw firm conclusions about the B- or T- cell origin of ALL in dogs. Although we favor the idea that most canine ALLs are T cell, this hypothesis will require further studies using additional samples, comparisons with normal canine B and T cells, as well as detection of proteins by ICC and IHC.

There are a few limitations to this study. One is that our study population only included CD34+ AL cases. There are a few reasons for this: 1) In the authors' experience CD34- precursor neoplasms are rare. There are cases that present like precursor neoplasms based on clinical presentation and aggressive clinical course that do not express CD34, but they express other lineage antigens and therefore lineage assessment is not challenging. The goal of this study was to focus on CD34+ ALs which are more ambiguous and challenging to assign lineage. 2) CD34 is highly suggestive for a precursor hematopoietic neoplasm (if CD45 is also expressed)[4] and the use of CD34 to define these cases provides an objective criterion for diagnosis. The criteria used to diagnosis CD34+ AL in this study (>1,000 cells/uL or >10% CD34+ cells) may have omitted AL cases with minor populations of CD34+ cells. Clinical presentation and CBC findings should be interpreted along with flow cytometry findings to diagnose AL. 3) CD34 expression is

clinically relevant and known to be associated with shorter survival in dogs.[10] Therefore, we decided to validate our panel with CD34+ AL cases.

Another limitation is the limited probe gene list used in our study. Our probe list was based on a literature review of both veterinary and human medicine. We used probes that would identify a wide variety of hematopoietic lineages, primarily focusing on B, T, and myeloid lineages. We recognize the potential bias for hand-selecting probes. We attempted to remove any potential bias by identifying multi-locus genes that were expressed and clustered together. In this study set it was MHCII (*DLA-DQA1, DLA-DRA,* and *HLA-DRB1*) and immunoglobulin heavy chains (IgG and IgM). Only one of the genes from each of these gene families were chosen for the final clustering algorithm given that their transcription is similarly regulated. The selection of which TRGC loci was not unbiased either. Canines have eight TRGC loci that can be rearranged and incorporated into the T cell receptor.[207] We designed probes specifically for *TRGC2, TRGC3*, and *TRGC8* because previous groups have shown that these loci are preferentially rearranged.[208] It is conceivable that the other TRGC loci not included in our study could have been useful for differentiating these neoplasms.

Finally, we developed this classification scheme with antibodies directed at surface antigens that are used routinely for immunophenotyping in most laboratories.[209] It is likely that additional markers/combinations can elucidate AL subtypes similarly. There is some indirect evidence for this provided in our gene expression data. For instance, CD11c, CD11b, and Galectin 3 are overexpressed in AML compared to ALL and cross-reactive antibodies are commercially available. Interestingly, myeloperoxidase was not considered differentially expressed between subtypes (FDR = 0.42, p value = 0.03), even though other groups have shown

it to be useful for distinguishing myeloid neoplasms.[98] Additional studies interrogating the specificity of these antigens for delineating AL subtypes are warranted.

Here, we show that AL subtypes (i.e. lymphoid vs. myeloid) can be differentiated using commercially available, directly conjugated antibodies. Additional work using a separate cohort is needed to validate our flow cytometry diagnostic criteria. We were able to show acceptable correlation between mRNA and expression of surface protein measured by flow cytometry using NanoString technology and we identified potential markers that can be attempted to further classify AL subtypes.

CHAPTER 3: Transcriptomic profiling of canine acute myeloid leukemia and the comparative features with human acute myeloid leukemia

Summary

Acute myeloid leukemia is an aggressive heterogeneous hematopoietic neoplasm that afflicts both dogs and people. The purpose of this study was to characterize the expression profiles of cAML, identify deviations from normal in canonical pathways, and highlight overlapping comparative features with human AML, including both pediatric and adult AML. Transcriptome sequencing was performed in 10 healthy blood, 5 healthy bone marrow, and 110 CD34+ canine acute leukemia samples classified via immunophenotyping. Unsupervised hierarchical clustering revealed 2 major transcriptomic groups, which were consistent with a myeloid and lymphoid gene signature. In general, cAML samples overexpressed genes associated with leukemogenesis and leukemic stem cells. GSVA of the myeloid subgroups revealed that they were enriched for MYC and TGF-β signaling pathways. Deconvolution using a single cell hematopoietic atlas to predict cell type abundances revealed that primitive myeloid cell types were overrepresented in cAML cases and the distribution of these cell types was variable between predicted cAML subgroups. Additionally, we show that cAML samples have more overlapping features with pediatric AML than adult AML at the transcriptomic level. Overall, this study adds further evidence to the canine AML model and highlights comparative features shared between both species.

Introduction

Acute myeloid leukemia (AML) is a heterogeneous neoplasm in people and dogs that arises from hematopoietic progenitors and myeloid precursors located within the bone marrow. The disease course, clinical presentation, and macroscopic biologic features (e.g. cellular

morphology and antigen expression) are similar between the two species.[102] Human AML (hAML) has been extensively characterized over the last few decades, revealing distinguishing genotypic and phenotypic features that are prognostically significant and clinically relevant.[7] However, treatment and clinical management of these patients remains challenging given the complexity and variation of the tumor's biology between molecular subtypes.[2,6] hAML even has unique features between age groups (i.e. pediatric vs. adult AML).[9,59] Large multi-institutional studies address such challenges, with the goal to provide precision medicine for patients with AML.[2,6,25] If canine AML (cAML) and hAML have overlapping molecular features, investigations into the efficacy of targeted therapeutics could benefit both species.

Dogs spontaneously develop acute leukemia (AL) and the outcome in dogs with any subtype, AML or acute lymphoid leukemia (ALL) is poor, with a median survival time reported between 9-19 days.[3,4,210] While commercially available antibodies can distinguish acute lymphoid from myeloid leukemias in some cases, many cases do not express lineage antigens and remain unclassifiable by flow cytometry.[96]

Dogs with AML present with similar hematologic abnormalities as people, including anemia, thrombocytopenia, neutropenia, and an expansion of CD34+ hematopoietic progenitors within the blood and/or bone marrow.[3,4,210] The mutational repertoire of cAML has only been investigated in one previous study that targeted genes commonly mutated in hAML (i.e. *FLT3, NRAS, KRAS, HRAS, KIT*), and this study found overlapping mutations between the two species.[114] Treatment options for cAML in veterinary medicine are limited, with most dogs receiving supportive care and/or cytotoxic chemotherapy regimens, which only increases median survival time by a week to months.[4,210] Given the quick clinical progression and similar clinical presentation, we hypothesize that cAML will have overlapping molecular features with hAML

subtypes. Characterizing the transcriptome cAML could further credential the dog as a model for human hematopoietic malignancies and aid in the development of targeted therapeutics for both veterinary and human medical fields.

In this study we started our approach by defining the gene expression profile of cAML compared to that of other subtypes (e.g. ALL). Next, we utilized unsupervised clustering to predict cAML subgroups and performed deconvolution to impute cell fractions using a single cell transcriptomic atlas of normal canine bone marrow. Finally, we determined if cAML subgroups share features with hAML subtypes, including both pediatric and adult hAML subtypes. Multiple groups have utilized similar approaches previously for evaluation of other spontaneous dog tumors. Promising data from these studies highlight similarities between the gene expression profiles of canine and the human "equivalent" diseases, If the transcriptomic programs of cAML share overlapping features with hAML, then translational studies could be initiated to investigate targeted therapies.

Methods

Sample collection and case selection:

Samples were submitted to Colorado State University's Clinical Hematopathology laboratory for routine immunophenotyping between August 2015 to August 2020. Samples were not solicited for this study and considered exempt from approval by the Animal Care and Use Committee. Control samples consisted of 10 fresh discarded EDTA peripheral blood samples that were previously submitted to the Colorado State University's Veterinary Diagnostic Laboratory and five flash frozen bone marrow samples from healthy dogs collected at the Fred Hutchinson Cancer Research Center. Neoplastic samples included EDTA peripheral blood samples from dogs (n = 111) diagnosed with AL by flow cytometry. Bone marrow aspirations

are not routinely performed in veterinary medicine and were not available for evaluation in this study. Inclusion criteria included samples with >10% of the total leukocytes expressed CD34 or there was >1000 CD34+ cells/uL which lacked expression of class II major histocompatibility complex (MHCII).[96] There were eight samples that had < 10% CD34+ and/or < 1000 CD34+ cells/uL at the time of diagnosis but were included after review of the clinical history because AL was considered the top clinical differential and neoplastic cells were described as having a blast morphology.

Hematology and Immunophenotyping:

CBC results were submitted concurrently with the patient's sample. CBCs were either performed in the submitting clinic with a bench top analyzer, by a veterinary diagnostic reference laboratory, or performed at the Clinical Pathology laboratory at Colorado State University's Veterinary Teaching Hospital. Given that defined reference intervals are different between instruments used for complete blood counts in this study, we considered patients to have a hematology abnormality using the following values: Patients were considered to have a leukocytosis if >18,000 WBC/uL, anemic if <35% hematocrit, and thrombocytopenic if < 200,000 platelets/uL without evidence of platelet clumps. Platelet counts were excluded from analysis in 80 patients due to platelet clumps being identified.

Flow cytometry was performed as previously described and analyzed using Kaluza software (Beckman Coulter, www.beckmancoulter.com).[96] Samples were acquired over a period when the staining panel changed in our clinical laboratory. The two panels are provided in Chapter 2's Supplemental Table 8. The panel does not detect intracellular antigens. All neoplasms expressed the pan-leukocyte marker, CD45. The CD18 antibody used in this study is a cross-reactive anti-human CD18 and a prior study demonstrated that this antibody binds

primarily to canine neutrophils and monocytes, and only at low levels to lymphocytes.[201] AL cases were comprised of a myriad of immunophenotypes that we routinely diagnose in CSU clinical hematopathology laboratory, which included CD5+ (n = 31), CD14+/CD18+ (n = 54), and unclassifiable (n = 25). CD5+, CD14+/CD18+MHCII- phenotypes were tentatively classified as lymphoid, myeloid, and unclassifiable, respectively. One of the cases expressed both CD5 and CD14 but was considered tentatively diagnosed as AML for downstream analysis. One of these included a plasma cell tumor. The original sample was considered CD34+MHCII^{low}, but was found to express *IRF4, JCHAIN,* and other B cell lineage markers by RNA sequencing. This sample was not included in subsequent analysis. Total RNA was extracted from peripheral blood, post RBC lysis, if the majority of the nucleated cells were considered viable upon review (i.e., <33% Propidium Iodide +). Neoplastic cells were not sorted from the other peripheral blood leukocytes in this study, and PBMCs were not enriched with density gradient centrifugation

Bulk RNA quantification and qualification:

Total RNA was extracted from leukocytes using the PureLink RNA mini kit (ThermoFisher, Waltham, MA). DNA digestion was performed on the column using PureLinke DNAse (ThermoFisher). Initial RNA integrity was assessed using an Agilent 2200 Tapestation (Agilent Technologies, CA, USA) and quantified using a Nanodrop One Spectrophotometer (ThermoFisher). Samples were selected if the total RNA concentration was above 20ng/uL and if the RNA integrity score was above 7. Once selected, samples were shipped to Novogene Co., LTD (Beijing, China) for sample processing, library preparation, and transcriptome sequencing. Post-shipment, samples were reassessed for quantification, integrity, and purity. Per Novogene, RNA degradation and contamination were monitored on 1% agarose gels. RNA purity was

checked using the NanoPhotometer spectrophotometer (IMPLEN, Westlake Village, CA). RNA integrity and quantitation were assessed using the RNA Nano 6000 Assay Kit of the Bioanalyzer 2100 system (Agilent Technologies, Santa Clara, CA). Eleven samples were considered impure (i.e. contained genomic DNA) and underwent purification using DNase I and column selection.

Library Preparation and bulk RNA sequencing:

A total amount of 1ug RNA per sample was used as input material for the RNA sample preparations. Sequencing libraries were generated using NEBNext Ultra RNA Library Prep Kit for Illumina (NEB, USA) following manufacturer's recommendations and index codes were added to attribute sequences to each sample. The stranded barcoded libraries underwent paired end 150bp sequencing on an Illumina Novoseq 6000 instrument. We targeted a minimal depth of ~77 million 150bp paired end reads per sample, approximately 23Gb per sample.

Clinical Data Statistical Analysis:

All statistical analysis was performed using either R programming language or in GraphPad prism (source). The Shapiro-Wilk test was used to determine normality for all clinical continuous variables presented. Gaussian distributed continuous variables were assessed via unpaired t-tests and variables that failed normality (p value < 0.05) were assessed via Wilcoxon ranked sum test. The top 3 outliers were identified, visually inspected, and then removed from downstream statistical comparisons using the boxplot function in R only for the CBC data. Statistically significant observations were defined as p values and adjusted p values < 0.05. P-values were corrected for multiple testing using the Benjamini-Hochberg approach, unless otherwise specified.

Bulk RNA Sequencing Data Quality Control and Processing:

Raw read files (FASTQ format) were first processed using FASTQC.[211] FASTQC reports were inspected for each sample prior to further processing. Sequence reads were then trimmed of low-quality reads (Phred score <30) and adapter sequences using TrimGalore.[212] Reads were then aligned to the CanFam3.1 reference genome using STAR.[213] Genome reference files (i.e. genome CanFam3.1 fasta and gtf files) were downloaded from Ensembl (release version 104).[214] Sorted BAM files were then processed through featureCounts to generate raw read counts using CanFam3.1 GTF annotations.[215] BAM files were indexed with SAMtools and subsequently visually inspected in the Broad Institute's Integrative Genome Viewer to insure alignment to exonic regions.[216,217] Once completed, all output files were then assessed using MultiQC to ensure high quality samples were input into downstream data analysis.[218] The count matrix output from featureCounts was imported into R for downstream analysis.

Differential gene expression (DGE) analysis:

Prior to DGE analysis, exploratory analysis of the count matrix was performed using NOISeq to assess the count distribution, investigate the biotype features, and filter low count reads (CPM <1) (Supplemental Figure 9).[219] Unsupervised hierarchical clustering of the top 1500 genes with the greatest dispersion around the median was used to define the major AL groups (e.g. myeloid vs. lymphoid). Genes and samples were clustered by Euclidean distance with ward.D2 metrics. DGE analysis between the two major groups of AL was performed using DESeq2 v1.28.1.[158] Differentially expressed genes (DEG) were defined as having an adjusted p value <0.05 and a $\log_2$foldchange >1 or <-1. Subgroups of cAML were identified by unsupervised clustering using uniform manifold approximation and projection (UMAP). Gene counts underwent variance stabilizing transformation prior to UMAP embedding using the Seurat package.[151] UMAP cluster assignment of the UMAP reduced dimension data was

performed with the Louvain algorithm with multilevel refinement.[151,154] Default UMAP parameters were used, in addition to min_dist=0.25, with n.neighbors = 8 and the number of dimensions incorporated using dims = 1:6, while the Louvain algorithm with multilevel refinement was completed with default parameters and resolution = 1.0. The number of dimensions were chosen based on the JackStraw scores to predict significant principal components using a p-value cutoff < 0.05. We assessed the total within-cluster sum of squares to determine the number of nearest neighbors predicted by k means clustering. Default settings to calculate the optimal number of clusters via the within-cluster sum of squares were used by factorextra R package.[220] Results were visualized and the total number of clusters were determined using the "elbow method". Once cAML subgroups were identified, we performed receiver operating characteristic analysis using the Seurat R package and pairwise DEG analysis with DESeq2 to identify genes that defined each subgroup.[151,158]

Gene set enrichment/variation analysis:

Publicly available gene sets including the Molecular Signature Databases' (MSigDB) curated gene sets, Kyoto Encyclopedia of Genes and Genomes (KEGG), Gene Ontology, and REACTOME were referenced for gene set enrichment analysis (GSEA) or gene set variation analysis (GSVA).[157,221–226] All publicly curated gene sets were imported using the msigdb R package.[227] Significant genes were ranked in descending order prior to performing GSEA using the R package clusterProfiler 4.0 with default settings for the fgsea algorithm, except eps was set to 0.[228] Prior to GSVA, gene counts of our samples underwent variance stabilizing transformation. Gene set variation of MSigDB's Hallmark pathways were assessed using default settings of the gsva algorithm in the GSVA R package.[157,222] GSVA enrichment scores were

compared between each UMAP subgroup and normal bone marrow controls with the limma R package to identify differentially expressed gene sets.[229]

Deconvolution and cell type enrichment of bulk RNA sequencing data:

We utilized a single cell transcriptomic atlas to impute cell fractions and investigate cell signatures enriched in our bulk RNA sequencing data sets. To do this, we used the CIBERSORTx algorithm and Gene Set Variation analysis (GSVA) to investigate the cell composition and the cell type signatures, respectively. To impute cell fractions and calculate the relative fractions of each cell type, we first generated a signature matrix using the cell types found in the CD34+ sorted cells and bulk bone marrow data sets from Chapter 1 (see above). We excluded cycling cell populations, poor quality cells, the ambiguous HSPC group, and the B cell subtypes enriched for in the CD34+ sorting process, other than the CLP cell type. We randomly down sampled our matrix to include 8000 cells and their respective gene expression. We utilized the CIBERSORTx algorithm to impute the relative fractions of our controls and samples with a myeloid gene signature using permutations = 500 and with S-mode batch correction. Quantile normalization was disabled. Variance stabilizing transformed gene expression data from our samples were imported into the CIBERSORTx Web site. The output was then compared between the control samples and the myeloid cases and between each myeloid UMAP subgroup. Additionally, we extracted the top 100 genes (ranked by log2 fold change) that defined each of the single cell clusters to generate our gene matrix transposed file for reference. Similar as above, we utilized the GSVA R package to calculate gene set enrichment scores across the control and myeloid samples. Differential gene set expression analysis was performed using limma R package.

External datasets:

Raw read counts from the TARGET (pAML) and BEAT AML (aAML) cohorts were used to generate representative pediatric and adult AML gene sets, respectively.[2,6,9,59] To do this, we performed pairwise DGE analysis between each pAML and aAML subtype and their respective bone marrow control samples from each study. These gene sets from the DGE analysis were restricted to the top 250 genes up- and down- regulated for each pAML and aAML subtype that also concurrently had a matching dog gene symbol. Matching human to dog gene symbols were identified according to Ensembl's BioMart v104 database.[230] Gene symbols were not restricted based on the high or low confidence prediction of ortholog similarity. Subtype annotation was based on the pAML "AML subtype" and the aAML "specific diagnosis at sample acquisition" categories provided in the patient manifest files, respectively. For instance, in the BEAT AML dataset we used the collective normal bone marrow mononuclear cells (NBM-MNC) group and in the TARGET AML dataset we used the normal bone marrow (NBM) group for comparisons. 7 subtypes in the BEAT AML data were excluded because they contained less than 5 biological replicates for each, which included: "Acute erythroid leukaemia", "Acute megakaryoblastic leukaemia", "Acute undifferentiated leukaemia", "AML with DEK-NUP214", "Mixed phenotype Acute leukaemia B myeloid NOS", "Mixed phenotype Acute leukaemia T myeloid NOS", and "Myeloid leukaemia associated with Down syndrome". In total, we generated 56 gene sets, 22 of which were from the TARGET data set and 34 were from the BEAT AML data set. GSEA was performed as described previously using pre-ranked gene lists from the DGE analysis between our cAML subgroups and normal bone marrow controls. To identify gene sets with the highest similarity shared with each cAML subgroup, we combined the absolute value of the normalized enrichment scores (NES) from the paired up- and down-

regulated gene sets. Leading edge analysis from clusterProfiler's GSEA output was performed to identify shared genes of the top 3 gene sets with the highest combined NES.[228]

Results

Overview of study population:

Table 5: Clinical data of all canine acute leukemia cases and myeloid and lymphoid gene signature subgroups.

	Dogs with available data (n)	Number affected (%) or median (IQR)			Myeloid vs. Lymphoid p value[β]
Gene signature		Acute leukemia	Myeloid	Lymphoid	
n	110	110	56	54	
Signalment					
Sex	110				NS
Intact male		7 (6.4%)	4 (7.1%)	3 (5.6%)	
Neutered male		52 (47.3%)	25 (44.6%)	27 (50%)	
Intact female		3 (2.7%)	0 (0%)	3 (5.6%)	
Spayed female		48 (43.6%)	27 (48.2%)	21 (38.9%)	
Age at diagnosis (years)	110	8.1 (6.4-10.0)	8.3 (6.5-10.0)	8.0 (6.1-10.0)	NS
Breed (top 4 most common)	109*				NS
Mixed breed		33 (30%)	16 (28.6%)	17 (32.1%)	
Labrador retriever		16 (14.7%)	8 (14.3%)	8 (15.1%)	
German shepherd		13 (11.9%)	6 (10.7%)	7 (13.2%)	
Golden retriever		10 (9.2%)	7 (12.5%)	3 (5.7%)	
Hematologic data					
WBC (cells/uL)	110	54,750 (28,507-117,882)	31,715 (16,800-56,410)	95,650 (54,525-182,007)	<0.0001
HCT (%)	110	28 (23-36)	31 (24-36)	26 (22-33)	NS
PLT (cells/uL) without clumping	30	62,000 (44,500-101,500)	65,000 (57,000-103,000)	56,500 (40,000-99,750)	NS
Immunophenotyping data					
CD34+ cells (%)	110	56.1 (25.7-73.3)	28.7 (16.1-58.6)	68.1 (53.9-89.1)	<0.0001
CD5+CD3- cells (%)	110	8.0 (4.7-14.1)	7.1 (4.8-10.9)	10.0 (4.7-18.3)	NS

CD14+MHCII- cells (%)	110	1.0 (0.1-5.1)	3.9 (1.4-11.2)	0.3 (0.0-0.8)	<0.0001
CD18+MHCII-CD4-CD14- cells (%)	110	14.9 (4.6-35.5)	29.2 (14.7-50.3)	4.9 (1.7-14.8)	<0.0001
PN-Neutrophils (%)	110	3.6 (1.0-11.8)	9.9 (3.7-22.2)	1.3 (0.5-2.8)	<0.0001
PN-T cells (%)	110	2.6 (1.0-4.8)	4.3 (2.2-7.2)	1.4 (0.8-3.0)	<0.0001
PN-B cells (%)	110	0.8 (0.4-1.4)	1.0 (0.6-2.0)	0.6 (0.3-0.9)	0.0004
PN-Monocytes (%)	110	0.3 (0.1-1.1)	0.6 (0.3-2.2)	0.1 (0.0-0.2)	<0.0001

Abbreviations: WBC: White blood cell concentration; HCT: Hematocrit; PLT: Platelet concentration; PN: Phenotypically normal, NS: Not Significant (p value > 0.05)
* Breed data was not available for 1 dog with a lymphoid gene signature
β p values were calculated using either a Welch's t test or Mann-Whitney U test for parametric and nonparametric data sets, respectively. A chi-squared test was utilized to assess the distribution of sex and top four breeds between the myeloid and lymphoid groups.

Bulk RNA sequencing was performed on 110 canine acute leukemia cases diagnosed in the peripheral blood. Control samples included 5 immunophenotypically normal bone marrow samples and 10 immunophenotypically normal blood samples, as assessed by flow cytometry. Signalment data was not available for the 5 bone marrow control samples. The 10 normal blood samples were comprised of 6 males/4 females, a mixture of breeds, the majority of which were Beagles, and of various ages (median = 2 years, range = 1.0-11.2 years). Mixed breed, Labrador retriever, German shepherd, Golden retriever dogs represented the four most common breeds in the AL cohort (Table 5). The rest consisted of a variety of other breeds that encompassed between 1-4 dogs of each. The occurrence of AL in this cohort was most prevalent in older patients (median: 8.0 years; Table 5). The population consisted of 54% males, 46% females, and 91% were neutered or spayed. AL cases often presented with a leukocytosis (n = 93/110), low platelet counts (n= 25/25), and/or with a low hematocrit (81/110). Overall, the median proportion of CD34+ cells was 56.1% with an interquartile range (IQR) between 25.7-73.3%.

Canine acute leukemias are enriched for gene sets associated with primitive cell development and suppress genes associated with mature leukocyte differentiation:

Principal component analysis (PCA) revealed that normal control samples, both the blood (BLCNTRL) and bone marrow (BMCNTRL), discretely separated from AL cases (Figure 15A). 5,594 genes were considered differentially expressed (DE) (adjusted p value <0.05) between AL and BLCNTRL and 3,710 genes were DE between AL and BMCNTRL, Figure 15B. AL cases overexpressed genes associated with leukemic stem cells and/or implemented in the pathogenesis of acute leukemia in people (Figure 15C). GSEA of the DEG revealed that AL cases were activated for gene ontology biological pathways associated with cell development (e.g. embryonal morphogenesis) and suppressed pathways associated with leukocyte differentiation/function (Supplemental Figure 10A). This finding is consistent with prior observations that neoplastic hematopoietic progenitors are activated for embryonic cell development pathways and have dysregulation of the HOX genes.[231] Additionally, similar pathways were found to be activated or suppressed when using KEGG and REACTOME gene sets (Supplemental Figure 10B-10C).

Unsupervised hierarchical clustering of acute leukemia cases revealed two main groups, consistent with myeloid and lymphoid gene signatures:

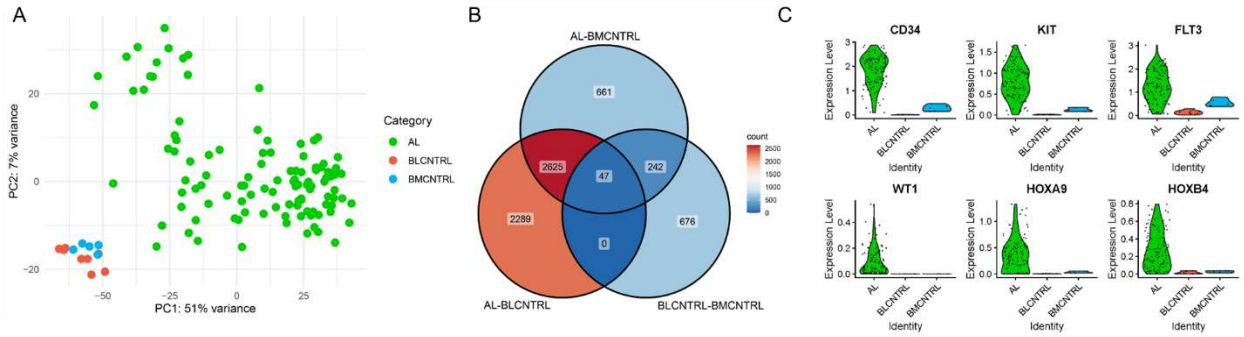

Figure 15: Overview of transcriptomic gene expression of canine acute leukemia, peripheral blood, and bone marrow control samples. A) Principal component analysis of the normalized gene counts from all samples revealed discrete separation of the canine acute leukemia samples away from the control samples. B) Venn diagram of differentially expressed genes between each comparison. C) Violin plots of select genes that are overexpressed in the canine acute leukemia samples and are associated with human acute leukemia. Abbreviations: AL, Acute leukemia; BLCNTRL, blood control; BMCNTRL, bone marrow control.

After excluding controls, unsupervised hierarchical clustering of the AL cases using the top 1500 genes with the highest dispersion around the median revealed two large groups (Figure 16A). 56 cases clustered together in group 1 and 54 cases clustered in group 2 (Figure 16B). Altogether, 1,555 and 681 genes were considered differentially expressed and up- and down-regulated respectively, between group 1 and group 2. Group 1 overexpressed myeloid associated

genes (e.g. *ANPEP, LYZ, BPI)* compared to group 2. GSEA of the DEG revealed that group 1

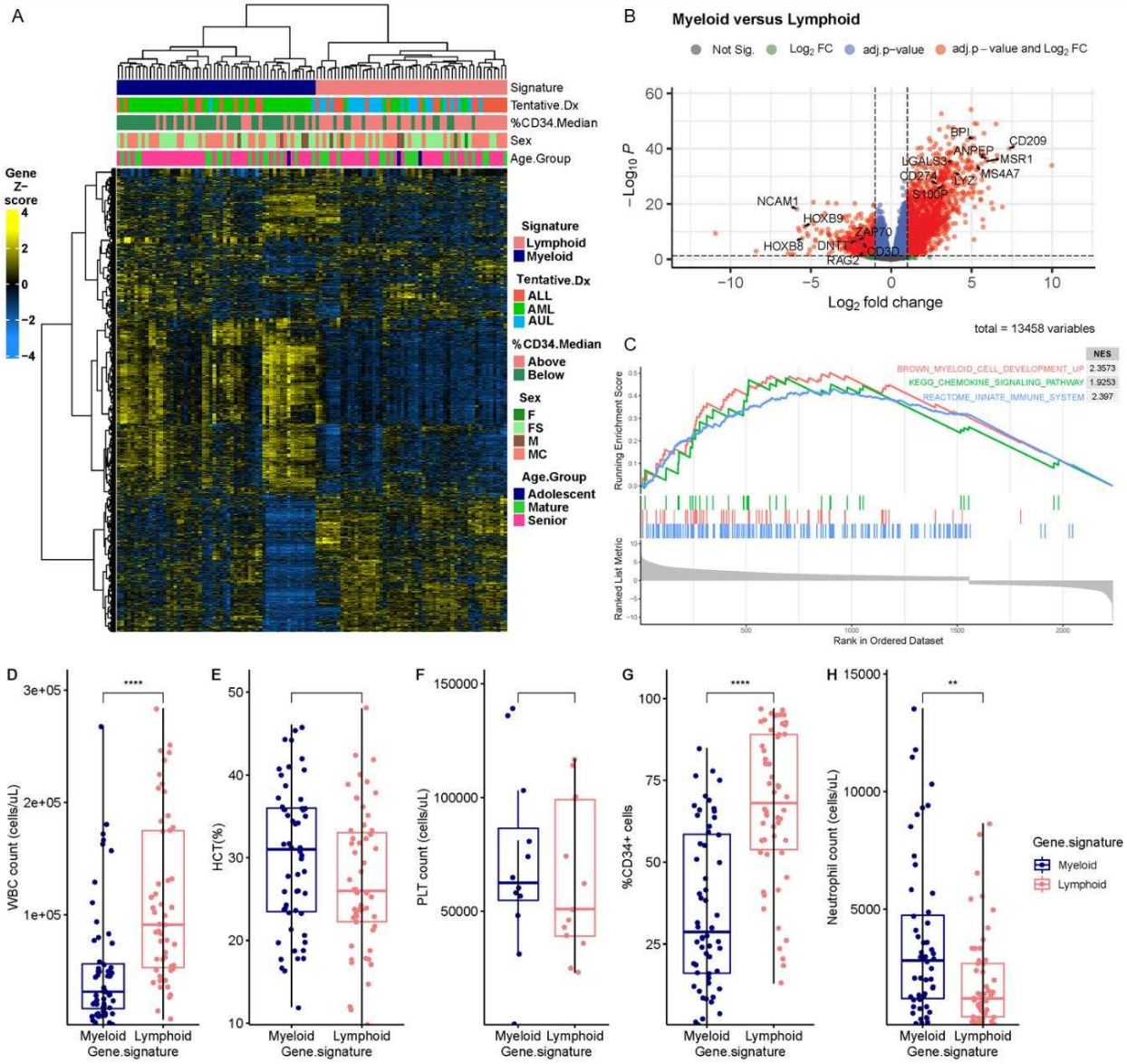

Figure 16: Canine acute leukemia samples separate into two groups, one consistent with myeloid and one consistent with lymphoid. A) Heat map of the top 1500 genes revealed two groups. The heat map shows the row *z* score of variance stabilized transformed normalized read counts determined by using the DESeq2 R package. Columns represent individual acute leukemia samples. At the top, the overall gene signature, tentative diagnosis, categorical classification of the percentage of CD34+ cells in that sample compared to the median, sex, and age group are represented by colored bars. B) Volcano plot of the differentially expressed genes comparing the two groups. One group overexpressed myeloid-associated genes and the other overexpressed lymphoid-associated genes. C) Gene set enrichment plot of select myeloid gene sets using the DEG expressed between the myeloid vs. Lymphoid groups. D-H) Box plots with individual data points comparing the hemogram and immunophenotyping data between the myeloid and lymphoid groups. Abbreviations: Tentative.Dx, Tentative diagnosis; Sig, Significant; adj., adjusted; WBC, white blood cell; HCT, hematocrit; PLT, Platelet Count.

was activated for myeloid associated gene sets, including those involved in myeloid cell development and myeloid cellular processes, such as chemokine signaling and innate immune responses (Figure 16C). Additionally, group 2 overexpressed canonical genes associated with immature lymphocytes (e.g., *DNTT, RAG2*) and with T cell (e.g., *CD3D and ZAP70*) lineage compared to group 1.

Immunophenotyping results corroborated with our suspicion of lineage (i.e., myeloid vs. lymphoid), as 44/54 cases (81.4%, Chi-square = 42.93, p value < 0.0001) tentatively diagnosed as myeloid by flow cytometry were in group 1. Conversely, the majority of tentatively diagnosed lymphoid and unclassifiable cases by flow cytometry aggregated in group 2. Group 1, the samples with a myeloid gene signature, overall presented with lower proportions of CD34+ cells and higher proportions of myeloid cell types (e.g., neutrophils, monocytes, and neoplastic myeloid populations) compared to group 2 (p value <0.05, Table 5). Group 2 had a higher concentration of WBC, and overexpressed genes associated with a precursor hematopoietic cell phenotype (e.g., *HOXB8, HOXB9, DNTT, RAG2)* compared to group 1 (Figures 16B and 16D-16H). Given the gene expression profile and the concurrent immunophenotyping data, we concluded that group 1 was most consistent with acute myeloid leukemias and will furthermore be referred to as cAML. Group 2, the lymphoid signature group, will be referred to as cALL. In alignment with our goals, we focused our approach by extracting the cases defined as myeloid (cAML) based on gene expression for downstream comparisons and concentrated on characterizing this population.

DGE analysis between cAML samples and the canine bone marrow controls revealed 2,846 DEG, of which 1,796 and 1,049 genes were up- and down-regulated, respectively. When we referenced the genes found in the 17-gene leukemic stem cell (LSC) scoring system, we found that the myeloid cases were enriched for multiple genes that confer stemness in hAML.[65] Compared to the bone marrow control, the myeloid cases overexpressed multiple genes in the 17-LSC panel including *CD34*, *ADGRG1*, *EMP1*, *SOCS2*, *MMRN1*, *ZBTB46*, and *DNMT3B* (Supplemental Figure 11). Additionally, *PEAR1* gene expression has recently been shown to be overexpressed in poorly differentiated hAML samples and correlative with a poor outcome in

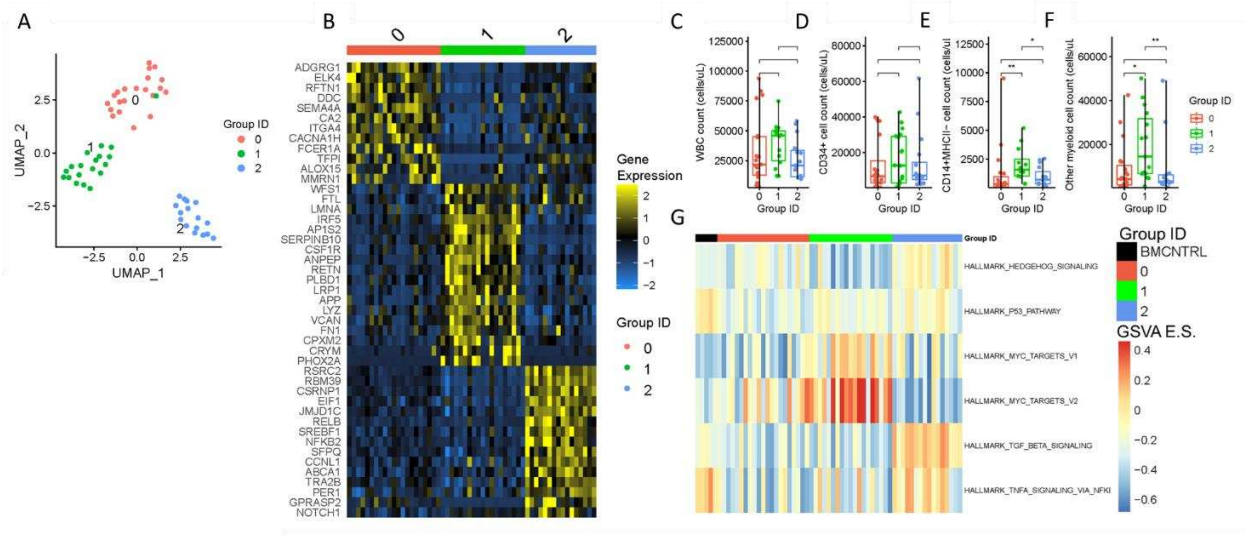

Figure 17: Multiple canine acute myeloid leukemia subgroups are predicted, and each have unique features. A) Uniform manifold approximation and projection of cAML samples revealed three subgroups. B) Heatmap of the top 15 genes that define each cAML subgroup based on receiver operating characteristic analysis. Group 0 and 2 overexpressed genes associated with granulocytes and group 1 overexpressed genes associated with myelomonocytic/monocytic lineage. C-F) Box plots with individual data points comparing the hemogram/immunophenotyping data between the cAML subgroups. Group 1, which overexpressed myelomonocytic/monocytic genes, also presented with the highest neoplastic CD14+MHCII- and CD18+MHCII- cell counts at sample acquisition (p value < 0.05). G) Heatmap of gene set variation analysis enrichment scores of select MSigDB hallmark pathway gene sets from normal bone marrow (BMCNTRL) and cAML subgroups. Group 1 had the highest GSVA enrichment scores for MYC targets and Group 2 had the highest GSVA enrichment scores for TGFB and TNFA signaling. Abbreviations: BMCNTRL, Bone marrow control; E.S. Enrichment Score; GSVA, gene set variation analysis; ID, Identification.

hAML. We found *PEAR1* to be overexpressed by a $\log_2$ fold change >3 (p value < 0.001) in our cAML samples compared to the normal bone marrow samples.[2]

Unsupervised clustering of myeloid cases predicted multiple subgroups with unique gene expression and clinical features:

Three subgroups of cAML were identified using unsupervised clustering with UMAP (Figure 17A and Supplemental Table 15). UMAP groups 0, 1, and 2 consisted of 21, 19, and 16 cases, respectively. UMAP groups 0 and 2 had similar proportions of the top 4 most common breeds within this cohort (Supplemental Figure 12). However, Golden retrievers were not represented in UMAP group 1 (Supplemental Figure 12). No significant difference was noted in the age at diagnosis between the UMAP subgroups (Table 6).

All UMAP subgroups overexpressed genes associated with the RAS and/or PI3K/AKT signaling pathways and were found to be activated for unique MSigDB hallmark cancer pathways compared to normal bone marrow (Figure 17G & Supplemental Figure 13A). For instance, groups 1 and 2 had the highest GSVA enrichment scores for MYC targets and TGF beta signaling pathways, respectively (Figure 17G and Supplemental Tables 15-17).

We evaluated the gene expression between the UMAP groups with two methodologies, receiver operating characteristic (ROC) analysis and pairwise DGE analysis. First, we performed ROC analysis to identify genes that defined each UMAP group (Supplemental Table 14). We found that UMAP group 1 had the highest expression of genes typically associated with monocytic lineage, including *ANPEP*, *RETN*, and *LYZ*.[139] These results also corroborated with the flow cytometry data available, as UMAP group 1 had the highest CD14+MHCII- and other neoplastic myeloid cell counts (cells/uL) compared to UMAP groups 0 and 2 (adj. p value < 0.05, Figures 17C-17F and Table 6). Interestingly, the genes that defined UMAP groups 0 and 2

were not considered specific for a particular leukocyte lineage but have been previously shown to be expressed in multiple myeloid cell types, including granulocytes (e.g., *ABCA1, CSRNP1, FCER1A*, and *RELB*) and erythroid cell types (e.g., *CA2* and *ABCA1*).[139,232,233] Pairwise comparisons between each cAML subgroup revealed that UMAP Groups 0 and 2 overexpressed genes typically associated with leukemic stem cells and poorly differentiated hAML subtypes (Supplemental Figure 13B).

Imputed cell populations of primitive myeloid precursors are variable between subgroups of canine acute myeloid leukemias:

We utilized CIBERSORTx to predict the relative proportions of cell types in our control and cAML samples. The cAML samples had a higher median relative fraction predicted for primitive myeloid cell types (e.g. CD34+ common myeloid progenitors (CMP), CD34+ granulocyte-monocyte progenitors (GMP), and CD34+ megakaryocytic-erythroid progenitors (MEP)) and the lowest median relative fractions for mature leukocytes (e.g. neutrophils, pre-neutrophils, monocytes), compared to the control samples (Kruskal–Wallis test p value < 0.05, Supplemental Figure 14). Whenever we separated the cAML based on their UMAP grouping, we noted that UMAP group 1 had the highest median relative proportions of GMP and early monocytic and dendritic cell precursors. UMAP group 0 had the highest median proportions of MEPs and had similar proportions of CD34+ CMPs predicted as UMAP group 2. Interestingly, UMAP group 2 had high proportions of mature granulocytic cell types compared to the others, which corroborated with their overexpression of granulocytic marker genes (Figure 17B).

Although biologically expected results were computed with CIBERSORTx (e.g., Blood samples had the highest proportion of Neutrophils, Monocyte_1, and Immature B cells), we suspected some cell types were overcalculated with the CIBERSORTx approach alone

(Supplemental Figure 14). For instance, blood samples had the highest proportions of HSC_early_multipotential_progenitors cell types and plasma cells were imputed to be between ~14-22% in the bone marrow samples (Supplemental Figure 14). Given these findings, we also assessed the enrichment of cell type gene signatures across samples using GSVA. The CIBERSORTx and GSVA results were considered comparable (Figure 18A-C). For instance, the blood and bone marrow control samples had the highest enrichment scores for mature leukocyte populations compared to the myeloid/cAML samples (Figure 18B). UMAP groups 0 and 1 had the highest GSVA enrichment scores for CD34+ MEPs and developing monocytic cell types, respectively (Figure 18C). Whereas, UMAP group 2 was the most enriched for B cell precursor cell types compared to both UMAP groups 0 and 1. B-cell developmental gene regulatory network activation and B cell associated gene enrichment have been described in subgroups of pAML, particularly infant AML, which could explain our findings.[234]

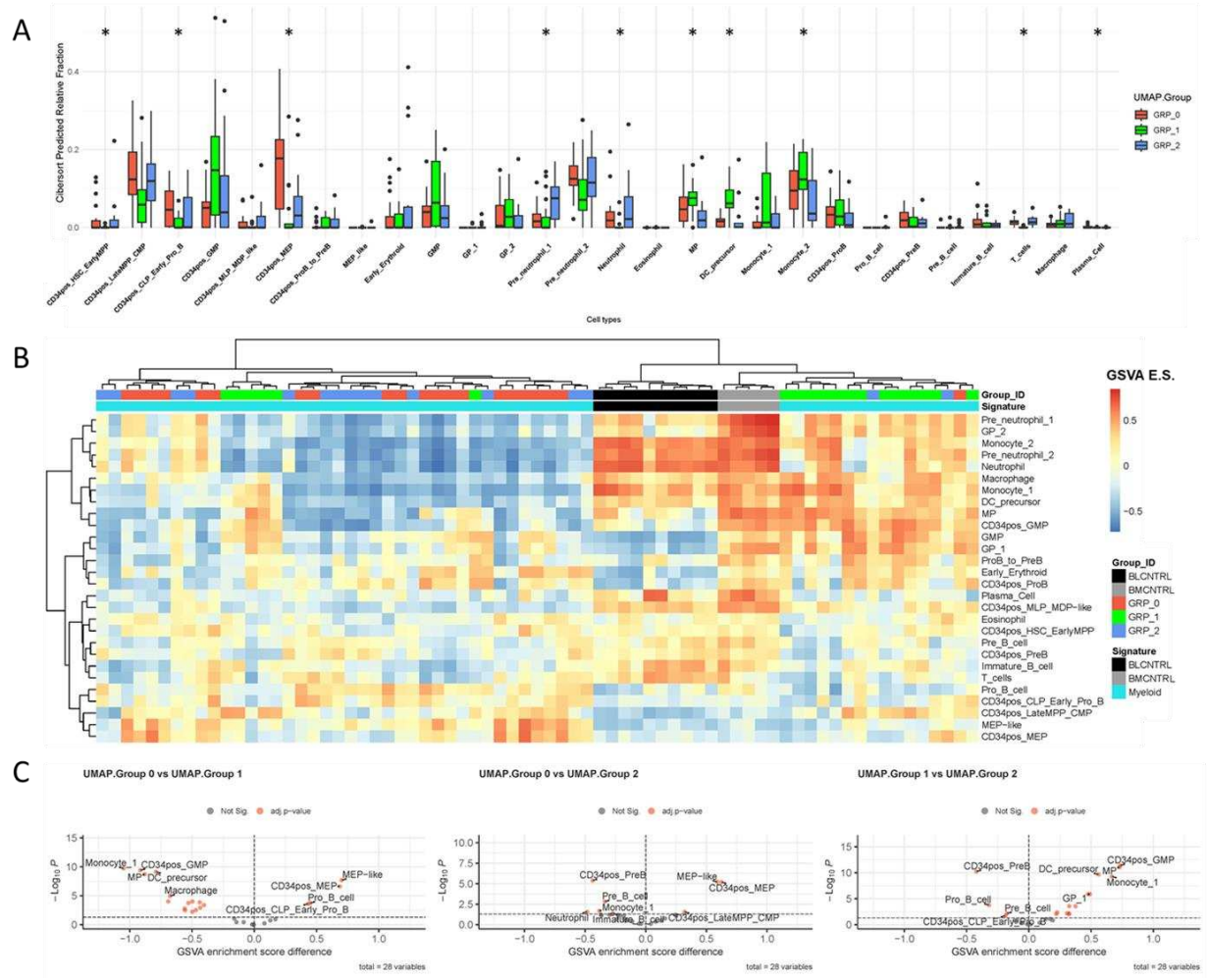

Figure 18: Imputed cell fractions and cell type gene set variation analysis of cAML subgroups. A) Boxplot of the predicted relative fractions of cell types across each cAML UMAP subgroup. UMAP groups are color coded. The * at the top represents statistical significance and p value < 0.05 using a Kruskal-Wallis test. B) Heatmap of GSVA results comparing cell type enrichment scores across samples. Sample types are color-coded based on the signature or UMAP group ID. The scale corresponds to increased (red) or decreased (blue) enrichment score results. C) Volcano plots depicting the differential gene set enrichment analysis results as pairwise comparisons between each UMAP group. Red dots represent gene sets that were considered differentially expressed (adj. p value <0.05) in that comparison and gray dots were not considered statistically significant. Abbreviations: HSC, Hematopoietic stem cell; pos, positive, GMP, Granulocyte-monocyte precursor; MPP, Multipotent progenitor; MEP, Megakaryocytic-erythroid progenitor; CLP, Common lymphoid progenitor; MLP, Multi-lymphoid progenitor; MDP, Monocyte-dendritic precursor; GP, Granulocyte precursor; MP, Monocyte precursor; DC, Dendritic cell; MLP, Multi-lymphoid progenitor; GSVA E.S., Gene set variation analysis enrichment score; Sig, Significant.

Table 6: Clinical data of cAML subgroups identified by unsupervised clustering

	Dogs with available data (n)	Number affected (%) or median (IQR)			Comparison between cAML subgroups p value[β]
UMAP.Group		0	1	2	
n	56	21	19	16	
Signalment					
Sex	56				
Intact male		0 (0%)	3 (15.8%)	1 (6.3%)	
Neutered male		8 (38.1%)	7 (36.8%)	10 (62.5%)	
Intact female		0 (0%)	0 (0%)	0 (0%)	
Spayed female		13 (61.9%)	9 (47.4%)	5 (31.3%)	
Age at diagnosis (years)	56	9.0 (7.5-10.4)	8.0 (4.0-8.8)	7.9 (6.7-9.6)	NS
Breed (top 4 most common)	56				
Mixed breed		5 (23.8%)	5 (26.3%)	6 (37.5%)	
Labrador retriever		4 (19.0%)	2 (10.5%)	2 (12.5%)	
German shepherd		3 (14.3%)	1 (5.3%)	2 (12.5%)	
Golden retriever		4 (19.0%)	0 (0%)	3 (18.8%)	
Hematologic data					
WBC concentration (cells/uL)	56	25,360 (14,360-77,300)	49,840 (31,400-118,855)	22,615 (11,950-38,910)	0.03
HCT (%)	56	28 (24-35)	26 (8.5-56.7)	33 (22-39)	NS
PLT (cells/uL) without clumping*	13	65,500 (42,774-81,250)	73,000 (60,750-121,000)	60,000 (58,000-136,000)	NS
Immunophenotyping data					
CD34+ cells (%)	56	26.7 (18.6-49.9)	25.7 (8.5-56.7)	36.5 (24.9-64.2)	NS

CD5+CD3- cells (%)	56	8.3 (5.2-12.9)	6.7 (4.8-8.1)	8.2 (5.6-20.4)	NS
CD14+MHCII- cells (%)	56	2.6 (0.6-4.3)	7.3 (3.2-20.1)	4.1 (1.4-7.6)	0.02
CD18+MHCII-CD4-CD14-cells (%)	56	26.5 (12.4-32.7)	50.0 (28.3-63.4)	20.1 (13.7-31.3)	0.02
PN-Neutrophils (%)	56	12.6 (3.7-20.6)	8.2 (4.6-18.2)	11.0 (3.5-32.3)	NS
PN-T cells (%)	56	4.5 (2.8-9.4)	3.7 (1.6-5.9)	3.1 (1.9-6.4)	NS
PN-B cells (%)	56	1.0 (0.6-3.1)	1.0 (0.5-1.8)	1.0 (0.6-1.8)	NS
PN-Monocytes (%)	56	0.4 (0.2-2.1)	0.9 (0.5-1.6)	0.9 (0.3-4.0)	NS

Abbreviations: cAML: canine acute myeloid leukemia; WBC: White blood cell concentration; HCT: Hematocrit; PLT: Platelet concentration; PN: Phenotypically normal
*: No clumping was reported in 4, 4, and 5 dogs from groups 0, 1, and 2, respectively.
β: p values were calculated using either a Brown-Forsythe and Welch ANOVA or one-way ANOVA for parametric and nonparametric data sets, respectively.

cAML subgroups have overlapping and unique features compared to both pediatric and adult AML and are activated for gene sets of hAML subtypes:

Next, we set out to investigate the overlapping features between hAML, both pAML and aAML, and cAML subgroups. To do this, we referenced the generated gene sets representing of the TARGET and BEAT AML cohorts. The TARGET (pAML) and BEAT (aAML) data sets consisted of 1110 and 697 samples, respectively. 11 and 24 different AML subtypes were described in the TARGET and BEAT AML patient manifests, respectively. We extracted the top 250 DEG that matched the dog's gene symbol and were both up- and down-regulated to generate a total of 56 gene sets. These 56 gene sets were used to perform GSEA in each cAML subgroup.

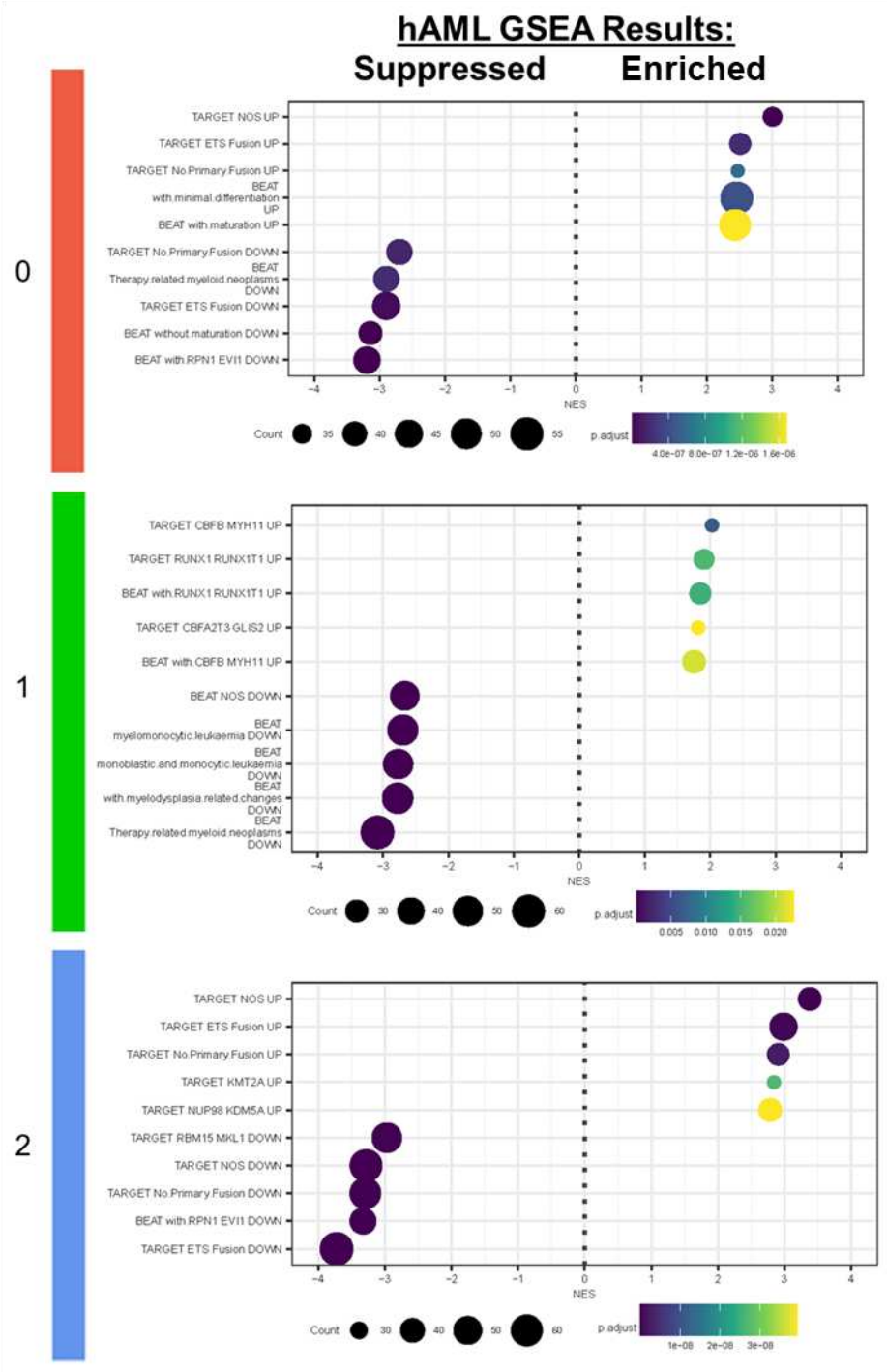

Figure 19: Gene set enrichment analysis results using DEG between each cAML subgroup versus the bone marrow control samples. Each dot represents a hAML gene set enriched in our cAML subgroups. The top 5 up (enriched) and down (suppressed) gene sets with the highest and lowest normalized enrichment scores are shown. The cAML groups 0, 1, and 2, are identified to the left and by their corresponding-colored bar. The size of each dot corresponds to the gene count, and the color of each dot corresponds to the adjusted p-value.

GSEA revealed that each cAML subgroup was enriched for multiple pAML and aAML gene sets (Table 7, Figure 19, and Supplemental Table 18). We noted that Group 1 had the highest number of enriched gene sets from the aAML cohort and had the lowest number of enriched gene sets from pAML, compared to the other predicted cAML subgroups (Table 7). Additionally, Group 2 had the highest number and proportion of enriched gene sets from the pAML cohort, compared to the other groups (Table 7). Although more aAML gene sets were found to be enriched across all cAML subgroups, we found that the TARGET Not otherwise specified (NOS) and TARGET ETS Fusion subtypes were amongst the top 3 in both cAML groups 0 and 2 when we combined the absolute value of NES from the enriched and suppressed gene sets (Table 7). Conversely, group 1 had the highest combined NES for aAML subtypes, including BEAT Therapy related myeloid neoplasms, BEAT AML with RUNX1-RUNX1T1 fusion, and BEAT AML NOS (Supplemental Table 18). Leading edge analysis of the top 3 gene sets with the highest NES revealed that there are multiple genes considered enriched in cAML and shared between the associated hAML subtypes (Supplemental Figure 15). Some of these genes (e.g. WT1, FLT4) are potential therapeutic targets or have been implicated in drug resistance in hAML patients (e.g. NCAM1).[2,235,236]

Table 7: Summarized CIBERSORTx, cell type GSVA, and gene set enrichment results using the differentially expressed genes from each cAML subgroup with hAML gene sets

UMAP. Group	0	1	2
	CIBERSORTx		
Imputed cell type with the highest median proportion	CD34pos_MEP	CD34pos_GMP	CD34pos_LateMPP_CMP
	GSVA		
Cell type with the highest pairwise GSVA score	CD34pos_MEP	CD34pos_GMP	CD34pos_Pre_B
	Number of gene sets enriched (%) [β]		
Total human AML gene sets enriched with q value < 0.05*	46 (82.1%)	33 (58.9%)	52 (92.9%)
Total human AML gene sets enriched with q value < 0.05 and ES >0.5 or <-0.5*	17 (30.4%)	18 (31.1%)	27 (48.2%)
TARGET gene sets enriched with q value < 0.05 and ES >0.5 or <-0.5*	6 (27.3%)	2 (9.1%)	12 (54.5%)
BEAT AML gene sets enriched with q value < 0.05 and ES >0.5 or <-0.5*	11 (32.4%)	16 (47.1%)	15 (44.1%)
TARGET AML subtypes with paired gene sets enriched with q value <0.05 and ES >0.5 or -0.5*	0	0	3
BEAT AML subtypes with paired gene sets enriched with q value	1	0	2

<0.05 and ES >0.5 or <-0.5*			
Top 3 (highest combined NES from paired hAML gene sets)*	TARGET NOS	BEAT Therapy related myeloid neoplasms	TARGET ETS Fusion
	TARGET ETS Fusion	BEAT AML with RUNX1-RUNX1T1	TARGET NOS
	BEAT AML without maturation	BEAT NOS	TARGET No Primary Fusion

Abbreviations: cAML: canine acute myeloid leukemia; ES: enrichment score; hAML: human acute myeloid leukemia; NOS: Not otherwise specified

*: Gene sets were excluded if their enrichment score was in the opposite direction as the gene set generated (e.g. + ES but DOWN gene set).

β: Proportion of gene sets were calculated using the total gene sets (n=56) or the total number per TARGET (n = 22) or BEAT AML (n = 34) gene sets, respectively.

Discussion

In this study, we utilized gene expression profiling to characterize canine acute leukemias, define their lineage as myeloid or lymphoid, impute their cell composition, and compare cAML predicted subgroups to hAML subtypes. The canine acute leukemia cohort overexpressed genes that have been implicated in leukemogenesis and in both human acute myeloid and lymphoid leukemias.[237–239] For instance, the HOX genes were repeatedly found to be enriched in both of our myeloid and lymphoid subgroups. Myeloid cases were identified based on overexpression of myeloid-associated genes and enrichment for myeloid leukocyte gene sets, relative to the lymphoid group. Conversely, myeloid cases under-expressed genes associated with lymphoid lineage, such as *ZAP70*, *DNTT*, *RAG2*, and *CD3*.[139] This finding might suggest that the cases within lymphoid subgroup are compatible with a T cell acute

lymphoblastic leukemia. However, additional analysis focusing on characterizing this cALL group is needed and beyond the scope of this initial work.

Classification methods traditionally used in the diagnosis of hAML, include cytomorphology review, flow cytometry panels, cytogenetic analysis, and mutational profiling.[96,102] There is mounting evidence that gene expression profiling is a reliable methodology for defining subtypes of acute leukemia in people, and gene expression profiling can also be indicative of underlying favorable or unfavorable prognostic factors.[64,240–243] Currently, diagnostic options are limited in veterinary medicine for subclassifying canine acute leukemia. Therefore, we implemented an unsupervised approach to define lineage using gene expression profiling, which revealed a dichotomy of acute leukemia subtypes (i.e., myeloid vs. lymphoid). Our results corroborated our suspicions of acute leukemia subtype and revealed that most cases that were tentatively diagnosed as AML by flow cytometry clustered in the myeloid group. Additionally, most lymphoid cases and unclassifiable cases (determined by flow cytometry) clustered together in the lymphoid group. For downstream comparisons, we stratified the cases broadly as myeloid versus lymphoid using gene expression alone, rather than by flow cytometry results, and extracted the myeloid cases for assessing comparative features with hAML.

We identified three cAML subgroups, predicted by unsupervised clustering methods, with unique clinical variables, gene expression, imputed cell compositions, and gene set enrichment. All of which shared overlapping features with multiple pAML and aAML subtypes. 5-year relative survival for hAML patients is currently reported at ~20% and novel targeted therapeutics are needed to advance the care for these patients.[2,8] cAML patients could bridge the

gaps in clinical translation of novel therapeutics, especially given the quick clinical progression seen in dogs and the patterns of gene expression defined here.

Similar as hAML, cAML overexpressed genes associated with hAML leukemogenesis and primitive hematopoietic cell types. For instance, genes in the 17-gene LSC panel, a panel designed to identify individuals with a LSC signature and at risk for therapy resistance, were noted to be enriched in our myeloid group.[244] Additionally, we found that the myeloid cases overexpressed *PEAR1*, which was recently shown to be associated with a poor outcome.[2] cAML cases overexpressed genes that are of interest for novel and/or developing therapeutics for hAML, including *MYC*, *FLT3*, *WT1*, and *KIT*, to name a few.[2,6] Additionally, cAML samples were found to be enriched for multiple targets along the RAS and PI3K/AKT signaling pathway, both of which have been implicated in hAML pathogenesis and >50% of aAML patients have one or more activating mutations associated with the RAS pathway.[29,30] It is possible that the RAS signaling pathway plays a similar role in cAML pathogenesis. Ultimately, we propose that cAML could serve as a model for investigating leukemogenesis, leukemic stem cell biology, environmental factors that lead to the development of AML, and/or therapy resistance/development, and additional work is needed to confirm these predicted overlapping features.

There are limitations to this study. Our study consisted of only 110 cases, and approximately half were consistent with myeloid lineage. As previously mentioned, acute myeloid leukemia in people is considered a heterogeneous disease with over 26 different WHO classification subtypes for aAML.[7] This scheme does not perfectly fit for pAML subtypes, as the molecular landscape of pAML is different than aAML.[9] We suspect that our cohort of 56 cases does not fully capture the repertoire of cAML cases that dogs develop. Additionally, our

laboratory routinely identifies acute leukemia cases based on the proportion of CD34+ cells. Eight cases in this cohort were CD34 low or negative and we suspect CD34- canine acute leukemia cases are underrepresented in this data set. This could explain why most of our cohort overexpressed markers associated with immature acute leukemias phenotypes. Additional studies focused on CD34- canine acute leukemias, both myeloid and lymphoid lineages, are required. Furthermore, fusion gene analysis and validation was beyond the initial scope of this work. However, fusion gene detection is considered imperative for hAML subtyping and often fusion genes are correlative with gene expression profiling. Future investigations are ongoing and devoted to fusion gene identification and validation for canine acute leukemias. It is possible that canine acute leukemias, both myeloid and lymphoid, either develop unique or similar translocations and that these will also be correlative with transcriptomic programs. Regardless, we provide evidence that cAML have overlapping features with hAML and that cAMLs are activated for gene sets associated with hAML subtypes.

Here we show that canine acute leukemias can be discretely separated into two groups, one consistent with myeloid lineage and the other consistent with lymphoid. Of the acute myeloid leukemias, we identified molecular features implicated in hAML. Additionally, we found that predicted cAML subgroups are comprised of heterogeneous populations of myeloid cell types and are enriched for genes associated with both adult and pediatric AML subtypes. Our global analysis of gene expression in cAML samples offers insight into the comparative features with hAML. Future studies can be specifically devoted to the function/impact of these highlighted features and their role in acute myeloid leukemia biology and clinical translation.

CHAPTER 4: Mutational landscape of the canine acute myeloid leukemia exome

Summary

Acute myeloid leukemia (AML) is an aggressive heterogenous hematopoietic neoplasm that afflicts both dogs and people. The underlying somatic mutations that occur in human AML (hAML) have been described but are yet to be defined in canine AML (cAML). The goal of this work was to identify somatic mutation candidates in cAML and determine their overlap with hAML. Here, we utilize whole exome sequencing to identify candidate mutations in 44 cAML samples. We focused our approach by limiting our analysis to variants predicted to have a moderate to high impact and that occurred in a known gene implicated in cancer. At least one mutation in common oncogenes mutated in hAML (e.g. *NRAS, KRAS, PTPN11, FLT3, KIT*) were also identified in over 75% of cAML samples. Mutations in *DNMT3A* were uncommon (n=3/44) and *NPM1* mutations were not identified in our cohort, both of which are common aAML-associated genes. However, mutations in other epigenetic modifiers, such as *KDM5C* and *KDM6A*, occurred at a high frequency. This data provides insight into the candidate mutations potentially driving cAML pathogenesis and their overlapping features with hAML.

Introduction

Over 21,000 newly diagnosed cases of human acute myeloid leukemia (hAML) and 10,000 hAML-related deaths are reported in the United States every year.[1] hAML is considered a highly diverse aggressive hematopoietic malignancy, with over 16 recurrent gene rearrangements, 60 recurrent point mutations, and thousands of rarely mutated genes.[2,7,50] Not only are there substantial differences in disease biology associated with AML subtypes, but there are even unique features between age groups. For instance, pediatric AML (pAML) is

characterized by fusion genes and somatic mutations not seen in the adult counterpart, making finding a cure even more challenging.[9,59] Substantial breakthroughs in targeted therapeutics for AML have been slow to develop and only 20% of patients experience durable remission.[2,6] A translational model could help bridge gaps in clinical translation of experimental therapeutics and move towards one cure.

Dogs spontaneously develop AML and there are major clinical and biological features that overlap with the human disease. However, very little is known about the molecular landscape of canine AML (cAML). Mutations in *NRAS/KRAS*, *KIT*, and *FLT3*, have previously been described in canine acute leukemia. Our group set out to investigate the molecular alterations in this neoplasm using whole exome sequencing. The goal of this work was to identify somatic mutation candidates in cAML via whole exome sequencing (WES). We hypothesize that some of the somatic mutations that occur in cAML will be similar to ones seen in hAML, and some will be unique to dogs.

Methods

Sample Collection:

Genomic DNA from 43 cAML samples with concurrent RNA-seq data and 1 cAML sample without paired RNA-seq data was submitted for whole exome library preparation and sequencing to University of Colorado's Genomics Core for processing. Banked Genomic DNA from 39 age-matched dogs without hematopoietic malignancy, acquired through our collaboration with the Dog Aging Project and previous studies, was performed to generate our panel of normal population variants.[245,246]

Genomic DNA extraction and Sequencing:

Genomic DNA was extracted from frozen leukocyte pellets using a QIAamp DNA Mini Kit (Qiagen). DNA integrity and concentration were assessed using an Agilent Tapestation and Qubit Fluorometer, respectively. Whole exome libraries were prepped using the Agilent Sure SureSelectXT CD Canine All Exon V2, 96, auto, Community Design kit. Libraries were sequenced by the University of Colorado's Genomics Core using an Illumina NovaSeq6000, with paired end reads, 150 cycles at 300x coverage.

Data Analysis:

Read quality was assessed with FastQC/MultiQC.[218] Trim galore software was used to trim adapter sequences and filter low quality reads (Phred score < 30). Processing followed GATK best practices.[247] Alignment was completed using the canine reference genome, CanFam3.1 ensembl v.104, and BWA-aln. Post-alignment BAM files we marked duplicate reads and sequences underwent base recalibration. Next, we generated a panel of normals (PON) using the sequencing data from the 39 clinically healthy dog samples using Mutect2. Variant calling on the AML samples was performed using Mutect2 after importing the PON and using the reported *Canis lupus familiaris* germline variants variant call file (vcf) available through the Broad Institute to filter out population polymorphisms.[248] Variants were manually filtered by setting the minimum depth required for variant calling to 5. Next, we placed less priority on variants that had a variant allele frequency (i.e. variant allele reads/total allele reads; VAF) between 47.5-52.5% or >97.5% for heterozygous and homozygous genes, respectively. Variants labeled as "PASS" were selected for downstream annotation using Ensembl's Variant Effect Predictor.[249,250] cAML-candidate mutations were prioritized if they were considered novel (i.e., were not previously reported in the dbSNP database), occur in protein-coding regions, predicted to have moderate to high impact using Ensembl's Variant Effect Predictor, are identified as

either a Tier 1 or Tier 2 COSMIC cancer gene.[249,250] Final candidate variants were inspected in the Broad Institute's Integrative Genome Viewer and mapped to functional sites within the affected protein.[251] We utilized cBioPortal to interrogate the variants in human oncologic study data sets, including the TARGET AML, BEAT AML, and TCGA pancancer studies.[252] Publicly available gene sets were accessed through the Broad's Molecular Signature Database (MSigDB) for gene set enrichment analysis (GSEA).[157,221–226]

Statistical Analysis:

Statistical analysis and data interrogation was performed using variant call file processing software, maftools.[253] Summary statistics of the variants identified across this cohort, the prevalence and co-occurrence of variants, enrichment analysis, and gene pathway enrichment of associated mutated genes, were assessed using maftools. We performed oncodriver gene analysis using the OncodriveCLUST algorithm in maftools using the oncodrive() function.[33] Statistically significant observations for this study were defined as p values, adjusted p values, or q values < 0.05. P values were corrected for multiple testing using the Benjamini-Hochberg approach, unless otherwise specified.

Results

Overview of study population:

Whole exome sequencing was performed on genomic DNA extracted from 44 canine peripheral blood AML samples submitted for immunophenotyping to Colorado State University's Clinical Hematopathology Laboratory. 43/44 samples were previously submitted for bulk RNA-seq (see Chapter 3). Summarized patient demographic data is provided in Table 8. There was a minor predominance of females in our cohort (52.3% females compared to 47.7% males). Most of the patients included in this cohort were older (median = 8.1 years) and were considered purebred status (68.2%). Of the purebreds, large breed dogs, including Golden

Table 8: Overview of canine cohort

	Total dogs with available data (n)		Number affected (% of group) or median (IQR)		
UMAP.Group		Entire cohort	0	1	2
n		44	14	16	13
Sex	44				
Male		21 (47.7%)	4 (28.6%)	8 (50%)	9 (69.2%)
Female		23 (52.3%)	10 (71.5%)	8 (50%)	4 (30.8%)
Age	44				
Reported age at sample acquisition (years)		8.1 (6.0-9.7)	8.7 (7.2-11.2)	7.5 (3.8-8.8)	7.6 (6.8-10)
Reported breed status	44				
Purebred		30 (68.2%)	11 (78.6%)	11 (68.8%)	7 (53.8%)
Mixed		14 (31.8%)	3 (21.4%)	5 (31.3%)	6 (46.2%)
Top 4 most common breeds	44				
Mixed		14 (38.8%)	3 (21.4%)	5 (31.3%)	6 (46.2%)
Golden Retriever		7 (15.9%)	3 (21.4%)	0 (0%)	3 (23.1%)
Labrador retriever		5 (11.4%)	3 (21.4%)	2 (12.5%)	0 (0%)
German shepherd		4 (9.1%)	2 (14.3%)	1 (6.3%)	1 (7.7%)

Abbreviations: IQR, Interquartile range.

retrievers, Labrador retrievers, and German shepherds, were the most common. The clinical metadata associated with each sample are provided in Supplemental Table 19.

Mutational landscape of the cAML exome:

In total, 2,614,582 variants were identified across the 44 samples. Post-filtering, 688 and 167 of the variants were predicted to have a moderate or high impact, respectively, in 341 genes (Supplemental Table 20). The median number of significant prioritized variants per sample was 13 (Figure 20A). Single nucleotide variants (SNV) were the most frequent variant type (n=736/855, 86.1%) (Figure 20A). Of the SNVs, 53 truncating mutations were found in 44 genes. Cytosine to adenine transversions had the highest frequency (55.3%), followed by cytosine to thymine transitions (26.2%, Figure 20C & Supplemental Figure 16). 252 of the SNVs had a deleterious SIFT score predicted with high confidence. 107 variants were characterized as either an insertion or deletion (indel) and 73 of those were classified as either a frame shift insertion or frame shift deletion. One nonsense indel mutation was identified in *MED12*. A graphical representation of the top 15 most frequent genes with a detectable variant identified in our cohort is provided in Figure 20B. Two samples contained a higher tumor mutational burden (n=269 and 86) of prioritized variants identified compared to the rest of the cohort. Gene set enrichment analysis of the mutated genes revealed that these samples were enriched for variants

in genes associated with the G2/M cell cycle checkpoint (HALLMARK_G2M_CHECKPOINT q-value: < 0.001), an important step involved in DNA repair.

The variant allele frequencies (VAF) ranged between 2.1-97.3% (average VAF = 31.2%) and the VAF for the top 10 most common cAML variants is provided in Figure 21A. We cross-referenced the genes found to have a variant in our study with their corresponding gene family provided by MSigDB, the majority of which (n =137) occurred in known oncogenes

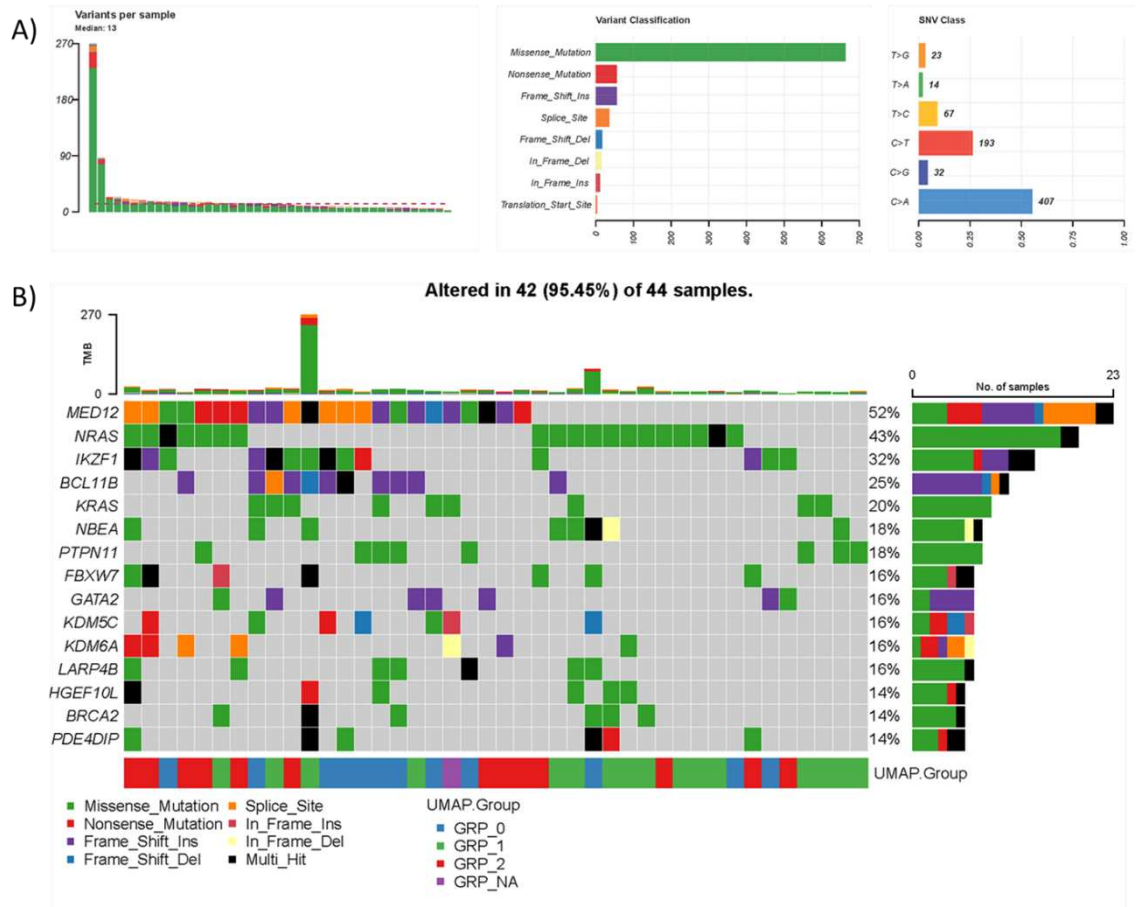

Figure 20: Overview of the variants identified in canine acute myeloid leukemia. A) From left to right, the bar plots represent the number of variants identified in each sample, the breakdown of the variant types, and the count of each SNV class. The dashed line in the far-left bar plot represents the median number of variants prioritized. B) The oncoplot displayed represents the top 15 genes with significant variants that are altered in 42 of the 44 samples. Each column represents an individual cAML sample. The number of mutations identified in each sample is represented by the top bar plot. The bar plot and the associated percentages listed to the right represent the count of each variant classifications and the relative frequency of that gene with a variant, respectively. The bar at the bottom represents the associated UMAP group for each sample.

(Supplemental Table 21). Additionally, 88 transcription factors and 44 tumor suppressors were identified to have a variant. The distribution of the other gene families consisted of 35 protein kinases and fewer cell differentiation markers (n=14), cytokines and growth factors (n =6), and homeodomain proteins (n=5). Numerous genes were classified into multiple gene families (e.g., *TP53, FLT3, KIT*, etc.).

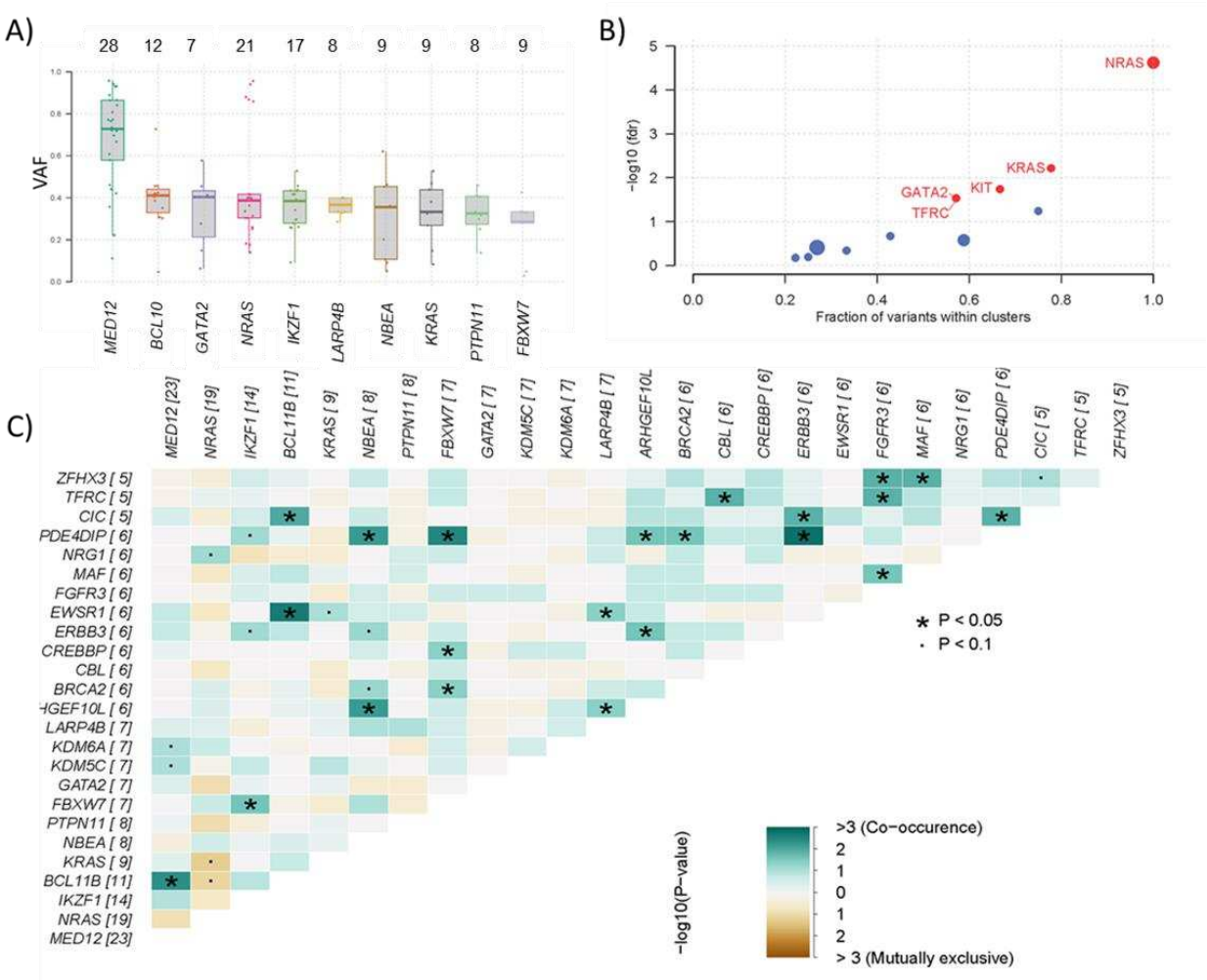

Figure 21: Variant allele frequency, hotspot variants and variant interaction of cAML variants. A) Box plot depicting the variant allele frequency of the top 10 genes. The numbers at the top represent the number of variants identified in that gene. The y-axis represents the variant allele frequency. B) Scatterplot of genes that are enriched for specific loci (i.e., "hot spots"). The size of the dot corresponds to the number of loci considered enriched in that gene. Red dots are considered statistically significant. C) Correlation plot representing the variant interaction analysis results to identify co-occurring (green) and mutually exclusive (gold/yellow) gene interactions. The * denotes statistically significant results (p value < 0.05) and the "." signifies p values between 0.05-0.1.

Given that mutations of epigenetic factors are a common motif in hAML pathogenesis, we investigated the epigenetic factors that may play a role in cAML pathogenesis. First, we cross-referenced our genes with a human epigenetic factor database to assess each gene's epigenetic function/modification (Supplemental Table 22).[254] 64 genes were identified as being an epigenetic factor. Of those, histone modification writers (i.e., *KMT2D, EZH2, SETD1B, KMT2A, PRKCB, NSD1, RARA,* and *PRDM16*), histone modification erasers (i.e., *ASXL1, KDM6A, KDM5C, KDM5A, USP44*), and/or chromatin remodelers (i.e., *NBN, IKZF1, ATRX, FOXA1, CHD4, KEAP1,* and *PSIP1*) were amongst the most common classes. No variant was identified in the epigenetic modifier *NPM1,* a common feature of adult AML, but infrequently mutated in pediatric AML.[9,30] Additionally, variants in epigenetic modifiers implicated in hAML, such as *DNMT3A* (n=3/44), *TET2* (n=3/44), and *ASXL1* (n=2/44), were considered an uncommon feature of cAML.

Potential oncodrivers, co-occurring variants, and enrichment analysis of variants identified in canine AML:

Next, we interrogated the potential role of the common genes identified to have a significant variant. *MED12*, a protein subunit of the mediator complex that is involved in transcriptional regulation of genes that maintain HSC-stemness, has previously been reported to be mutated in multiple canine cell lines and human solid tumor types, and was found to be the most common (n=23/44, 52.3%) cAML gene with a detected variant.[252,255–258] Both *IKZF1* and *GATA2* are hematopoietic transcription factors that are involved in hematopoietic stem cell maintenance and differentiation and were also amongst the top 15 genes with a significant variant.[163,259] Additionally, we identified point mutations that have previously been reported in other canine oncology studies. For instance, the missense mutation D815V in exon 17 of the *KIT*

gene has previously been reported in canine acute leukemias.[114] We identified other variants, such as the E76K in exon 3 of *PTPN11* and the D815V in exon 17 of *KIT*, in this cohort.[260,261] We utilized the OncodriveCLUST algorithm to identify possible driver mutations using positional clustering. Potential driver mutations were predicted at 2 loci in the *NRAS* gene and at 1 locus in each of the following genes: *KRAS, KIT, GATA2,* and *TFRC* based on positional clustering (Figure 21B and Supplemental Table 23).

Our ability to assess for co-occurrence of variants was limited by the small sample size of genes with >5 variants. However, we did note that multiple genes with variants were considered to co-occur including gene pairs such as *MED12:BCL11B*, *IKZF1:FBXW7*, and *NBEA:LARP4B*, to name a few (Figure 21C). Interestingly, mutations in *NRAS* and *KRAS* trended towards being mutually exclusive (p value: 0.05-0.1), a pattern seen with pAML.[9] Next, we performed enrichment analysis using a groupwise fisher exact test to investigate if the cAML variants we identified were enriched in any of the following categories: UMAP.group, breed, sex, and age group. After adjustment for multiple statistical testing, we did not yield any statistically significant results (adj. p value > 0.05), which may indicate that our statistical comparisons are underpowered.

Variants in the RTK-RAS pathway are a common motif of cAML:

Mutations in common hAML-associated genes (i.e. *NRAS*, *KRAS*, *PTPN11,* and *GATA2*) were amongst the top 15 genes with a detectable variant in this cohort.[9,30] Of those variants prioritized, the RTK-RAS pathway was ubiquitously affected (Figure 22A). Additionally, recurrent point mutations, potential "hot spots", were identified in *NRAS* and *KRAS* genes in this cohort (Figure 22B and Supplemental Table 20). We also noted that variants occurred at similar locations and protein domains in genes involved in the RTK-RAS pathway between cAML and

hAML and other human malignancies (Supplemental Table 20 and Supplemental Figure 17). For instance, the codon changes G13R in exon 2 and Q61R/H of the *NRAS* gene were shared between human and canine AML. Interestingly, the proportion of cAML samples (43%) with a detectable *NRAS* variants was much higher than both pAML and aAML patients (Figure 22C).[9,30] We previously noted that the downstream targets of *NRAS/KRAS* (e.g., *CCND2, MYB, CDK6,*

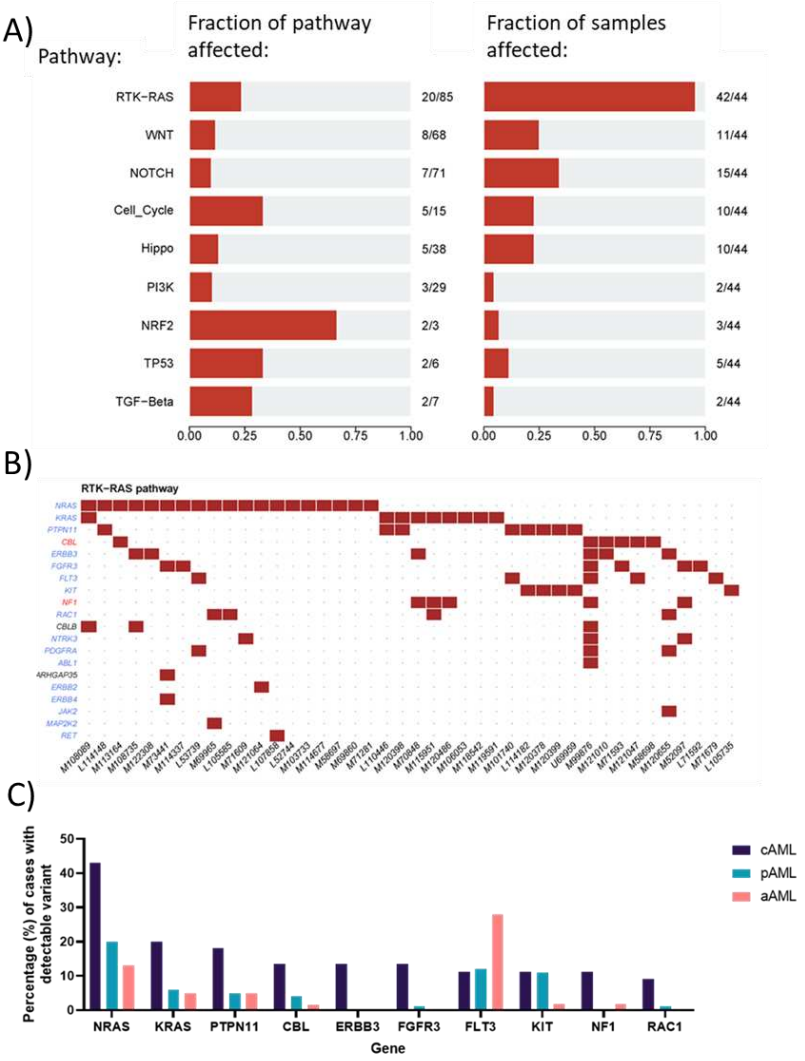

Figure 22: Variants in cAML are commonly involved in the RTK-RAS canonical cancer pathway. A) Bar plot depicting the distribution of prioritized variants across canonical cancer pathways. The left bar plot represents the proportion of genes affected in the pathway ad the bar plot on the right represents the proportion of samples with a variant in the associated pathway. B) Box plot highlighting the distribution of genes with variants across samples in the RTK-RAS pathway. Genes in red represent tumor suppressors and genes in blue represent oncogenes. C) Bar plot comparing the proportion of cases with a variant identified in the top 10 most frequently mutated genes in the RTK-RAS pathway between cAML, pAML, and aAML.

etc.) were upregulated in cAML samples compared to normal bone marrow controls (see Chapter 3 Supplemental Figure 13), which is further supportive evidence that this pathway is dysregulated in cAML.

Discussion

Here, we sought to broadly investigate the unique and comparative features of cAML's mutational landscape using whole exome sequencing. We identified variants in common hAML-associated genes, such as *NRAS*, *KRAS*, *PTPN11*, *FLT3, GATA2*, and *TP53,* and genes not often associated with hAML, such as *MED12.* Although variants in epigenetic modifiers that are implicated in hAML (e.g., *DNMT3A, TET2, ASXL1*) were considered uncommon in this cohort. However, variants in other epigenetic factors were readily identified cAML. Even though there are differences in the mutational landscape of the exome between cAML and hAML, it is possible that the genetic alterations observed have similar biological consequences and converge on canonical cancer pathways. Additional studies are required to investigate the functional impact of these variants and their role in cAML pathogenesis.

The prevalence of the *MED12* variants identified is surprising. As previously mentioned, *MED12* is involved in regulating gene expression and maintenance of hematopoietic stem cell homeostasis.[257] Mutations in *MED12* are considered uncommon in humans.[255,262,263] Recurrent mutations in early exons have been described in multiple benign neoplasms in humans (e.g. leiomyomas and chronic lymphocytic leukemia).[255,262] One study found that truncating nonsense mutations towards the 5' end of exon 1 may allow the protein to avoid nonsense-mediated mRNA decay.[263] In our samples, most of the variants identified were within or neighboring the PQL beta-catenin-binding domain, which is considered an important interaction for regulating Wnt-responsive genes.[264] Our current studies did not yield that the WNT-Beta-Catenin pathway

was dysregulated in any of the cAML subgroups compared to the bone marrow controls (see Chapter 3). However, we suspect that the functional impact of the variants identified are dependent on the variant type and location within the gene. Focused studies are required to assess the functional impacts of these *MED12* variants and other variants identified in this study.

Our data revealed that signaling through the RTK-RAS pathway appears to be a common motif shared between hAML and cAML. In our study, ~95% of samples contained a variant within this pathway. This proportion is slightly higher than what has been previously reported for hAML.[30] Regardless, over 50% of aAML patients are identified to have at least one activating mutation in this pathway, which is considered an important final step in leukomogenesis.[30] Additionally, we noted that the gene list with prioritized variants was more similar to pAML than aAML, which also corroborates our findings at the gene expression level (see Chapter 3). These findings could indicate that the underlying pathogenesis between pAML and cAML are comparable between the two entities.

This study is not without limitations. First, we suspect that there are other molecular abnormalities that contribute to cAML pathogenesis, which cannot be identified by WES alone (e.g., large tandem duplications or translocations). Although, RAS mutations were a common feature, these alone are not sufficient to cause leukemogenesis. Additional alterations that lead to either inhibition of hematopoietic cell differentiation, alternative splicing, and/or aberrant epigenetic modifications are required. Given the high prevalence of recurrent translocations found in hAML, additional investigations focused on characterizing and validating cAML fusion genes/structural variations and their co-occurrence with SNV/indels are warranted. Additionally, the small sample size of our cohort (n=44) limited our statistical power for performing

enrichment analysis of variants across groups. Increasing the cohort size could improve our ability to make biologically meaningful and statistically significant observations.

In essence, the data presented provides insight into the genetic alterations of cAML and adds further credentials to the dog as a spontaneous model for hAML. We identified conserved recurrent molecular pathway alterations shared between the two species. Additionally, we suspect that even though dogs have unique somatic mutations in non-hAML associated genes, their effects likely converge on similar canonical cancer pathways, especially given the corresponding RNA-seq data analysis results. However, additional investigations are warranted to further interrogate the prevalence and functional impact of these mutations in cAML pathogenesis.

CONCLUSIONS

The heterogeneous nature of hAML, the diversity of recurrent mutations, and differences in biology between adult and pediatric neoplasms, make investigating targeted therapeutics challenging. The use of a canine model to interrogate the efficacy of novel therapies has proven to be beneficial in other oncologic research areas, such as primary bone, brain, and bladder cancers. It is conceivable that cAML patients could serve as a spontaneous large animal model for investigating targeted therapeutics if canonical cancer pathways are shared between the two species. Before researchers can utilize the canine model for AML research, a comprehensive understanding of the molecular features of cAML is needed. The goal of this work was to further investigate the molecular features of this poorly characterized canine cancer.

Prior to our investigations in chapter 1, very little was known about the overarching features of the canine hematopoietic system and differentiation pathways of hematopoietic cell subsets. In this work, we utilized single cell transcriptomic profiling of normal canine hematopoietic tissue to generate a reference database of healthy gene expression programs. Additionally, we compared these features with canonical features of human hematopoiesis. This database served as a reference for Chapter 3 investigations, where we inferred the cell type composition of cAML subgroups. This reference atlas may aid in additional studies investigating deviations from normal hematopoietic cell gene expression programs.

In chapter 2, we show the utility of using a targeted gene expression panel for distinguishing lineage of canine acute leukemias. We also correlated immunophenotyping results with the gene expression profile to formulate flow cytometric diagnostic criteria for classifying these tumors broadly into lymphoid vs. myeloid. We showed that the expression of CD14 and CD5 could distinguished cAML from cALL, respectively. Additional investigations are required

to validate our proposed criteria using a separate test cohort. Regardless, flow cytometry is widely available, and the proposed criteria could benefit other institutions who perform immunophenotyping of canine lymphomas/leukemias.

Studies implemented in Chapters 3 and 4 were devoted to gene expression and mutational profiling of cAML samples. Our results yielded commonalities shared between cAML and hAML. In particular, cAML samples appear to be enriched for genes associated with leukemogenesis and leukemic stem cells. Additionally, cAML samples overexpressed downstream targets of RAS genes and often had recurrent point mutations in *NRAS/KRAS* genes. Also, we described novel candidate mutations that have not been previously reported in canine leukemia/lymphoma. We noted that cAML samples were enriched for genes of pAML subtypes and have a similar distribution of variants as pAML-associated genes. However, while our initial research provides insight into the underlying features of cAML, additional studies are required to validate our results. Additionally, these studies likely do not capture the full spectrum of cAML, especially given how heterogeneous AML is in people. Focused investigations are required to pinpoint the underlying pathogenesis of cAML.

Overall, this work has helped improve our understanding of cAML in dogs. With this data in hand, we hope to focus future investigations on validating our results and test novel therapeutic to improve care for veterinary patients and further contribute to the field of comparative oncology.

REFERENCES

1. Cancer Statistics Review, 1975-2018 - SEER Statistics. Accessed November 4, 2021. https://seer.cancer.gov/csr/1975_2018/
2. Bottomly D, Long N, Schultz AR, et al. Integrative analysis of drug response and clinical outcome in acute myeloid leukemia. *Cancer Cell*. 2022;40(8):850-864.e9. doi:10.1016/J.CCELL.2022.07.002
3. Bennett AL, Williams LE, Ferguson MW, et al. Canine acute leukaemia: 50 cases (1989–2014). *Vet Comp Oncol*. Published online 2017. doi:10.1111/vco.12251
4. Davis LL, Hume KR, Stokol T. A retrospective review of acute myeloid leukaemia in 35 dogs diagnosed by a combination of morphologic findings, flow cytometric immunophenotyping and cytochemical staining results (2007-2015). *Vet Comp Oncol*. Published online 2018. doi:10.1111/vco.12377
5. Khoury JD, Solary E, Abla O, et al. The 5th edition of the World Health Organization Classification of Haematolymphoid Tumours: Myeloid and Histiocytic/Dendritic Neoplasms. *Leukemia*. 2022;36(7):1703-1719. doi:10.1038/S41375-022-01613-1
6. Tyner JW, Tognon CE, Bottomly D, et al. Functional genomic landscape of acute myeloid leukaemia. *Nat 2018 5627728*. 2018;562(7728):526-531. doi:10.1038/s41586-018-0623-z
7. Arber DA, Orazi A, Hasserjian R, et al. The 2016 revision to the World Health Organization classification of myeloid neoplasms and acute leukemia. *Blood*. Published online 2016. doi:10.1182/blood-2016-03-643544
8. Pulte D, Jansen L, Castro FA, et al. Survival in patients with acute myeloblastic leukemia in Germany and the United States: Major differences in survival in young adults. *Int J Cancer*. 2016;139(6):1289-1296. doi:10.1002/IJC.30186

9. Bolouri H, Farrar JE, Triche T, et al. The molecular landscape of pediatric acute myeloid leukemia reveals recurrent structural alterations and age-specific mutational interactions. *Nat Med 2017 241*. 2017;24(1):103-112. doi:10.1038/nm.4439

10. Chaudhury S, O'Connor C, Cañete A, et al. Age-specific biological and molecular profiling distinguishes paediatric from adult acute myeloid leukaemias. *Nat Commun*. 2018;9(1). doi:10.1038/S41467-018-07584-1

11. Aung MMK, Mills ML, Bittencourt-Silvestre J, Keeshan K. Insights into the molecular profiles of adult and paediatric acute myeloid leukaemia. *Mol Oncol*. 2021;15(9):2253-2272. doi:10.1002/1878-0261.12899

12. De Kouchkovsky I, Abdul-Hay M. 'Acute myeloid leukemia: a comprehensive review and 2016 update.' *Blood Cancer J 2016 67*. 2016;6(7):e441-e441. doi:10.1038/bcj.2016.50

13. Østgård LSG, Medeiros BC, Sengeløv H, et al. Epidemiology and clinical significance of secondary and therapy-related acute myeloid leukemia: A national population-based cohort study. *J Clin Oncol*. 2015;33(31):3641-3649. doi:10.1200/JCO.2014.60.0890

14. Hulegårdh E, Nilsson C, Lazarevic V, et al. Characterization and prognostic features of secondary acute myeloid leukemia in a population-based setting: A report from the Swedish Acute Leukemia Registry. *Am J Hematol*. 2015;90(3):208-214. doi:10.1002/AJH.23908

15. Song X, Peng Y, Wang X, et al. Incidence, Survival, and Risk Factors for Adults with Acute Myeloid Leukemia Not Otherwise Specified and Acute Myeloid Leukemia with Recurrent Genetic Abnormalities: Analysis of the Surveillance, Epidemiology, and End Results (SEER) Database, 2001-2013. *Acta Haematol*. 2018;139(2):115-127. doi:10.1159/000486228

16. Appelbaum FR, Gundacker H, Head DR, et al. Age and acute myeloid leukemia. *Blood*. 2006;107(9):3481-3485. doi:10.1182/BLOOD-2005-09-3724

17. Juliusson G, Antunovic P, Derolf Å, et al. Age and acute myeloid leukemia: Real world data on decision to treat and outcomes from the Swedish Acute Leukemia Registry. *Blood*. 2009;113(18):4179-4187. doi:10.1182/BLOOD-2008-07-172007

18. Chaudhury SS, Morison JK, Gibson BES, Keeshan K. Insights into cell ontogeny, age, and acute myeloid leukemia. *Exp Hematol*. 2015;43(9):745-755. doi:10.1016/J.EXPHEM.2015.05.008

19. Gibson BES, Webb DKH, Howman AJ, de Graaf SSN, Harrison CJ, Wheatley K. Results of a randomized trial in children with Acute Myeloid Leukaemia: medical research council AML12 trial. *Br J Haematol*. 2011;155(3):366-376. doi:10.1111/J.1365-2141.2011.08851.X

20. Döhner H, Estey E, Grimwade D, et al. Diagnosis and management of AML in adults: 2017 ELN recommendations from an international expert panel. *Blood*. 2017;129(4):424-447. doi:10.1182/BLOOD-2016-08-733196

21. Klein K, de Haas V, Kaspers GJL. Clinical challenges in de novo pediatric acute myeloid leukemia. *Expert Rev Anticancer Ther*. 2018;18(3):277-293. doi:10.1080/14737140.2018.1428091

22. Krug U, Röllig C, Koschmieder A, et al. Complete remission and early death after intensive chemotherapy in patients aged 60 years or older with acute myeloid leukaemia: a web-based application for prediction of outcomes. *Lancet (London, England)*. 2010;376(9757):2000-2008. doi:10.1016/S0140-6736(10)62105-8

23. Gamis AS, Alonzo TA, Meshinchi S, et al. Gemtuzumab ozogamicin in children and

adolescents with de novo acute myeloid leukemia improves event-free survival by reducing relapse risk: Results from the randomized phase iII children's oncology group Trial AAML0531. *J Clin Oncol*. 2014;32(27):3021-3032. doi:10.1200/JCO.2014.55.3628

24. McNeer NA, Philip J, Geiger H, et al. Genetic mechanisms of primary chemotherapy resistance in pediatric acute myeloid leukemia. *Leukemia*. 2019;33(8):1934. doi:10.1038/S41375-019-0402-3

25. Therapeutically Applicable Research to Generate Effective Treatments (TARGET). Accessed September 8, 2022. https://ocg.cancer.gov/programs/target

26. Beat AML Functional Genomic Study - NCI. Accessed September 8, 2022. https://www.cancer.gov/about-nci/organization/ccg/blog/2019/beataml

27. Davis LL, Hume KR, Stokol T. A retrospective review of acute myeloid leukaemia in 35 dogs diagnosed by a combination of morphologic findings, flow cytometric immunophenotyping and cytochemical staining results (2007-2015). *Vet Comp Oncol*. 2018;16(2):268-275. doi:10.1111/VCO.12377

28. Burd A, Levine RL, Ruppert AS, et al. Precision medicine treatment in acute myeloid leukemia using prospective genomic profiling: feasibility and preliminary efficacy of the Beat AML Master Trial. *Nat Med*. 2020;26(12):1852-1858. doi:10.1038/S41591-020-1089-8

29. TJ L, C M, L D, et al. Genomic and epigenomic landscapes of adult de novo acute myeloid leukemia. *N Engl J Med*. 2013;368(22):2059-2074. doi:10.1056/NEJMOA1301689

30. Papaemmanuil E, Gerstung M, Bullinger L, et al. Genomic Classification and Prognosis in Acute Myeloid Leukemia. *N Engl J Med*. 2016;374(23):2209-2221.

doi:10.1056/NEJMOA1516192

31. Mardis ER, Ding L, Dooling DJ, et al. Recurring mutations found by sequencing an acute myeloid leukemia genome. *undefined*. 2009;361(11):1058-1066. doi:10.1056/NEJMOA0903840

32. Naoe T, Kiyoi H. Gene mutations of acute myeloid leukemia in the genome era. *Int J Hematol*. 2013;97(2):165-174. doi:10.1007/S12185-013-1257-4

33. Lawrence MS, Stojanov P, Polak P, et al. Mutational heterogeneity in cancer and the search for new cancer-associated genes. *Nature*. 2013;499(7457):214-218. doi:10.1038/NATURE12213

34. Wen XM, Xu ZJ, Jin Y, et al. Association Analyses of TP53 Mutation With Prognosis, Tumor Mutational Burden, and Immunological Features in Acute Myeloid Leukemia. *Front Immunol*. 2021;12:4283. doi:10.3389/FIMMU.2021.717527/BIBTEX

35. Bolouri H, Farrar JE, Triche T, et al. The molecular landscape of pediatric acute myeloid leukemia reveals recurrent structural alterations and age-specific mutational interactions. *Nat Med*. 2018;24(1):103-112. doi:10.1038/NM.4439

36. Minucci S, Maccarana M, Cioce M, et al. Oligomerization of RAR and AML1 transcription factors as a novel mechanism of oncogenic activation. *Mol Cell*. 2000;5(5):811-820. doi:10.1016/S1097-2765(00)80321-4

37. Lin RJ, Evans RM. Acquisition of oncogenic potential by RAR chimeras in acute promyelocytic leukemia through formation of homodimers. *Mol Cell*. 2000;5(5):821-830. doi:10.1016/S1097-2765(00)80322-6

38. Liquori A, Ibañez M, Sargas C, Sanz MÁ, Barragán E, Cervera J. Acute Promyelocytic Leukemia: A Constellation of Molecular Events around a Single PML-RARA Fusion

Gene. *Cancers (Basel)*. 2020;12(3). doi:10.3390/CANCERS12030624

39. Grisolano JL, Wesselschmidt RL, Pelicci PG, Ley TJ. Altered Myeloid Development and Acute Leukemia in Transgenic Mice Expressing PML-RARα Under Control of Cathepsin G Regulatory Sequences. *Blood*. 1997;89(2):376-387. doi:10.1182/BLOOD.V89.2.376

40. He LZ, Tribioli C, Rivi R, et al. Acute leukemia with promyelocytic features in PML/RARalpha transgenic mice. *Proc Natl Acad Sci U S A*. 1997;94(10):5302-5307. doi:10.1073/PNAS.94.10.5302

41. Grinev V V., Barneh F, Ilyushonak IM, et al. RUNX1/RUNX1T1 mediates alternative splicing and reorganises the transcriptional landscape in leukemia. *Nat Commun*. 2021;12(1). doi:10.1038/S41467-020-20848-Z

42. Gardini A, Cesaroni M, Luzi L, et al. AML1/ETO oncoprotein is directed to AML1 binding regions and co-localizes with AML1 and HEB on its targets. *PLoS Genet*. 2008;4(11). doi:10.1371/JOURNAL.PGEN.1000275

43. Ptasinska A, Assi SA, Mannari D, et al. Depletion of RUNX1/ETO in t(8;21) AML cells leads to genome-wide changes in chromatin structure and transcription factor binding. *Leukemia*. 2012;26(8):1829-1841. doi:10.1038/LEU.2012.49

44. Castilla LH, Perrat P, Martinez NJ, et al. Identification of genes that synergize with Cbfb-MYH11 in the pathogenesis of acute myeloid leukemia. *Proc Natl Acad Sci U S A*. 2004;101(14):4924. doi:10.1073/PNAS.0400930101

45. Foucar K, Reichard K, Czuchlewski D. Bone marrow pathology. :933.

46. Gary Gilliland D, Griffin JD. The roles of FLT3 in hematopoiesis and leukemia. *Blood*. 2002;100(5):1532-1542. doi:10.1182/BLOOD-2002-02-0492

47. Kao HW, Liang DC, Wu JH, et al. Gene mutation patterns in patients with minimally

differentiated acute myeloid leukemia. *Neoplasia*. 2014;16(6):481-488. doi:10.1016/J.NEO.2014.06.002

48. Lavau C, Luo RT, Du C, Thirman MJ. Retrovirus-mediated gene transfer of MLL-ELL transforms primary myeloid progenitors and causes acute myeloid leukemias in mice. *undefined*. 2000;97(20):10984-10989. doi:10.1073/PNAS.190167297

49. Castilla LH, Wijmenga C, Wang Q, et al. Failure of embryonic hematopoiesis and lethal hemorrhages in mouse embryos heterozygous for a knocked-in leukemia gene CBFB-MYH11. *Cell*. 1996;87(4):687-696. doi:10.1016/S0092-8674(00)81388-4

50. Papaemmanuil E, Gerstung M, Bullinger L, et al. Genomic Classification and Prognosis in Acute Myeloid Leukemia. *N Engl J Med*. 2016;374(23):2209-2221. doi:10.1056/NEJMOA1516192/SUPPL_FILE/NEJMOA1516192_DISCLOSURES.PDF

51. Jaiswal S, Fontanillas P, Flannick J, et al. Age-Related Clonal Hematopoiesis Associated with Adverse Outcomes. *N Engl J Med*. 2014;371(26):2488-2498. doi:10.1056/NEJMoa1408617

52. Xie M, Lu C, Wang J, et al. Age-related mutations associated with clonal hematopoietic expansion and malignancies. *Nat Med*. 2014;20(12):1472-1478. doi:10.1038/nm.3733

53. Genovese G, Kähler AK, Handsaker RE, et al. Clonal Hematopoiesis and Blood-Cancer Risk Inferred from Blood DNA Sequence. *N Engl J Med*. 2014;371(26):2477-2487. doi:10.1056/NEJMoa1409405

54. Arends CM, Galan-Sousa J, Hoyer K, et al. Hematopoietic lineage distribution and evolutionary dynamics of clonal hematopoiesis. *Leukemia*. 2018;32(9):1908-1919. doi:10.1038/s41375-018-0047-7

55. Morita K, Wang F, Jahn K, et al. Clonal evolution of acute myeloid leukemia revealed by

high-throughput single-cell genomics. *Nat Commun*. 2020;11(1). doi:10.1038/S41467-020-19119-8

56. Bochtler T, StolÏzel F, Heilig CE, et al. Clonal heterogeneity as detected by metaphase karyotyping is an indicator of poor prognosis in acute myeloid leukemia. *J Clin Oncol*. 2013;31(31):3898-3905. doi:10.1200/JCO.2013.50.7921

57. Medeiros BC, Othus M, Fang M, Appelbaum FR, Erba HP. Cytogenetic heterogeneity negatively impacts outcomes in patients with acute myeloid leukemia. *Haematologica*. 2015;100(3):331-335. doi:10.3324/HAEMATOL.2014.117267

58. Lindsley RC, Mar BG, Mazzola E, et al. Acute myeloid leukemia ontogeny is defined by distinct somatic mutations. *Blood*. 2015;125(9):1367-1376. doi:10.1182/BLOOD-2014-11-610543

59. Farrar JE, Schuback HL, Ries RE, et al. Genomic profiling of pediatric acute myeloid leukemia reveals a changing mutational landscape from disease diagnosis to relapse. *Cancer Res*. 2016;76(8):2197-2205. doi:10.1158/0008-5472.CAN-15-1015/652018/AM/GENOMIC-PROFILING-OF-PEDIATRIC-ACUTE-MYELOID

60. Ho PA, Kutny MA, Alonzo TA, et al. Leukemic mutations in the methylation-associated genes DNMT3A and IDH2 are rare events in pediatric AML: a report from the Children's Oncology Group. *Pediatr Blood Cancer*. 2011;57(2):204-209. doi:10.1002/PBC.23179

61. Bullinger L, Döhner K, Bair E, et al. Use of Gene-Expression Profiling to Identify Prognostic Subclasses in Adult Acute Myeloid Leukemia. *N Engl J Med*. 2004;350(16):1605-1616. doi:10.1056/NEJMOA031046/SUPPL_FILE/NEJM_BULLINGER_1605SA1-7.PDF

62. Walker CJ, Mrózek K, Ozer HG, et al. Gene expression signature predicts relapse in adult

patients with cytogenetically normal acute myeloid leukemia. *Blood Adv*. 2021;5(5):1474. doi:10.1182/BLOODADVANCES.2020003727

63. Verhaak RGW, Wouters BJ, Erpelinck CAJ, et al. Prediction of molecular subtypes in acute myeloid leukemia based on gene expression profiling. *Haematologica*. 2009;94(1):131. doi:10.3324/HAEMATOL.13299

64. Golub TR, Slonim DK, Tamayo P, et al. Molecular classification of cancer: Class discovery and class prediction by gene expression monitoring. *Science (80-)*. Published online 1999. doi:10.1126/science.286.5439.531

65. Ng SWK, Mitchell A, Kennedy JA, et al. A 17-gene stemness score for rapid determination of risk in acute leukaemia. *Nature*. 2016;540(7633):433-437. doi:10.1038/nature20598

66. Ng SWK, Murphy T, King I, et al. A clinical laboratory-developed LSC17 stemness score assay for rapid risk assessment of patients with acute myeloid leukemia. *Blood Adv*. 2022;6(3):1064-1073. doi:10.1182/BLOODADVANCES.2021005741

67. Elsayed AH, Rafiee R, Cao X, et al. A six-gene leukemic stem cell score identifies high risk pediatric acute myeloid leukemia. *Leuk 2019 343*. 2019;34(3):735-745. doi:10.1038/s41375-019-0604-8

68. Bennett JM, Catovsky D, Daniel M -T, et al. Proposals for the classification of the acute leukaemias. French-American-British (FAB) co-operative group. *Br J Haematol*. 1976;33(4):451-458. doi:10.1111/J.1365-2141.1976.TB03563.X

69. Bennett JM, Catovsky D, Daniel MT, et al. Proposed revised criteria for the classification of acute myeloid leukemia. A report of the French-American-British Cooperative Group. *Ann Intern Med*. 1985;103(4):620-625. doi:10.7326/0003-4819-103-4-620

70. Rousselot P, Hardas B, Patel A, et al. The PML-RAR alpha gene product of the t(15;17) translocation inhibits retinoic acid-induced granulocytic differentiation and mediated transactivation in human myeloid cells. *Oncogene*. 1994;9(2):545-551. Accessed December 5, 2022. https://europepmc.org/article/med/8290265

71. Paulson K, Serebrin A, Lambert P, et al. Acute promyelocytic leukaemia is characterized by stable incidence and improved survival that is restricted to patients managed in leukaemia referral centres: a pan-Canadian epidemiological study. *Br J Haematol*. 2014;166(5):660-666. doi:10.1111/BJH.12931

72. Kayser S, Schlenk RF, Platzbecker U. Management of patients with acute promyelocytic leukemia. *Leukemia*. 2018;32(6):1277-1294. doi:10.1038/S41375-018-0139-4

73. Rahmé R, Thomas X, Recher C, et al. Early death in acute promyelocytic leukemia (APL) in French centers: a multicenter study in 399 patients. *Leukemia*. 2014;28(12):2422-2424. doi:10.1038/LEU.2014.240

74. Tazi Y, Arango-Ossa JE, Zhou Y, et al. Unified classification and risk-stratification in Acute Myeloid Leukemia. *Nat Commun*. 2022;13(1). doi:10.1038/S41467-022-32103-8

75. Bersanelli M, Travaglino E, Meggendorfer M, et al. Classification and Personalized Prognostic Assessment on the Basis of Clinical and Genomic Features in Myelodysplastic Syndromes. *J Clin Oncol*. 2021;39(11):1223-1233. doi:10.1200/JCO.20.01659

76. Estey E, Hasserjian RP, Döhner H. Distinguishing AML from MDS: a fixed blast percentage may no longer be optimal. *Blood*. 2022;139(3):323-332. doi:10.1182/BLOOD.2021011304

77. Buccisano F, Maurillo L, Spagnoli A, et al. Cytogenetic and molecular diagnostic characterization combined to postconsolidation minimal residual disease assessment by

flow cytometry improves risk stratification in adult acute myeloid leukemia. *Blood*. 2010;116(13):2295-2303. doi:10.1182/BLOOD-2009-12-258178

78. Loken MR, Alonzo TA, Pardo L, et al. Residual disease detected by multidimensional flow cytometry signifies high relapse risk in patients with de novo acute myeloid leukemia: a report from Children's Oncology Group. *Blood*. 2012;120(8):1581-1588. doi:10.1182/BLOOD-2012-02-408336

79. Weinberg OK, Arber DA. Mixed-phenotype acute leukemia: historical overview and a new definition. *Leuk 2010 2411*. 2010;24(11):1844-1851. doi:10.1038/leu.2010.202

80. Weir EG, Ali Ansari-Lari M, Batista DAS, et al. Acute bilineal leukemia: a rare disease with poor outcome. *Leukemia*. 2007;21(11):2264-2270. doi:10.1038/SJ.LEU.2404848

81. Charles NJ, Boyer DF. Mixed-Phenotype Acute Leukemia: Diagnostic Criteria and Pitfalls. *Arch Pathol Lab Med*. 2017;141(11):1462-1468. doi:10.5858/ARPA.2017-0218-RA

82. Alexander TB, Gu Z, Iacobucci I, et al. The genetic basis and cell of origin of mixed phenotype acute leukaemia. *Nature*. 2018;562(7727):373-406. doi:10.1038/S41586-018-0436-0

83. Kobayashi R, Tawa A, Hanada R, Horibe K, Tsuchida M, Tsukimoto I. Extramedullary infiltration at diagnosis and prognosis in children with acute myelogenous leukemia. *Pediatr Blood Cancer*. 2007;48(4):393-398. doi:10.1002/PBC.20824

84. Kantarjian H, O'Brisn S, Cortes J, et al. Results of intensive chemotherapy in 998 patients age 65 years or older with acute myeloid leukemia or high-risk myelodysplastic syndrome: *Cancer*. 2006;106(5):1090-1098. doi:10.1002/CNCR.21723

85. Khan AM, Lancet JE, Kharfan-Dabaja MA, Al Ali NH, List AF, Komrokji RS. Albumin

Is a Prognostic Factor for Overall Survival in Newly Diagnosed Patients with Acute Myeloid Leukemia (AML). *Blood*. 2011;118(21):4253-4253. doi:10.1182/BLOOD.V118.21.4253.4253

86. Kumar S, Dispenzieri A, Lacy MQ, et al. Serum uric acid: novel prognostic factor in primary systemic amyloidosis. *Mayo Clin Proc*. 2008;83(3):297-303. doi:10.4065/83.3.297

87. Xu W, Wang YH, Fan L, et al. Prognostic significance of serum immunoglobulin paraprotein in patients with chronic lymphocytic leukemia. *Leuk Res*. 2011;35(8):1060-1065. doi:10.1016/J.LEUKRES.2010.12.005

88. Ferrara F, Mirto S. Serum LDH value as a predictor of clinical outcome in acute myelogenous leukaemia of the elderly. *Br J Haematol*. 1996;92(3):627-631. doi:10.1046/J.1365-2141.1996.00398.X

89. Walter RB, Othus M, Borthakur G, et al. Prediction of early death after induction therapy for newly diagnosed acute myeloid leukemia with pretreatment risk scores: a novel paradigm for treatment assignment. *J Clin Oncol*. 2011;29(33):4417-4424. doi:10.1200/JCO.2011.35.7525

90. Mrożek K, Marcucci G, Nicolet D, et al. Prognostic significance of the European LeukemiaNet standardized system for reporting cytogenetic and molecular alterations in adults with acute myeloid leukemia. *J Clin Oncol*. 2012;30(36):4515-4523. doi:10.1200/JCO.2012.43.4738

91. Döhner H, Estey EH, Amadori S, et al. Diagnosis and management of acute myeloid leukemia in adults: recommendations from an international expert panel, on behalf of the European LeukemiaNet. *Blood*. 2010;115(3):453-474. doi:10.1182/BLOOD-2009-07-

235358

92. Welch JS, Ley TJ, Link DC, et al. The origin and evolution of mutations in Acute Myeloid Leukemia. *Cell*. 2012;150(2):264. doi:10.1016/J.CELL.2012.06.023

93. Adam F, Villiers E, Watson S, Coyne K, Blackwood L. Clinical pathological and epidemiological assessment of morphologically and immunologically confirmed canine leukaemia. *Vet Comp Oncol*. Published online 2009. doi:10.1111/j.1476-5829.2009.00189.x

94. Novacco M, Comazzi S, Marconato L, et al. Prognostic factors in canine acute leukaemias: a retrospective study. *Vet Comp Oncol*. Published online 2016. doi:10.1111/vco.12136

95. Tasca S, Carli E, Caldin M, Menegazzo L, Furlanello T, Gallego LS. Hematologic abnormalities and flow cytometric immunophenotyping results in dogs with hematopoietic neoplasia: 210 cases (2002-2006). *Vet Clin Pathol*. Published online 2009. doi:10.1111/j.1939-165X.2008.00099.x

96. Harris RA, Rout ED, Yoshimoto JA, Avery PR, Avery AC. Using digital RNA counting to establish flow cytometry diagnostic criteria for subtypes of CD34+ canine acute leukaemia. *Vet Comp Oncol*. 2022;20(3):710-719. doi:10.1111/VCO.12825

97. Stokol T, Schaefer DM, Shuman M, Belcher N, Dong L. Alkaline phosphatase is a useful cytochemical marker for the diagnosis of acute myelomonocytic and monocytic leukemia in the dog. *Vet Clin Pathol*. 2015;44(1):79-93. doi:10.1111/vcp.12227

98. Villiers E, Baines S, Law A-M, Mallows V. Identification of acute myeloid leukemia in dogs using flow cytometry with myeloperoxidase, MAC387, and a canine neutrophil-specific antibody. *Vet Clin Pathol*. 2006;35(1):55-71. doi:10.1111/j.1939-

165X.2006.tb00089.x

99. Bennett AL, Williams LE, Ferguson MW, et al. Canine acute leukaemia: 50 cases (1989–2014). *Vet Comp Oncol*. 2017;15(3):1101-1114. doi:10.1111/VCO.12251

100. McManus PM, Hess RS. Myelodysplastic changes in a dog with subsequent acute myeloid leukemia. *Vet Clin Pathol*. 1998;27(4):112-115. doi:10.1111/J.1939-165X.1998.TB01029.X

101. Tolle D V., Seed TM, Fritz TE, Lombard LS, Poole CM, Norris WP. Acute Monocytic Leukemia in an Irradiated Beagle. *http://dx.doi.org/101177/030098587901600210*. 2016;16(2):243-254. doi:10.1177/030098587901600210

102. Jain NC, Blue JT, Grindem CB, et al. Proposed criteria for classification of acute myeloid leukemia in dogs and cats. *Vet Clin Pathol*. 1991;20(3):63-82. doi:10.1111/J.1939-165X.1991.TB00571.X

103. Stokol T, Nickerson GA, Shuman M, Belcher N. Dogs with acute myeloid leukemia have clonal rearrangements in T and B cell receptors. *Front Vet Sci*. Published online 2017. doi:10.3389/fvets.2017.00076

104. Epperly E, Hume KR, Moirano S, et al. Dogs with acute myeloid leukemia or lymphoid neoplasms (large cell lymphoma or acute lymphoblastic leukemia) may have indistinguishable mediastinal masses on radiographs. *Vet Radiol Ultrasound*. 2018;59(5):507-515. doi:10.1111/VRU.12622

105. Froment R, Bédard C. Marked hyperphosphatasemia associated with an acute leukemia in a Great Dane. *Vet Clin Pathol*. 2016;45(3):459-465. doi:10.1111/VCP.12389

106. Tan E, Abrams-Ogg ACG, Defarges A, Bienzle D. Automated analysis of bone marrow aspirates from dogs with haematological disorders. *J Comp Pathol*. 2014;151(1):67-79.

doi:10.1016/J.JCPA.2014.02.005

107. Miglio A, Antognoni MT, Miniscalco B, et al. Acute undifferentiated leukaemia in a dog. *Aust Vet J*. 2014;92(12):499-503. doi:10.1111/AVJ.12273

108. Figueiredo JF, Culver S, Behling-Kelly E, Breen M, Friedrichs KR. Acute myeloblastic leukemia with associated BCR-ABL translocation in a dog. *Vet Clin Pathol*. 2012;41(3):362-368. doi:10.1111/J.1939-165X.2012.00450.X

109. Gelain ME, Martini V, Giantin M, et al. CD44 in canine leukemia: analysis of mRNA and protein expression in peripheral blood. *Vet Immunol Immunopathol*. 2014;159(1-2):91-96. doi:10.1016/J.VETIMM.2014.02.008

110. Bronzini I, Aresu L, Paganin M, et al. DNA methylation and targeted sequencing of methyltransferases family genes in canine acute myeloid leukaemia, modelling human myeloid leukaemia. *Vet Comp Oncol*. Published online 2017. doi:10.1111/vco.12231

111. Rochel D, Abadie J, Robveille C, et al. Thrombocytosis and central nervous system involvement in a case of canine acute megakaryoblastic leukemia. *Vet Clin Pathol*. 2018;47(3):363-367. doi:10.1111/VCP.12642

112. Nair M, Kusumakumary P, Nair PS. Acute myeloid leukemia presenting as mediastinal mass. *Indian J Pediatr*. 2014;81(8):824-825. doi:10.1007/S12098-013-1121-9

113. Ganzel C, Manola J, Douer D, et al. Extramedullary disease in adult acute myeloid leukemia is common but lacks independent significance: Analysis of patients in ECOG-ACRIN cancer research group trials, 1980-2008. *J Clin Oncol*. 2016;34(29):3544-3553. doi:10.1200/JCO.2016.67.5892

114. Usher SG, Radford AD, Villiers EJ, Blackwood L. RAS, FLT3, and C-KIT mutations in immunophenotyped canine leukemias. *Exp Hematol*. Published online 2009.

doi:10.1016/j.exphem.2008.09.005

115. Daver N, Wei AH, Pollyea DA, Fathi AT, Vyas P, DiNardo CD. New directions for emerging therapies in acute myeloid leukemia: the next chapter. *Blood Cancer J*. 2020;10(10). doi:10.1038/S41408-020-00376-1

116. Döhner H, Estey E, Grimwade D, et al. Diagnosis and management of AML in adults: 2017 ELN recommendations from an international expert panel. *Blood*. 2017;129(4):424-447. doi:10.1182/BLOOD-2016-08-733196

117. DiNardo CD, Jonas BA, Pullarkat V, et al. Azacitidine and Venetoclax in Previously Untreated Acute Myeloid Leukemia. *N Engl J Med*. 2020;383(7):617-629. doi:10.1056/NEJMOA2012971

118. Vail DM, Thamm DH, Liptak JM. Withrow and MacEwen's Small Animal Clinical Oncology. *Withrow MacEwen's Small Anim Clin Oncol*. Published online December 15, 2006:1-842. doi:10.1016/C2016-0-01939-3

119. Suter SE, Hamilton MJ, Sullivan EW, Venkataraman GM. Allogeneic hematopoietic cell transplantation in a dog with acute large granular lymphocytic leukemia. *J Am Vet Med Assoc*. 2015;246(9):994-997. doi:10.2460/JAVMA.246.9.994

120. Nestorowa S, Hamey FK, Pijuan Sala B, et al. A single-cell resolution map of mouse hematopoietic stem and progenitor cell differentiation. *Blood*. 2016;128(8):e20-e31. doi:10.1182/BLOOD-2016-05-716480

121. Velten L, Haas SF, Raffel S, et al. Human haematopoietic stem cell lineage commitment is a continuous process. *Nat Cell Biol 2017 194*. 2017;19(4):271-281. doi:10.1038/ncb3493

122. Haas S, Trumpp A, Milsom MD. Causes and Consequences of Hematopoietic Stem Cell

Heterogeneity. *Cell Stem Cell*. 2018;22(5):627-638. doi:10.1016/J.STEM.2018.04.003

123. Chao MP, Seita J, Weissman IL. Establishment of a normal hematopoietic and leukemia stem cell hierarchy. *Cold Spring Harb Symp Quant Biol*. 2008;73:439-449. doi:10.1101/SQB.2008.73.031

124. Kondo M, Weissman IL, Akashi K. Identification of clonogenic common lymphoid progenitors in mouse bone marrow. *Cell*. 1997;91(5):661-672. doi:10.1016/S0092-8674(00)80453-5

125. Akashi K, Traver D, Miyamoto T, Weissman IL. A clonogenic common myeloid progenitor that gives rise to all myeloid lineages. *Nature*. 2000;404(6774):193-197. doi:10.1038/35004599

126. Notta F, Zandi S, Takayama N, et al. Distinct routes of lineage development reshape the human blood hierarchy across ontogeny. *Science*. 2016;351(6269). doi:10.1126/SCIENCE.AAB2116

127. Haas S. Hematopoietic Stem Cells in Health and Disease—Insights from Single-Cell Multi-omic Approaches. *Curr Stem Cell Reports*. 2020;6(3):67-76. doi:10.1007/S40778-020-00174-2/FIGURES/1

128. Triana S, Vonficht D, Jopp-Saile L, et al. Single-cell proteo-genomic reference maps of the hematopoietic system enable the purification and massive profiling of precisely defined cell states. *Nat Immunol*. 2021;22(12):1577-1589. doi:10.1038/S41590-021-01059-0

129. Wu M, Kwon HY, Rattis F, et al. Imaging hematopoietic precursor division in real time. *Cell Stem Cell*. 2007;1(5):541-554. doi:10.1016/J.STEM.2007.08.009

130. Baldridge MT, King KY, Boles NC, Weksberg DC, Goodell MA. Quiescent

haematopoietic stem cells are activated by IFN-gamma in response to chronic infection. *Nature*. 2010;465(7299):793-797. doi:10.1038/NATURE09135

131. Essers MAG, Offner S, Blanco-Bose WE, et al. IFNα activates dormant haematopoietic stem cells in vivo. *Nat 2009 4587240*. 2009;458(7240):904-908. doi:10.1038/nature07815

132. van Galen P, Hovestadt V, Wadsworth MH, et al. Single-cell RNA-seq reveals AML hierarchies relevant to disease progression and immunity. *Cell*. 2019;176(6):1265. doi:10.1016/J.CELL.2019.01.031

133. Velten L, Story BA, Hernández-Malmierca P, et al. Identification of leukemic and pre-leukemic stem cells by clonal tracking from single-cell transcriptomics. *Nat Commun*. 2021;12(1). doi:10.1038/S41467-021-21650-1

134. Kowalczyk MS, Tirosh I, Heckl D, et al. Single-cell RNA-seq reveals changes in cell cycle and differentiation programs upon aging of hematopoietic stem cells. *Genome Res*. 2015;25(12):1860-1872. doi:10.1101/GR.192237.115

135. Pellin D, Loperfido M, Baricordi C, et al. A comprehensive single cell transcriptional landscape of human hematopoietic progenitors. *Nat Commun*. 2019;10(1). doi:10.1038/S41467-019-10291-0

136. Xie X, Liu M, Zhang Y, et al. Single-cell transcriptomic landscape of human blood cells. *Natl Sci Rev*. 2020;8(3). doi:10.1093/NSR/NWAA180

137. Roy A, Wang G, Iskander D, et al. Transitions in lineage specification and gene regulatory networks in hematopoietic stem/progenitor cells over human development. *Cell Rep*. 2021;36(11). doi:10.1016/J.CELREP.2021.109698

138. Dolgalev I, Tikhonova AN. Connecting the Dots: Resolving the Bone Marrow Niche Heterogeneity. *Front cell Dev Biol*. 2021;9. doi:10.3389/FCELL.2021.622519

139. Hay SB, Ferchen K, Chetal K, Grimes HL, Salomonis N. The Human Cell Atlas bone marrow single-cell interactive web portal. *Exp Hematol*. 2018;68:51-61. doi:10.1016/J.EXPHEM.2018.09.004

140. Stuart T, Butler A, Hoffman P, et al. Comprehensive Integration of Single-Cell Data Resource Comprehensive Integration of Single-Cell Data. *Cell*. 2019;177. doi:10.1016/j.cell.2019.05.031

141. Azimuth. Accessed February 3, 2023. https://azimuth.hubmapconsortium.org/

142. Ayers J, Milner RJ, Cortés-Hinojosa G, et al. Novel application of single-cell next-generation sequencing for determination of intratumoral heterogeneity of canine osteosarcoma cell lines. *J Vet Diagn Invest*. 2021;33(2):261-278. doi:10.1177/1040638720985242

143. Vandamme C, Rytkönen-Nissinen M, Lönnberg T, et al. Single-cell characterization of dog allergen–specific T cells reveals TH2 heterogeneity in allergic individuals. *J Allergy Clin Immunol*. 2022;149(5):1732-1743.e15. doi:10.1016/J.JACI.2021.11.018

144. Gingrich AA, Reiter TE, Judge SJ, et al. Comparative Immunogenomics of Canine Natural Killer Cells as Immunotherapy Target. *Front Immunol*. 2021;12:3721. doi:10.3389/FIMMU.2021.670309/BIBTEX

145. Chen D, Sun J, Zhu J, et al. Single cell atlas for 11 non-model mammals, reptiles and birds. *Nat Commun 2021 121*. 2021;12(1):1-17. doi:10.1038/s41467-021-27162-2

146. Fastrès A, Pirottin D, Fievez L, et al. Characterization of the Bronchoalveolar Lavage Fluid by Single Cell Gene Expression Analysis in Healthy Dogs: A Promising Technique. *Front Immunol*. 2020;11:1707. doi:10.3389/FIMMU.2020.01707/BIBTEX

147. Jackson K, Milner RJ, Doty A, et al. Analysis of canine myeloid-derived suppressor cells

(MDSCs) utilizing fluorescence-activated cell sorting, RNA protection mediums to yield quality RNA for single-cell RNA sequencing. *Vet Immunol Immunopathol*. 2021;231. doi:10.1016/J.VETIMM.2020.110144

148. Fastrès A, Pirottin D, Fievez L, et al. Identification of Pro-Fibrotic Macrophage Populations by Single-Cell Transcriptomic Analysis in West Highland White Terriers Affected With Canine Idiopathic Pulmonary Fibrosis. *Front Immunol*. 2020;11:3313. doi:10.3389/FIMMU.2020.611749/BIBTEX

149. Cambien B, Lebrigand K, Baeri A, et al. Identification of oncolytic vaccinia restriction factors in canine high-grade mammary tumor cells using single-cell transcriptomics. *PLoS Pathog*. 2020;16(10). doi:10.1371/JOURNAL.PPAT.1008660

150. Früh SP, Saikia M, Eule J, et al. Elevated circulating Th2 but not group 2 innate lymphoid cell responses characterize canine atopic dermatitis. *Vet Immunol Immunopathol*. 2020;221. doi:10.1016/J.VETIMM.2020.110015

151. Satija R, Farrell JA, Gennert D, Schier AF, Regev A. Spatial reconstruction of single-cell gene expression data. *Nat Biotechnol*. 2015;33(5):495-502. doi:10.1038/NBT.3192

152. McGinnis CS, Murrow LM, Gartner ZJ. DoubletFinder: Doublet Detection in Single-Cell RNA Sequencing Data Using Artificial Nearest Neighbors. *Cell Syst*. 2019;8(4):329-337.e4. doi:10.1016/J.CELS.2019.03.003

153. Zappia L, Oshlack A. Clustering trees: a visualization for evaluating clusterings at multiple resolutions. *Gigascience*. 2018;7(7):1-9. doi:10.1093/GIGASCIENCE/GIY083

154. Rotta R, Noack A. Multilevel local search algorithms for modularity clustering. *ACM Ref Format*. 2011;16(2):27. doi:10.1145/1963190.1970376

155. Aran D, Looney AP, Liu L, et al. Reference-based analysis of lung single-cell sequencing

reveals a transitional profibrotic macrophage. *Nat Immunol*. 2019;20(2):163-172. doi:10.1038/S41590-018-0276-Y

156. Kuleshov M V., Jones MR, Rouillard AD, et al. Enrichr: a comprehensive gene set enrichment analysis web server 2016 update. *Nucleic Acids Res*. 2016;44(W1):W90-W97. doi:10.1093/NAR/GKW377

157. Liberzon A, Subramanian A, Pinchback R, Thorvaldsdóttir H, Tamayo P, Mesirov JP. Molecular signatures database (MSigDB) 3.0. *Bioinformatics*. 2011;27(12):1739-1740. doi:10.1093/BIOINFORMATICS/BTR260

158. Love MI, Huber W, Anders S. Moderated estimation of fold change and dispersion for RNA-seq data with DESeq2. *Genome Biol*. 2014;15(12):1-21. doi:10.1186/S13059-014-0550-8/FIGURES/9

159. Cao J, Spielmann M, Qiu X, et al. The single-cell transcriptional landscape of mammalian organogenesis. *Nat 2019 5667745*. 2019;566(7745):496-502. doi:10.1038/s41586-019-0969-x

160. Tirosh I, Izar B, Prakadan SM, et al. Dissecting the multicellular ecosystem of metastatic melanoma by single-cell RNA-seq. *Science (80-)*. 2016;352(6282):189-196. doi:10.1126/SCIENCE.AAD0501/SUPPL_FILE/TIROSH.SM.PDF

161. Vagapova ER, Spirin P V., Lebedev TD, Prassolov VS. The Role of TAL1 in Hematopoiesis and Leukemogenesis. *Acta Naturae*. 2018;10(1):15. doi:10.32607/20758251-2018-10-1-15-23

162. Welinder E, Mansson R, Mercer EM, Bryder D, Sigvardsson M, Murre C. The transcription factors E2A and HEB act in concert to induce the expression of FOXO1 in the common lymphoid progenitor. *Proc Natl Acad Sci U S A*. 2011;108(42):17402-17407.

doi:10.1073/PNAS.1111766108/SUPPL_FILE/PNAS.201111766SI.PDF

163. Morgan D, Tergaonkar V. Unraveling B cell trajectories at single cell resolution. *Trends Immunol*. 2022;43(3):210-229. doi:10.1016/J.IT.2022.01.003

164. Shyamsunder P, Shanmugasundaram M, Mayakonda A, et al. Identification of a novel enhancer of CEBPE essential for granulocytic differentiation. *Blood*. 2019;133(23):2507-2517. doi:10.1182/BLOOD.2018886077

165. Sichien D, Scott CL, Martens L, et al. IRF8 Transcription Factor Controls Survival and Function of Terminally Differentiated Conventional and Plasmacytoid Dendritic Cells, Respectively. *Immunity*. 2016;45(3):626-640. doi:10.1016/J.IMMUNI.2016.08.013

166. Zhang Z, Bossila EA, Li L, Hu S, Zhao Y. Central gene transcriptional regulatory networks shaping monocyte development in bone marrow. *Front Immunol*. 2022;13. doi:10.3389/FIMMU.2022.1011279

167. Clark MR, Mandal M, Ochiai K, Singh H. Orchestrating B cell lymphopoiesis through interplay of IL-7 receptor and pre-B cell receptor signalling. *Nat Rev Immunol*. 2014;14(2):69-80. doi:10.1038/NRI3570

168. Platonova N, Miquel G, Regenfuss B, et al. Evidence for the interaction of fibroblast growth factor-2 with the lymphatic endothelial cell marker LYVE-1. *Blood*. 2013;121(7):1229-1237. doi:10.1182/BLOOD-2012-08-450502

169. Galvagni F, Nardi F, Maida M, et al. CD93 and dystroglycan cooperation in human endothelial cell adhesion and migration adhesion and migration. *Oncotarget*. 2016;7(9):10090-10103. doi:10.18632/ONCOTARGET.7136

170. Lin G, Finger E, Gutierrez-Ramos JC. Expression of CD34 in endothelial cells, hematopoietic progenitors and nervous cells in fetal and adult mouse tissues. *Eur J*

Immunol. 1995;25(6):1508-1516. doi:10.1002/eji.1830250606

171. Pantelyushin S, Ranninger E, Bettschart-Wolfensberger R, vom Berg J. OMIP-065: Dog Immunophenotyping and T-Cell Activity Evaluation with a 14-Color Panel. *Cytom Part A*. 2020;97(10):1024-1027. doi:10.1002/cyto.a.24168

172. Hohaus S, Petrovick MS, Voso MT, Sun Z, Zhang DE, Tenen DG. PU.1 (Spi-1) and C/EBP alpha regulate expression of the granulocyte-macrophage colony-stimulating factor receptor alpha gene. *Mol Cell Biol*. 1995;15(10):5830-5845. doi:10.1128/mcb.15.10.5830

173. Collin M, Bigley V. Human dendritic cell subsets: an update. *Immunology*. 2018;154(1):3-20. doi:10.1111/IMM.12888

174. Bae S, Kim H, Lee N, et al. α-Enolase Expressed on the Surfaces of Monocytes and Macrophages Induces Robust Synovial Inflammation in Rheumatoid Arthritis. *J Immunol*. 2012;189(1):365-372. doi:10.4049/JIMMUNOL.1102073

175. Doty RT, Yan X, Lausted C, et al. Single-cell analyses demonstrate that a heme-GATA1 feedback loop regulates red cell differentiation. *Blood*. 2019;133(5):457-469. doi:10.1182/BLOOD-2018-05-850412

176. Hu N, Mora-Jensen H, Theilgaard-Mönch K, et al. Differential Expression of Granulopoiesis Related Genes in Neutrophil Subsets Distinguished by Membrane Expression of CD177. *PLoS One*. 2014;9(6):e99671. doi:10.1371/JOURNAL.PONE.0099671

177. Bai M, Grieshaber-Bouyer R, Wang J, et al. CD177 modulates human neutrophil migration through activation-mediated integrin and chemoreceptor regulation. *Blood*. 2017;130(19):2092-2100. doi:10.1182/BLOOD-2017-03-768507

178. Anderson DA, Dutertre CA, Ginhoux F, Murphy KM. Genetic models of human and

mouse dendritic cell development and function. *Nat Rev Immunol*. 2021;21(2):101-115. doi:10.1038/S41577-020-00413-X

179. Kelly LM, Englmeier U, Lafon I, Sieweke MH, Graf T. MafB is an inducer of monocytic differentiation. *EMBO J*. 2000;19(9):1987-1997. doi:10.1093/EMBOJ/19.9.1987

180. Chinenov Y, Kerppola TK. Close encounters of many kinds: Fos-Jun interactions that mediate transcription regulatory specificity. *Oncogene*. 2001;20(19):2438-2452. doi:10.1038/SJ.ONC.1204385

181. Chieppa M, Bianchi G, Doni A, et al. Cross-Linking of the Mannose Receptor on Monocyte-Derived Dendritic Cells Activates an Anti-Inflammatory Immunosuppressive Program. *J Immunol*. 2003;171(9):4552-4560. doi:10.4049/JIMMUNOL.171.9.4552

182. Grajales-Reyes GE, Iwata A, Albring J, et al. Batf3 maintains autoactivation of Irf8 for commitment of a CD8α+ conventional DC clonogenic progenitor. *Nat Immunol 2015 167*. 2015;16(7):708-717. doi:10.1038/ni.3197

183. Almeida ARM, Neto JL, Cachucho A, et al. Interleukin-7 receptor α mutational activation can initiate precursor B-cell acute lymphoblastic leukemia. *Nat Commun*. 2021;12(1). doi:10.1038/S41467-021-27197-5

184. Wallaert A, Durinck K, Taghon T, Van Vlierberghe P, Speleman F. T-ALL and thymocytes: a message of noncoding RNAs. *J Hematol Oncol 2017 101*. 2017;10(1):1-17. doi:10.1186/S13045-017-0432-0

185. Qiu P. Embracing the dropouts in single-cell RNA-seq analysis. *Nat Commun*. 2020;11(1). doi:10.1038/S41467-020-14976-9

186. Vernau W, Moore PF. An immunophenotypic study of canine leukemias and preliminary assessment of clonality by polymerase chain reaction. *Vet Immunol Immunopathol*.

Published online 1999. doi:10.1016/S0165-2427(99)00051-3

187. D B, R T, D B, et al. Expression of haematopoietic progenitor cell-associated antigen BI-3C5/CD34 in leukemia. *Leuk Res*. 1989;13(1):83-85. doi:10.1016/0145-2126(89)90035-0

188. Avery AC. The Genetic and Molecular Basis for Canine Models of Human Leukemia and Lymphoma. *Front Oncol*. 2020;10:23. doi:10.3389/fonc.2020.00023

189. You MJ, Medeiros LJ, Hsi ED. T-Lymphoblastic Leukemia/Lymphoma. *Am J Clin Pathol*. 2015;144(3):411-422. doi:10.1309/AJCPMF03LVSBLHPJ

190. Coustan-Smith E, Mullighan CG, Onciu M, et al. Early T-cell precursor leukaemia: a subtype of very high-risk acute lymphoblastic leukaemia. *Lancet Oncol*. 2009;10(2):147-156. doi:10.1016/S1470-2045(08)70314-0

191. Williams MJ, Avery AC, Lana SE, Hillers KR, Bachand AM, Avery PR. Canine lymphoproliferative disease characterized by lymphocytosis: Immunophenotypic markers of prognosis. *J Vet Intern Med*. Published online 2008. doi:10.1111/j.1939-1676.2008.0041.x

192. Kozlov I, Beason K, Yu C, Hughson M. CD79a expression in acute myeloid leukemia t(8;21) and the importance of cytogenetics in the diagnosis of leukemias with immunophenotypic ambiguity. *Cancer Genet Cytogenet*. 2005;163(1):62-67. doi:10.1016/j.cancergencyto.2005.06.002

193. Lai R, Juco J, Lee SF, Nahirniak S, Etches WS. Flow cytometric detection of CD79a expression in T-cell acute lymphoblastic leukemias. *Am J Clin Pathol*. 2000;113(6):823-830. doi:10.1309/391R-93YF-DB4D-1L35

194. Pantelyushin S, Ranninger E, Bettschart-Wolfensberger R, vom Berg J. OMIP-065: Dog Immunophenotyping and T-Cell Activity Evaluation with a 14-Color Panel. *Cytom Part*

A. 2020;97(10):1024-1027. doi:10.1002/cyto.a.24168

195. Bacher U, Schnittger S, Haferlach C, Haferlach T. Molecular diagnostics in acute leukemias. *Clin Chem Lab Med*. Published online 2009. doi:10.1515/CCLM.2009.324

196. Bullinger L, Valk PJM. Gene expression profiling in acute myeloid leukemia. *J Clin Oncol*. Published online 2005. doi:10.1200/JCO.2005.05.020

197. Rao S, Lana S, Eickhoff J, et al. Class II Major Histocompatibility Complex Expression and Cell Size Independently Predict Survival in Canine B-Cell Lymphoma. *J Vet Intern Med*. 2011;25(5):1097-1105. doi:10.1111/j.1939-1676.2011.0767.x

198. Gelain ME, Mazzilli M, Riondato F, Marconato L, Comazzi S. Aberrant phenotypes and quantitative antigen expression in different subtypes of canine lymphoma by flow cytometry. *Vet Immunol Immunopathol*. 2008;121(3-4):179-188. doi:10.1016/j.vetimm.2007.09.018

199. Rout ED, Shank AMM, Waite AHK, Siegel A, Avery AC, Avery PR. Progression of cutaneous plasmacytoma to plasma cell leukemia in a dog. *Vet Clin Pathol*. 2017;46(1):77-84. doi:10.1111/vcp.12463

200. Seelig DM, Avery P, Webb T, et al. Canine t-zone lymphoma: Unique immunophenotypic features, outcome, and population characteristics. *J Vet Intern Med*. 2014;28(3):878-886. doi:10.1111/jvim.12343

201. Chabanne L, Marchal T, Kaplanski C, et al. Screening of 78 monoclonal antibodies directed against human leukocyte antigens for cross-reactivity with surface markers on canine lymphocytes. *Tissue Antigens*. 1994;43(3):202-205. doi:10.1111/j.1399-0039.1994.tb02324.x

202. Hughes KL, Labadie JD, Yoshimoto JA, Dossey JJ, Burnett RC, Avery AC. Increased

frequency of CD45 negative T cells (T zone cells) in older Golden retriever dogs. *Vet Comp Oncol*. Published online 2018. doi:10.1111/vco.12343

203. Reith W, LeibundGut-Landmann S, Waldburger JM. Regulation of MHC class II gene expression by the class II transactivator. *Nat Rev Immunol*. 2005;5(10):793-806. doi:10.1038/nri1708

204. Staudt LM, Lenardo MJ. Immunoglobulin gene transcription. *Annu Rev Immunol*. 1991;9:373-398. doi:10.1146/annurev.iy.09.040191.002105

205. Chapiro E, Delabesse E, Asnafi V, et al. Expression of T-lineage-affiliated transcripts and TCR rearrangements in acute promyelocytic leukemia: Implications for the cellular target of t(15;17). *Blood*. Published online 2006. doi:10.1182/blood-2005-09-009977

206. Hashimoto M, Yamashita Y, Mori N. Immunohistochemical detection of CD79a expression in precursor T cell lymphoblastic lymphoma/leukaemias. *J Pathol*. 2002;197(3):341-347. doi:10.1002/path.1126

207. Massari S, Bellahcene F, Vaccarelli G, et al. The deduced structure of the T cell receptor gamma locus in Canis lupus familiaris. *Mol Immunol*. Published online 2009. doi:10.1016/j.molimm.2009.05.008

208. Keller SM, Moore PF. Rearrangement patterns of the canine TCRγ locus in a distinct group of T cell lymphomas. *Vet Immunol Immunopathol*. 2012;145(1-2):350-361. doi:10.1016/J.VETIMM.2011.12.008

209. Meichner K, Stokol T, Tarigo J, et al. Multicenter flow cytometry proficiency testing of canine blood and lymph node samples. *Vet Clin Pathol*. 2020;49(2):249-257. doi:10.1111/vcp.12843

210. Novacco M, Comazzi S, Marconato L, et al. Prognostic factors in canine acute

leukaemias: a retrospective study. *Vet Comp Oncol*. 2016;14(4):409-416. doi:10.1111/VCO.12136

211. Babraham Bioinformatics - FastQC A Quality Control tool for High Throughput Sequence Data. Accessed September 9, 2022. https://www.bioinformatics.babraham.ac.uk/projects/fastqc/

212. Babraham Bioinformatics - Trim Galore! Accessed October 6, 2022. https://www.bioinformatics.babraham.ac.uk/projects/trim_galore/

213. A D, CA D, F S, et al. STAR: ultrafast universal RNA-seq aligner. *Bioinformatics*. 2013;29(1):15-21. doi:10.1093/BIOINFORMATICS/BTS635

214. Aken BL, Ayling S, Barrell D, et al. The Ensembl gene annotation system. *Database J Biol Databases Curation*. 2016;2016. doi:10.1093/DATABASE/BAW093

215. Liao Y, Smyth GK, Shi W. featureCounts: an efficient general purpose program for assigning sequence reads to genomic features. *Bioinformatics*. 2014;30(7):923-930. doi:10.1093/BIOINFORMATICS/BTT656

216. Danecek P, Bonfield JK, Liddle J, et al. Twelve years of SAMtools and BCFtools. *Gigascience*. 2021;10(2). doi:10.1093/GIGASCIENCE/GIAB008

217. Robinson JT, Thorvaldsdóttir H, Winckler W, et al. Integrative genomics viewer. *Nat Biotechnol 2011 291*. 2011;29(1):24-26. doi:10.1038/nbt.1754

218. Ewels P, Magnusson M, Lundin S, Käller M. MultiQC: summarize analysis results for multiple tools and samples in a single report. *Bioinformatics*. 2016;32(19):3047-3048. doi:10.1093/BIOINFORMATICS/BTW354

219. Tarazona S, Furió-Tarí P, Turrà D, et al. Data quality aware analysis of differential expression in RNA-seq with NOISeq R/Bioc package. *Nucleic Acids Res*.

2015;43(21):e140-e140. doi:10.1093/NAR/GKV711

220. factoextra package - RDocumentation. Accessed October 6, 2022. https://www.rdocumentation.org/packages/factoextra/versions/1.0.7

221. Subramanian A, Tamayo P, Mootha VK, et al. Gene set enrichment analysis: a knowledge-based approach for interpreting genome-wide expression profiles. *Proc Natl Acad Sci U S A*. 2005;102(43):15545-15550. doi:10.1073/PNAS.0506580102

222. Hänzelmann S, Castelo R, Guinney J. GSVA: Gene set variation analysis for microarray and RNA-Seq data. *BMC Bioinformatics*. 2013;14(1):1-15. doi:10.1186/1471-2105-14-7/FIGURES/7

223. Kanehisa M, Goto S. KEGG: kyoto encyclopedia of genes and genomes. *Nucleic Acids Res*. 2000;28(1):27-30. doi:10.1093/NAR/28.1.27

224. The Gene Ontology resource: enriching a GOld mine. doi:10.1093/nar/gkaa1113

225. Ashburner M, Ball CA, Blake JA, et al. Gene Ontology: tool for the unification of biology. *Nat Genet*. 2000;25(1):25. doi:10.1038/75556

226. Gillespie M, Jassal B, Stephan R, et al. The reactome pathway knowledgebase 2022. *Nucleic Acids Res*. 2022;50(D1):D687-D692. doi:10.1093/NAR/GKAB1028

227. Title An ExperimentHub Package for the Molecular Signatures Database (MSigDB). Accessed October 6, 2022. https://orcid.org/0000-0001-9221-2892

228. Wu T, Hu E, Xu S, et al. clusterProfiler 4.0: A universal enrichment tool for interpreting omics data. *Innov*. 2021;2(3):100141. doi:10.1016/J.XINN.2021.100141

229. Ritchie ME, Phipson B, Wu D, et al. limma powers differential expression analyses for RNA-sequencing and microarray studies. *Nucleic Acids Res*. 2015;43(7):e47-e47. doi:10.1093/NAR/GKV007

230. Kinsella RJ, Kähäri A, Haider S, et al. Ensembl BioMarts: a hub for data retrieval across taxonomic space. *Database (Oxford)*. 2011;2011. doi:10.1093/DATABASE/BAR030

231. Sun Y, Zhou B, Mao F, et al. HOXA9 Reprograms the Enhancer Landscape to Promote Leukemogenesis. *Cancer Cell*. 2018;34(4):643-658.e5. doi:10.1016/J.CCELL.2018.08.018

232. Monaco G, Lee B, Xu W, et al. RNA-Seq Signatures Normalized by mRNA Abundance Allow Absolute Deconvolution of Human Immune Cell Types. *Cell Rep*. 2019;26(6):1627-1640.e7. doi:10.1016/J.CELREP.2019.01.041

233. Zheng S, Papalexi E, Butler A, Stephenson W, Satija R. Molecular transitions in early progenitors during human cord blood hematopoiesis. *Mol Syst Biol*. 2018;14(3). doi:10.15252/MSB.20178041

234. Bolouri H, Ries R, Pardo L, et al. A B-cell developmental gene regulatory network is activated in infant AML. *PLoS One*. 2021;16(11). doi:10.1371/JOURNAL.PONE.0259197

235. Chapuis AG, Egan DN, Bar M, et al. T cell receptor gene therapy targeting WT1 prevents acute myeloid leukemia relapse post-transplant. *Nat Med 2019 257*. 2019;25(7):1064-1072. doi:10.1038/s41591-019-0472-9

236. Sasca D, Szybinski J, Schüler A, et al. NCAM1 (CD56) promotes leukemogenesis and confers drug resistance in AML. *Blood*. 2019;133(21):2305-2319. doi:10.1182/BLOOD-2018-12-889725

237. Alharbi RA, Pettengell R, Pandha HS, Morgan R. The role of HOX genes in normal hematopoiesis and acute leukemia. *Leuk 2013 275*. 2012;27(5):1000-1008. doi:10.1038/leu.2012.356

238. Wang YY, Zhou GB, Yin T, et al. AML1-ETO and C-KIT mutation/overexpression in t(8;21) leukemia: Implication in stepwise leukemogenesis and response to Gleevec. *Proc Natl Acad Sci U S A*. 2005;102(4):1104-1109. doi:10.1073/PNAS.0408831102/SUPPL_FILE/08831FIG6.PDF

239. Meshinchi S, Appelbaum FR. Structural and functional alterations of FLT3 in acute myeloid leukemia. *Clin Cancer Res*. 2009;15(13):4263-4269. doi:10.1158/1078-0432.CCR-08-1123

240. Armstrong SA, Staunton JE, Silverman LB, et al. MLL translocations specify a distinct gene expression profile that distinguishes a unique leukemia. *Nat Genet 2001 301*. 2001;30(1):41-47. doi:10.1038/ng765

241. Valk PJM, Verhaak RGW, Beijen MA, et al. Prognostically Useful Gene-Expression Profiles in Acute Myeloid Leukemia. *N Engl J Med*. 2004;350(16):1617-1628. doi:10.1056/NEJMOA040465/SUPPL_FILE/1617SA1.PDF

242. Lee S, Chen J, Zhou G, et al. Gene expression profiles in acute myeloid leukemia with common translocations using SAGE. *Proc Natl Acad Sci U S A*. 2006;103(4):1030-1035. doi:10.1073/PNAS.0509878103/SUPPL_FILE/09878TABLE6.XLS

243. Haferlach T, Kohlmann A, Schnittger S, et al. Global approach to the diagnosis of leukemia using gene expression profiling. *Blood*. 2005;106(4):1189-1198. doi:10.1182/BLOOD-2004-12-4938

244. Qiu LL, Levinson SS, Keeling KL, Elin RJ. Convenient and effective method for removing fibrinogen from serum specimens before protein electrophoresis. *Clin Chem*. 2003;49(6 Pt 1):868-872.

245. Hoffman JM, Creevy KE, Franks A, O'Neill DG, Promislow DEL. The companion dog as

a model for human aging and mortality. *Aging Cell*. 2018;17(3):e12737. doi:10.1111/ACEL.12737

246. Labadie JD, Elvers I, Feigelson HS, et al. Genome-wide association analysis of canine T zone lymphoma identifies link to hypothyroidism and a shared association with mast-cell tumors. *BMC Genomics*. 2020;21(1):464. doi:10.1186/s12864-020-06872-9

247. Best Practices Workflows – GATK. Accessed September 8, 2022. https://gatk.broadinstitute.org/hc/en-us/sections/360007226651-Best-Practices-Workflows

248. J P, J K, BW D, et al. Whole genome sequencing of canids reveals genomic regions under selection and variants influencing morphology. *Nat Commun*. 2019;10(1). doi:10.1038/S41467-019-09373-W

249. McLaren W, Gil L, Hunt SE, et al. The Ensembl Variant Effect Predictor. *Genome Biol*. 2016;17(1):122. doi:10.1186/s13059-016-0974-4

250. Forbes SA, Beare D, Boutselakis H, et al. COSMIC: Somatic cancer genetics at high-resolution. *Nucleic Acids Res*. 2017;45(D1):D777-D783. doi:10.1093/NAR/GKW1121

251. Robinson JT, Thorvaldsdóttir H, Winckler W, et al. Integrative Genomics Viewer. *Nat Biotechnol*. 2011;29(1):24. doi:10.1038/NBT.1754

252. Gao J, Aksoy BA, Dogrusoz U, et al. Integrative analysis of complex cancer genomics and clinical profiles using the cBioPortal. *Sci Signal*. 2013;6(269). doi:10.1126/scisignal.2004088

253. Mayakonda A, Lin DC, Assenov Y, Plass C, Koeffler HP. Maftools: efficient and comprehensive analysis of somatic variants in cancer. *Genome Res*. 2018;28(11):1747-1756. doi:10.1101/GR.239244.118

254. Medvedeva YA, Lennartsson A, Ehsani R, et al. EpiFactors: a comprehensive database of

human epigenetic factors and complexes. *Database (Oxford)*. 2015;2015. doi:10.1093/DATABASE/BAV067

255. Markowski DN, Huhle S, Nimzyk R, Stenman G, Löning T, Bullerdiek J. MED12 mutations occurring in benign and malignant mammalian smooth muscle tumors. *Genes Chromosomes Cancer*. 2013;52(3):297-304. doi:10.1002/GCC.22029

256. Das S, Idate R, Cronise KE, Gustafson DL, Duval DL. Identifying candidate druggable targets in canine cancer cell lines using whole-exome sequencing. *Mol Cancer Ther*. 2019;18(8):1460-1471. doi:10.1158/1535-7163.MCT-18-1346/88320/AM/IDENTIFYING-CANDIDATE-DRUGGABLE-TARGETS-IN-CANINE

257. Aranda-Orgilles B, Saldaña-Meyer R, Wang E, et al. MED12 Regulates HSC-Specific Enhancers Independently of Mediator Kinase Activity to Control Hematopoiesis. *Cell Stem Cell*. 2016;19(6):784-799. doi:10.1016/J.STEM.2016.08.004

258. Gola C, Giannuzzi D, Rinaldi A, et al. Genomic and Transcriptomic Characterization of Canine Osteosarcoma Cell Lines: A Valuable Resource in Translational Medicine. *Front Vet Sci*. 2021;8:394. doi:10.3389/FVETS.2021.666838/BIBTEX

259. Hoang T, Lambert JA, Martin R. SCL/TAL1 in Hematopoiesis and Cellular Reprogramming. *Curr Top Dev Biol*. 2016;118:163-204. doi:10.1016/bs.ctdb.2016.01.004

260. Takada M, Smyth LA, Thaiwong T, et al. Activating Mutations in PTPN11 and KRAS in Canine Histiocytic Sarcomas. *Genes (Basel)*. 2019;10(7). doi:10.3390/GENES10070505

261. Rodrigues L, Watson J, Feng Y, et al. Shared hotspot mutations in spontaneously arising cancers position dog as an unparalleled comparative model for precision therapeutics. *bioRxiv*. Published online October 25, 2021:2021.10.22.465469. doi:10.1101/2021.10.22.465469

262. Kämpjärvi K, Kim NH, Keskitalo S, et al. Somatic MED12 mutations in prostate cancer and uterine leiomyomas promote tumorigenesis through distinct mechanisms. *Prostate*. 2016;76(1):22-31. doi:10.1002/PROS.23092

263. Heikkinen T, Kämpjärvi K, Keskitalo S, et al. Somatic MED12 Nonsense Mutation Escapes mRNA Decay and Reveals a Motif Required for Nuclear Entry. *Hum Mutat*. 2017;38(3):269-274. doi:10.1002/HUMU.23157

264. Kim S, Xu X, Hecht A, Boyer TG. Mediator is a transducer of Wnt/beta-catenin signaling. *J Biol Chem*. 2006;281(20):14066-14075. doi:10.1074/JBC.M602696200

APPENDIX

SUPPLEMENTARY MATERIAL FOR CHAPTER 1

Supplemental Table 1. Antibody panels for canine flow cytometry immunophenotyping and fluorescence activated cell sorting (FACS).

Antibody tube §	Antibody specificity and fluorochrome ‡
Panel 1	
1	No antibodies
2	CD5-FITC/CD45-PE/CD21-Alexa 647
3	CD21-Alexa 647/Class II MHC-FITC/CD22-PE/CD25-SB436
4	CD4-PECy7/CD5-APCe780/CD8-Pacific Blue/Class II MHC-APC/CD14-A700/CD18-PE/CD3-FITC
5	CD117-PE/CD5-APCe780/Class II MHC-APC/CD34-FITC
Panel 2	
1	No antibodies
2	CD5-FITC/CD22-PE/CD21-Alexa 647/CD45-EF450
3	CD4-PECy7/CD5-APCe780/CD8-SB702/CD34-PE/Class II MHC-APC/CD21-A647/CD25-SB600/CD3-FITC
FACS Panel	
1	No antibodies
2	CD4-Pacific Blue/Class II MHC-APC/CD34-FITC

§ Immunophenotyping data was gathered using antibody panels 1 & 2. Two of the samples were analyzed on a three laser Coulter Gallios with Panel 1. One sample was analyzed on a Sony ID7000 spectral flow cytometer using Panel 2. CD34+ cells were enriched from 2 samples using the FACS panel on a Sony SH800 cell sorter.

‡ Except where noted, antibodies were purchased from Bio-Rad, Hercules, CA. Clones are as follows: CD45 = YKIX716.13, CD18 = YFC118.3 (human CD18), CD4 = YKIX302.9, CD8 = YCATE55.9, CD5 = YKIX322.3, CD21 = CA2.1D6, CD22 = RFB4 (human CD22, AbCam, Cambridge, MA), CD3 = CA17.2A12, CD14 = TUK4 (human CD14), class II MHC = YKIX334.2, CD34 = 1H6, CD25 = P2A10 (eBioscience, San Diego, CA), and CD117 = 104D2 (BioLegend, San Diego, CA). All tubes contain propidium iodide for dead cell exclusion.

Supplemental Table 2. Top 100 enriched genes from each cluster of sorted CD34+ cells. Genes were restricted to genes with gene symbols.

Cluster ID	Tentative cell type annotation	Top 100 enriched genes
0	CD34pos_PreB	AKAP12, DLA-DRA, VPREB1, DNTT, PAX5, FOXO1, NINJ1, RAG1, EPB41, GYPC, SPTBN1, DPEP1, SEPTIN6, DLA-64, YBX3, ADGRF1, CHD1, CD74, TPM2, TRAF3IP3, EIF1, MRC1, PNISR, TCF4, TOP2B, LAMA4, MARCKS, FAM107B, HLA-DQB2, DDX5, ASNS, FRG1, DCK, CXCR4, CD19, BLNK, PLAC8, TPT1, JCHAIN, MLLT10, EBF1, MEF2C, IGHM, MTA3, ALDH3A1, NPNT, GALK1, GMFG, BPTF, KRTCAP2, LDHB, PLS1, TFDP2, ERBIN, ABRACL, PSAT1, ATRX, SYK, KMT2E, SLC25A6, CRYBG1, TARS3, YPEL3, FBLN1, AP2B1, ARHGAP5, ANKRD54, MDP1, GNAI3, ZC3H13, SNW1, PMPCB, ZNF638, AGPAT3, EXOC6, GRAMD1A, RMDN1, SNRPN, C7H18orf32, TRIP12, UBE2V2, PNN, SDHAF4, PM20D2, RTN4, LRP10, UBB, NFKBIB, HUWE1, COA1, KRAS, TIMM29, BOLA1, ZNF800, MLH3, FRA10AC1, NXF1, SPOP, ATP8A1, MRPS31
1	CD34pos_GMP	MPO, ARHGAP45, PRSS57, SERPINB1, MGST1, ALAS1, MT2A, PYCARD, FKBP11, ALOX5AP, PTGR1, ANXA2, NFKBID, RBP7, NME1, GCAT, LY86, PYGL, FABP3, SPI1, NQO2, GGH, NPC2, COX7A1, PLBD1, CTSA, NT5DC2, ANXA1, AP1S2, POLR1G, MT1E, TFEC, CASP4, RAB44, PIR, SLAMF9, TNFSF13, LYG1, SPNS3, CEBPE, RASL11A, F5, STBD1, SERPINB10, ERO1A, LRRK2, SH2B2, NLRP3, FCGR1A, CYBB, KIF17, GADD45B, ENO1, SERPINB8, GNPAT, SMIM4, MFSD10, ALPL, CERS4, BPI, DBI, ACTN1, PDIA4, PPA1, ATP6V0E1, CALR, SRGN, NPM1, COX5A, SCARB2, PGM1, UNC93B1, GCSH, DNASE2, DCLRE1A, APRT, MBOAT1, FNBP1, CAT, PPM1J, ATP5MC1, FUCA1, EBNA1BP2, HSP90AB1, ZNF593, ENDOG, RPN1, EIF4A1, LAMTOR2, COQ10B, RPN2, PHC2, P4HB, MECR, HSP90B1, PPP1R14B, PSTPIP2, SMIM12, GPX1, AIFM2

2	CD34pos_LateMPP_CMP	HPGD, HSP90AB1, APOC1, ENPP3, RARRES2, RACK1, GCSAML, RGS2, ALPL, MSRB3, NPM1, TFPT, DMD, ADGRG1, PRSS57, GPRC5C, KIT, TNFSF13B, EEF1B2, FCER2, FKBP11, TFPI, RBP7, TIMP2, TAL1, PGLYRP2, PMP22, VKORC1, NAV3, RCAN2, UBA52, RASAL3, C9H17orf64, FCER1A, RFTN1, NACA, SNX30, SYNGR1, NFE2, NUDT2, DYRK1B, ESAM, SLA, CCND2, TBXAS1, PTPN7, FAU, PYGL, TSTD1, RGS19, TM6SF1, OGA, FXYD5, SSR4, USP20, TKT, LRRC71, NFKBID, GUCY1B1, SLC6A6, IGFLR1, EEF1D, GCHFR, IMPDH2, TRAP1, REV3L, RANGRF, FAM117A, ACSL5, PEPD, GLUL, NBN, FBL, NPC2, GCAT, PCBD1, DDX56, POLR2H, TTLL12, RRAGD, EIF4A1, PCYT1A, SH3BP5, HMGA1, CTSA, LARS1, LAMTOR4, EIF3E, PABPC1, GTF3A, DKC1, BCAP29, EEF2, ITM2B, EBNA1BP2, GSTP1, MMD, COQ10B, MYCBP, APRT
3	CD34pos_HSC_EarlyMPP	TFPI, VIM, RGS2, RARRES2, FCER2, LGALS1, BPI, EGFL7, ST7, FBN2, S100A8, ADGRE3, NRIP1, NKX2-3, S100A5, ADGRG1, LSP1, HOXA6, REV3L, LTF, C9H17orf64, MFAP2, RBPMS, MSRB3, ITM2B, UBA52, NPTX1, CALML4, HSPB1, SLA, EMP3, IGFBP7, FAU, MLLT3, APOC1, HLA-DQB2, CD34, PMP22, ESAM, SPP1, TNFSF13B, DLA-DOA, UGT2A1, CD79A, CCND2, PTPRE, LRRC71, RND2, EMID1, CD3D, CD74, RGS19, RCAN2, FLNB, DLA-DRA, CLEC3B, LAG3, PCDH17, TFEC, AIF1, CDO1, ALOX5, STMN3, SKAP1, NAV3, NACA, GCNT2, IGFLR1, SULT1B1, IL12RB2, PABPC1, GPRC5C, DHRS1, EVA1B, PTGS1, FAM171B, PHACTR1, STOM, JUP, PTP4A3, GNG11, TAL1, KRT18, FOSB, PARD3B, RFTN1, NCOA7, TFPT, PAM, HHEX, FXYD5, PTGER4, KCNN4, NUDT14, ARHGDIB, FYN, USP21, DMD, PTPN6, CYSTM1
4	Cycling_1	H1-5, TOP2A, MKI67, H2AC18, TUBA1B, ASPM, HMGB2, AURKB, SMC2, DUT, DHDDS, TPX2, CENPF, KNL1, H1-4, CENPE, KIF11, H2AZ1, KIF15, NDC80, SYNE2, NUSAP1, HMGB1, SMC4, NUF2, UBE2S, PTMA, TUBB4B, SGO1, ARHGEF39, MIS18BP1, SPC24, KIF22, CKAP2L, CALM3, TMPO, NCAPG, STMN1, GTSE1, EZH2, TUBB6, TACC3, CDK1, KIF23, KIFC1, TK1,

		ESCO2, CLSPN, PIMREG, CYBA, CCNA2, INCENP, UBE2C, NUCKS1, CDCA3, PSIP1, PRC1, CCNB2, VPREB3, DIAPH3, E2F8, BUB1, HJURP, FBXO5, KIF14, RACGAP1, E2F2, DEPDC1, ARL4C, ANLN, CDKN2C, NEIL3, KIF18B, H2AZ2, BUB1B, ANP32E, KIF20B, H2AC11, H2AC21, BRCA2, CDKN3, TTK, SUMO2, CTCF, ATAD2, PLK1, NPNT, USP1, ECT2, PSMB9, DDX39A, UBB, MTFR2, KIF4A, CDC20, HMMR, DEK, SPAG5, UHRF1, CKAP2
5	CD34pos_MEP	CA2, FCER1A, GATA1, NOSTRIN, MICAL3, EPOR, ITGA2B, KLF1, KCTD1, GFI1B, LMNA, RHAG, MUC13, PTGS1, FN3K, CA1, NRP2, PRKG1, AQP1, DCSTAMP, SLC38A8, ACKR1, ADD2, F2RL3, PLXNC1, TAL1, SELP, TIMP2, DLC1, UCHL1, SPTA1, DNAJA4, NCOA7, GUCY1A1, STON2, EMID1, ADGRG1, GUCY1B1, SNX30, PRDX2, FTH1.1, SH3BGRL2, VKORC1, PDCD4, ALOX15, DMD, DAAM1, SELENBP1, ANXA9, ENPP3, PSEN2, GNG11, NBN, PARVB, CCND1, PRIM2, NUDT2, GGTA1, PARD3B, HK1, TNIK, TEX15, RFTN1, OAS1, CBFA2T3, FYB1, CSF1, SLC16A7, PBX1, SPTLC2, APOC1, UROD, ZMYND8, TIMP1, BLVRA, SELENOW, DCXR, CDC42BPA, HMBS, RASSF8, ZNRF1, ST7, GPX1, NAV3, PIP4K2A, REXO2, MSRB3, WRN, TBXAS1, TGFB1, EEF1B2, TAOK3, RNPEP, IGFLR1, RBPMS, LGALS9, TEC, ACSL5, SDF4, RAB13
6	CD34pos_CLP_Early_Pro_B	CD2, TXLNB, CAPN6, RNASEH2B, IL7R, FGFR2, CD34, MICAL2, PIK3R1, PLAC8, GALNTL6, HOPX, MAP7, NDST3, HIVEP3, RASSF9, TIMP1, BMP2K, CD7, PAK3, PTGER4, ATP1B1, TOX2, RASA3, SATB1, IRAG2, BAHCC1, CD96, IGFBP7, GRN, ITGA4, TSC22D4, ESR1, PDE9A, CD79A, CORO1B, PARP1, SLC17A8, CD44, MACROH2A1, FLT3, TESC, GAS6, OGFOD3, CLEC3B, BHLHB9, SELPLG, DDIT4, GBP1, SEMA4D, URI1, SH3BP4, CCDC50, CORO1A, GBP6, ST3GAL1, CDIP1, TSPAN5, TESPA1, DTNBP1, KRTCAP2, ABAT, UHRF1, GLUL, MMD, STING1, RALGPS2, RCSD1, JUP, MAN2A1, FUT8, ALCAM, DNTT, ASNS, RYBP, CD48, B2M, EEF1B2, PSD2, KCNK12, DNAJC25, ATP8B4, APBB1IP, SEPTIN6, PTPRF, SSR4, BACE1,

		ACTG1, VRK1, ANKRD28, CMA1, ADGRG1, AFF3, MSH6, HOXA7, TRIM17, PAN3, PABPC1, DPEP1, MCTP2
7	CD34pos_ProB	VPREB3, STMN1, PTMA, PAX5, ASNS, DHDDS, BLNK, TFDP2, HMGB1, DEK, MSH6, HMGB2, UHRF1, DPEP1, CNN2, FBLN1, MCM6, H2AZ1, AKAP12, VPREB1, YBX3, CD19, HNRNPA2B1, NINJ1, IGHM, PDCD1, DNTT, SOD1, CYBA, BARD1, DNMT1, INKA1, TPM2, ARHGEF39, CCNE2, TYMS, HNRNPM, PLS1, TPT1, H2AZ2, RFC4, GBP6, EPB41, PSIP1, LDHB, GYPC, POU2AF1, DCK, SMC4, HNRNPD, DNAJC9, HNRNPA3, SLC4A11, PCNA, MCM3, CHD1, E2F2, MCM7, UGDH, ATP5PF, AMDHD1, PSAT1, TSPO, ACOT13, MARCKS, ZCCHC7, ARPC5L, CASP8AP2, CECR2, CHAF1A, NMRAL1, FAM107B, SIVA1, AKR1B1, GAPDH, CDC6, HELLS, ATAD5, PCP4L1, LAMA4, ALDH3A1, TCF4, CCT2, ORC6, SMC6, NPNT, PSMB1, TOP2B, RASGRP2, RNASEH2B, NASP, SULT1B1, EBF1, SEPTIN6, CENPW, ERBIN, GAS6, BRCA2, NAP1L1, SPTBN1
8	CD34pos_MLP_MDP-like	IGKC, PACSIN1, TPM4, RUNX2, ADGRG5, TTYH1, NIBAN3, IRF8, COBLL1, CYB561A3, SELL, CYP2D15, ATP1B1, TLR3, RUBCNL, TMEM132A, ITGB7, IRAG2, FUCA1, APBB1IP, OCIAD2, IL7R, SPATS2L, CTSS, CCR7, CLEC2D, PPM1J, TNFRSF13C, PLAC8, QSOX1, FYB1, GRN, CTSZ, SLC8A1, SQLE, LCP1, CCDC50, GLB1, SCAP, ZYX, SELPLG, CD96, GNG10, TMSB10, MT2A, RHOQ, SEMA4A, PRDX4, CRIP1, ALCAM, MED25, EGFL7, NAGA, B2M, GPX1, AGBL4, SORL1, FMNL1, FAM118A, CORO1A, VCL, SOD1, CAPG, CTSB, CYSTM1, METRNL, CBLB, DSE, MSMO1.1, JPT1, CSNK1G1, EZR, UGCG, FCGRT, TXNDC5, IGFBP7, RIPOR2, PLD4, CD48, PPM1H, TXNDC17, DGKA, DOCK8, FCHO1, MED13L, NAPSA, STING1, UNC93B1, SCPEP1, ACAT2, MPZL1, CBWD1, DESI1, EFHC1, DCPS, CRELD2, LGALS1, GSN, PRCP, KLC4

9	ProB_to_PreB	FCRLA, LEF1, IRF4, CD55, CAMK4, HVCN1, VPREB3, TCEA3, ODC1, IRAG2, USP53, DERL3, NME1, RAPGEF5, KLHL18, MCUB, PRXL2B, APLP2, SEPTIN11, IL7R, NOP10, TXNDC5, CFAP251, IGHM, KRT23, CD3D, PAX5, TCEA1, INSYN1, APEX1, SIAH2, CHCHD10, POLD1, ID3, GNAS, COQ10B, ATP5MC1, TRMT112, MYO1B, IMP4, NHP2, ENO1, PRDX1, PRDX4, RSL1D1, PDCD1, PTMA, UQCRQ, COQ7, NME2, HERPUD1, PSMA7, PPA1, ZNF706, PDAP1, PSMB9, SIVA1, CASP3, ALYREF, MTAP, TCF3, DCTPP1, COX5A, TRIP13, CD74, PFDN6, HSDL2, GMPS, PSMB2, CLSPN, CYCS, CLEC2D, RAB3IP, CNBP, RASSF7, CD164, PA2G4, ERH, LSM7, CDC6, COX4I1, TPI1, SSB, EIF4A1, POLR2E, LYAR, SUB1, SOD1, PCNA, CENPU, DDX54, ZNF593, APRT, SRM, ATP5F1D, BZW1, COX5B, UHRF1, NMRAL1, MRPL55
10	Cycling_2	PLK1, CDKN3, CCNB3, TROAP, UBE2C, NUSAP1, DEPDC1, ASPM, CDCA3, DLGAP5, BUB1, CENPA, GTSE1, PIMREG, KIF23, BUB1B, AURKA, NUF2, REEP4, CCNB2, ECT2, CKAP2L, TMEM71, CEP55, NEK2, CDC20, CENPF, KIF14, KIF20A, CCNA2, KIF11, CDK1, TOP2A, CKAP2, TPX2, HMMR, CENPE, MKI67, KIFC1, TACC3, KNL1, PRC1, TUBB6, ARHGEF39, CDCA8, MTFR2, CDCA2, HJURP, KIF20B, NDC80, SGO1, DEPDC1B, AURKB, RACGAP1, TUBB4B, NUCKS1, SGO2, SMG1, KIF22, UBE2S, INCENP, CKAP5, HMGB2, JPT1, KIF18A, NPNT, RAD21, SMC4, GPSM2, SECISBP2, KIF15, MIS18BP1, KIF4A, ODF2, NCAPD2, BUB3, CKS1B, HP1BP3, POU2AF1, H2AZ2, KNSTRN, HMGB1, TRIM59, TUBA1B, DHDDS, SH2D3C, SPAG5, SMTN, LYZ, CALM3, HMGN3, G2E3, EBF1, DUT, KIF18B, HSP90B1, FAM107B, TTK, TMPO, SPC25
11	T_cells	KLK11, CRLF2, SYTL3, MPP4, IL13, IL1RL1, ICOS, ZNF683, EGFL6, ITK, GATA3, PTGES, IL2RA, RGS1, RGS16, C1orf54, LRRN3, KHDRBS3, TNFRSF18, IL17RB, SRGN, ARL4C, KLRG1, MS4A2, CYTIP, KCNQ2, BHLHE40, EMB, INPP4B, IL7R, REM1, GPR183, PODNL1, AHR, LGALS1, SAMSN1, CD3D, CD7, ETS1, SAMHD1, CALM1, L2HGDH, CRIP1, CSGALNACT1, LSP1, STK17B, PTPRC, CLINT1,

		GPX1, PLAC8A, EVL, VIM, S100A11, LAMTOR4, CDA, FGL2, TTC38, DLA-64, ITGB7, SELENOW, ANTXR2, CD48, ST3GAL6, TAGAP, CORO1A, PPARG, GRAP2, PPP2R5A, CHN2, SLC4A4, GIMAP8, HSBP1, B2M, ETHE1, LPAR6, PLCL1, TNIK, AHNAK, SKAP1, ARID5B, MCUB, ACTB, ARHGAP18, PDCD4, SH3BGRL3, DLA88, TNFRSF25, DBP, TESPA1, ARPC2, ABRACL, LRRFIP1, SEPTIN11, PLIN2, CTSH, ERN1, SERPINB6, DDIT4, TGFB1, RGS19
12	Endothelial	MAFB, FCN1, CCDC80, CCL14, SERPINH1, CXADR, KDR, STAB2, ARHGAP29, CD36, RDH16, PRSS23, PLPP3, TM4SF18, LYVE1, ADGRL2, PLVAP, DNASE1L3, ADGRF5, SOX18, GPIHBP1, IL13RA2, FERMT2, SELE, ADGRL4, TINAGL1, EMP2, SERPING1, TJP1, VCAM1, FAM167B, FILIP1, NR2F1, NR2F2, LDB2, CDH5, EMCN, SASH1, NFIB, PLA2R1, GPX3, DYSF, OLFM1, SLC39A8, GALNT18, TMEM47, ROBO4, CPNE8, PECAM1, COL4A1, KANK3, CALD1, ARHGAP28, PDK4, NRP1, COL4A2, ADM5, F8, PLAC8A, FXYD6, BCAM, TMEM150C, DAB2, BMP2, DLL4, CD93, SRGAP1, CDC42BPB, SELENOP, CHRNE, TIMP3, HGF, FLT1, CNN3, STAB1, FLT4, CALCRL, RGS16, SULT1A1, NUPR1, ACKR1, FGL2, PHLDB2, RASIP1, NECTIN2, TSPAN12, IL6ST, ID1, TEK, S1PR1, DOCK9, PLPP1, MRC1, ITGA2, PLK2, ID3, CFI, EGFL7, ASAH1, FCGRT

Supplemental Table 3. Top 100 enriched genes from each cluster of bulk bone marrow cells. Genes were restricted to genes with gene symbols.

Cluster ID	Tentative cell type annotation	Top 100 enriched genes
0	Pre_neutrophil_2	PGLYRP, PADI3, MMP9, FADS1, C9H17orf64, VIM, LGALS3, MGAT4A, ABTB1, RGS2, LSP1, S100A12, GMFG, CCPG1, CAPG, HMGB2, SH3BGRL3, DHRS7, TPI1, ACTR3, S100A8, RGS19, CDA, OAZ1, PFN1, S100P, LCP1, GADD45A, NFKBID, ACTB, ACTG1, PLA2G7, MSRB1, SELENOW, PGLS, C30H15orf48, GABARAP, CYBA, GGH, C5AR1, GLRX, EMB, VASP, AP1S2, GAPDH, PTPRC, ARPC2, SELL, PYGL, PLAC8, SPI1, DDX5, CKAP4, FGL2, SERPINA1, LTF, MXD1, GALK1, SQOR, IL17RA, LAMTOR4, PLBD1, PLAUR, ARPC3, ALOX5, RNASEK, ISG20, SAT1, C17H1orf162, TWF2, COTL1, FCGR1A, ITM2B,SEC14L1, MCPH1, EIF1, PHACTR2, TESC, CORO1A, UBE2B, PAK2, PTPN6, RCSD1, ABCA7, TPD52, TRIB1, MGST1, YPEL3, STK4, SVIL, KLF6, SKAP2, ARG2, CLTA, BCL2A1, CFL1, ATP6V0E1, TLN1, ALOX5AP, PPP4R1
1	Neutrophil	CXCL8, SOD2, CD4, ISG20, PLA2G7, SERPINA1, FTH1.1, CEACAM28, SELL, RGS2, ADGRE3, CDA, GGH, EMB, ITM2B, GADD45A, C5AR1, ABTB1, NFKBID, GALK1, MSRB1, ARHGAP45, DHRS7, GABARAP, FTL, RGS19, OAZ1, LCP1, GMFG, VIM, C30H15orf48, FCGR1A, EIF1, SRGN, CAPG, GPCPD1, DDX5, PADI3, FOS, CLTA, TIMP2, LGALS3, STX11, GAPDH, PGLS, RNASEK, C9H17orf64, UBE2B, ACTB, SEC14L1, SKAP2, SAT1, ATP6V0E1, MAPK13, ZFP36, SPI1, ARG2, CCPG1, MXD1, VASP, MCPH1, ASPH, ZFAND5, GLIPR1, CLIC1, PTPN1, COTL1, SNX10, RESF1, FGL2, BCL2A1, STK17B, NAMPT, IL17RA, ARPC3, B2M, TNFSF9, YPEL3, SORL1, PLAUR, HMGB2, BTG1, KLF6, MCTP2, PFN1, ARPC2, PTPN6, LRRK2, SH3BGRL3, GADD45B, KTN1, ANTXR2, PYURF, PLEK, MGST1, ARFIP1, PPP1R2, SNRNP27, FYB1, ACTR2
2	Pre_neutrophil_1	MMP8, LTF, PGLYRP1, FADS1, TCN1, PRNP, MMP9, BDH1, TESC, S100A12, S100A8, CKAP4, CD177, S100P, PPA2, CAMP, CPNE3, SERPINB1, SH3BGRL3, ACTR3, PLBD1, SELENOW, APMAP, CP, C9H17orf64, MGAT4A, ENO1, CSTA, PFN1, FAM107B, OXCT1, GSN, CYSTM1, WIPI1, LGALS3, CFP, INHBA, AP1S2, LSP1, ACSS1, SQOR, SRI, PYGL, CRISP2, PADI3, CAPG, GLRX, ACTG1, PTPRC, LCP1, KLF5, CYBA, TSPO, TIAM2, CCPG1, TPI1, MSRB1, ABRACL, LAMTOR4, GMFG, SLC45A2, PLAC8,

		SUCLG1, HIBCH, ALOX5AP, CXCR4, ETHE1, CYBB, DDIT4, QPCT, SVIP, GOT1, LCN2, HK3, CLINT1, PGD, NT5C3A, SLCO4C1, ARPC2, DOCK8, GAPDH, ATP8B4, SERPINB8, BRI3, ANXA3, RRAGD, GTF2B, ALOX5, C20H19orf38, VIM, CFL1, ACTB, SUCLG2, SYNE1, POLR3B, ANP32A, STBD1, SVIL, TRIB1, CCDC125
3	GMP	ELANE, SLPI, GZMB, MPO, PLAC8A, BPI, ALOX15, ALAS1, SSR4, SERPINB1, SSR3, PPA1, NME2, H2AZ1, EEF1B2, SEC61B, CENPW, RBP7, SDF2L1, MMD, COQ10B, COX7A1, CD63, SYNGR1, PCBD2, METTL7A, LDHB, UBA52, URI1, PAFAH1B3, SERF1A, THEM4, ETFB, CANX, PES1, RAB13, MRPS18C, PDIA6, FKBP11, MYCBP, RNASEH2B, C4H1orf131, TNFSF13, EBNA1BP2, SMIM4, SIVA1, RASL11A, CHI3L1, FABP3, CD302, PPP1R14B, EMC8, AGPAT3, CROT, NHP2, APRT, RCN1, ACOT7, LBHD1, SOD1, APIP, SPNS3, MRPL51, SLC29A1, VMA21, SRGN, FAIM, LRMDA, LYRM2, PCBD1, ERO1A, POP5, ANXA5, MAPKAPK5, SULT1C4, MYB, NUCB1, SCCPDH, HSDL1, SEPTIN5, P4HA2, ATP5MC1, SVBP, BBIP1, ANP32E, TMX1, GLT8D1, NUCB2, HMGN3, NPC2, SNRPG, DNPH1, AKAP7, PDIA3, NACA, GGCT, HOMER2, METTL5, TMEM126A, VPS29
4	GP_2	CAMP, CP, TCN1, CD177, MMP8, LTF, CRISP2, CSTA, DHDDS, PRNP, GSN, TESC, CEBPE, CA6, C3, CPNE3, LCN2, RETN, BDH1, ANXA1, PLAC8A, SRI, APMAP, ENO1, INHBA, CFP, LYZ, CYBB, PPA2, GPI, CYSTM1, OXCT1, S100A8, ARHGDIB, STOM, SLC45A2, TIAM2, C1orf54, AGL, PHYH, S100P, ACAT1, STBD1, SVIP, CKAP4, BASP1, S100A12, FADS1, LAMTOR4, SERPINB1, P4HA1, ACSS1, C20H19orf38, SUCLG1, RTN3, LAMP2, HIBCH, HK3, TKT, APOM, BRI3, CCDC125, FUNDC1, PSTPIP2, NT5C3A, GSTO1, GTF2B, GADD45B, ALOX5AP, VCL, RCN1, ABRACL, FAM107B, ATP8B4, AK2, ARFGEF1, PYGL, EIF4G3, KLF5, NUCB2, UGP2, PLSCR1, CLINT1, ACTR3, POLR3B, SELENOW, CYBA, SLA, LYG1, ANP32A, SEM1, WIPI1, SLCO4C1, ETHE1, RRAGD, ZNF414, TSPAN8, ATG3, PGK1, TSPO
5	Granulocyte_2	PGLYRP1, PADI3, MMP9, C9H17orf64, VIM, S100A12, FADS1, GMFG, LGALS3, LSP1, CAPG, SH3BGRL3, OAZ1, PFN1, HMGB2, RGS2, ABTB1, ACTB, PLA2G7, S100A8, ACTR3, LCP1, MGAT4A, GADD45A, DHRS7, CCPG1, RGS19, MSRB1, GAPDH, S100P, CDA, TPI1, C5AR1, NFKBID, PGLS, ARPC2, C30H15orf48, ACTG1, GGH, PTPRC, PYGL, GABARAP, DDX5, CYBA, GLRX, SELENOW, EMB, VASP, ALOX5, SPI1, SELL, PLAUR, SERPINA1, MXD1, PLAC8, SAT1, CKAP4, GALK1, LTF,

		AP1S2, FGL2, IL17RA, SQOR, ARPC3, TWF2, C17H1orf162, CORO1A, PLBD1, LAMTOR4, TRIB1, COTL1, ISG20, RNASEK, TESC, KLF6, MCPH1, FCGR1A, SEC14L1, PHACTR2, RNF10, TPD52, MGST1, ABCA7, RCSD1, STK4, CLTA, ITM2B, SVIL, YPEL3, PGD, UBE2B, IL16, CFL1, RAB11FIP2, STX11, SAMSN1, FBXO9, ETHE1, VSTM1, SKAP2
6	Cycling_Gran_1	RETN, CAMP, H2AZ1, H1-5, DHDDS, CENPW, TUBA1B, SPC24, H2AC18, CD177, TYMS, NUSAP1, PTMA, PLAC8A, DCXR, ACAT1, CCNB2, SMC2, RRM2, CEBPE, CA6, AURKB, ASPM, H2AC11, TPX2, TOP2A, CRISP2, KIF11, MKI67, NDC80, H2AC13, SKA2, DUT, H2AC21, CDK1, CP, HMMR, ANXA1, CKS1B, SNRPD1, UBE2S, LCN2, NUCB2, STMN1, CKAP2L, H2AZ2, PAFAH1B3, PRC1, NUF2, H2AC2, H1-4, GTSE1, PPA1, NCAPG, SPCS3, SRI, AK2, UBE2C, CCNA2, CPNE3, MYCBP, RAD51AP1, KNL1, APPL1, SGO1, PPA2, SMC4, C1orf54, SUMO2, TCN1, AURKA, SERF1A, CALM3, HMGB1, METTL7A, TMX1, NDUFS8, LYZ, OXCT1, MRPL52, SMG1, VDAC1, CKAP2, CENPF, ANP32E, ACOT7, MIS18BP1, ATAD2, RCN1, NCAPD3, GPI, SMC1A, THEM4, RUNDC3B, LSM5, ARHGDIB, E2F8, MMP8, ESCO2, BBLN
7	Pre_B_cell	VPREB3, PAX5, AKAP12, FCRLA, IGHM, SPTBN1, TOP2B, NIBAN3, ODC1, ACTC1, TPM2, AOX2, IRF4, RAG1, TCF3, VPREB1, ZNF704, C5H16orf74, FOXO1, CD72, FBXO25, POU2AF1, EBF1, BACH2, RAB3IP, DERL3, CECR2, TNFRSF13C, GNAS, PRDX1, SEPTIN6, DLA-DRA, TCEA1, CD19, EFR3A, EEF1A1, BLNK, TCF4, SEPTIN11, FRG1, ATRX, H3-3A, CD74, CD79A, PTMA, HLA-DQB2, SYK, GLCCI1, ZCCHC7, PIK3AP1, INPP5D, CNBP, IFI30, TBC1D1, PARP4, STMN1, PRRC2C, CORO1B, PNN, NCL, NPM1, MCUB, CSK, LGALS1, SUB1, PNISR, CXCR4, MCFD2, CLEC2D, CD37, NKTR, DLA-64, FRYL, JMJD1C, OGT, DEK, ATP8A1, HNRNPK, SERBP1, UBB, TMSB10, PSIP1, ATF7IP, SPATS2, HIVEP1, OPTN, HSP90AB1, ZEB2, DYRK1B, PEPD, KDM1B, PM20D2, RHEB, YBX3, SLC25A6, SNRPG, LUC7L3, FAM53B, NME2, HNRNPH1
8	Monocyte_1	CTSS, MAFB, LGALS1, TIMP1, ARHGAP45, S100A5, SLAMF9, VCAN, MT2A, BPI, TMSB10, CCDC88A, DLA-DRA, LY86, ABCA5, ANPEP, EIF4A1, CD300H, HLA-DQB2, VMP1, GPX1, NPC2, SULF2, DLA-DMA, TFEC, ZEB2, MNDA, CD74, FUCA1, TNFSF13, SAMHD1, IFI30, MX2, CASP4, CD86, SERPINB10, MARCHF1, PSAP, CTSZ, SAMD9L, TREM1, PYCARD, MBOAT1, CLEC12A, UNC93B1, SLC46A2, OAS2, AIF1, SEC61A1, TPM4, PLEC,

		KARS1, FKBP15, SHTN1, XDH, ATP2B1, HNMT, BANK1, DLA-DQA1, FN1, MYOF, TET2, DDX60, ATP1B1, SLC37A2, MAN1A1, UTRN, AHNAK, CSF1R, NLRP3, TCIRG1, LRRK2, SH2B2, OGFRL1, VRK2, GIMAP4, CCDC50, CHN2, CAPN2, ST3GAL5, PARP4, ADAM28, TGFBI, TRPS1, GIMAP8, GIMAP1, TCEA3, NRG1, METRNL, CASP12, IKBKE, LRP1, FGD2, PLEKHO1, TBXAS1, AHR, DGKG, NLRP1, TLR4, IRF5
9	Granulocyte_1	MMP8, LTF, PRNP, TCN1, FADS1, S100A8, MMP9, CD177, BDH1, TESC, CAMP, PPA2, CP, S100A12, S100P, PGLYRP1, CKAP4, CSTA, SRI, APMAP, CYSTM1, CPNE3, ENO1, SH3BGRL3, GSN, CFP, PLBD1, CYBB, C9H17orf64, SERPINB1, INHBA, SELENOW, FAM107B, OXCT1, MGAT4A, ACTR3, CRISP2, PFN1, HK3, DHDDS, GPI, SQOR, ACSS1, SUCLG1, WIPI1, PYGL, HIBCH, MSRB1, ATP8B4, LSP1, ACTG1, KLF5, GAPDH, ARPC2, PADI3, LGALS3, CYBA, FCER1G, C3, BASP1, PLAC8, LAMTOR4, CAPG, BRI3, GOT1, ETHE1, GTF2B, QPCT, TIAM2, STBD1, AP1S2, CA6, LCN2, GLRX, TSPO, SVIP, CCDC125, ALOX5AP, SLC45A2, PSTPIP2, NT5C3A, ABRACL, ARRB2, CFL1, GRK6, TPI1, SERPINB8, CORO1A, CEBPE, PTPRC, ZNF414, PGK1, AGL, TSPAN8, DDIT4, PGD, SYNE1, C20H19orf38, POLR3B, STOM
10	Granulocyte_3	CXCL8, SOD2, ISG20, PLA2G7, CD4, SERPINA1, SELL, GGH, GADD45A, FTH1.1, RGS2, CDA, OAZ1, NFKBID, CEACAM28, EMB, C5AR1, ITM2B, ABTB1, GALK1, FTL, LCP1, DHRS7, C30H15orf48, CAPG, GABARAP, ADGRE3, CYP4F22, VIM, MSRB1, GMFG, FCGR1A, RGS19, PADI3, GAPDH, SRGN, DDX5, ARHGAP45, LGALS3, C9H17orf64, MXD1, STX11, ACTB, SEC14L1, GPCPD1, ARG2, PGLS, EIF1, CLTA, SAT1, ZFP36, MAPK13, SPI1, RNASEK, TIMP2, NAMPT, VASP, GLIPR1, CLIC1, PTPN1, IL17RA, SKAP2, CCPG1, ZFAND5, SNX10, STK17B, FOS, ARPC2, UBE2B, HMGB2, KLF6, ARPC3, ASPH, BCL2A1, PLAUR, ATP6V0E1, FGL2, PFN1, COTL1, TNFSF9, YPEL3, MCTP2, MCPH1, PLEK, KTN1, RESF1, LRRK2, SH3BGRL3, MARCKS, SORL1, CYBA, IL13RA1, GRAMD1A, ANTXR2, BTG1, PTPN6, FYB1, ACTR3, ARFIP1, PAK2
11	Early_Erythroid	HBM, AHSP, PRDX2, CA2, CA1, BLVRB, GYPA, ALAS2, MGST3, ALAD, GPX1, SPTA1, CCDC34, HMBS, RHCE, ATP5IF1, UROD, HEMGN, AQP1, NANS, KLF1, SOD1, MIOX, GYPC, TSPO2, MKI67, ACADSB, TK1, IFT27, SELENBP1, METAP2, PPOX, UBE2S, NAA16, DUT, DEK, CENPF, GATA1, IMPDH2, UROS, TFRC, LMNA, NT5C, PIGQ, EPOR, VDAC3, PRDX3, NDUFS3, REXO2, PRKAR2B, DNAJA4, TTLL12, GADD45GIP1, ABCB6,

		TYMS, HAGH, CENPE, MYBL2, FN3K, CLTB, TAL1, UBAC1, SMC2, RAD23A, RHAG, RRM2, USP14, MCM6, CYC1, GFI1B, UBE2K, MUC13, SMC1A, MYH10, GMNN, TPX2, EIF2AK1, ORC1, SPTB, NOSTRIN, SSRP1, FECH, ANK1, MCM7, BOLA3, NCAPG, HMGA1, PON2, NMRAL1, AGPAT3, ERMAP, KIF20B, GCHFR, RNASEH2A, ADK, TRAK2, ASPM, RFC4, SPC24, SEPTIN4
12	MP	CENPF, LGALS1, PYCARD, LY86, SLAMF9, TUBB6, CENPE, MKI67, CCDC88A, CDC20, CTSA, KIF20B, MNDA, LYG1, FABP3, TNFSF13, TMPO, KIF15, TIMP1, TFEC, KIF11, PLK1, CASP4, SERPINB10, IFI30, KIFC1, CCDC50, RNASEH2C, UNC93B1, TK1, KIF22, RRBP1, INCENP, SULF2, DDX39A, CTSS, HSPH1, NCAPD2, PLEC, ANPEP, BUB1B, VCAN, TPM4, NQO2, NT5DC2, MYBL2, FKBP11, MBOAT1, NCAPG, IQGAP2, CCNA2, MTFR2, SLC43A3, CDCA3, COX7A1, LIG1, CEP55, TCIRG1, BUB1, MX2, DLA-DMA, THY1, ST3GAL5, MAN1A1, MS4A7, ANLN, KIF4A, SHTN1, SPATS2L, REEP4, HMGB3, CERS4, CXCL14, AKR1B1, MYOF, IKBKE, CNDP2, SH2B2, GALNT12, HNMT, CD86, SAMHD1, SPHK1, GLB1, KCNN4, XDH, GIMAP4, CEP128, VRK2, ANXA4, CASP12, ST7, ITGA6, PRPSAP1, MELK, TRIP13, SPAG5, FAM120A, CTNNA1, FBXO6
13	Immature_B_cell	LTB, TNFRSF13C, DLA-DRA, HLA-DQB2, CD74, DLA-DQA1, DLA-DOA, MS4A1, FCER2, CD3D, BTLA, CD22, PAX5, IGHM, CLEC2D, SP140, CORO1B, ID3, PLEKHO1, CD79A, ODC1, MEF2C, FAU, DLA-DMA, FCMR, MNDA, BANK1, BIN1, DYRK1B, PRDX1, ARPC5L, EEF1A1, RALGPS2, SWAP70, NACA, SNRPG, ETS1, HOPX, NOP53, TAP1, FCRLA, ACP5, SEPTIN11, DLA-64, ZNF318, REL, SLC4A7, UBA52, PTPN6, TRIM34, CD37, TFPT, SEPTIN6, GSPT2, IFI30, SLC25A6, EEF1B2, CNBP, SMCHD1, EEF1D, CCDC50, WDFY4, RASA3, DNASE2, SEC11C, PFDN5, B2M, STMN1, DLA88, HIF1A, COQ10B, RESF1, JAK1, OPTN, ZCCHC7, C9H17orf99, HVCN1, SP110, ZBTB38, MACF1, EIF4B, ICAM2, CD53, PLAC8, PRRC2C, PSIP1, SMC6, RACK1, SERBP1, EPHX1, BTF3, TRMT112, NPM1, PSMB9, EIF3K, ATF7IP, CHD2, SRRM2, CTSZ, MYCBP2

14	T_cells	CCL5, CD3E, CD3D, CCL4, GZMK, KLRB1, CD7, CD2, CORO1B, IL2RB, LTB, NCR3, SKAP1, KLRK1, CD3G, GIMAP8, IFGGB2, SH2D1A, CTSW, ITK, CD96, CAMK4, CD160, GATA3, ZAP70, TRAT1, LYSMD2, ETS1, FLT3LG, EVL, HOPX, CLEC2D, STAT4, SSBP4, B2M, CD79A, GIMAP4, IL7R, CRIP1, DLA-64, HLA-DQB2, MACF1, DYRK1B, UBA52, FAU, EEF1A1, OPTN, CBLB, DLA88, NOP53, DOCK10, GIMAP1, TAP1, MNDA, JAK1, TRIM34, ARL4C, CALM1, NACA, PSIP1, PLEKHA1, EEF1D, EVA1B, SNRPG, TMSB10, MYCBP2, DLA-79, RDX, PFDN5, PTPRC, SLC25A6, COQ10B, EZR, DLA-DRA, THY1, EIF4B, GNAS, EEF1B2, PIK3R1, EPB41, SEPTIN6, TRAF3IP3, SP110, APOL6, SLC4A7, ICAM2, NPM1, CELF2, RESF1, KAT6B, SERBP1, TRMT112, HSP90AA1, BTF3, PDCD4, TAPBPL, SRRM2, RACK1, CNBP, PRRC2C
15	GP_1	RETN, PLAC8A, DHDDS, CENPW, CD177, CA6, CRISP2, OLR1, LYZ, CP, CAMP, ANXA1, METTL7A, BPI, CEBPE, H2AZ1, SERF1A, NUCB2, AK2, ACOT7, ACAT1, SRI, THEM4, CHI3L1, BARD1, PTMA, RRM2, CPNE3, TYMS, LCN2, ARHGDIB, ALOX15, NQO1, RCN1, TMX1, VDAC1, PPA1, SNRPD1, MYCBP, SSR4, MCM6, LDHB, FAIM, GPI, MGST1, SAP18, CROT, OXCT1, STMN1, RAD51AP1, SMC2, SPC24, SEM1, ATAD2, PCNA, DCXR, GSN, SLC20A1, STBD1, DBI, SIVA1, AGL, SPCS3, NDUFB4, RFC4, RAB13, PAFAH1B3, MCM3, SERPINB1, CSTA, EIF1AX, SSR3, CYBB, C3, SMIM4, LAMP2, COX5A, NMRAL1, LYRM2, SLBP, APPL1, VCL, C4H1orf131, PLSCR1, TESC, NUDT1, TUBA1B, CCNE2, NDUFS8, DNMT1, TUSC3, MRPL52, P4HA1, RBP7, SPTLC2, BDH1, RNASEH2B, H2AZ2, MRPL40, SVIP
16	Pro_B_cell	VPREB1, DNTT, AKAP12, ASNS, DPEP1, GYPC, PAX5, UHRF1, SYNE2, SULT1B1, BLNK, TCF4, PLS1, TPM2, FBLN1, NPNT, ADGRF1, CD34, FOXO1, LAMA4, RAB3IP, BAHCC1, EBF1, INKA1, LIMD1, POU2AF1, ZNF608, ALDH3A1, VPREB3, CD19, IL7R, TIFA, GAS6, PIMREG, LEF1, INSYN1, SLC4A11, YBX3, PSAT1, DCK, TLE1, CD72, MRC1, MARCKSL1, CASP3, SPTBN1, CA9, PEAR1, RAPGEF5, NINJ1, IGHM, TOP2B, MEF2C, MYB, SEPTIN6, SPATS2, RAG1, TCF3, CECR2, EFR3A, RTKN2, EPB41, CCSAP, HSPA2, CRYBG1, TLR7, N4BP2, VEGFC, PTMA, MDFIC, SEPTIN11, SOX4, PSIP1, ID3, CD2AP, PARP1, SLC39A6, MLLT10, CHD1, AKR1B1, MAP7D3, USP53, PRDX1, ARHGEF39, MSH6, XRCC1, ZCCHC7, TCF12, GNAS, CD22, CDIP1, SREK1, TTC3, EPHX1, SMC4, S100A13, TDP2, ILF2, NAP1L1, ATRX

17	Macrophage	C1QC, C1QA, C1QB, HMOX1, CD5L, GSTP1, CCL14, AIF1, SPIC, FXYD6, LGMN, BLVRB, FAM151A, VSIG4, MAFB, MRC1, VCAM1, CD163, DAB2, CD68, SERPINB6, PCOLCE2, MSR1, EPB41L3, NR1H3, IL18, FSCN1, PID1, TMEM47, SLC7A8, SELENOP, PLA2R1, SDC2, MYO1B, SAT2, CREG1, HAVCR1, PPARG, LGALS1, NRP1, MS4A7, ARL4C, FCGRT, CTSS, CXCL16, NIBAN3, HLA-DQB2, DNASE2, FTL, PRDX1, IL1R2, ACSF2, FTH1.1, EGFL7, TSPAN4, SLC40A1, GLUL, CTSC, DLA-DQA1, DLA-DRA, PECAM1, CD86, TTC38, B2M, CTSZ, FUCA1, MARCKS, ITGAV, DLA-DMA, CSTB, CCND1, SCPEP1, PSAP, NPC2, LY86, CD74, CNDP2, CFP, RNASEK, BPI, EPHX1, CD2, DSE, SAT1, ABCA1, PEPD, GPX1, FKBP11, VEGFB, DLA-64, CD63, RGS10, SLC37A2, GCSH, IFI30, GRN, CD300H, AP2M1, DLA88, ATP2B1
18	Plasma_Cell	JCHAIN, FKBP11, PRDX4, TXNDC5, DERL3, MZB1, TNFRSF17, MAN1A1, RARRES2, POU2AF1, IRF4, PRDM1, SPATS2L, XBP1, SELENOM, PDIA5, ZBTB38, SPATS2, CLEC2D, DNAJB9, CHPF, KRT18, TNFRSF13B, DGKI, GOLM1, MGLL, STN1, BMP6, LAPTM4A, SPINK2, SMIM1, NBEA, ELL2, FICD, EAF2, SLAMF7, ITIH5, TENT5C, SLC41A2, ICAM2, RRBP1, PIGT, BCAT2, SEL1L, LMAN1, TP53I13, QPCTL, MYDGF, GOLPH3L, HYOU1, DERL1, MAN1A2, CRELD2, AK1, PDCD4, HSPA13, PDIA4, SRM, PER3, DSE, GMPPB, STMN3, FNDC3A, HDLBP, ARFGAP3, MANF, SLC17A9, GSPT2, DNAJC1, TSPYL2, ARSG, BLNK, MS4A1, FKBP2, PLA2G12A, TXNDC11, NME1, PLEKHA8, MEF2C, SEC11C, TRAM1, DDRGK1, HSP90B1, HUS1, OSTC, SLC33A1, ERN1, DNAJB11, FUT8, TCF4, SPCS2, SDF2L1, TNFSF10, ANGPTL6, DLA-79, IPO4, DNAJC3, HOPX, SLC30A7, SEC61A1
19	Monocyte_2	THBS1, CTSS, VCAN, SLC2A3, FPR2, IL18, MAPK13, PLBD1, LRRK2, MARCHF1, MYOF, SLAMF9, LY86, LYST, TREM1, SULF2, CASP4, ATP2B1, CLEC12A, ARHGAP45, AOAH, SLC30A1, LCN2, VMP1, NBEAL2, LGALS1, ITGB7, CXCL8, RGS2, CLEC5A, MX2, TKT, DDIT4, C5AR1, ACTB, CYP27A1, APOBR, TLR4, EMP3, PLXNC1, DLA88, MYO9B, ZNF414, LYZ, MYH9, BTG1, HIPK2, ABCA1, REL, SERPINA1, SYNE1, IL17RA, UTRN, FCGR1A, IQGAP1, HIF1A, DLA-64, IGF2R, NLRP3, TUT7, APP, ARG2, AKAP13, SELL, UNC93B1, MCL1, LSP1, QSOX1, ARHGAP30, SLC6A6, LRRFIP1, CD37, LYG1, NFKBID, MAFB, ENO1, ZSWIM6, CTSZ, FOS, SLC37A2, SYK, CXCR4, PLAUR, XDH, WDFY3, LTF, ZFAND5,

		GGH, FMNL1, DPYD, B2M, FTH1.1, RBPJ, EMB, SORL1, BCL2A1, PDLIM2, RNASEL, GLRX, BANK1
20	UNKNWN	CA2, PRDX2, CA1, ALAS2, BLVRB, GYPA, HEMGN, KLF1, AHSP, CD79A, NOSTRIN, EEF1B2, IMPDH2, TSPO2, SPTA1, DNAJA4, GATA1, TUBA1B, ATP5IF1, COQ10B, ALAD, NPM1, NACA, LMNA, UBA52, EEF1A1, , PPOX, GPX1, HMGB1, EIF4A1, H1-5, SNRPG, UROD, SSR4, MGST3, SLC25A6, HSP90AB1, HSP90AA1, SOD1, H2AZ1, HSPA8, RAN, HMBS, TMSB10, IFT27, EEF1D, APEX1, CCDC34, TK1, GYPC, PLAC8A, PRDX3, UBE2S, STMN1, DYRK1B, ACADSB, RACK1, EIF3F, SERBP1, NME1, DUT, REXO2, EIF4B, EIF3K, TPX2, GADD45GIP1, ATP5F1D, CALM3, UROS, NT5C, TOP2A, TTLL12, NANS, NCL, PTMA, TRMT112, SMC2, TYMS, MKI67, HSPA9, PRKAR2B, CHCHD2, UQCR10, NDUFS3, UBAC1, STMP1, DEK, EIF3M, VDAC3, ATP5PF, HMGA1, MPO, POLR2H, SNRPD1, CCT6A, HNRNPA2B1, CENPF, DYNLL1.1, NUCKS1
21	HSPC	CD34, AKR1B1, RARRES2, EBPL, ENPP3, TNFSF13B, SULT1B1, ESAM, LRRC71, CBFA2T3, CEP68, DMD, DNTT, KIT, ALPL, ADGRG1, TFPI, APOC1, CCND2, NRIP1, GSTA4, FLT3, MSRB3, NAV3, IRAK1BP1, RCAN2, MNS1, MARCKSL1, FLNB, PEG3, NTHL1, PEAR1, HOXA9, PTP4A3, FBN2, GUCY1A1, RAI14, GLT8D2, FAM171B, CCDC30, PPP1R9A, HPGD, IL12RB2, CC2D2A, POGLUT2, VKORC1, SHMT2, SCML2, NUDT2, SH3BGRL2, AEN, RANGRF, SCRN2, CLEC3B, ZDHHC8, CDK6, SSBP4, GCAT, NFE2L3, CNTLN, FAM216A, RFTN1, DTWD1, MORN2, PDCD2L, MAGED2, ENOPH1, UTP20, POLR1G, PTOV1, PLXNA1, MYL6B, SNX30, KIF17, TRMT1, MAP3K6, SURF2, SRM, SOX4, NT5DC2, TCOF1, METTL1, MYC, PARP1, MTG1, FAAP100, TBRG4, FCER1A, MDN1, CAMKK2, ARHGAP5, NSG1, NBN, TRAP1, IARS1, PSD2, HMGA1, CEP89, JUP, MSH2
22	Poor-quality	ND4L

23	DC_precursor	S100A5, CD300H, PKIB, NAPSA, FCER1A, AHNAK, SHTN1, MRC1, GOLM1, BATF3, AHR, ADAM15, AK8, PPM1J, ECM1, ACOT9, FLT3, CCDC146, CLEC1B, PPP1R14A, CCND1, CCDC136, NAV1, CD1C, MT3, F11, PTH1R, PLD4, PLEKHA5, WNT10B, NECTIN1, TLR3, HIP1, SPHK1, SLC8A1, GPR183, FGD2, PLEKHO1, HAVCR1, CD86, TBC1D9, CAPN2, TPM4, FBP1, ATP1B1, DLA-DQA1, EGFL8, MYOF, IFI30, IRF4, ABCA5, METRNL, TARS2, FXYD1, CCR5, UCP2, BIN1, HOMER3, SULF2, TIMP1, CAMK1D, DLA-DMA, MT2A, RUNX2, GNGT2, CHN2, JUP, LY86, LRRC25, ALDOC, PPP2R3C, UNC119, SLC46A2, CBFA2T3, MDFIC, ABI3, FCGRT, CCDC6, TJP2, CD74, ZNF385A, MICAL2, MAP4K1, TCEA3, TMEM144, CCDC88A, ACAT2, HNMT, RGS10, TNFSF8, PYCARD, DSE, ZMIZ2, AIF1, SLC27A3, PARP15, GLB1, ZNF296, PRCP, EBPL
24	Cycling_Gran_2	NUSAP1, CCNB2, ASPM, CDKN3, PLK1, HMMR, CDC20, NUF2, KNL1, GTSE1, TOP2A, CENPF, DLGAP5, AURKA, TPX2, REEP4, UBE2C, CKS1B, KIF11, CENPW, CCNA2, CKAP2L, CEP55, CKAP2, UBE2S, SMG1, KIF23, PRC1, AURKB, BUB1B, CD177, NEK2, SGO2, GPSM2, MKI67, JPT1, KIF20B, DEPDC1, CCNB3, CDK1, CA6, ANXA1, PTGES, CP, CENPE, CAMP, SKA2, SECISBP2, G2E3, TACC3, C1orf54, CEBPE, SPC24, ECT2, C5orf58, P4HA1, KIF14, CRISP2, BUB1, DHDDS, SMC4, NDC80, TUBB6, SPC25, HP1BP3, H2AZ1, H2AZ2, CDCA8, TCN1, KIFC1, PLAC8A, TMEM229A, TUBA1B, ACAT1, DYNLL1.1, PEX3, TRIM59, CDCA3, CETN3, CSTA, RETN, SRI, SMIM12, OXCT1, LYG1, ARHGEF39, NUCKS1, CALM3, PPA2, MMP8, POLR3B, TMEM71, RSBN1, UGP2, SNRPD1, KIF18A, ARHGDIB, MIS18BP1, LCN2, RUNDC3B
25	Eosinophil	CPA3, HPGD, EPX, DPP4, IL3RA, ADGRE2, APCDD1L, ELAPOR1, GATM, MMP1, ADORA3, CMA1, TNIK, MS4A2, FCER1A, NDRG2, SMPD1, ALPL, CSF2RB, PLPP1, PTPN7, STXBP5, PON2, SYNE1, RAB44, RTN3, LMO4, ACSL4, ALOX15, TEC, ACLY, RUNX1, SCAP, DLA88, CELF2, MLLT6, MAN1A1, CD63, SERAC1, USP20, TMED7, MYH9, PPP3CA, ARFGEF1, TMBIM6, CXCR4, ANXA1, SNX30, LGALS1, DENND6A, TASOR, KIAA1109, DLA-DOA, NBEAL2, DYRK1B, CAT, ATF4, HNRNPH1, PHC2, CERS4, HSPA8, TBC1D10C, CTSA, TGFB1, SYNGR1, TENT5A, GSE1, SPINT2, ALAS1, TES, CABIN1, VEGFA, ITPR2, VPS13D, PCNX4, PFKFB3, SEMA4D, CA2, KIF21B, RABGAP1L, ANKRD44, BPTF, PRKDC, ATP5F1A, TUBA1B, CLTC, CNN2, MACF1, CANX, TAL1,

		PDZD8, ETS1, RACK1, MATR3, KAT6B, STT3A, TRAM1, IBTK, HSP90B1, TRIP12
26	MLP-CLP-like	CCND1, RARRES2, OCIAD2, FCER1A, IL7R, RYR1, IGF1, IGFBP7, FZD2, TMEM132A, EGFL7, CDH1, ADGRG5, PACSIN1, STYXL2, IRF8, CYB561A3, MT3, CYP2D15, TTYH1, COBLL1, TLR9, TLR3, TGFB2, RUNX2, THEM5, SQLE, JAM2, RAB3C, WDR27, HOMER3, FAM167A, FLNB, GALNTL6, CWH43, ZDHHC1, MCOLN2, P2RY14, SULF1, EPHA2, PTPRS, PLD4, NIBAN3, BACE1, AGBL4, SPATS2L, SPATA6, OSCAR, RIIAD1, CCR5, CD1C, BLNK, ATP1B1, TPM4, CDIP1, SCAP, AK8, ARHGAP31, TSPAN5, FAM118A, FCRLA, DGKI, DSE, PRKCI, TCF4, TM7SF2, MSMO1.1, GPR183, PLEKHA5, CXCL16, MPZL1, PRCP, MT2A, PSD2, SLC8A1, EBPL, MYO1E, CLEC2D, PARP15, SLC41A2, GYPC, FLT3, RUBCNL, CYP51A1, MAP4K1, UGCG, EFHC1, CCDC50, CD2AP, FCHO1, MT1E, SUSD1, ARF5, CBLB, SLC38A1, IRAG2, TLR7, BCL11A, SEMA4A, ERP29
27	MEP-like	NOSTRIN, UCHL1, SELENBP1, GATA1, KLF1, TSPO2, EPOR, MUC13, GFI1B, MICAL3, FN3K, DNAJA4, ENPP3, CD320, DMD, PDIA2, EMID1, AK1, CDC42BPA, PODXL, KCTD1, ADD2, CCND1, PLOD2, GUCY1B1, RHAG, PAQR5, CA9, PSEN2, KIT, MBOAT2, MARCHF3, ADGRG1, MNS1, SH3BGRL2, ITGA2B, SH2D4A, MAP3K6, TOM1L1, TERT, FAR2, PTPRF, RMDN2, SLC1A3, TEX15, MMEL1, KIF21A, VDR, CDK14, AGAP3, PRKG1, MYH10, LMNA, VEGFC, SCO2, NPR2, AQP1, PLSCR4, TRIM58, THAP4, PARD3B, ACKR1, RNF11, EGFL7, ENDOG, DLC1, SEPTIN8, PARD3, PTGS1, B9D1, VKORC1, IRAK1BP1, CDKL2, AEN, TRIP6, NR2F6, DAAM1, STN1, DST, CBFA2T3, FXYD1, PLEK2, MRRF, TTC38, MDN1, FKBP4, GCAT, EMC9, MYBBP1A, PTOV1, PIK3R2, KIF3A, SPTA1, RRP9, CDK6, KAT2A, CNN3, ARHGEF12, NNT, PCYOX1

Supplemental Table 4. Trajectory analysis results for the granulocytic/neutrophilic lineage. Selected results are shown for genes that have a q value < 0.05 and Moran's I > 0.25.

Gene/Gene Symbol	status	p_value	morans_test_statistic	morans_I	q_value
CAMP	OK	0	271.1838	0.939722	0
SLPI	OK	0	259.7576	0.899783	0
ENSCAFG00000031869	OK	0	258.5822	0.895781	0
ELANE	OK	0	256.799	0.889438	0
S100A8	OK	0	255.0812	0.8838	0
LTF	OK	0	254.7746	0.882828	0
S100A12	OK	0	254.4333	0.881594	0
RPL18	OK	0	253.1505	0.877062	0
RPS12	OK	0	251.7372	0.872157	0
RPS24	OK	0	250.8356	0.869153	0
RPL35A	OK	0	249.3506	0.86397	0
MT-CO3	OK	0	249.1692	0.862943	0
RPS23	OK	0	248.6303	0.8614	0
MT-CO2	OK	0	248.5522	0.860956	0
RPL13	OK	0	247.9856	0.859152	0
RPL32	OK	0	247.6668	0.858127	0
ENSCAFG00000032259	OK	0	246.3641	0.853661	0
RPS17	OK	0	243.0695	0.842171	0
ENSCAFG00000042212	OK	0	242.25	0.839314	0
RPS13	OK	0	241.2524	0.835859	0
RPS15A	OK	0	240.6676	0.833798	0
MT-ATP6	OK	0	240.6249	0.833052	0
RPS26	OK	0	240.2314	0.832369	0
RPS5	OK	0	239.567	0.82996	0
RPS18	OK	0	239.1584	0.828536	0
ENSCAFG00000029884	OK	0	238.5593	0.826431	0
RPS27A	OK	0	237.9164	0.824286	0
CD79A	OK	0	237.4794	0.822729	0
PGLYRP1	OK	0	236.7403	0.820264	0
RPS10	OK	0	235.461	0.815873	0
PTMA	OK	0	234.9122	0.813859	0
RPL9	OK	0	234.8605	0.813653	0
RPS25	OK	0	233.9729	0.810692	0
RPS4X	OK	0	233.956	0.810539	0
ENSCAFG00000031952	OK	0	232.8026	0.806629	0
ENSCAFG00000017688	OK	0	232.5221	0.805473	0
ENSCAFG00000046992	OK	0	231.9104	0.803415	0
RPS11	OK	0	231.2381	0.801095	0
ENSCAFG00000018784	OK	0	230.9803	0.800203	0

RPL8	OK	0	230.4534	0.79845	0
RPS7	OK	0	229.7322	0.79596	0
RPL21	OK	0	228.8189	0.792717	0
DHDDS	OK	0	227.7846	0.789091	0
RPS14	OK	0	227.738	0.789072	0
RPL27A	OK	0	226.9742	0.786185	0
RPL24	OK	0	226.7442	0.785558	0
FTH1.1	OK	0	226.6103	0.784511	0
RPS28	OK	0	225.912	0.782712	0
RPS27	OK	0	224.3847	0.777503	0
RPS3A	OK	0	224.3259	0.777181	0
VIM	OK	0	224.0494	0.776334	0
ENSCAFG00000019044	OK	0	223.3056	0.773664	0
MT-ND4	OK	0	222.7084	0.771132	0
MT-CYB	OK	0	222.2802	0.769488	0
PLAC8A	OK	0	222.0455	0.769104	0
RPL22	OK	0	221.9828	0.769092	0
RPL23	OK	0	221.4029	0.76699	0
RPL12	OK	0	220.7731	0.764779	0
RPL15	OK	0	217.4945	0.753461	0
SSR4	OK	0	217.4139	0.753245	0
RPL28	OK	0	216.4314	0.749803	0
RPS8	OK	0	214.0496	0.741629	0
EEF1B2	OK	0	213.8302	0.740711	0
RPL7A	OK	0	213.6172	0.739998	0
ENSCAFG00000009523	OK	0	213.244	0.73887	0
SNRPG	OK	0	213.0926	0.738231	0
ENSCAFG00000043173	OK	0	212.224	0.735139	0
H2AZ1	OK	0	211.4166	0.732341	0
LYZ	OK	0	209.2586	0.724987	0
NACA	OK	0	208.1638	0.721187	0
RPL3	OK	0	208.0783	0.720742	0
RPL11	OK	0	207.8787	0.720277	0
RPL7	OK	0	202.8902	0.702842	0
RPS6	OK	0	200.7767	0.695419	0
ENSCAFG00000045333	OK	0	199.3155	0.690405	0
PADI3	OK	0	199.0564	0.689675	0
RPLP0	OK	0	198.9995	0.689277	0
UBA52	OK	0	198.3752	0.687312	0
RPL35	OK	0	197.2284	0.683259	0
RPL27	OK	0	196.2621	0.680007	0
RPL34	OK	0	194.7764	0.674834	0
ENSCAFG00000031706	OK	0	194.6224	0.674078	0

MPO	OK	0	196.8384	0.673057	0
COQ10B	OK	0	192.353	0.666147	0
RETN	OK	0	191.9164	0.664196	0
GADD45A	OK	0	190.9915	0.661573	0
RPL5	OK	0	189.7946	0.657542	0
SERPINA1	OK	0	189.6461	0.656784	0
PLA2G7	OK	0	189.4251	0.655938	0
BPI	OK	0	193.504	0.65578	0
MT-ND1	OK	0	189.1805	0.654865	0
CENPW	OK	0	189.0492	0.654679	0
RPSA	OK	0	187.3574	0.648989	0
C9H17orf64	OK	0	186.5514	0.646361	0
FTL	OK	0	186.4403	0.644618	0
NME2	OK	0	184.795	0.640167	0
ISG20	OK	0	183.3147	0.634827	0
FKBP11	OK	0	181.9426	0.62887	0
FADS1	OK	0	181.0509	0.627275	0
DYRK1B	OK	0	180.4612	0.625159	0
SOD2	OK	0	180.4343	0.62477	0
STMN1	OK	0	180.1184	0.623742	0
ENSCAFG00000049043	OK	0	176.7752	0.61243	0
RPL10A	OK	0	175.8029	0.60906	0
NFKBID	OK	0	174.6006	0.604805	0
ENSCAFG00000005768	OK	0	174.1958	0.603471	0
GGH	OK	0	173.6968	0.601543	0
OAZ1	OK	0	172.5886	0.597884	0
CP	OK	0	171.2101	0.592989	0
SELL	OK	0	171.0505	0.592388	0
MMP9	OK	0	170.1238	0.58914	0
ENSCAFG00000030087	OK	0	170.1709	0.588891	0
MT-CO1	OK	0	169.0116	0.585347	0
ENSCAFG00000015122	OK	0	168.9606	0.58533	0
ENSCAFG00000044682	OK	0	167.0299	0.578552	0
GZMB	OK	0	167.0165	0.576874	0
HSP90AB1	OK	0	165.5041	0.573002	0
ACTB	OK	0	163.1972	0.565358	0
MMP8	OK	0	161.1976	0.558345	0
RGS2	OK	0	160.0917	0.554465	0
HSP90B1	OK	0	159.6028	0.552465	0
RPL19	OK	0	158.9094	0.550537	0
ENSCAFG00000006102	OK	0	157.2301	0.544653	0
SSR3	OK	0	156.7232	0.542928	0
GMFG	OK	0	156.3578	0.541662	0

CEACAM28	OK	0	155.893	0.539558	0
RPL13A	OK	0	155.4644	0.538553	0
ENSCAFG00000008873	OK	0	153.8113	0.532799	0
LCP1	OK	0	152.4136	0.52799	0
ENSCAFG00000013366	OK	0	152.3502	0.527685	0
EMB	OK	0	151.2683	0.523837	0
HMGB2	OK	0	151.0164	0.523109	0
ARHGAP45	OK	0	150.1816	0.519824	0
ENSCAFG00000048610	OK	0	149.4398	0.517614	0
TYMS	OK	0	148.6935	0.513583	0
CD177	OK	0	148.1891	0.513234	0
CAPG	OK	0	147.7819	0.511955	0
RACK1	OK	0	146.1576	0.506096	0
RPS15	OK	0	145.8091	0.504997	0
H1-5	OK	0	146.0641	0.503319	0
CSNK1G1	OK	0	145.2882	0.502855	0
MT-ND2	OK	0	145.0449	0.500977	0
CDA	OK	0	142.9721	0.495031	0
PPA1	OK	0	142.6497	0.493846	0
C30H15orf48	OK	0	142.7778	0.493625	0
NPM1	OK	0	141.813	0.490689	0
ENSCAFG00000017824	OK	0	141.4218	0.489851	0
SH3BGRL3	OK	0	140.8066	0.487804	0
ENSCAFG00000000118	OK	0	139.8448	0.483878	0
RPS3	OK	0	139.3467	0.482681	0
RPL14	OK	0	139.1379	0.481873	0
NAP1L1	OK	0	139.1319	0.481363	0
SERPINB1	OK	0	138.8902	0.481157	0
ENSCAFG00000023205	OK	0	138.645	0.480194	0
ENSCAFG00000002215	OK	0	138.1555	0.478595	0
ENSCAFG00000000443	OK	0	138.1881	0.478125	0
ENSCAFG00000048619	OK	0	137.4607	0.476081	0
B2M	OK	0	134.8943	0.466799	0
TESC	OK	0	133.6758	0.463001	0
ENSCAFG00000017264	OK	0	133.7012	0.461735	0
ITM2B	OK	0	132.8934	0.459999	0
ABTB1	OK	0	132.5731	0.459149	0
RPS21	OK	0	132.3668	0.458486	0
CD4	OK	0	131.982	0.4561	0
MT-ND3	OK	0	131.9971	0.455837	0
MMD	OK	0	130.982	0.453105	0
ENSCAFG00000009113	OK	0	130.7146	0.452106	0
CXCL8	OK	0	129.7561	0.448518	0

TUBA1B	OK	0	128.6263	0.445173	0
DHRS7	OK	0	128.4641	0.444929	0
ENSCAFG00000013905	OK	0	127.3193	0.440953	0
SEC61B	OK	0	127.153	0.440271	0
COX7A1	OK	0	127.3786	0.440053	0
ENO1	OK	0	126.9334	0.439719	0
LGALS3	OK	0	126.91	0.439594	0
NUSAP1	OK	0	127.3789	0.439415	0
RGS19	OK	0	126.3376	0.437592	0
SNRPD1	OK	0	125.4746	0.434568	0
GABARAP	OK	0	125.426	0.434392	0
TCN1	OK	0	125.3673	0.434126	0
PFN1	OK	0	124.145	0.430041	0
ENSCAFG00000050001	OK	0	124.4406	0.429423	0
LSP1	OK	0	123.8323	0.428944	0
ENSCAFG00000005978	OK	0	122.8147	0.425269	0
EIF1	OK	0	122.2869	0.423437	0
SEC11C	OK	0	122.2387	0.423277	0
ACTG1	OK	0	121.7162	0.421643	0
S100P	OK	0	121.3887	0.420528	0
GALK1	OK	0	120.9456	0.418604	0
SPC24	OK	0	120.3372	0.415544	0
EIF3K	OK	0	119.1855	0.412887	0
ENSCAFG00000042472	OK	0	117.3997	0.406122	0
ENSCAFG00000049566	OK	0	117.1287	0.405122	0
MSRB1	OK	0	115.3547	0.39946	0
ATP5MC1	OK	0	115.274	0.399093	0
CKAP4	OK	0	115.08	0.398479	0
EEF1A1	OK	0	113.85	0.394167	0
ENSCAFG00000031588	OK	0	112.8073	0.390761	0
RASL11A	OK	0	113.7876	0.387475	0
THEM4	OK	0	111.4683	0.385624	0
FCGR1A	OK	0	110.6491	0.383058	0
ENSCAFG00000032392	OK	0	110.1834	0.381515	0
ENSCAFG00000049108	OK	0	108.8897	0.377022	0
ANXA1	OK	0	108.7898	0.376294	0
GPCPD1	OK	0	108.808	0.37623	0
SMC2	OK	0	107.9451	0.372981	0
SIVA1	OK	0	107.9012	0.372475	0
DDX5	OK	0	106.9027	0.370044	0
CCNB2	OK	0	106.5343	0.367576	0
CANX	OK	0	106.5463	0.367284	0
TIMP2	OK	0	105.8947	0.366376	0

CXCR4	OK	0	104.8205	0.360888	0
TFPT	OK	0	104.0178	0.360298	0
RPL26	OK	0	103.7407	0.359139	0
ENSCAFG00000049156	OK	0	103.2335	0.357408	0
BDH1	OK	0	103.1352	0.357185	0
PAFAH1B3	OK	0	103.2454	0.35687	0
NOP10	OK	0	103.0892	0.356387	0
NIFK	OK	0	102.1983	0.353448	0
ENSCAFG00000019220	OK	0	102.0044	0.353172	0
HMGB1	OK	0	101.8768	0.352851	0
HMGN3	OK	0	101.8322	0.352197	0
TNFSF13	OK	0	101.719	0.351475	0
SDF2L1	OK	0	100.6737	0.34842	0
PDIA4	OK	0	100.9435	0.348202	0
C5AR1	OK	0	100.6009	0.348188	0
ACTR3	OK	0	100.1793	0.346983	0
METTL7A	OK	0	100.2025	0.346615	0
SERF1A	OK	0	99.95316	0.345408	0
PLBD1	OK	0	98.94035	0.342533	0
ENSCAFG00000046564	OK	0	98.89951	0.342454	0
FAU	OK	0	98.76268	0.342064	0
PPA2	OK	0	98.69994	0.341853	0
CPNE3	OK	0	98.05759	0.339645	0
ALAS1	OK	0	98.00342	0.339346	0
URI1	OK	0	98.14732	0.339117	0
PRNP	OK	0	97.85464	0.338532	0
ENSCAFG00000042554	OK	0	97.71338	0.33847	0
SLC25A6	OK	0	96.27238	0.33341	0
SNRPD2	OK	0	95.64535	0.331244	0
SRI	OK	0	94.5811	0.327607	0
PGLS	OK	0	93.85342	0.324978	0
NMRAL1	OK	0	94.01597	0.324751	0
GAPDH	OK	0	93.68242	0.324481	0
RNASEK	OK	0	93.53356	0.323853	0
UBE2B	OK	0	93.39172	0.323237	0
NUCB2	OK	0	93.33934	0.323233	0
ENSCAFG00000025063	OK	0	93.37679	0.323041	0
ENSCAFG00000032036	OK	0	93.18096	0.321222	0
SAT1	OK	0	92.74643	0.32098	0
SRGN	OK	0	92.57868	0.320271	0
ADGRE3	OK	0	92.40727	0.31902	0
CALR	OK	0	92.4155	0.318483	0
DLA-64	OK	0	91.80927	0.317504	0

ACAT1	OK	0	91.66544	0.317357	0
CCPG1	OK	0	90.80899	0.31444	0
LDHB	OK	0	91.03356	0.314198	0
RFC4	OK	0	90.63461	0.313103	0
SEC14L1	OK	0	90.38911	0.312873	0
RAD51AP1	OK	0	90.6942	0.312598	0
RRM2	OK	0	90.25678	0.311316	0
HMMR	OK	0	89.31387	0.308434	0
CYBA	OK	0	88.81911	0.307636	0
COX5A	OK	0	88.7075	0.307153	0
ENSCAFG00000048539	OK	0	88.88078	0.30713	0
ALOX15	OK	0	88.90571	0.306655	0
VASP	OK	0	88.53506	0.306569	0
PTPRC	OK	0	88.27303	0.305691	0
CLTA	OK	0	88.23745	0.305439	0
MRTO4	OK	0	88.00786	0.303209	0
KRTCAP2	OK	0	87.06184	0.301416	0
ENSCAFG00000029155	OK	0	86.93697	0.301125	0
CHCHD2	OK	0	86.32558	0.298936	0
ENSCAFG00000035349	OK	0	86.12898	0.297787	0
MGAT4A	OK	0	85.25189	0.29523	0
AP1S2	OK	0	84.73222	0.293379	0
SPI1	OK	0	84.62827	0.292989	0
IL17RA	OK	0	84.55523	0.292712	0
PTPN1	OK	0	84.53218	0.292528	0
TOP2A	OK	0	85.52563	0.29227	0
TPX2	OK	0	83.94759	0.288835	0
ENSCAFG00000043730	OK	0	83.39197	0.288757	0
FABP3	OK	0	82.84397	0.284476	0
SKAP2	OK	0	82.0473	0.283983	0
UBE2C	OK	0	82.54371	0.283666	0
SEM1	OK	0	81.57442	0.282491	0
DBI	OK	0	81.59764	0.282482	0
PPP1R14B	OK	0	81.55602	0.281282	0
GLIPR1	OK	0	80.7964	0.27948	0
ERH	OK	0	80.77124	0.279328	0
CDC20	OK	0	81.17579	0.278977	0
KNL1	OK	0	80.15696	0.275849	0
RESF1	OK	0	79.24904	0.273944	0
BTF3	OK	0	78.83777	0.272992	0
ENSCAFG00000016065	OK	0	78.79182	0.272739	0
CRISP2	OK	0	78.69695	0.272422	0
NUCKS1	OK	0	78.63225	0.271885	0

ATAD2	OK	0	78.73953	0.270958	0
LBHD1	OK	0	78.06121	0.268629	0
PCBD1	OK	0	77.44575	0.264744	0
ENSCAFG00000043193	OK	0	76.06286	0.263184	0
STK17B	OK	0	76.05299	0.263149	0
FBL	OK	0	76.31828	0.263079	0
ENSCAFG00000004842	OK	0	75.99084	0.262865	0
ENSCAFG00000045775	OK	0	75.98393	0.262467	0
ARPC2	OK	0	75.60535	0.261816	0
C1QBP	OK	0	75.65228	0.261155	0
NME1	OK	0	75.48413	0.259811	0
ARG2	OK	0	74.66872	0.258415	0
YPEL3	OK	0	74.43512	0.257592	0
CA6	OK	0	74.31776	0.257151	0
CYBB	OK	0	74.22063	0.25696	0
ENSCAFG00000008311	OK	0	74.10572	0.256373	0
AK2	OK	0	73.99087	0.255993	0
RNASEH2B	OK	0	73.96964	0.255944	0
RBP7	OK	0	73.96953	0.255712	0
FGL2	OK	0	73.67534	0.254971	0
ZFAND5	OK	0	73.72124	0.254454	0
CCNE2	OK	0	73.67169	0.253643	0
SYNGR1	OK	0	73.34434	0.253617	0
AKAP13	OK	0	73.37707	0.253453	0
ENSCAFG00000019360	OK	0	73.04977	0.25285	0
OXCT1	OK	0	72.83706	0.252146	0
SNX10	OK	0	72.83786	0.251951	0
CD63	OK	0	72.71917	0.251789	0
BCL2A1	OK	0	72.77249	0.251361	0
TPI1	OK	0	72.48704	0.250964	0
CENPF	OK	0	72.90817	0.250422	0

Supplemental Table 5. Trajectory analysis results for the monocytic/dendritic cell lineage.
Selected results are shown for genes that have a q value < 0.05 and Moran's I > 0.25.

Gene/ Gene Symbol	status	p_value	morans_test_statistic	morans_I	q_value
H2AZ1	OK	0	105.5169	0.873319	0
TUBA1B	OK	0	105.4264	0.871732	0
STMN1	OK	0	102.5409	0.848403	0
PTMA	OK	0	102.0356	0.844449	0
HMGB1	OK	0	101.9882	0.844042	0
TOP2A	OK	0	102.3126	0.844002	0
S100A12	OK	0	100.1107	0.827572	0
UBE2S	OK	0	97.12333	0.801837	0
ASPM	OK	0	96.81193	0.797364	0
PLK1	OK	0	95.61931	0.788303	0
CENPF	OK	0	95.20766	0.784796	0
S100A8	OK	0	94.79835	0.783799	0
TMSB10	OK	0	93.79441	0.775121	0
ENSCAFG00000008661	OK	0	93.15139	0.767225	0
DHDDS	OK	0	92.40906	0.764363	0
TUBB6	OK	0	92.3501	0.762515	0
CDC20	OK	0	92.07933	0.7592	0
LTF	OK	0	91.85342	0.758	0
SMC4	OK	0	91.52384	0.756144	0
KIF20B	OK	0	90.73244	0.748696	0
NUCKS1	OK	0	90.4804	0.748037	0
MKI67	OK	0	90.32753	0.745349	0
TPX2	OK	0	89.17722	0.736367	0
NUSAP1	OK	0	88.85027	0.732346	0
ENSCAFG00000000443	OK	0	88.44217	0.7308	0
ENSCAFG00000017264	OK	0	88.43929	0.729903	0
CENPE	OK	0	88.32111	0.7281	0
ENSCAFG00000028765	OK	0	88.08907	0.726301	0
CCNB2	OK	0	87.96893	0.726269	0
HMGB2	OK	0	87.15415	0.720746	0
ENSCAFG00000030087	OK	0	86.53646	0.714537	0
PADI3	OK	0	86.48294	0.713995	0
GTSE1	OK	0	86.5104	0.713465	0
ENSCAFG00000007705	OK	0	86.42203	0.712041	0
TYMS	OK	0	85.31254	0.704433	0
H1-5	OK	0	84.93701	0.701117	0
SERPINA1	OK	0	84.49914	0.695647	0
CENPW	OK	0	84.02424	0.694788	0
KNL1	OK	0	84.18524	0.694257	0
RGS2	OK	0	84.00515	0.692224	0

ENSCAFG00000050001	OK	0	83.54105	0.689482	0
FTH1.1	OK	0	83.68618	0.689372	0
KIF11	OK	0	82.78114	0.682904	0
SPC24	OK	0	82.00014	0.677947	0
NUF2	OK	0	82.17689	0.677452	0
CDCA3	OK	0	82.04909	0.675802	0
ENSCAFG00000042212	OK	0	81.32855	0.672812	0
NFKBID	OK	0	80.73455	0.667101	0
C9H17orf64	OK	0	80.30391	0.662563	0
SMC2	OK	0	80.06603	0.661512	0
DUT	OK	0	79.90983	0.660605	0
GADD45A	OK	0	80.11258	0.660318	0
RPL13	OK	0	79.69634	0.659321	0
DLA-DRA	OK	0	80.2701	0.658292	0
ENSCAFG00000009113	OK	0	79.79561	0.658225	0
ARHGEF39	OK	0	79.72633	0.657742	0
ARHGAP45	OK	0	79.5474	0.657542	0
KIF15	OK	0	79.46063	0.656078	0
AURKB	OK	0	79.37289	0.655278	0
BUB1B	OK	0	79.16656	0.653009	0
DLGAP5	OK	0	78.95084	0.650781	0
FABP3	OK	0	78.75725	0.650727	0
CD79A	OK	0	78.4749	0.649142	0
NDC80	OK	0	78.50977	0.647062	0
KIF22	OK	0	78.39842	0.646909	0
RPL3	OK	0	78.17938	0.646819	0
ENSCAFG00000016482	OK	0	78.20842	0.645961	0
TK1	OK	0	78.07287	0.644745	0
ENSCAFG00000002332	OK	0	78.07709	0.642932	0
KIF23	OK	0	77.8006	0.641552	0
PLBD1	OK	0	77.58929	0.641482	0
EMB	OK	0	77.53041	0.638881	0
CKAP2L	OK	0	76.83683	0.633591	0
IFI30	OK	0	76.78715	0.633342	0
CDK1	OK	0	76.68088	0.632138	0
MIS18BP1	OK	0	76.35217	0.630119	0
RRM2	OK	0	76.22038	0.628859	0
NMRAL1	OK	0	75.93049	0.627003	0
SGO2	OK	0	75.95097	0.626164	0
RPS11	OK	0	75.62754	0.625478	0
PLA2G7	OK	0	75.07823	0.617963	0
GGH	OK	0	74.82625	0.617488	0
RPL18	OK	0	74.54574	0.616622	0

KIFC1	OK	0	74.57561	0.614833	0
ISG20	OK	0	74.89868	0.6138	0
COQ10B	OK	0	74.1917	0.613673	0
HMMR	OK	0	74.19677	0.610356	0
RPSA	OK	0	73.5363	0.608364	0
NCAPG	OK	0	73.37294	0.606269	0
CCNA2	OK	0	73.46563	0.605644	0
CKAP2	OK	0	73.40852	0.60475	0
ENSCAFG00000043319	OK	0	73.15005	0.603336	0
LYZ	OK	0	72.77224	0.601947	0
RPL7A	OK	0	72.74893	0.601784	0
RPS15A	OK	0	72.50644	0.599769	0
RPS23	OK	0	72.5005	0.599736	0
CTSS	OK	0	72.51172	0.598816	0
CALM3	OK	0	71.9904	0.595265	0
JPT1	OK	0	71.74535	0.591485	0
HLA-DQB2	OK	0	72.13492	0.589976	0
RPL32	OK	0	71.27024	0.589472	0
RPS27A	OK	0	71.20919	0.589027	0
SELL	OK	0	71.24068	0.588043	0
BPI	OK	0	70.83114	0.585744	0
C5AR1	OK	0	70.82192	0.583143	0
ENSCAFG00000013905	OK	0	70.48426	0.583054	0
CDK4	OK	0	70.40725	0.582131	0
MCM6	OK	0	70.62768	0.581753	0
ENSCAFG00000049566	OK	0	70.05717	0.578841	0
ENSCAFG00000017688	OK	0	69.59451	0.575646	0
RPL10A	OK	0	69.54415	0.575197	0
MYBL2	OK	0	69.75935	0.574988	0
MCM3	OK	0	69.56036	0.572579	0
ENSCAFG00000048539	OK	0	68.75638	0.568233	0
ENSCAFG00000029884	OK	0	68.58129	0.567229	0
CEP55	OK	0	68.86816	0.566565	0
BUB1	OK	0	68.73861	0.56619	0
ENSCAFG00000018784	OK	0	68.13385	0.563475	0
SGO1	OK	0	68.31222	0.563149	0
PRC1	OK	0	67.84397	0.559458	0
RPL15	OK	0	67.58276	0.558981	0
RPS5	OK	0	67.53684	0.558605	0
RPS4X	OK	0	67.50222	0.55829	0
RPL8	OK	0	67.48328	0.558075	0
H2AZ2	OK	0	67.49345	0.557798	0
AURKA	OK	0	67.87488	0.55765	0

RPL12	OK	0	67.40381	0.557501	0
FCGR1A	OK	0	67.60571	0.557277	0
RPS26	OK	0	67.00949	0.554227	0
SMG1	OK	0	67.16161	0.553305	0
HSP90AB1	OK	0	66.74999	0.551953	0
RFC4	OK	0	66.61399	0.550251	0
MTFR2	OK	0	66.49279	0.548538	0
MCM7	OK	0	66.41155	0.548378	0
BRCA2	OK	0	66.20594	0.54669	0
TACC3	OK	0	65.95504	0.54479	0
RPS18	OK	0	65.78112	0.544034	0
ANP32E	OK	0	65.61147	0.542326	0
DLA-DQA1	OK	0	66.23671	0.542154	0
ANLN	OK	0	65.89102	0.541993	0
NAP1L1	OK	0	65.2886	0.539758	0
REEP4	OK	0	65.46337	0.538861	0
CSNK1G1	OK	0	65.13281	0.53878	0
MSRB1	OK	0	65.52795	0.538296	0
IL17RA	OK	0	65.21287	0.538199	0
ENO1	OK	0	64.81662	0.536137	0
ENSCAFG00000006102	OK	0	64.80154	0.535911	0
ENSCAFG00000045333	OK	0	64.34674	0.532149	0
CKS1B	OK	0	64.22024	0.530447	0
SIVA1	OK	0	64.0761	0.5291	0
DDX39A	OK	0	64.0217	0.528967	0
RAN	OK	0	63.86843	0.528213	0
ENSCAFG00000013366	OK	0	63.79883	0.527656	0
LSP1	OK	0	63.74123	0.526771	0
MT-ATP6	OK	0	63.60402	0.52601	0
S100P	OK	0	63.61465	0.525869	0
SOD2	OK	0	64.00958	0.52221	0
PYGL	OK	0	63.38891	0.521865	0
RPS8	OK	0	62.88203	0.520032	0
DDX5	OK	0	63.01494	0.518555	0
RPS6	OK	0	62.63508	0.518033	0
ENSCAFG00000046992	OK	0	62.61446	0.517691	0
RPL24	OK	0	62.58389	0.517491	0
SPAG5	OK	0	62.07498	0.510905	0
MT-ND4	OK	0	61.69926	0.510107	0
RPS12	OK	0	61.4758	0.508145	0
ENSCAFG00000046600	OK	0	61.53072	0.507375	0
DEPDC1	OK	0	61.44507	0.503563	0
HELLS	OK	0	61.26631	0.503497	0

MT-CO3	OK	0	60.78916	0.502717	0
HSP90B1	OK	0	60.8309	0.502546	0
NME1	OK	0	60.69883	0.501492	0
VIM	OK	0	60.57556	0.500571	0
KIF4A	OK	0	60.59532	0.499377	0
RPL9	OK	0	60.30053	0.498678	0
LGALS1	OK	0	60.28117	0.498546	0
CAMP	OK	0	61.80256	0.49788	0
HJURP	OK	0	60.68281	0.497831	0
DNMT1	OK	0	60.23357	0.497511	0
CLSPN	OK	0	60.3649	0.497062	0
GMFG	OK	0	60.11368	0.496198	0
PA2G4	OK	0	60.01265	0.496135	0
APEX1	OK	0	60.03207	0.495904	0
CHAF1A	OK	0	60.08179	0.495764	0
CXCR4	OK	0	60.16685	0.495705	0
BARD1	OK	0	59.92475	0.494999	0
SPCS3	OK	0	59.8488	0.494943	0
CRIP1	OK	0	60.16113	0.494761	0
SKA2	OK	0	59.91359	0.494509	0
PKIB	OK	0	61.24771	0.489741	0
ENSCAFG00000029470	OK	0	59.40797	0.489629	0
ABTB1	OK	0	59.9908	0.489483	0
GALK1	OK	0	59.56854	0.489267	0
RUNDC3B	OK	0	59.26801	0.488815	0
H2AC18	OK	0	59.27309	0.487395	0
CD74	OK	0	59.31354	0.486906	0
INCENP	OK	0	58.82058	0.485798	0
STK17B	OK	0	59.07169	0.485755	0
RPS17	OK	0	58.71609	0.485497	0
CCPG1	OK	0	58.84258	0.485179	0
ATAD2	OK	0	58.77525	0.484906	0
KIF14	OK	0	58.68661	0.482677	0
RPL35A	OK	0	58.01935	0.479671	0
TTK	OK	0	58.22804	0.47866	0
RBBP7	OK	0	57.88794	0.478445	0
ENSCAFG00000023111	OK	0	57.79356	0.477407	0
SNRPG	OK	0	57.66975	0.47695	0
ERH	OK	0	57.58934	0.476229	0
CP	OK	0	58.2476	0.474053	0
EIF1	OK	0	57.37851	0.473946	0
MT-CYB	OK	0	57.20713	0.472883	0
CXCL8	OK	0	58.12295	0.472841	0

ENSCAFG00000015122	OK	0	57.01264	0.471375	0
MSH6	OK	0	57.18979	0.471018	0
RPL19	OK	0	56.93244	0.470738	0
RPL13A	OK	0	56.92207	0.470605	0
PSME2	OK	0	56.87891	0.469762	0
ENSCAFG00000044628	OK	0	57.48537	0.468358	0
RPS3A	OK	0	56.48046	0.466995	0
ATAD5	OK	0	56.3731	0.465197	0
CKAP4	OK	0	56.30746	0.464129	0
RPS25	OK	0	56.11555	0.463968	0
TROAP	OK	0	56.44766	0.463687	0
NME2	OK	0	55.93873	0.462554	0
CYBA	OK	0	55.86001	0.461716	0
SMC1A	OK	0	55.81797	0.461129	0
ENSCAFG00000048610	OK	0	55.63863	0.460138	0
RPL23	OK	0	55.64873	0.460106	0
MT-CO2	OK	0	55.55901	0.459342	0
AK8	OK	0	56.16984	0.458011	0
MMP8	OK	0	56.40437	0.457679	0
DYNLL1.1	OK	0	55.2132	0.456306	0
TKT	OK	0	55.14187	0.455542	0
CCT6A	OK	0	54.89195	0.453848	0
KIF18B	OK	0	55.12162	0.453103	0
PPA1	OK	0	54.82244	0.452471	0
NCAPD2	OK	0	54.89442	0.452463	0
MAPK13	OK	0	54.94231	0.452116	0
CDKN3	OK	0	55.00002	0.451462	0
ACTB	OK	0	54.58204	0.450988	0
RPS13	OK	0	54.43881	0.450031	0
CCNE2	OK	0	54.75664	0.449961	0
EEF1A1	OK	0	54.29991	0.448955	0
PRDX1	OK	0	54.23283	0.448382	0
ALOX5AP	OK	0	54.12023	0.447307	0
CD4	OK	0	54.85916	0.447181	0
CDCA8	OK	0	54.17246	0.445961	0
RPL7	OK	0	53.8512	0.445255	0
HNRNPAB	OK	0	53.80237	0.444831	0
CBX5	OK	0	53.82918	0.444784	0
RPLP0	OK	0	53.71695	0.444095	0
CDA	OK	0	53.78387	0.443093	0
ENSCAFG00000003970	OK	0	53.60515	0.441538	0
FBL	OK	0	53.35953	0.441112	0
SERPINB1	OK	0	53.34545	0.440377	0

OAZ1	OK	0	53.20544	0.439228	0
PSIP1	OK	0	53.08814	0.438659	0
RPS7	OK	0	53.0071	0.438252	0
LCN2	OK	0	52.94603	0.436538	0
DHRS7	OK	0	52.9825	0.43632	0
RGS10	OK	0	52.88696	0.435571	0
NASP	OK	0	52.65986	0.435277	0
CENPK	OK	0	52.78205	0.435178	0
CHCHD2	OK	0	52.5334	0.434396	0
ECT2	OK	0	52.74157	0.433858	0
CDCA2	OK	0	52.7716	0.433823	0
AMDHD1	OK	0	52.4888	0.433724	0
TUBB4B	OK	0	52.54713	0.433099	0
NUDT1	OK	0	52.47362	0.432837	0
ODF2	OK	0	52.39768	0.431931	0
FADS1	OK	0	52.54399	0.42948	0
ORC6	OK	0	52.07858	0.429003	0
ENSCAFG00000009523	OK	0	51.77726	0.427855	0
NPM1	OK	0	51.74992	0.427695	0
ENSCAFG00000011598	OK	0	52.15316	0.427046	0
RAD51	OK	0	51.97122	0.426179	0
HNRNPD	OK	0	51.54859	0.426142	0
ENSCAFG00000049156	OK	0	51.47292	0.425668	0
SMC6	OK	0	51.49176	0.425317	0
RAD51AP1	OK	0	51.49502	0.424474	0
SPC25	OK	0	51.49972	0.424074	0
SYNGR2	OK	0	51.45511	0.423854	0
GLRX	OK	0	51.2611	0.4235	0
PPM1J	OK	0	51.43181	0.42307	0
CEACAM28	OK	0	51.92711	0.422975	0
ANXA2	OK	0	50.79724	0.420018	0
GSN	OK	0	50.88799	0.419562	0
PPP1R14B	OK	0	50.67007	0.418607	0
PRDX4	OK	0	50.60888	0.417409	0
ESCO2	OK	0	50.58619	0.416677	0
RACGAP1	OK	0	50.49646	0.414604	0
RPS28	OK	0	50.09713	0.414188	0
ENSCAFG00000031869	OK	0	50.1123	0.413941	0
ENSCAFG00000023735	OK	0	50.62351	0.413926	0
DLA-DMA	OK	0	50.16638	0.413844	0
PTPRC	OK	0	50.12326	0.4132	0
UBE2C	OK	0	50.1832	0.411917	0
UHRF1	OK	0	49.97976	0.411415	0

SKA3	OK	0	49.94879	0.410885	0
RPL5	OK	0	49.58227	0.409886	0
ENSCAFG00000018277	OK	0	49.48315	0.408374	0
FBXO5	OK	0	49.56756	0.407444	0
RRM1	OK	0	49.42956	0.406272	0
SLC20A1	OK	0	49.15615	0.405669	0
VCAN	OK	0	49.79013	0.404785	0
IMPDH2	OK	0	49.02423	0.404763	0
GPX1	OK	0	48.95937	0.404531	0
LSM3	OK	0	48.81777	0.403521	0
MT-CO1	OK	0	48.74424	0.402834	0
LBHD1	OK	0	48.73987	0.402686	0
CDC6	OK	0	48.93367	0.402038	0
ENSCAFG00000015834	OK	0	48.60657	0.401885	0
NT5DC2	OK	0	48.64551	0.401673	0
NOP10	OK	0	48.38878	0.40004	0
CSTA	OK	0	48.66704	0.40004	0
DLA-DOA	OK	0	50.09987	0.399963	0
LCP1	OK	0	48.41285	0.399264	0
NAPSA	OK	0	48.65966	0.399058	0
BTG1	OK	0	48.88738	0.39904	0
RGS19	OK	0	48.23957	0.397867	0
HNRNPA3	OK	0	48.12124	0.397656	0
DDIT4	OK	0	48.34085	0.396191	0
CCND1	OK	0	48.43387	0.396172	0
DBI	OK	0	47.90881	0.396042	0
RACK1	OK	0	47.87789	0.395781	0
DYRK1B	OK	0	47.86206	0.395619	0
TFPT	OK	0	47.84462	0.395497	0
TESC	OK	0	47.93013	0.395162	0
NANS	OK	0	47.7804	0.394959	0
RPL35	OK	0	47.72802	0.394541	0
MRC1	OK	0	48.82742	0.393972	0
TRMT112	OK	0	47.5933	0.393433	0
SAT1	OK	0	48.63468	0.393188	0
CD300H	OK	0	47.7069	0.392941	0
SEPTIN6	OK	0	47.75048	0.392825	0
E2F8	OK	0	47.53298	0.391318	0
CCT5	OK	0	47.33354	0.391201	0
GNAS	OK	0	47.29187	0.390845	0
TRIM59	OK	0	47.41961	0.390264	0
SNRPD1	OK	0	47.11477	0.389492	0
SLC25A6	OK	0	47.052	0.388938	0

ENSCAFG00000031952	OK	0	46.99535	0.388473	0
ATP5MC1	OK	0	46.91806	0.387844	0
ENSCAFG00000032036	OK	0	46.86069	0.386838	0
ENSCAFG00000015217	OK	0	46.98254	0.386563	0
COX5A	OK	0	46.67684	0.385797	0
ENSCAFG00000049108	OK	0	46.61653	0.385313	0
TMPO	OK	0	46.64084	0.38523	0
ENSCAFG00000005292	OK	0	47.0011	0.384498	0
CKAP5	OK	0	46.60769	0.384125	0
ZFAND5	OK	0	46.74711	0.383586	0
DNAJC9	OK	0	46.39024	0.382125	0
MT-ND1	OK	0	46.21463	0.381935	0
RPS24	OK	0	46.13234	0.381259	0
APOBR	OK	0	46.24363	0.380779	0
RPL22	OK	0	46.05572	0.380595	0
GOLM1	OK	0	46.18406	0.380139	0
ENSCAFG00000020220	OK	0	46.8067	0.379651	0
TUT7	OK	0	46.1204	0.379285	0
ALOX5	OK	0	46.16452	0.378833	0
DCTPP1	OK	0	45.87898	0.377772	0
PLAUR	OK	0	46.90414	0.377667	0
FTL	OK	0	45.73748	0.377342	0
RPL27	OK	0	45.57473	0.376687	0
ENSCAFG00000002541	OK	0	45.52271	0.376349	0
HSPA8	OK	0	45.29664	0.374095	0
ENSCAFG00000046637	OK	0	44.79373	0.370291	0
SRM	OK	0	44.88217	0.37002	0
ILF2	OK	0	44.79215	0.369952	0
GMNN	OK	0	44.77594	0.369769	0
HSPH1	OK	0	44.80577	0.369449	0
NACA	OK	0	44.5819	0.368428	0
NOP58	OK	0	44.63443	0.36827	0
CCNB3	OK	0	45.3572	0.368105	0
MELK	OK	0	44.63745	0.367762	0
ENSCAFG00000044682	OK	0	44.42417	0.367227	0
VASP	OK	0	44.61147	0.367054	0
DEK	OK	0	44.40168	0.366955	0
ENSCAFG00000043646	OK	0	44.46789	0.366729	0
ENSCAFG00000019044	OK	0	44.31341	0.366271	0
IRF4	OK	0	44.91053	0.366183	0
MYH9	OK	0	44.41174	0.365919	0
TIMP1	OK	0	44.27114	0.365425	0
LGALS3	OK	0	44.23233	0.365418	0

RETN	OK	0	44.55903	0.36499	0
HMGA1	OK	0	44.23481	0.364568	0
HSP90AA1	OK	0	44.11452	0.364355	0
ENSCAFG00000005768	OK	0	44.26434	0.364152	0
ENSCAFG00000035349	OK	0	44.00281	0.36366	0
EIF4A1	OK	0	43.97665	0.36345	0
NEK2	OK	0	44.21016	0.362779	0
SEC14L1	OK	0	44.02045	0.362416	0
ENSCAFG00000008221	OK	0	43.84903	0.362036	0
ENSCAFG00000043173	OK	0	43.75529	0.361702	0
ENSCAFG00000023205	OK	0	43.66704	0.36079	0
ENSCAFG00000004842	OK	0	43.62236	0.36057	0
ENSCAFG00000032259	OK	0	44.70892	0.360351	0
CENPU	OK	0	43.73108	0.359872	0
HMGB3	OK	0	44.0295	0.359785	0
EBNA1BP2	OK	0	43.55224	0.359772	0
NPC2	OK	0	43.55652	0.359503	0
COX5B	OK	0	43.49294	0.359494	0
AIF1	OK	0	43.41546	0.358187	0
SEC61B	OK	0	43.27769	0.357629	0
ACTR3	OK	0	43.2259	0.356897	0
PTPN1	OK	0	43.60125	0.355718	0
ARID5B	OK	0	43.19469	0.354931	0
UQCRB	OK	0	42.92865	0.354826	0
CFL1	OK	0	42.92997	0.354788	0
SUMO2	OK	0	42.87798	0.354412	0
ZNF414	OK	0	43.15333	0.354241	0
SLC2A3	OK	0	43.44152	0.353978	0
RPS3	OK	0	42.77327	0.353457	0
ENSCAFG00000031706	OK	0	43.13982	0.352768	0
CENPH	OK	0	42.83446	0.352761	0
ENSCAFG00000025063	OK	0	42.90988	0.352379	0
NCAPD3	OK	0	42.63623	0.35161	0
MT-ND2	OK	0	42.56777	0.351434	0
RPS15	OK	0	42.46227	0.350812	0
TRIP13	OK	0	42.47972	0.350141	0
ENSCAFG00000019360	OK	0	42.3786	0.349822	0
SERBP1	OK	0	42.30014	0.349636	0
PYCARD	OK	0	42.15685	0.348337	0
LYST	OK	0	42.29555	0.348004	0
DEPDC1B	OK	0	42.25073	0.347668	0
ENSCAFG00000032728	OK	0	41.99608	0.347087	0
B2M	OK	0	42.01761	0.346964	0

CENPQ	OK	0	42.08449	0.346621	0
GAPDH	OK	0	42.03498	0.346323	0
MARCHF1	OK	0	41.76722	0.344648	0
HNRNPA2B1	OK	0	41.62504	0.343666	0
ACTG1	OK	0	41.57571	0.343542	0
NUCB2	OK	0	41.56145	0.343404	0
POLA1	OK	0	41.69217	0.342801	0
MRPL20	OK	0	41.2249	0.340753	0
ENSCAFG00000032392	OK	0	41.22394	0.340636	0
WDHD1	OK	0	41.31098	0.340571	0
PTH1R	OK	0	41.83505	0.340197	0
FCGRT	OK	0	41.19274	0.339594	0
MCM10	OK	0	41.22121	0.339547	0
ATP2B1	OK	0	41.66914	0.339535	0
SQOR	OK	0	41.34226	0.338775	0
DKC1	OK	0	41.03962	0.338713	0
DIAPH3	OK	0	41.29253	0.338684	0
TIPIN	OK	0	41.07325	0.338289	0
SNX3	OK	0	40.70945	0.336059	0
PRSS57	OK	0	40.64121	0.335819	0
RPL27A	OK	0	40.56431	0.335243	0
MGST1	OK	0	40.57771	0.335188	0
MMP9	OK	0	41.32779	0.335098	0
RRP1B	OK	0	40.87017	0.334372	0
SYK	OK	0	40.66572	0.334333	0
MCL1	OK	0	40.79614	0.334239	0
MYCBP	OK	0	40.4916	0.334002	0
CLEC1B	OK	0	45.95244	0.333904	0
RAD21	OK	0	40.43807	0.333723	0
TPI1	OK	0	40.48975	0.333559	0
RPL28	OK	0	40.10361	0.331454	0
LSM5	OK	0	40.07643	0.330715	0
THBS1	OK	0	40.27208	0.329736	0
PGLYRP1	OK	0	40.7715	0.329543	0
ATP5F1D	OK	0	39.86284	0.329421	0
WIPI1	OK	0	40.09276	0.328652	0
ENSCAFG00000017604	OK	0	40.80331	0.328106	0
ARG2	OK	0	39.7421	0.327848	0
ITM2B	OK	0	39.61844	0.326046	0
SECISBP2	OK	0	39.50388	0.324909	0
CALR	OK	0	39.33234	0.324776	0
POLQ	OK	0	39.36909	0.32409	0
CAPG	OK	0	38.95101	0.321848	0

USP1	OK	0	38.97052	0.321692	0
GRAMD1A	OK	0	39.25243	0.321168	0
RANBP1	OK	0	38.81987	0.320415	0
MANF	OK	0	38.69214	0.319506	0
FAU	OK	0	38.64228	0.319137	0
KIF18A	OK	0	38.77728	0.318994	0
MCM5	OK	0	38.94368	0.318854	0
AP1S2	OK	0	38.47794	0.317952	0
RPS14	OK	0	38.23164	0.315893	0
RNASEH2C	OK	0	38.24256	0.315694	0
YPEL3	OK	0	38.30507	0.315692	0
FOXM1	OK	0	38.2482	0.315	0
ENSCAFG00000010086	OK	0	38.08779	0.31471	0
ENSCAFG00000010865	OK	0	38.10167	0.314461	0
ATP5F1A	OK	0	38.05622	0.314459	0
CIP2A	OK	0	38.17266	0.313941	0
PSMA7	OK	0	37.97459	0.31379	0
PFN1	OK	0	38.02205	0.31375	0
PDIA4	OK	0	37.97903	0.313725	0
RPS10	OK	0	37.95907	0.31364	0
SLAMF9	OK	0	37.91802	0.313269	0
PSMB2	OK	0	37.90846	0.313252	0
SSRP1	OK	0	37.85625	0.312647	0
MARCKS	OK	0	38.81069	0.312446	0
RPS27	OK	0	37.78821	0.312255	0
ENSCAFG00000049043	OK	0	37.7402	0.311895	0
POLD2	OK	0	37.90012	0.311783	0
CHEK1	OK	0	37.82156	0.311012	0
MND1	OK	0	37.55757	0.309351	0
LRRK2	OK	5.94E-308	37.49323	0.308635	1.51E-306
HNRNPM	OK	1.11E-305	37.35346	0.308595	2.83E-304
SRGN	OK	0	37.57325	0.307571	0
MAD2L2	OK	3.73E-304	37.25943	0.306973	9.45E-303
ENSCAFG00000013864	OK	2.86E-302	37.14289	0.306875	7.21E-301
GABARAP	OK	1.30E-302	37.16408	0.306127	3.29E-301
PHACTR2	OK	7.17E-302	37.11811	0.305921	1.80E-300
MAFB	OK	4.29E-307	37.44049	0.30585	1.09E-305

SOD1	OK	3.47E-302	37.13768	0.305616	8.74E-301
ENSCAFG00000045775	OK	1.04E-298	36.9215	0.305008	2.60E-297
NCAPG2	OK	4.47E-299	36.94444	0.304134	1.12E-297
EZH2	OK	8.82E-299	36.92606	0.304096	2.20E-297
SYNE1	OK	2.62E-299	36.95886	0.304015	6.58E-298
NDUFS7	OK	1.35E-295	36.72716	0.303037	3.35E-294
SSR4	OK	2.03E-294	36.65332	0.302848	5.01E-293
SSR3	OK	3.53E-293	36.5753	0.302231	8.68E-292
ANPEP	OK	8.48E-294	36.61426	0.302182	2.09E-292
ENSCAFG00000049181	OK	6.32E-302	37.1215	0.302157	1.59E-300
LSM4	OK	3.67E-293	36.57426	0.301477	9.00E-292
PLXNC1	OK	5.23E-294	36.62748	0.301241	1.29E-292
DPYD	OK	7.44E-295	36.68062	0.301129	1.84E-293
FGL2	OK	2.46E-291	36.45924	0.300074	6.01E-290
NSD2	OK	1.42E-290	36.41109	0.299577	3.47E-289
CSTB	OK	3.90E-287	36.19317	0.298929	9.49E-286
PSAT1	OK	1.04E-288	36.29304	0.298759	2.54E-287
CENPJ	OK	4.29E-287	36.19052	0.29815	1.04E-285
TREM1	OK	1.84E-284	36.02275	0.297172	4.47E-283
ATP5IF1	OK	1.21E-282	35.90645	0.296723	2.93E-281
BCL2A1	OK	4.34E-295	36.69531	0.296174	1.08E-293
ARID3A	OK	2.20E-284	36.01784	0.296112	5.32E-283
HAT1	OK	2.01E-282	35.89237	0.295721	4.84E-281

NHP2	OK	2.86E-281	35.81835	0.295607	6.87E-280
GINS2	OK	2.08E-282	35.89144	0.294857	5.00E-281
ABCA5	OK	3.32E-278	35.62099	0.293188	7.94E-277
CENPA	OK	3.96E-279	35.68055	0.292688	9.49E-278
EMC8	OK	1.19E-275	35.45549	0.292685	2.84E-274
RPL14	OK	9.07E-274	35.33322	0.291956	2.14E-272
ESPL1	OK	2.32E-277	35.56634	0.291785	5.54E-276
PAK1	OK	2.97E-275	35.42977	0.291631	7.06E-274
ALYREF	OK	9.55E-273	35.26661	0.29121	2.25E-271
PARP1	OK	5.59E-275	35.41195	0.2912	1.33E-273
CCDC88A	OK	1.14E-272	35.26158	0.291148	2.68E-271
DLA-64	OK	1.21E-271	35.19457	0.290682	2.84E-270
MT-ND3	OK	1.82E-271	35.18296	0.290423	4.26E-270
SSB	OK	8.95E-271	35.13773	0.290269	2.08E-269
NQO2	OK	8.90E-271	35.13787	0.289798	2.07E-269
CTSA	OK	9.17E-270	35.07151	0.289725	2.13E-268
SDF2L1	OK	1.11E-269	35.06595	0.289578	2.58E-268
ENSCAFG00000010412	OK	2.44E-273	35.3052	0.289505	5.76E-272
EBPL	OK	1.94E-271	35.18123	0.289127	4.52E-270
MSH2	OK	8.06E-271	35.14069	0.288701	1.88E-269
VMP1	OK	3.63E-274	35.35915	0.288271	8.58E-273
NDUFS8	OK	5.06E-266	34.82516	0.287737	1.17E-264
FUS	OK	5.15E-266	34.82467	0.28753	1.19E-264

SELENOW	OK	5.55E-265	34.75637	0.286692	1.28E-263
CD1C	OK	3.99E-278	35.61579	0.286061	9.53E-277
FANCD2	OK	1.68E-264	34.7245	0.285932	3.87E-263
TXNDC17	OK	2.78E-261	34.5106	0.284849	6.38E-260
LIG1	OK	6.67E-261	34.48528	0.284483	1.52E-259
ENSCAFG00000024792	OK	3.33E-258	34.30479	0.283057	7.58E-257
CCT2	OK	1.06E-257	34.27094	0.282783	2.41E-256
TSPO	OK	4.27E-257	34.23039	0.282761	9.64E-256
EMP3	OK	1.47E-257	34.26149	0.282549	3.33E-256
FYB1	OK	7.81E-258	34.27994	0.282422	1.77E-256
TBC1D23	OK	4.42E-261	34.4972	0.28194	1.01E-259
ENSCAFG00000017824	OK	1.47E-252	33.92419	0.280125	3.28E-251
SMC3	OK	6.34E-252	33.88102	0.279732	1.42E-250
GPCPD1	OK	6.76E-255	34.08226	0.279698	1.52E-253
ENSCAFG00000029155	OK	3.71E-251	33.82889	0.279349	8.27E-250
ENSCAFG00000045013	OK	9.59E-251	33.80082	0.279158	2.14E-249
BATF3	OK	4.41E-253	33.95952	0.27792	9.90E-252
NCL	OK	3.15E-248	33.62912	0.277457	6.97E-247
ENSCAFG00000008311	OK	1.44E-247	33.58401	0.277373	3.17E-246
ENSCAFG00000024944	OK	3.18E-250	33.76533	0.277243	7.06E-249
FOS	OK	1.60E-260	34.45988	0.277019	3.65E-259
ZFP36	OK	7.83E-255	34.07793	0.276469	1.76E-253
DNAJC19	OK	1.28E-245	33.45005	0.276323	2.84E-244

TCP1	OK	6.16E-244	33.33424	0.27533	1.36E-242
S100A5	OK	5.96E-244	33.33525	0.275094	1.31E-242
RPL34	OK	7.15E-243	33.26068	0.274713	1.57E-241
MRPS12	OK	4.71E-243	33.27322	0.27461	1.03E-241
SYNCRIP	OK	3.80E-242	33.21051	0.274161	8.31E-241
FCER1A	OK	1.97E-250	33.77954	0.272819	4.38E-249
SAMHD1	OK	5.35E-241	33.13083	0.272782	1.17E-239
SEMA4D	OK	5.95E-241	33.12762	0.272739	1.30E-239
ENSCAFG00000006545	OK	1.81E-239	33.02441	0.272597	3.92E-238
MRPL51	OK	1.41E-239	33.03195	0.272554	3.06E-238
RAD18	OK	7.54E-241	33.12046	0.272427	1.64E-239
ADAM15	OK	2.06E-241	33.15954	0.272011	4.51E-240
ENSCAFG00000014612	OK	3.51E-258	34.30327	0.271998	7.98E-257
EIF3K	OK	3.71E-238	32.93296	0.271917	7.99E-237
SPATS2L	OK	1.24E-238	32.96609	0.271274	2.69E-237
RPN2	OK	3.78E-236	32.79241	0.270842	8.09E-235
ILF3	OK	2.08E-236	32.81055	0.270695	4.46E-235
SLC25A5	OK	3.35E-235	32.72585	0.270343	7.16E-234
RPL21	OK	2.93E-234	32.65956	0.269759	6.25E-233
ENSCAFG00000000118	OK	4.63E-234	32.64554	0.269665	9.87E-233
AHNAK	OK	8.64E-240	33.04682	0.269293	1.87E-238
PECAM1	OK	8.38E-238	32.90824	0.268063	1.80E-236
HHEX	OK	1.18E-237	32.89795	0.267895	2.53E-236

LRRC25	OK	7.20E-232	32.49075	0.267456	1.53E-230
KNTC1	OK	2.53E-232	32.52295	0.267307	5.37E-231
RPL11	OK	6.04E-230	32.35428	0.267199	1.27E-228
COX7A1	OK	3.29E-230	32.37304	0.267014	6.93E-229
FBXO9	OK	1.81E-231	32.46245	0.266797	3.83E-230
ENSCAFG00000028613	OK	3.51E-229	32.29988	0.266696	7.35E-228
CYBB	OK	1.23E-228	32.26099	0.266232	2.58E-227
ERCC6L	OK	2.47E-231	32.45281	0.265616	5.23E-230
CDC45	OK	2.97E-231	32.44716	0.265605	6.27E-230
ORC1	OK	1.77E-229	32.32102	0.265023	3.72E-228
ENSCAFG00000017655	OK	1.13E-226	32.12068	0.264999	2.36E-225
ENSCAFG00000008236	OK	5.93E-229	32.28368	0.264373	1.24E-227
PAFAH1B3	OK	8.54E-225	31.98597	0.263946	1.77E-223
PSMB6	OK	3.23E-224	31.94437	0.263858	6.67E-223
HMGN3	OK	3.21E-224	31.94465	0.263416	6.62E-223
CALCOCO2	OK	2.99E-224	31.94679	0.263269	6.19E-223
ABCA1	OK	4.68E-226	32.07653	0.263135	9.72E-225
CENPT	OK	2.17E-226	32.10046	0.262952	4.51E-225
ENSCAFG00000017667	OK	6.81E-222	31.77662	0.262425	1.40E-220
RPL22L1	OK	5.17E-222	31.78531	0.262404	1.06E-220
NIFK	OK	3.31E-221	31.72691	0.261991	6.77E-220
EEF1B2	OK	1.87E-220	31.67231	0.261609	3.82E-219
ETHE1	OK	6.22E-221	31.70703	0.261383	1.27E-219

GPSM2	OK	1.25E-222	31.82976	0.260871	2.58E-221
TCN1	OK	4.21E-256	34.16354	0.260836	9.49E-255
ECM1	OK	1.79E-227	32.1781	0.260348	3.73E-226
ENSCAFG00000003331	OK	2.73E-220	31.6604	0.259752	5.56E-219
MLEC	OK	1.11E-215	31.32358	0.258527	2.26E-214
HP1BP3	OK	4.01E-215	31.28273	0.257853	8.13E-214
COMMD4	OK	3.45E-214	31.2139	0.257603	6.99E-213
STEAP4	OK	4.04E-230	32.36669	0.257289	8.50E-229
MRPL40	OK	5.60E-212	31.05057	0.256337	1.13E-210
CD37	OK	1.58E-212	31.09118	0.256172	3.20E-211
FLT3	OK	1.30E-217	31.46528	0.256123	2.64E-216
HNRNPR	OK	6.10E-211	30.97366	0.255486	1.22E-209
NOP56	OK	1.54E-210	30.94388	0.255359	3.07E-209
EEF1D	OK	3.29E-210	30.91924	0.255337	6.57E-209
SLC6A6	OK	8.20E-212	31.0383	0.254913	1.65E-210
SERF1A	OK	3.61E-211	30.99057	0.254547	7.23E-210
SHCBP1	OK	2.46E-211	31.003	0.254348	4.93E-210
CENPM	OK	1.39E-212	31.09547	0.254282	2.80E-211
UBE2B	OK	7.27E-212	31.04221	0.254211	1.46E-210
PLEKHO1	OK	1.96E-208	30.78695	0.253864	3.89E-207
RBPJ	OK	6.54E-208	30.74782	0.253213	1.30E-206
PDCD5	OK	2.48E-206	30.62947	0.252282	4.90E-205
ARFGEF1	OK	8.71E-207	30.66359	0.25223	1.73E-205

NDUFB4	OK	4.44E-205	30.53525	0.252172	8.74E-204
FPR2	OK	4.60E-204	30.45864	0.250239	9.03E-203

Supplemental Table 6. Trajectory analysis results for the lymphocytic (B cell) cell lineage. Selected results are shown for genes that have a q value < 0.05 and Moran's I > 0.25.

Gene/Gene Symbol	status	p_value	morans_test_statistic	morans_I	q_value
TUBA1B	OK	0	97.86195	0.814501	0
HMGB2	OK	0	97.58605	0.812028	0
TOP2A	OK	0	95.66797	0.792654	0
ASPM	OK	0	95.80948	0.79204	0
GRN	OK	0	92.81004	0.770095	0
VPREB1	OK	0	91.37372	0.761227	0
FYB1	OK	0	90.63263	0.749425	0
TPX2	OK	0	90.3672	0.749056	0
CTSS	OK	0	89.32635	0.739254	0
HMGB1	OK	0	88.49447	0.737755	0
ENSCAFG00000014139	OK	0	88.12236	0.735359	0
CDC20	OK	0	88.6152	0.730129	0
H2AZ1	OK	0	87.27439	0.727336	0
ENSCAFG00000007705	OK	0	88.06351	0.724193	0
CENPE	OK	0	87.42497	0.721709	0
NUF2	OK	0	85.97982	0.711148	0
ENSCAFG00000030087	OK	0	85.18385	0.707201	0

CENPF	OK	0	86.79073	0.706144	0
ENSCAFG00000017264	OK	0	85.51225	0.705979	0
ENSCAFG00000028765	OK	0	84.89304	0.704801	0
NUSAP1	OK	0	85.2796	0.702479	0
KIF11	OK	0	84.38569	0.699542	0
DHDDS	OK	0	83.22402	0.693573	0
H1-5	OK	0	83.51487	0.693059	0
GTSE1	OK	0	83.97168	0.690399	0
ENSCAFG00000000443	OK	0	82.30388	0.684773	0
ENSCAFG00000048539	OK	0	82.16234	0.682841	0
ENSCAFG00000009113	OK	0	81.59933	0.676587	0
DNTT	OK	0	81.14833	0.673207	0
SGO1	OK	0	79.80115	0.661002	0
PTMA	OK	0	79.3216	0.660968	0
MKI67	OK	0	80.16089	0.659328	0
ENSCAFG00000002332	OK	0	77.81539	0.641109	0
ENSCAFG00000000697	OK	0	76.68031	0.634632	0
CCND1	OK	0	75.77736	0.624749	0
SPC24	OK	0	74.89497	0.622983	0
RARRES2	OK	0	74.96268	0.617511	0
BUB1B	OK	0	74.60768	0.615244	0
CLSPN	OK	0	73.14542	0.606027	0
STMN1	OK	0	72.48451	0.604198	0
RPS23	OK	0	72.33194	0.60355	0
NCAPG	OK	0	72.54667	0.600881	0
NUCKS1	OK	0	71.77399	0.596839	0
KNL1	OK	0	71.49925	0.590235	0
FZD2	OK	0	71.13231	0.582032	0
RPSA	OK	0	69.13019	0.576993	0
KIF15	OK	0	69.28231	0.574883	0
ASNS	OK	0	68.95534	0.572279	0
ENSCAFG00000008661	OK	0	69.17705	0.570651	0
KIF22	OK	0	68.55042	0.56743	0
UBE2C	OK	0	69.37695	0.567071	0
PLK1	OK	0	68.81284	0.566334	0
BRCA2	OK	0	68.18289	0.565729	0

FAU	OK	0	67.5384	0.563549	0
SPATS2L	OK	0	68.02326	0.558381	0
DPEP1	OK	0	67.19288	0.557816	0
TK1	OK	0	67.15131	0.557758	0
CDK1	OK	0	67.01406	0.553467	0
NDC80	OK	0	66.23116	0.54524	0
UHRF1	OK	0	65.75441	0.544595	0
KIF23	OK	0	65.47114	0.541216	0
ENSCAFG00000030875	OK	0	64.91316	0.538343	0
AURKB	OK	0	64.68049	0.537924	0
SMC2	OK	0	64.63336	0.537097	0
ENSCAFG00000046600	OK	0	64.63824	0.536837	0
TUBB6	OK	0	64.86604	0.536713	0
CDKN3	OK	0	65.71968	0.536336	0
DUT	OK	0	63.996	0.532869	0
RPL32	OK	0	63.84013	0.532745	0
BUB1	OK	0	64.55744	0.532005	0
RPS14	OK	0	63.34417	0.528542	0
TACC3	OK	0	63.36388	0.526573	0
LTB	OK	0	63.16004	0.525192	0
CDH1	OK	0	63.36371	0.519819	0
ENSCAFG00000009523	OK	0	61.92688	0.516824	0
CCNB2	OK	0	62.19487	0.514802	0
DLA-DRA	OK	0	61.27125	0.511071	0
CKAP2L	OK	0	61.87405	0.509713	0
KIFC1	OK	0	60.80453	0.504077	0
DEPDC1	OK	0	61.28454	0.504061	0
ENSCAFG00000050001	OK	0	60.16555	0.498121	0
IFI30	OK	0	59.32425	0.494023	0
ENSCAFG00000016482	OK	0	59.5052	0.493684	0
RGS18	OK	0	59.69096	0.49368	0
CD79A	OK	0	58.61717	0.489069	0
AKAP12	OK	0	58.64575	0.488316	0
EGFL7	OK	0	58.48912	0.481667	0
PIMREG	OK	0	58.64855	0.481516	0
TTYH1	OK	0	57.43718	0.47107	0
MTFR2	OK	0	57.02394	0.468652	0
KIF20B	OK	0	56.20941	0.466912	0
RPS7	OK	0	55.96186	0.466884	0

TYMS	OK	0	55.99032	0.465695	0
CALM3	OK	0	55.91151	0.46525	0
RPL8	OK	0	55.58777	0.463744	0
KIF14	OK	0	56.34094	0.463082	0
GADD45A	OK	0	55.58476	0.462371	0
RPL13	OK	0	55.40922	0.462304	0
DLGAP5	OK	0	56.15045	0.461362	0
RPS15A	OK	0	55.23449	0.460799	0
SPTBN1	OK	0	55.34564	0.460642	0
FUCA1	OK	0	54.95656	0.457416	0
HLA-DQB2	OK	0	54.54185	0.454812	0
ENSCAFG00000010412	OK	0	54.07814	0.446056	0
SULT1B1	OK	0	53.99739	0.444752	0
VPREB3	OK	0	53.40694	0.44444	0
IGHM	OK	0	53.0827	0.442519	0
PRC1	OK	0	53.15456	0.438564	0
CCNB3	OK	0	53.85667	0.438438	0
UBE2S	OK	0	52.65577	0.437689	0
RPS28	OK	0	52.05893	0.43431	0
RPL11	OK	0	51.57057	0.430185	0
INCENP	OK	0	51.5264	0.428135	0
TUBB4B	OK	0	51.51972	0.427423	0
RPL19	OK	0	51.20925	0.427185	0
STYXL2	OK	0	54.4314	0.42664	0
ENSCAFG00000007461	OK	0	51.46023	0.425545	0
ENSCAFG00000043319	OK	0	51.37357	0.425502	0
PAX5	OK	0	51.0412	0.425214	0
TPM4	OK	0	51.12634	0.423968	0
PLAC8	OK	0	50.9384	0.423948	0
NIBAN3	OK	0	51.0634	0.422749	0
HJURP	OK	0	51.48938	0.422001	0
CCNA2	OK	0	51.83691	0.421874	0
DIAPH3	OK	0	50.96753	0.421372	0
CCR5	OK	0	51.44522	0.421266	0
CENPW	OK	0	50.21618	0.417879	0
MT2A	OK	0	50.47641	0.414852	0
SMC4	OK	0	49.76793	0.414243	0
TOP2B	OK	0	49.73627	0.414219	0
AOX2	OK	0	49.83376	0.412898	0
ECT2	OK	0	49.86277	0.411297	0

MSMO1.1	OK	0	49.6878	0.41123	0
CCNE2	OK	0	49.75359	0.41049	0
S100A8	OK	0	51.59827	0.41	0
RPL21	OK	0	49.03397	0.408999	0
ENSCAFG00000042212	OK	0	48.92774	0.408125	0
YBX3	OK	0	49.05996	0.40805	0
RPS11	OK	0	48.68796	0.406137	0
RACGAP1	OK	0	48.66342	0.401712	0
GYPC	OK	0	47.85125	0.398235	0
ENSCAFG00000025115	OK	0	47.24512	0.393391	0
HMGB3	OK	0	47.4673	0.391728	0
CEP55	OK	0	47.97888	0.38944	0
JPT1	OK	0	46.67267	0.387463	0
LGALS1	OK	0	46.49996	0.387213	0
CDCA3	OK	0	47.65894	0.385425	0
TMPO	OK	0	46.24531	0.385091	0
SELL	OK	0	46.21406	0.384282	0
TFDP2	OK	0	45.87882	0.382038	0
S100A12	OK	0	48.4749	0.381846	0
ENSCAFG00000006485	OK	0	45.634	0.379553	0
MCM3	OK	0	45.81965	0.378771	0
ERCC6L	OK	0	45.97029	0.378615	0
GNAS	OK	0	45.16724	0.376474	0
H2AC18	OK	0	45.25223	0.375865	0
KIF18B	OK	0	45.81538	0.375519	0
NINJ1	OK	0	45.19509	0.374264	0
TMSB10	OK	0	44.8961	0.374039	0
CXCR4	OK	0	44.8961	0.373902	0
TLR3	OK	0	45.4341	0.371833	0
TNFRSF13C	OK	0	44.63117	0.371815	0
RYR1	OK	0	47.34413	0.371609	0
CENPA	OK	0	45.9011	0.368941	0
RPL35A	OK	0	44.22514	0.36883	0
RAD51AP1	OK	0	44.49059	0.367374	0
ACTC1	OK	0	44.06718	0.365165	0
SYNE2	OK	0	43.98457	0.36354	0
ENSCAFG00000011598	OK	0	44.36521	0.36198	0
RAD51	OK	0	44.19227	0.361189	0
RAG1	OK	0	43.25032	0.35921	0

RPL24	OK	0	43.08008	0.359179	0
SOD1	OK	0	43.00004	0.35827	0
TBC1D1	OK	0	42.82556	0.356555	0
SH3BGRL3	OK	0	42.84041	0.356279	0
RPL5	OK	0	42.6834	0.355948	0
ENSCAFG00000019044	OK	0	42.53118	0.3547	0
RPS12	OK	0	42.52254	0.354615	0
SGO2	OK	0	42.4051	0.352373	0
FBXO5	OK	0	42.92076	0.352281	0
RRM2	OK	0	42.45575	0.350899	0
RPS8	OK	0	42.03647	0.350577	0
SCPEP1	OK	0	42.10988	0.349648	0
VIM	OK	0	42.43626	0.348961	0
CYP2D15	OK	0	42.75161	0.348629	0
ESCO2	OK	0	42.10682	0.34797	0
RNASEH2B	OK	0	41.72484	0.347119	0
CDCA2	OK	0	42.23104	0.346713	0
TPM2	OK	0	41.83321	0.346611	0
CYBA	OK	0	41.30704	0.344196	0
ANLN	OK	0	41.8665	0.344032	0
ENSCAFG00000017688	OK	0	41.20616	0.343658	0
PLEKHO1	OK	0	41.33981	0.343355	0
NAP1L1	OK	0	41.17805	0.343315	0
ENSCAFG00000029542	OK	0	41.99143	0.34302	0
ORC6	OK	0	41.25282	0.342177	0
E2F8	OK	0	41.57427	0.341873	0
ENSCAFG00000050027	OK	0	41.04747	0.34113	0
RPS25	OK	0	40.82473	0.340408	0
B2M	OK	0	40.8408	0.340364	0
ENSCAFG00000013905	OK	0	40.80567	0.340238	0
RPL10A	OK	0	40.52331	0.337946	0
RPS17	OK	0	40.519	0.33789	0
AURKA	OK	0	40.93863	0.33769	0
ENSCAFG00000017604	OK	0	41.09528	0.335995	0
RPS5	OK	0	40.03722	0.333825	0
RPL9	OK	0	39.9838	0.333433	0
OSCAR	OK	0	41.5082	0.333423	0
RPS27	OK	0	39.92422	0.332901	0

CDCA8	OK	0	40.74228	0.332063	0
NT5DC2	OK	0	40.15639	0.331113	0
MIS18BP1	OK	0	39.62657	0.328821	0
FAM107B	OK	0	39.44123	0.32798	0
ZDHHC1	OK	0	40.36069	0.327875	0
RPS6	OK	0	39.18941	0.326829	0
RPS13	OK	0	39.19275	0.32677	0
FCRLA	OK	0	39.17824	0.325953	0
ENSCAFG00000005292	OK	0	39.87189	0.325165	0
MCM10	OK	0	39.42739	0.324927	0
DCK	OK	0	39.36627	0.324844	0
CCDC50	OK	0	39.03723	0.324839	0
PBK	OK	0	39.39801	0.322761	0
ENSCAFG00000045333	OK	0	38.49462	0.320922	0
ENSCAFG00000029884	OK	0	38.03407	0.317169	0
IRF4	OK	0	38.08376	0.316269	0
PTPN6	OK	0	37.81704	0.315091	0
CHD1	OK	0	37.7784	0.313881	0
SQLE	OK	0	38.14189	0.313148	0
MT-CO3	OK	0	37.52456	0.312737	0
NCAPD2	OK	0	37.73298	0.312711	0
RPL23	OK	5.02E-308	37.49772	0.312622	2.66E-306
ENSCAFG00000046992	OK	4.58E-307	37.43872	0.31211	2.41E-305
RPL7A	OK	6.85E-306	37.36647	0.311557	3.59E-304
RPL18	OK	9.46E-306	37.35784	0.311485	4.94E-304
RPL12	OK	4.51E-304	37.25433	0.310622	2.34E-302
RPL3	OK	1.48E-302	37.16058	0.309855	7.63E-301
CENPH	OK	5.65E-308	37.49457	0.308665	2.98E-306
TROAP	OK	0	38.68408	0.307876	0
RTKN2	OK	0	37.5619	0.307866	0
LMNB1	OK	7.06E-300	36.99436	0.305999	3.62E-298
RPS24	OK	1.34E-294	36.66458	0.305617	6.77E-293
ADGRF1	OK	0	37.63026	0.305014	0
ENSCAFG00000006557	OK	0	37.6518	0.304905	0
FANCM	OK	1.31E-299	36.97772	0.30466	6.65E-298
C9H17orf64	OK	0	39.73882	0.304109	0
RAN	OK	1.80E-291	36.46775	0.303917	9.02E-290
NCAPG2	OK	5.34E-296	36.75231	0.303885	2.71E-294
HSP90AB1	OK	1.08E-289	36.3554	0.303022	5.37E-288

SPAG5	OK	2.59E-303	37.20741	0.301537	1.34E-301
FCER1A	OK	0	42.59234	0.301407	0
SCAP	OK	7.06E-291	36.43028	0.300806	3.53E-289
HDGF	OK	1.83E-283	35.95899	0.299247	9.07E-282
SLC8A1	OK	9.21E-293	36.54911	0.29793	4.64E-291
MT-ATP6	OK	3.59E-278	35.61872	0.296903	1.75E-276
MS4A1	OK	1.68E-278	35.6401	0.29606	8.21E-277
FBLN1	OK	6.96E-282	35.85777	0.295584	3.43E-280
SMG1	OK	1.04E-277	35.58884	0.295507	5.07E-276
RPS18	OK	3.90E-273	35.29199	0.294196	1.86E-271
MRC1	OK	4.48E-280	35.74153	0.293923	2.20E-278
CRYBG1	OK	3.01E-274	35.36444	0.293334	1.46E-272
TFPT	OK	2.13E-271	35.17855	0.293257	1.01E-269
ACTG1	OK	3.37E-270	35.09997	0.292433	1.58E-268
ATP8A1	OK	1.67E-270	35.11995	0.291869	7.85E-269
ATP1B1	OK	1.15E-273	35.32656	0.291358	5.54E-272
RPS26	OK	9.12E-267	34.87429	0.290754	4.25E-265
KIF4A	OK	3.86E-273	35.29226	0.290122	1.85E-271
ENSCAFG00000008873	OK	3.53E-263	34.63682	0.288646	1.63E-261
H3-3A	OK	1.89E-262	34.58832	0.288271	8.73E-261
RPS4X	OK	1.35E-260	34.46492	0.287326	6.18E-259
LYZ	OK	4.35E-271	35.15825	0.286296	2.06E-269
DEPDC1B	OK	7.76E-273	35.27246	0.285813	3.70E-271
COBLL1	OK	1.19E-270	35.12953	0.284823	5.63E-269
ENSCAFG00000046564	OK	8.21E-254	34.00898	0.283474	3.74E-252
PADI3	OK	8.02E-300	36.99091	0.283416	4.10E-298
MCM6	OK	6.77E-249	33.67476	0.280006	3.04E-247
RGS10	OK	6.75E-253	33.94703	0.279707	3.05E-251
ZNF704	OK	3.30E-249	33.69604	0.278914	1.49E-247
GSN	OK	9.09E-248	33.59761	0.278705	4.07E-246
NPNT	OK	1.25E-264	34.73308	0.278285	5.80E-263
ENSCAFG00000044682	OK	3.07E-244	33.35508	0.277922	1.36E-242
LAMA4	OK	6.10E-253	33.95002	0.277041	2.77E-251
SORL1	OK	2.60E-243	33.29109	0.276049	1.14E-241
CYP51A1	OK	9.14E-245	33.39139	0.275832	4.07E-243
LGALS3	OK	1.31E-256	34.19774	0.272421	5.98E-255
MT-CO2	OK	2.05E-233	32.59998	0.271676	9.00E-232
HSPA8	OK	3.94E-233	32.58	0.271327	1.72E-231
ENSCAFG00000017824	OK	1.15E-229	32.33428	0.269133	4.99E-228

CRIP1	OK	1.56E-230	32.39608	0.268805	6.77E-229
FAM167A	OK	1.05E-246	33.52464	0.265587	4.71E-245
PLS1	OK	3.87E-228	32.22553	0.265334	1.67E-226
ENSCAFG00000024198	OK	0	37.84563	0.265211	0
DEK	OK	1.82E-223	31.89025	0.265073	7.75E-222
SPC25	OK	3.54E-231	32.44178	0.26416	1.54E-229
ARHGAP45	OK	3.47E-218	31.50708	0.262371	1.46E-216
UBA52	OK	7.07E-216	31.33806	0.261186	2.95E-214
SGK2	OK	2.05E-221	31.74192	0.260726	8.70E-220
RPL34	OK	8.28E-215	31.25956	0.260534	3.44E-213
IL7R	OK	6.34E-216	31.34155	0.259395	2.65E-214
MYBL2	OK	1.72E-211	31.01446	0.25727	7.08E-210
ARHGEF39	OK	4.91E-210	30.90631	0.257053	2.01E-208
MPP6	OK	2.99E-212	31.07078	0.256561	1.23E-210
RRBP1	OK	5.18E-221	31.7128	0.256362	2.18E-219
ISG20	OK	4.85E-244	33.34144	0.256065	2.14E-242
MT3	OK	5.95E-227	32.14074	0.255948	2.55E-225
GAPDH	OK	7.71E-211	30.96612	0.255868	3.16E-209
ADGRG5	OK	3.08E-225	32.01778	0.255694	1.32E-223
ENSCAFG00000031806	OK	7.69E-206	30.59253	0.254262	3.11E-204
FTH1.1	OK	3.26E-205	30.54531	0.253844	1.32E-203
EPB41	OK	3.04E-204	30.47225	0.253552	1.22E-202
ENSCAFG00000000842	OK	9.15E-203	30.36044	0.252026	3.66E-201
CHAF1A	OK	3.09E-204	30.47173	0.251701	1.24E-202
CD34	OK	1.70E-206	30.64186	0.251565	6.91E-205
CSNK1G1	OK	6.16E-200	30.14539	0.251047	2.43E-198
NME1	OK	5.32E-200	30.15024	0.250596	2.11E-198
BANK1	OK	3.21E-200	30.167	0.250042	1.28E-198

Supplemental Table 7. Trajectory analysis results for the erythroid cell lineage. Selected results are shown for genes that have a q value < 0.05 and Moran's I > 0.25.

Gene/Gene Symbol	status	p_value	morans_test_statistic	morans_I	q_value
EEF1B2	OK	0	53.53824784	0.814571	0
NPM1	OK	0	52.21795835	0.795778	0
HSP90AB1	OK	0	51.17604603	0.779719	0
ENSCAFG00000045013	OK	0	50.3434304	0.763046	0
ENSCAFG00000030286	OK	0	49.60662021	0.757016	0
RPL12	OK	0	49.23472486	0.749578	0
RPS7	OK	0	49.08868566	0.747213	0
ACTG1	OK	0	48.80631917	0.741065	0
RPS5	OK	0	48.42049746	0.737344	0
ENSCAFG00000023111	OK	0	47.73601448	0.720093	0
RPL19	OK	0	46.27587363	0.704444	0
TMSB10	OK	0	45.40152751	0.689747	0
STMN1	OK	0	44.90518172	0.683482	0
SEPTIN6	OK	0	45.86215191	0.683243	0
HBM	OK	0	44.44873748	0.678279	0
RPL10A	OK	0	44.38280549	0.675857	0
RPL32	OK	0	44.15255763	0.672505	0
PFDN5	OK	0	43.72344999	0.665577	0
RPL18	OK	0	43.42661716	0.660918	0
RPL13	OK	0	43.15661457	0.657113	0
ENSCAFG00000032615	OK	0	42.9806295	0.655698	0
ENSCAFG00000015834	OK	0	43.01529934	0.655595	0
EEF1A1	OK	0	42.48944858	0.646775	0
AHSP	OK	0	42.23385897	0.643851	0
RPS10	OK	0	42.2466425	0.64359	0
ALAS2	OK	0	41.7683112	0.636711	0
CD79A	OK	0	41.80038407	0.636062	0
TSPO	OK	0	41.75493386	0.635424	0
ENO1	OK	0	41.87504233	0.634485	0
ENSCAFG00000031952	OK	0	41.49258385	0.631779	0
RPS17	OK	0	41.4062105	0.630876	0
RPL35A	OK	0	41.42036447	0.630785	0
CBFA2T3	OK	0	41.61760268	0.628319	0
PLXNC1	OK	0	41.51533646	0.626685	0

BTF3	OK	0	40.9742691	0.624682	0
FKBP11	OK	0	41.1292223	0.624561	0
UBA52	OK	0	40.89988478	0.622804	0
RPS12	OK	0	40.89495505	0.622788	0
FAU	OK	0	40.84000252	0.62184	0
NACA	OK	0	40.70947114	0.620112	0
EMP3	OK	0	41.16570854	0.618274	0
ENSCAFG00000045333	OK	0	40.57463439	0.617603	0
RPS4X	OK	0	40.38130045	0.614197	0
ENSCAFG00000032180	OK	0	40.26469955	0.613892	0
CFL1	OK	0	40.24409433	0.613272	0
RPL27	OK	0	40.17870344	0.612225	0
PRMT1	OK	0	40.08069426	0.609202	0
RPS14	OK	0	39.74747497	0.604512	0
RPL3	OK	0	39.61077412	0.603525	0
GYPA	OK	0	39.71222333	0.603107	0
RPL11	OK	0	39.53216657	0.602039	0
NBN	OK	0	39.15773641	0.593522	0
GMFG	OK	0	39.47353967	0.592099	0
ENSCAFG00000019044	OK	0	38.78184768	0.59035	0
NFKBID	OK	0	39.73013819	0.587547	0
RPS6	OK	0	38.45770059	0.585785	0
RSL1D1	OK	0	38.42976463	0.585189	0
ENSCAFG00000046992	OK	0	38.35705853	0.584007	0
CD63	OK	0	38.24187054	0.58046	0
ENSCAFG00000042554	OK	0	38.0591081	0.579773	0
ENSCAFG00000042212	OK	0	37.96583909	0.578444	0
MYB	OK	0	38.34415231	0.578219	0
CAPG	OK	0	38.43023327	0.577982	0
S100A8	OK	0	39.73708208	0.577916	0
COQ10B	OK	0	37.8971354	0.577707	0
ATP5IF1	OK	0	37.82932064	0.576563	0
UBE2S	OK	0	37.80230103	0.57623	0
RPS13	OK	0	37.84402565	0.575916	0
S100A12	OK	0	39.52946962	0.574597	0
RPL13A	OK	1.43E-307	37.46973083	0.57051	2.22E-305

EIF4A1	OK	4.44E-306	37.37808312	0.569761	6.68E-304
TOP2A	OK	4.18E-307	37.44119881	0.569189	6.37E-305
RPL7A	OK	2.01E-303	37.21421686	0.566964	2.95E-301
SELENOW	OK	0	37.69661539	0.565573	0
LSP1	OK	0	38.54160885	0.564098	0
DMD	OK	4.32E-305	37.31719466	0.563855	6.42E-303
RPS25	OK	1.02E-300	37.04650791	0.563836	1.48E-298
RPS18	OK	6.73E-297	36.80858467	0.560714	9.51E-295
RPS3A	OK	4.69E-297	36.81838949	0.560062	6.71E-295
ENSCAFG00000007705	OK	1.16E-295	36.73132018	0.559665	1.59E-293
ENSCAFG00000030359	OK	2.57E-296	36.77213857	0.558261	3.59E-294
C9H17orf64	OK	2.33E-308	37.51812757	0.558096	3.66E-306
ENSCAFG00000015122	OK	4.09E-293	36.57129644	0.556646	5.44E-291
RPS23	OK	1.86E-292	36.52987702	0.556594	2.45E-290
EIF4B	OK	3.64E-290	36.3852943	0.553768	4.73E-288
RPS15A	OK	3.72E-288	36.25799542	0.552075	4.78E-286
GPX1	OK	1.42E-285	36.09371583	0.549927	1.79E-283
ENSCAFG00000031706	OK	6.31E-294	36.62232139	0.549917	8.60E-292
SRM	OK	1.72E-286	36.15213631	0.549317	2.19E-284
RPL8	OK	7.41E-282	35.85602605	0.54609	9.12E-280
ENSCAFG00000001149	OK	1.26E-281	35.84129624	0.544558	1.53E-279
RPL24	OK	1.81E-280	35.76689934	0.544438	2.18E-278
S100P	OK	0	37.69758014	0.544022	0
TOMM7	OK	3.66E-278	35.61824092	0.542401	4.36E-276

HMBS	OK	1.33E-275	35.45236295	0.540412	1.54E-273
FTH1.1	OK	8.54E-276	35.46491253	0.540338	9.98E-274
PTMA	OK	2.86E-274	35.36584429	0.53904	3.24E-272
PLK1	OK	1.19E-273	35.32559155	0.537744	1.32E-271
PTGR1	OK	1.83E-274	35.37843297	0.537521	2.10E-272
PRRC2C	OK	4.01E-273	35.29118277	0.536923	4.41E-271
LCP1	OK	3.07E-293	36.57911952	0.536518	4.14E-291
PRDX1	OK	2.52E-276	35.4992406	0.533909	2.98E-274
GLRX	OK	1.77E-284	36.02384027	0.532349	2.20E-282
RHCE	OK	1.53E-266	34.85954932	0.530391	1.65E-264
RPL21	OK	1.63E-262	34.59264973	0.52673	1.70E-260
ENSCAFG00000018784	OK	8.86E-262	34.54371998	0.525908	9.13E-260
ENSCAFG00000002541	OK	1.07E-260	34.47151961	0.525035	1.09E-258
NOSTRIN	OK	1.59E-261	34.52678571	0.523815	1.62E-259
ENSCAFG00000017655	OK	1.96E-269	35.04979724	0.523037	2.14E-267
NIFK	OK	1.17E-256	34.20103873	0.520896	1.17E-254
APRT	OK	1.26E-264	34.73282166	0.520533	1.32E-262
SSB	OK	1.21E-256	34.19995979	0.520397	1.20E-254
LTF	OK	1.02E-273	35.32977826	0.520258	1.15E-271
ENSCAFG00000006102	OK	4.90E-256	34.1591134	0.519992	4.75E-254
RPSA	OK	2.82E-256	34.17523018	0.519813	2.76E-254
TIMP1	OK	2.04E-265	34.78517038	0.519279	2.18E-263
PRDX2	OK	1.39E-253	33.99354198	0.517997	1.32E-251

CLIC1	OK	2.05E-256	34.18451611	0.517731	2.03E-254
TKT	OK	3.09E-253	33.96997972	0.517274	2.93E-251
MIOX	OK	4.15E-253	33.9612977	0.516778	3.87E-251
PADI3	OK	5.66E-265	34.75580103	0.516744	6.00E-263
ENSCAFG00000029884	OK	7.44E-253	33.94415355	0.516675	6.81E-251
RPS27A	OK	9.86E-251	33.79998903	0.514487	8.89E-249
EEF1D	OK	5.53E-250	33.74901847	0.514156	4.94E-248
APEX1	OK	2.13E-249	33.70906683	0.513551	1.89E-247
CD37	OK	9.37E-252	33.86949768	0.513404	8.51E-250
RANGRF	OK	3.99E-253	33.96250988	0.512986	3.74E-251
MGST3	OK	6.10E-248	33.60948247	0.512014	5.37E-246
HMGN3	OK	9.69E-248	33.59571594	0.510698	8.46E-246
RPL9	OK	1.95E-246	33.5062633	0.510244	1.69E-244
ENPP3	OK	5.87E-255	34.0863989	0.508726	5.64E-253
ENSCAFG00000049108	OK	4.02E-241	33.13939998	0.504688	3.41E-239
ENSCAFG00000017688	OK	5.67E-240	33.05954117	0.50307	4.77E-238
HMGA1	OK	1.41E-239	33.03195321	0.502696	1.18E-237
OGA	OK	1.57E-237	32.88910065	0.500517	1.30E-235
ENSCAFG00000004260	OK	4.92E-236	32.78437252	0.499544	4.05E-234
EGFL7	OK	1.22E-241	33.17538315	0.499114	1.04E-239
RPS15	OK	3.25E-234	32.65644424	0.49758	2.65E-232
GTSE1	OK	3.01E-231	32.44670254	0.494277	2.43E-229
TESC	OK	5.66E-253	33.95218661	0.494141	5.23E-251

RPS11	OK	3.44E-230	32.37164876	0.492651	2.75E-228
ENSCAFG00000017824	OK	2.42E-232	32.52425198	0.492586	1.97E-230
GCAT	OK	5.92E-230	32.35489711	0.492181	4.70E-228
IMPDH2	OK	1.50E-228	32.2548341	0.491505	1.17E-226
NME1	OK	1.36E-228	32.25796439	0.490889	1.07E-226
PARK7	OK	8.93E-229	32.27098226	0.490363	7.05E-227
ENSCAFG00000010572	OK	1.02E-226	32.12396809	0.48921	7.84E-225
RPS26	OK	7.87E-226	32.06034971	0.488016	5.97E-224
ENSCAFG00000013515	OK	4.14E-226	32.08041173	0.487561	3.16E-224
NOP58	OK	8.69E-225	31.98544222	0.486976	6.50E-223
NME2	OK	1.10E-224	31.97819605	0.486909	8.14E-223
ENSCAFG00000032259	OK	3.89E-244	33.34804738	0.485793	3.35E-242
HMGB2	OK	1.07E-222	31.83480085	0.485007	7.84E-221
SSR4	OK	1.01E-222	31.83652904	0.484778	7.47E-221
ENSCAFG00000039767	OK	2.62E-222	31.80668147	0.48449	1.90E-220
HHEX	OK	1.99E-228	32.24613769	0.483857	1.54E-226
RPL23	OK	2.02E-222	31.81476396	0.483759	1.47E-220
TRMT112	OK	5.96E-221	31.7083495	0.482862	4.26E-219
COX5A	OK	7.24E-220	31.62959693	0.481148	5.11E-218
NOP53	OK	5.19E-221	31.71271335	0.481049	3.74E-219
CA1	OK	1.29E-217	31.46541601	0.478984	8.96E-216
THAP4	OK	3.14E-219	31.58322386	0.478723	2.19E-217
ENSCAFG00000043173	OK	3.69E-217	31.43208148	0.478713	2.54E-215

EBNA1BP2	OK	5.42E-217	31.41983521	0.478081	3.72E-215
CA2	OK	1.92E-216	31.37962541	0.477606	1.29E-214
ENSCAFG00000043616	OK	6.25E-215	31.26855824	0.476363	4.13E-213
ASPM	OK	2.56E-220	31.66235424	0.475839	1.82E-218
RACK1	OK	1.79E-216	31.38183439	0.475788	1.21E-214
TGFB1	OK	2.03E-215	31.30447353	0.474736	1.35E-213
RPS8	OK	4.77E-212	31.05573781	0.472808	3.14E-210
H1-5	OK	2.07E-210	30.93416408	0.471093	1.35E-208
DDX21	OK	2.10E-211	31.00810515	0.471037	1.37E-209
FBL	OK	8.36E-210	30.88910937	0.470277	5.41E-208
DDX18	OK	6.38E-208	30.74862192	0.467621	4.06E-206
ENSCAFG00000046600	OK	5.87E-208	30.75131357	0.467221	3.75E-206
RPL5	OK	2.33E-205	30.55634595	0.465077	1.46E-203
CEP68	OK	6.23E-217	31.41542078	0.464989	4.24E-215
ENSCAFG00000030556	OK	6.12E-207	30.6750631	0.464278	3.85E-205
ENSCAFG00000008221	OK	1.09E-204	30.50597609	0.463842	6.75E-203
MAP3K6	OK	2.13E-207	30.70941944	0.462274	1.35E-205
MRPL21	OK	1.20E-202	30.35158511	0.461922	7.33E-201
ENSCAFG00000042176	OK	2.24E-203	30.40670438	0.461558	1.38E-201
EBPL	OK	2.01E-203	30.41023455	0.460875	1.24E-201
LYAR	OK	3.26E-201	30.24261963	0.460225	1.96E-199
VKORC1	OK	4.11E-202	30.31096773	0.458725	2.49E-200
AKR1B1	OK	1.07E-209	30.88120531	0.458665	6.87E-208

LYZ	OK	1.37E-225	32.04313134	0.458571	1.03E-223
RPL22	OK	3.32E-199	30.08950947	0.457969	1.99E-197
RNPEP	OK	6.61E-199	30.06665133	0.456886	3.92E-197
MAP7D3	OK	1.57E-202	30.34274368	0.45643	9.53E-201
SYNGR1	OK	3.19E-197	29.93762243	0.455469	1.88E-195
ENSCAFG00000013366	OK	1.54E-196	29.88504313	0.455042	9.03E-195
RPL7	OK	6.94E-196	29.83465963	0.454154	4.03E-194
PTGS1	OK	2.88E-216	31.36670504	0.454132	1.93E-214
SEC61G	OK	1.37E-195	29.81192923	0.453932	7.87E-194
TXNL4A	OK	3.71E-194	29.70111246	0.452056	2.11E-192
ENSCAFG00000013905	OK	9.25E-194	29.67041029	0.451899	5.22E-192
EIF3E	OK	5.33E-195	29.76630852	0.451812	3.05E-193
CAMKK2	OK	4.75E-199	30.07765041	0.451459	2.83E-197
SEC11C	OK	2.35E-193	29.63897108	0.451096	1.32E-191
CDCA3	OK	4.11E-193	29.62012584	0.450386	2.30E-191
PABPC1	OK	5.06E-194	29.69072221	0.449024	2.87E-192
UROD	OK	1.70E-190	29.41631165	0.448055	9.30E-189
RPL34	OK	4.81E-192	29.53708973	0.447786	2.66E-190
CCND1	OK	7.15E-196	29.83368164	0.446437	4.13E-194
EIF3K	OK	3.64E-189	29.3120378	0.446221	1.98E-187
RPL4	OK	7.95E-189	29.28544448	0.445949	4.29E-187
KLF1	OK	1.54E-188	29.26285514	0.445768	8.24E-187
RPS28	OK	1.13E-188	29.27343533	0.445699	6.07E-187

CCT5	OK	4.41E-188	29.22697026	0.444896	2.35E-186
ENSCAFG00000028765	OK	3.15E-196	29.86110622	0.444557	1.84E-194
SOD1	OK	4.77E-187	29.14545174	0.443825	2.50E-185
PHPT1	OK	6.40E-187	29.13538877	0.443721	3.33E-185
HK1	OK	5.12E-187	29.14299092	0.44352	2.68E-185
EIF3G	OK	1.64E-186	29.10299521	0.443166	8.48E-185
SNRPG	OK	2.97E-186	29.08273504	0.442453	1.52E-184
RPS24	OK	3.86E-186	29.07366339	0.442346	1.97E-184
ENSCAFG00000009523	OK	4.07E-187	29.15093002	0.441332	2.14E-185
ERH	OK	1.19E-184	28.95561141	0.440827	5.96E-183
CCM2	OK	4.49E-186	29.06852626	0.439738	2.28E-184
NOP56	OK	1.21E-183	28.87564577	0.439378	5.98E-182
PSMG4	OK	9.59E-184	28.88362363	0.438979	4.77E-182
ENSCAFG00000047673	OK	5.51E-183	28.82307156	0.438515	2.72E-181
ENSCAFG00000042472	OK	1.27E-182	28.79408086	0.438243	6.25E-181
RGS19	OK	9.13E-185	28.96480748	0.436366	4.58E-183
CAMP	OK	1.88E-219	31.59940404	0.434691	1.32E-217
DUT	OK	1.22E-179	28.55506084	0.433818	5.94E-178
SSBP4	OK	7.17E-187	29.13150013	0.433697	3.71E-185
ADGRG1	OK	1.17E-187	29.19344618	0.433085	6.22E-186
CPNE3	OK	1.16E-190	29.42937575	0.432094	6.36E-189
ENSCAFG00000006545	OK	2.48E-176	28.28722465	0.430656	1.21E-174
MSRB1	OK	1.70E-192	29.57220676	0.429678	9.46E-191

HMGB1	OK	1.37E-175	28.2269568	0.429629	6.62E-174
SH3BGRL3	OK	5.53E-185	28.98208306	0.428123	2.80E-183
ITGA2B	OK	8.85E-185	28.96589212	0.427196	4.46E-183
DEK	OK	4.32E-173	28.02253212	0.426344	2.06E-171
CCT3	OK	9.85E-173	27.9931274	0.425852	4.68E-171
ENSCAFG00000009917	OK	1.57E-174	28.14042484	0.42583	7.58E-173
VIM	OK	7.23E-190	29.36708582	0.424715	3.94E-188
MCUB	OK	4.84E-172	27.93624113	0.42402	2.27E-170
SGO2	OK	4.46E-171	27.85677255	0.423598	2.07E-169
ENSCAFG00000010865	OK	2.91E-171	27.87200754	0.423525	1.36E-169
RPS3	OK	2.00E-172	27.9679043	0.423211	9.44E-171
PPOX	OK	5.57E-170	27.76608675	0.422675	2.57E-168
TPX2	OK	4.54E-172	27.93854033	0.422364	2.14E-170
FXYD5	OK	9.91E-174	28.07494447	0.422263	4.75E-172
PSMB1	OK	6.73E-168	27.59310729	0.420039	3.07E-166
HMMR	OK	1.30E-169	27.7356685	0.418608	5.96E-168
CCNB2	OK	3.79E-166	27.44687111	0.417849	1.71E-164
VCP	OK	2.67E-167	27.54317207	0.416989	1.21E-165
IFT27	OK	5.19E-165	27.35146314	0.41657	2.33E-163
CDK1	OK	9.60E-165	27.32899197	0.415839	4.29E-163
DKC1	OK	2.16E-164	27.29934167	0.415247	9.58E-163
ENSCAFG00000046564	OK	2.85E-164	27.28920745	0.415221	1.25E-162
BLVRB	OK	4.86E-163	27.18522263	0.414218	2.08E-161

ENSCAFG00000050001	OK	2.20E-164	27.29872572	0.413986	9.70E-163
ENSCAFG00000006580	OK	8.19E-164	27.25053317	0.413283	3.56E-162
SPTLC2	OK	2.21E-164	27.29857008	0.412982	9.71E-163
NUSAP1	OK	1.71E-163	27.2236284	0.412452	7.39E-162
TES	OK	1.87E-165	27.3886616	0.412437	8.43E-164
PTPN6	OK	3.95E-163	27.19278153	0.411792	1.70E-161
CDKN3	OK	1.81E-162	27.13682588	0.411426	7.71E-161
H2AC18	OK	1.83E-161	27.05161308	0.411006	7.69E-160
SOX4	OK	6.67E-174	28.08903205	0.410436	3.21E-172
ENSCAFG00000009692	OK	1.81E-160	26.96676468	0.409778	7.58E-159
EIF2S1	OK	3.92E-160	26.93819607	0.409553	1.63E-158
TXNL1	OK	1.58E-159	26.88647874	0.409266	6.55E-158
FMNL1	OK	3.57E-163	27.19654242	0.409061	1.54E-161
CCT2	OK	3.07E-159	26.86178442	0.408498	1.27E-157
RPL35	OK	2.30E-158	26.78688536	0.4078	9.42E-157
MICAL3	OK	1.29E-162	27.14926863	0.407399	5.52E-161
VDAC3	OK	4.94E-158	26.75835912	0.407094	2.02E-156
EPB42	OK	6.29E-159	26.83510867	0.406905	2.59E-157
ABRACL	OK	6.83E-164	27.25718481	0.406726	2.98E-162
NCL	OK	2.29E-162	27.12812094	0.406109	9.73E-161
CEACAM28	OK	1.83E-164	27.30540849	0.405711	8.15E-163
EIF3I	OK	1.46E-156	26.63154961	0.40533	5.94E-155
ENSCAFG00000018277	OK	3.11E-162	27.11690383	0.405312	1.31E-160

SERPINA1	OK	1.20E-171	27.90386765	0.404507	5.59E-170
RPS27	OK	5.57E-156	26.58138749	0.404228	2.25E-154
GSTA4	OK	4.89E-157	26.67265961	0.403845	1.99E-155
OXLD1	OK	1.14E-155	26.55464117	0.403384	4.57E-154
RFTN1	OK	7.60E-161	26.99897613	0.402102	3.18E-159
USP21	OK	1.40E-154	26.45999318	0.401842	5.60E-153
AFF2	OK	5.11E-169	27.68628187	0.40087	2.34E-167
DBI	OK	6.26E-154	26.40338272	0.398751	2.49E-152
PLAC8A	OK	2.47E-151	26.17637794	0.398564	9.74E-150
CAPRIN1	OK	1.39E-151	26.19827137	0.398501	5.51E-150
ST13	OK	1.77E-150	26.10102274	0.396939	6.96E-149
MRPS25	OK	2.99E-149	25.99276841	0.39542	1.16E-147
ALAD	OK	6.56E-149	25.96257988	0.39518	2.52E-147
SUB1	OK	6.41E-149	25.9634222	0.395047	2.47E-147
KTN1	OK	2.12E-149	26.00603841	0.39504	8.21E-148
MRTO4	OK	1.36E-148	25.93458542	0.394526	5.18E-147
MT-CYB	OK	8.72E-150	26.04006309	0.394253	3.40E-148
C5AR1	OK	2.71E-154	26.43502763	0.394247	1.08E-152
NOLC1	OK	8.69E-149	25.95172155	0.393887	3.33E-147
ENSCAFG00000047391	OK	3.05E-147	25.81443045	0.392994	1.15E-145
CCT4	OK	1.42E-146	25.75489062	0.391936	5.31E-145
RPLP0	OK	2.45E-146	25.73376419	0.391738	9.10E-145
ENSCAFG00000000604	OK	1.97E-146	25.74227194	0.391451	7.33E-145

NANS	OK	1.98E-148	25.91994027	0.391252	7.55E-147
KIF23	OK	1.94E-147	25.83194715	0.391233	7.36E-146
ACADSB	OK	1.33E-146	25.75736001	0.391118	5.00E-145
MATR3	OK	9.33E-151	26.12559492	0.390905	3.67E-149
CCND2	OK	3.12E-155	26.51657337	0.389139	1.25E-153
RRM2	OK	7.52E-144	25.51061265	0.388224	2.74E-142
FECH	OK	2.50E-144	25.55361576	0.388123	9.18E-143
FAM216A	OK	8.60E-145	25.59533747	0.387988	3.16E-143
GADD45GIP1	OK	2.39E-143	25.46537209	0.38767	8.67E-142
PSMA7	OK	3.22E-143	25.45357693	0.387168	1.17E-141
ENSCAFG00000017228	OK	6.65E-144	25.51541147	0.386872	2.43E-142
KIF11	OK	1.88E-142	25.38421892	0.38554	6.69E-141
KARS1	OK	3.49E-142	25.35997779	0.385513	1.23E-140
ENSCAFG00000032728	OK	3.26E-142	25.36267319	0.385283	1.15E-140
DDX56	OK	1.85E-142	25.384829	0.384245	6.61E-141
ENSCAFG00000014028	OK	5.33E-147	25.7928881	0.383944	2.01E-145
ENDOG	OK	2.34E-141	25.28491198	0.383867	8.19E-140
C30H15orf61	OK	1.54E-142	25.39206964	0.383704	5.54E-141
UQCRQ	OK	1.52E-140	25.21102284	0.383674	5.24E-139
PPP1R14B	OK	4.12E-146	25.71354368	0.383582	1.53E-144
SRFBP1	OK	2.30E-141	25.28562519	0.383545	8.07E-140
SERF2	OK	1.15E-140	25.2218865	0.383412	4.02E-139
TERT	OK	5.20E-146	25.70455321	0.383304	1.92E-144

ENSCAFG00000000118	OK	4.68E-140	25.16631551	0.383065	1.61E-138
SERBP1	OK	8.86E-140	25.14103414	0.382653	3.04E-138
PARP1	OK	1.29E-140	25.21753124	0.382443	4.48E-139
NT5C	OK	5.21E-138	24.97873048	0.380282	1.77E-136
ENSCAFG00000017264	OK	1.24E-137	24.94386638	0.379577	4.21E-136
SEC61B	OK	9.12E-139	25.04824686	0.379054	3.13E-137
KIT	OK	1.19E-149	26.02810397	0.378863	4.64E-148
COX4I1	OK	1.44E-136	24.84556262	0.377878	4.86E-135
SCRN2	OK	8.08E-138	24.96115802	0.375822	2.74E-136
EIF3M	OK	5.55E-135	24.6985021	0.375574	1.85E-133
CEBPZ	OK	1.44E-134	24.65984996	0.37439	4.79E-133
KIF22	OK	8.26E-135	24.68243258	0.374179	2.75E-133
HUS1	OK	4.11E-135	24.71068203	0.374137	1.37E-133
ME3	OK	1.37E-141	25.30603532	0.374026	4.83E-140
KIF21A	OK	2.86E-138	25.00268053	0.373046	9.76E-137
PCBD1	OK	3.17E-136	24.81393559	0.372704	1.06E-134
MRPL55	OK	4.73E-133	24.51816112	0.372451	1.56E-131
DNAJC19	OK	1.63E-132	24.46770678	0.372322	5.36E-131
RPL22L1	OK	3.66E-132	24.43473339	0.371789	1.20E-130
CFDP1	OK	3.74E-133	24.52775391	0.371191	1.24E-131
ENSCAFG00000008311	OK	2.40E-131	24.3578109	0.370668	7.79E-130
LAMTOR2	OK	1.78E-131	24.36998933	0.370495	5.82E-130
PSTPIP2	OK	4.28E-143	25.44247229	0.368812	1.54E-141

GTPBP4	OK	3.55E-131	24.34172748	0.368793	1.15E-129
ARHGDIB	OK	5.46E-143	25.43288286	0.368647	1.96E-141
GNL3	OK	1.45E-130	24.2839149	0.36852	4.63E-129
SEM1	OK	1.55E-129	24.18641969	0.367932	4.89E-128
MGST1	OK	1.42E-140	25.21371602	0.367699	4.91E-139
ZC3H15	OK	6.51E-129	24.12697987	0.366627	2.05E-127
MMP8	OK	1.77E-142	25.38667818	0.366389	6.33E-141
MTAP	OK	2.12E-131	24.3627657	0.365953	6.92E-130
EZR	OK	1.06E-129	24.20204503	0.365926	3.36E-128
SPINT2	OK	2.25E-129	24.17094176	0.365366	7.09E-128
DDX24	OK	2.90E-127	23.96944694	0.364495	9.00E-126
ENSCAFG00000008661	OK	1.37E-128	24.09622771	0.363618	4.29E-127
SLC38A1	OK	6.72E-131	24.31552633	0.363611	2.16E-129
UBFD1	OK	9.90E-128	24.01411598	0.363364	3.09E-126
SGO1	OK	1.59E-126	23.89835691	0.363073	4.93E-125
CNDP2	OK	5.71E-130	24.22751039	0.362776	1.81E-128
MIS18BP1	OK	1.06E-125	23.81913829	0.361988	3.26E-124
ENSCAFG00000049156	OK	3.11E-125	23.77392357	0.361738	9.49E-124
SNRPD1	OK	2.13E-125	23.78986883	0.36144	6.52E-124
ENSCAFG00000008336	OK	2.46E-131	24.3566559	0.360717	7.99E-130
ENSCAFG00000037735	OK	4.87E-137	24.88918558	0.360714	1.64E-135
SMARCE1	OK	2.06E-124	23.69441452	0.360359	6.20E-123
ENSCAFG00000023724	OK	4.84E-125	23.75533643	0.359991	1.47E-123

CKAP2L	OK	5.49E-125	23.75004295	0.359913	1.67E-123
SLC25A6	OK	1.39E-124	23.71106937	0.359696	4.20E-123
TFPT	OK	5.89E-123	23.55270544	0.358484	1.76E-121
ATP5MC1	OK	6.41E-123	23.54913617	0.358365	1.90E-121
CCT8	OK	5.21E-123	23.55786267	0.358022	1.56E-121
LAMTOR4	OK	8.53E-128	24.02029563	0.357475	2.67E-126
ENSCAFG00000044475	OK	1.73E-122	23.50691949	0.35739	5.10E-121
ENOPH1	OK	1.11E-122	23.52579442	0.357316	3.29E-121
TBCB	OK	1.96E-122	23.50164683	0.357021	5.76E-121
HDAC2	OK	2.11E-122	23.49853364	0.356747	6.18E-121
PAFAH1B3	OK	8.38E-122	23.43990754	0.356602	2.45E-120
PFN1	OK	2.90E-127	23.96935946	0.356097	9.00E-126
TK1	OK	1.58E-125	23.80232932	0.356068	4.86E-124
HSP90B1	OK	1.69E-123	23.60567109	0.355692	5.05E-122
CDK4	OK	4.92E-121	23.36439615	0.35549	1.42E-119
AURKB	OK	1.38E-122	23.51647309	0.355428	4.09E-121
TSFM	OK	6.55E-121	23.35218401	0.355248	1.88E-119
SYNCRIP	OK	3.43E-121	23.37976862	0.354959	9.97E-120
TIMP2	OK	5.03E-121	23.36345846	0.354916	1.45E-119
DYRK1B	OK	2.15E-121	23.3996737	0.354892	6.27E-120
TCP1	OK	1.56E-120	23.31495787	0.354485	4.46E-119
ACTB	OK	6.42E-124	23.64647679	0.354474	1.93E-122
SPI1	OK	2.60E-125	23.78146683	0.353857	7.95E-124

ACSL5	OK	1.09E-130	24.29578624	0.353738	3.48E-129
FTL	OK	6.18E-121	23.35468266	0.352757	1.78E-119
UBAC1	OK	3.69E-119	23.17915936	0.352693	1.04E-117
LCN2	OK	1.75E-130	24.27609979	0.352579	5.59E-129
ETFB	OK	5.92E-119	23.15883919	0.352352	1.67E-117
ABCB6	OK	7.67E-120	23.24675136	0.351995	2.17E-118
TPI1	OK	8.37E-120	23.24301577	0.351925	2.37E-118
MMP9	OK	4.47E-131	24.33224856	0.351268	1.44E-129
CCT6A	OK	3.14E-118	23.08684957	0.351106	8.80E-117
UQCRB	OK	5.58E-118	23.06198004	0.350783	1.56E-116
UQCR10	OK	1.03E-117	23.03550289	0.350535	2.86E-116
ECT2	OK	1.00E-120	23.33403738	0.350429	2.86E-119
PA2G4	OK	9.66E-118	23.03818464	0.350215	2.70E-116
ENSCAFG00000032392	OK	1.02E-117	23.03573585	0.349833	2.85E-116
YBX3	OK	4.47E-117	22.97168935	0.349157	1.23E-115
NUDT5	OK	1.98E-116	22.90688157	0.347988	5.46E-115
CKAP2	OK	4.05E-116	22.87580687	0.34753	1.11E-114
SLC16A7	OK	2.71E-117	22.99349156	0.347281	7.50E-116
APIP	OK	1.99E-115	22.8062403	0.34678	5.42E-114
NCOA7	OK	4.38E-117	22.97260555	0.346767	1.21E-115
GEMIN6	OK	5.06E-116	22.86604034	0.346591	1.39E-114
SSR3	OK	1.76E-115	22.81157747	0.346405	4.81E-114
HSP90AA1	OK	5.50E-115	22.76167963	0.345844	1.48E-113

SMN	OK	1.26E-114	22.72545115	0.345545	3.37E-113
REX1BD	OK	1.05E-114	22.73321028	0.345289	2.83E-113
ENSCAFG00000032063	OK	1.32E-114	22.72338157	0.345171	3.53E-113
ENSCAFG00000042945	OK	4.69E-121	23.36644473	0.345009	1.36E-119
BRIX1	OK	2.77E-114	22.69067747	0.344546	7.39E-113
VDAC1	OK	2.90E-115	22.78973386	0.344011	7.88E-114
KNL1	OK	5.48E-115	22.7618258	0.343555	1.48E-113
SURF2	OK	7.59E-114	22.64629426	0.343476	2.01E-112
LRRFIP1	OK	3.52E-115	22.78122092	0.343277	9.55E-114
ENSCAFG00000002332	OK	1.04E-113	22.63250314	0.343259	2.75E-112
PIGQ	OK	1.62E-114	22.71415033	0.343252	4.34E-113
SMIM12	OK	6.20E-113	22.55349887	0.342811	1.64E-111
RABAC1	OK	6.95E-114	22.6501357	0.342472	1.85E-112
DRAP1	OK	8.54E-113	22.53933516	0.341897	2.25E-111
ATP5F1D	OK	4.08E-112	22.46999382	0.341807	1.07E-110
CCDC34	OK	1.04E-113	22.63238372	0.34161	2.75E-112
AQP1	OK	1.64E-112	22.51042397	0.340835	4.31E-111
RGS2	OK	3.58E-120	23.27943682	0.340128	1.02E-118
MCM6	OK	6.56E-111	22.34629605	0.339604	1.70E-109
HSBP1	OK	6.54E-111	22.34641766	0.339548	1.70E-109
ESAM	OK	1.60E-122	23.51039416	0.338322	4.71E-121
NDFIP1	OK	7.44E-111	22.34066075	0.338322	1.92E-109
KIFC1	OK	4.29E-111	22.36522228	0.338156	1.12E-109

ANAPC13	OK	5.68E-110	22.24966077	0.338133	1.46E-108
ENSCAFG00000044682	OK	1.19E-109	22.21650586	0.337971	3.03E-108
GTF2A2	OK	1.18E-109	22.21677989	0.337819	3.02E-108
GSN	OK	3.38E-120	23.28192885	0.337595	9.62E-119
MDN1	OK	1.10E-110	22.32324788	0.337522	2.83E-109
AGPAT3	OK	3.04E-109	22.17431259	0.336999	7.68E-108
RNASEH2B	OK	1.35E-109	22.21087036	0.33647	3.43E-108
ELOB	OK	9.31E-109	22.12387124	0.336259	2.34E-107
SYTL1	OK	1.35E-110	22.31413221	0.336249	3.46E-109
SMG1	OK	4.07E-109	22.16117225	0.336089	1.03E-107
VDAC2	OK	2.42E-108	22.08077975	0.335736	6.06E-107
PGLS	OK	1.78E-109	22.19850448	0.335711	4.51E-108
RPS21	OK	3.57E-108	22.06316026	0.335487	8.90E-107
MYG1	OK	1.31E-107	22.0041485	0.334525	3.23E-106
HNRNPD	OK	1.12E-107	22.01155689	0.334524	2.75E-106
AIFM2	OK	9.35E-108	22.01955479	0.33336	2.32E-106
CORO1A	OK	1.81E-112	22.50603718	0.332894	4.74E-111
MSH6	OK	2.58E-106	21.86873193	0.332047	6.25E-105
MYCBP2	OK	4.05E-107	21.95306113	0.332003	9.94E-106
BCAP29	OK	1.32E-106	21.89928532	0.331938	3.21E-105
KDM5B	OK	2.47E-109	22.18361183	0.331507	6.26E-108
THUMPD3	OK	2.32E-106	21.87364642	0.331491	5.63E-105
EIF3F	OK	1.38E-105	21.7922047	0.33125	3.32E-104

IRAK1BP1	OK	1.08E-106	21.90841444	0.33106	2.64E-105
SLC25A37	OK	9.20E-106	21.81059822	0.331041	2.23E-104
LGALS3	OK	1.81E-124	23.69988742	0.330785	5.46E-123
ACBD6	OK	9.08E-107	21.91632173	0.330767	2.22E-105
NASP	OK	3.33E-105	21.75163149	0.330762	8.01E-104
SLC25A29	OK	6.07E-108	22.03911581	0.330152	1.51E-106
RHAG	OK	4.92E-107	21.94418921	0.329988	1.21E-105
CENPE	OK	1.09E-107	22.01246535	0.329591	2.70E-106
GAPDH	OK	2.70E-105	21.76125844	0.329222	6.51E-104
PTPMT1	OK	2.15E-104	21.66593411	0.329207	5.15E-103
LBHD1	OK	2.81E-104	21.65367557	0.329033	6.70E-103
ANXA2	OK	6.22E-108	22.03804506	0.328872	1.54E-106
PTPRC	OK	2.89E-108	22.07274086	0.328463	7.22E-107
FAM117A	OK	1.02E-108	22.119734	0.327307	2.56E-107
CLTA	OK	1.09E-102	21.48445325	0.326708	2.57E-101
ARHGEF39	OK	1.10E-103	21.59058256	0.326542	2.62E-102
MAT2A	OK	1.10E-104	21.69669684	0.326361	2.64E-103
ENSCAFG00000020220	OK	1.17E-111	22.42302743	0.326357	3.06E-110
GSPT1	OK	3.51E-102	21.43002539	0.325545	8.26E-101
AK1	OK	6.95E-102	21.3981531	0.325282	1.63E-100
SNRPD2	OK	3.77E-102	21.4266075	0.324991	8.87E-101
PFKM	OK	1.19E-101	21.37323215	0.324758	2.78E-100
EIF6	OK	9.55E-104	21.59717945	0.323714	2.28E-102

MTHFD1L	OK	2.98E-101	21.33008859	0.322674	6.94E-100
HNRNPK	OK	5.32E-100	21.19492621	0.322151	1.22E-98
RPL15	OK	5.43E-100	21.19396688	0.322079	1.24E-98
TIMM8A	OK	4.68E-101	21.30903001	0.321964	1.09E-99
TIMM10	OK	5.08E-100	21.19705428	0.321881	1.17E-98
HSPA8	OK	3.25E-100	21.21809306	0.321669	7.50E-99
CCNA2	OK	6.86E-100	21.1829077	0.320907	1.57E-98
EIF2AK1	OK	2.87E-103	21.54630955	0.320592	6.81E-102
COPRS	OK	1.55E-100	21.25296727	0.320182	3.58E-99
TOMM6	OK	3.39E-98	20.9984871	0.318935	7.63E-97
HARS1	OK	6.12E-99	21.07960994	0.31877	1.39E-97
SNRNP200	OK	8.93E-98	20.95234858	0.318394	2.00E-96
ARF4	OK	8.07E-99	21.06653075	0.318136	1.83E-97
JPT1	OK	5.66E-98	20.97403816	0.318105	1.27E-96
PSMG1	OK	1.40E-98	21.04043014	0.318006	3.16E-97
DCTPP1	OK	4.29E-100	21.2050258	0.317998	9.88E-99
CD320	OK	7.99E-98	20.95762831	0.317916	1.79E-96
BLVRA	OK	3.00E-97	20.89453504	0.317777	6.67E-96
MT-ND4	OK	8.99E-98	20.95203129	0.317038	2.01E-96
RSL24D1	OK	6.73E-97	20.85594963	0.316856	1.49E-95
DBN1	OK	2.31E-98	21.01659452	0.316436	5.22E-97
SMARCA2	OK	5.56E-98	20.97492737	0.315998	1.25E-96
CD302	OK	1.59E-101	21.35943469	0.315697	3.72E-100
UBL4A	OK	6.64E-96	20.74612335	0.315307	1.47E-94
DNAJA1	OK	3.04E-96	20.7836669	0.315117	6.72E-95
CDC20	OK	2.05E-95	20.69177717	0.314389	4.49E-94
ADD3	OK	4.85E-99	21.09062516	0.314031	1.11E-97
HAGH	OK	8.55E-95	20.62287761	0.313514	1.85E-93
PDCD11	OK	2.48E-95	20.68272426	0.313508	5.39E-94
GLRX3	OK	1.23E-95	20.71634474	0.313062	2.71E-94
TCOF1	OK	2.70E-96	20.78933945	0.312965	5.98E-95
DENR	OK	1.27E-94	20.60368215	0.312858	2.75E-93
PPID	OK	2.35E-95	20.6852336	0.312454	5.14E-94

PHF20	OK	1.19E-95	20.71812682	0.311672	2.62E-94
PHACTR2	OK	2.40E-95	20.68424529	0.3115	5.23E-94
GSTO1	OK	2.43E-100	21.23174495	0.311358	5.62E-99
HSDL2	OK	1.16E-93	20.49616706	0.311183	2.50E-92
MRPL32	OK	1.89E-93	20.4725338	0.31058	4.05E-92
TMED5	OK	2.82E-94	20.56515654	0.310492	6.06E-93
GADD45A	OK	7.88E-95	20.62685361	0.30979	1.71E-93
NUFIP1	OK	1.23E-92	20.38098909	0.309142	2.61E-91
ENSCAFG00000029155	OK	5.12E-93	20.4239409	0.309068	1.09E-91
RUVBL2	OK	4.53E-93	20.42993575	0.3087	9.64E-92
NDC80	OK	2.09E-93	20.46762595	0.308692	4.47E-92
HNRNPDL	OK	2.19E-92	20.35282307	0.308619	4.62E-91
HNRNPU	OK	2.96E-92	20.33803764	0.308608	6.23E-91
RAD23A	OK	8.70E-92	20.28514758	0.308294	1.82E-90
XAF1	OK	2.57E-101	21.3371077	0.308063	5.99E-100
POLR2H	OK	4.60E-92	20.31646509	0.308027	9.66E-91
AMDHD1	OK	1.37E-91	20.26293212	0.307982	2.85E-90
CD177	OK	8.11E-110	22.23371199	0.307767	2.08E-108
LDHB	OK	1.05E-92	20.38870788	0.3076	2.23E-91
RWDD1	OK	1.47E-91	20.25916981	0.307376	3.07E-90
AURKA	OK	1.25E-92	20.38048368	0.306972	2.63E-91
ENSCAFG00000046637	OK	4.61E-91	20.20300407	0.306882	9.52E-90
ENSCAFG00000016270	OK	2.45E-91	20.23407405	0.306802	5.09E-90
MESD	OK	2.45E-91	20.23409962	0.306749	5.09E-90
MRPL52	OK	2.82E-91	20.22728189	0.306704	5.83E-90
UCHL1	OK	1.81E-91	20.24894024	0.306347	3.78E-90
MYBL2	OK	9.33E-91	20.16811512	0.306065	1.92E-89
HRAS	OK	1.06E-91	20.27560274	0.305937	2.21E-90
COTL1	OK	1.77E-94	20.58776437	0.304712	3.81E-93
POLR1F	OK	3.54E-90	20.10202776	0.30453	7.25E-89
ZFP36	OK	5.17E-95	20.64726469	0.304368	1.12E-93
TRAP1	OK	1.02E-89	20.04928888	0.304285	2.08E-88
C1QBP	OK	5.37E-90	20.08140817	0.304253	1.09E-88
PNN	OK	2.35E-90	20.12240169	0.303488	4.82E-89
C9H17orf99	OK	3.70E-89	19.98530657	0.30339	7.47E-88
ATP5F1A	OK	5.82E-90	20.077357	0.303353	1.19E-88
SSNA1	OK	1.31E-88	19.92211606	0.30278	2.62E-87
SLC39A6	OK	9.27E-91	20.16844528	0.302086	1.91E-89

KLF6	OK	1.03E-93	20.50199028	0.302078	2.22E-92
COX5B	OK	3.13E-88	19.87845081	0.301918	6.23E-87
SSR2	OK	3.99E-88	19.86624632	0.301737	7.94E-87
DDX1	OK	2.44E-88	19.89093761	0.301673	4.87E-87
ZNF593	OK	8.79E-89	19.94202713	0.301541	1.77E-87
EPRS1	OK	5.31E-88	19.85189927	0.301341	1.05E-86
ENSCAFG00000004842	OK	9.05E-88	19.82506914	0.301289	1.79E-86
KMT2A	OK	9.09E-89	19.9403216	0.300358	1.83E-87
CSNK1G1	OK	2.88E-87	19.76670361	0.300267	5.68E-86
CDK14	OK	1.87E-89	20.01933603	0.300232	3.78E-88
MICOS13	OK	3.54E-87	19.75637533	0.300211	6.94E-86
MPG	OK	4.02E-87	19.74987973	0.300027	7.88E-86
NDUFB10	OK	3.36E-87	19.7588755	0.299988	6.62E-86
EIF3A	OK	7.80E-88	19.8325586	0.299941	1.54E-86
NDUFB2	OK	5.87E-87	19.73073533	0.299834	1.15E-85
TIMM8B	OK	1.30E-86	19.69034658	0.299251	2.55E-85
PRIM2	OK	2.49E-87	19.77404954	0.299236	4.91E-86
FGL2	OK	1.04E-98	21.05447607	0.297495	2.36E-97
ODC1	OK	6.01E-88	19.84566253	0.297465	1.19E-86
IPO5	OK	2.31E-84	19.42637958	0.295096	4.48E-83
NR2F6	OK	1.24E-88	19.92489101	0.295048	2.49E-87
TSHB	OK	2.89E-84	19.41487178	0.294953	5.58E-83
PGLYRP1	OK	3.29E-103	21.53995836	0.294281	7.79E-102
NAP1L1	OK	8.21E-84	19.36114934	0.29364	1.58E-82
BCL7C	OK	7.36E-84	19.36674947	0.29358	1.42E-82
ENSCAFG00000006821	OK	2.03E-83	19.31443726	0.293487	3.89E-82
HSPA9	OK	3.10E-83	19.29251791	0.292918	5.94E-82
CELF2	OK	1.80E-88	19.90621003	0.292666	3.60E-87
MT-CO2	OK	2.79E-84	19.41668069	0.29265	5.39E-83
EMID1	OK	1.19E-83	19.34199095	0.292643	2.29E-82
HEMGN	OK	1.53E-95	20.70583294	0.292436	3.36E-94
UBE2C	OK	4.06E-83	19.27865759	0.291999	7.75E-82
TOMM5	OK	1.43E-82	19.21331224	0.291865	2.73E-81
HYPK	OK	2.16E-82	19.19203701	0.291735	4.10E-81
BDH1	OK	7.55E-90	20.06442804	0.291606	1.53E-88
TSPAN2	OK	2.73E-84	19.41771308	0.291298	5.29E-83
LSM6	OK	4.45E-82	19.15434397	0.290609	8.44E-81
ENSCAFG00000029470	OK	1.04E-97	20.94496828	0.290471	2.32E-96
STOML2	OK	8.38E-82	19.12137218	0.290419	1.59E-80

ENSCAFG00000048610	OK	1.41E-81	19.09438769	0.289603	2.65E-80
CD4	OK	3.41E-93	20.44387031	0.289276	7.26E-92
ENSCAFG00000000842	OK	9.41E-85	19.47238744	0.289185	1.84E-83
ENSCAFG00000040846	OK	4.71E-81	19.03109544	0.289141	8.87E-80
HAGHL	OK	1.46E-84	19.45002064	0.288426	2.84E-83
SCP2	OK	5.13E-81	19.02661822	0.288258	9.65E-80
OSGEP	OK	5.37E-80	18.90316771	0.286904	9.95E-79
NNT	OK	9.89E-81	18.99223868	0.286825	1.85E-79
PABPC4	OK	2.03E-80	18.95438996	0.286768	3.79E-79
MYL6B	OK	1.56E-84	19.44656992	0.28664	3.03E-83
KAT2A	OK	3.63E-80	18.92383413	0.286561	6.75E-79
SEPTIN9	OK	3.81E-103	21.53315195	0.286404	9.01E-102
PMS1	OK	1.64E-80	18.96560914	0.286402	3.07E-79
DCXR	OK	8.54E-80	18.87867271	0.286359	1.57E-78
ENSCAFG00000043730	OK	2.05E-79	18.83228937	0.286173	3.77E-78
SLC29A1	OK	6.88E-80	18.89009191	0.286085	1.27E-78
SMC1A	OK	1.69E-79	18.84264224	0.28589	3.10E-78
YWHAB	OK	1.35E-79	18.85430154	0.285733	2.49E-78
DLGAP5	OK	1.72E-82	19.20391808	0.285071	3.27E-81
NFIC	OK	1.38E-80	18.97453696	0.2849	2.59E-79
CACYBP	OK	5.94E-79	18.77596412	0.284153	1.09E-77
CA9	OK	3.30E-79	18.80709203	0.284085	6.05E-78
S100A11	OK	5.13E-90	20.08360856	0.284033	1.05E-88
EIF3D	OK	3.56E-78	18.68066324	0.283489	6.47E-77
LRP8	OK	7.92E-78	18.63789811	0.283203	1.44E-76
CANX	OK	4.25E-80	18.91548743	0.283079	7.90E-79
IMP4	OK	4.50E-78	18.66812785	0.283018	8.17E-77
PRPF19	OK	1.16E-77	18.61734202	0.28274	2.10E-76
ENSCAFG00000047363	OK	1.69E-77	18.59723516	0.282699	3.05E-76
FADS1	OK	5.24E-91	20.19666263	0.282607	1.08E-89
DEPDC1	OK	2.79E-78	18.69356223	0.282541	5.09E-77
NUDC	OK	1.20E-77	18.61552421	0.281421	2.17E-76
PSMB10	OK	3.05E-77	18.56555754	0.28125	5.48E-76
SLC25A5	OK	2.02E-77	18.58775319	0.280992	3.64E-76
H2AZ1	OK	7.08E-77	18.52029854	0.28096	1.26E-75
CHD4	OK	6.99E-77	18.521021	0.28056	1.25E-75
BUD23	OK	1.84E-76	18.46870906	0.280326	3.28E-75
UQCC2	OK	2.68E-76	18.44849109	0.280326	4.74E-75

SIVA1	OK	2.41E-76	18.45434882	0.279925	4.26E-75
PSMD8	OK	2.30E-76	18.4567241	0.27992	4.09E-75
SNRPB2	OK	4.08E-76	18.42581039	0.279688	7.18E-75
CNN2	OK	7.98E-80	18.88227403	0.279472	1.47E-78
ENSCAFG00000048539	OK	1.27E-75	18.36409737	0.279085	2.22E-74
TUBA1B	OK	5.08E-76	18.41388752	0.278977	8.94E-75
SFPQ	OK	1.18E-75	18.36828352	0.278662	2.06E-74
UTP20	OK	7.13E-77	18.5199087	0.278451	1.27E-75
H1-4	OK	3.92E-76	18.42789599	0.278432	6.92E-75
RUVBL1	OK	5.12E-76	18.413477	0.277836	8.99E-75
LRPPRC	OK	8.40E-76	18.38665455	0.27766	1.47E-74
ATP5PF	OK	1.63E-74	18.22511249	0.276857	2.83E-73
ENSCAFG00000023691	OK	1.22E-88	19.92565432	0.276837	2.45E-87
RCAN2	OK	2.09E-77	18.58592225	0.276686	3.76E-76
SRSF11	OK	2.01E-74	18.21356438	0.2766	3.49E-73
CKAP4	OK	2.69E-80	18.9396275	0.276439	5.01E-79
UBL5	OK	4.46E-74	18.17002606	0.276145	7.70E-73
ATXN10	OK	2.69E-76	18.44828369	0.275887	4.75E-75
CHCHD2	OK	5.06E-74	18.1630281	0.275878	8.72E-73
ENSCAFG00000002215	OK	6.28E-74	18.15124602	0.275724	1.08E-72
SMC4	OK	2.52E-75	18.32694043	0.275552	4.39E-74
PFKFB3	OK	8.14E-76	18.38834665	0.274935	1.43E-74
PSME2	OK	1.48E-73	18.1040203	0.274774	2.52E-72
TSTD1	OK	6.05E-74	18.15323526	0.274642	1.04E-72
SRRM2	OK	2.88E-73	18.06736055	0.274396	4.86E-72
UROS	OK	2.52E-73	18.07476722	0.274359	4.27E-72
PRELID1	OK	3.29E-73	18.06010037	0.274317	5.53E-72
SP110	OK	2.88E-74	18.19400402	0.274208	4.98E-73
MYC	OK	4.70E-74	18.1671717	0.274193	8.09E-73
MDH1	OK	8.99E-74	18.13150402	0.274151	1.54E-72
PLA2G7	OK	5.24E-80	18.904484	0.274013	9.72E-79
BZW1	OK	4.39E-73	18.04405544	0.273702	7.38E-72
EIF2S3	OK	3.20E-73	18.06154672	0.2737	5.39E-72
TMEM126A	OK	2.80E-73	18.06892024	0.273573	4.74E-72
ILF3	OK	6.55E-73	18.02196246	0.273547	1.10E-71
B2M	OK	8.77E-75	18.25902393	0.273409	1.52E-73
RAB27A	OK	1.42E-73	18.10647341	0.273285	2.42E-72
UBA2	OK	9.15E-73	18.00349073	0.273217	1.53E-71
PWP1	OK	9.25E-77	18.50591424	0.272951	1.65E-75
EIF3H	OK	2.44E-72	17.94904887	0.27267	4.05E-71

PSMB6	OK	2.91E-72	17.93927623	0.272358	4.83E-71
ERMAP	OK	5.71E-75	18.28244835	0.272326	9.93E-74
LSM7	OK	3.39E-72	17.93084864	0.272224	5.61E-71
ARHGAP18	OK	2.05E-72	17.95887004	0.272159	3.40E-71
COA8	OK	2.41E-73	18.07708837	0.272154	4.10E-72
ANXA1	OK	2.72E-81	19.05983369	0.271375	5.13E-80
MT-ATP6	OK	1.06E-72	17.99527884	0.271365	1.77E-71
TMED3	OK	8.87E-72	17.87725795	0.271362	1.46E-70
VARS1	OK	1.40E-71	17.85172556	0.271091	2.29E-70
DHX9	OK	1.10E-71	17.8654146	0.271075	1.80E-70
ANLN	OK	3.82E-72	17.92415129	0.270576	6.32E-71
ACAP1	OK	9.83E-73	17.99950549	0.270154	1.64E-71
SUMO2	OK	3.47E-71	17.80106231	0.270108	5.66E-70
ENSCAFG00000017667	OK	1.68E-71	17.84155293	0.269726	2.75E-70
NDUFS3	OK	1.27E-70	17.72814941	0.269342	2.07E-69
ANK1	OK	9.28E-72	17.8747165	0.269119	1.52E-70
MKI67	OK	2.59E-82	19.18251991	0.268934	4.92E-81
IL2RG	OK	2.74E-78	18.69466479	0.268778	4.99E-77
ENSCAFG00000030143	OK	7.19E-71	17.76018495	0.268345	1.17E-69
GAR1	OK	1.65E-70	17.71342915	0.268147	2.68E-69
CCPG1	OK	8.83E-72	17.87748639	0.2679	1.45E-70
RARS1	OK	1.30E-69	17.59689882	0.267269	2.09E-68
KRTCAP2	OK	1.39E-69	17.59331793	0.266931	2.23E-68
GEMIN5	OK	7.07E-70	17.63138695	0.266906	1.14E-68
LXN	OK	3.50E-69	17.54070064	0.266356	5.61E-68
BUB1	OK	3.82E-69	17.53575184	0.26596	6.11E-68
NMRAL1	OK	9.03E-69	17.48683334	0.265687	1.43E-67
TMEM237	OK	1.26E-69	17.59854854	0.26544	2.04E-68
TSPO2	OK	6.40E-69	17.50645417	0.265019	1.02E-67
SCCPDH	OK	4.03E-69	17.53272051	0.264918	6.43E-68
RDX	OK	1.66E-68	17.4519866	0.264722	2.62E-67
FCGR1A	OK	2.80E-73	18.06885501	0.264711	4.74E-72
FAIM	OK	1.49E-68	17.45836347	0.264611	2.35E-67
EEF2	OK	3.10E-68	17.41629121	0.264439	4.87E-67
ACAT1	OK	1.69E-68	17.45098794	0.26397	2.67E-67
POLR1G	OK	5.67E-69	17.51328199	0.263888	9.03E-68
DYNLRB2	OK	5.36E-72	17.90530385	0.263873	8.84E-71
PIGX	OK	2.66E-69	17.55634825	0.263674	4.26E-68
MAP4K1	OK	1.10E-72	17.99340194	0.263584	1.83E-71
EIF2AK4	OK	4.23E-68	17.39850108	0.263539	6.63E-67
MRPL28	OK	1.19E-67	17.33924783	0.263424	1.85E-66

ENSCAFG00000018497	OK	9.34E-68	17.35313353	0.263366	1.45E-66
METAP2	OK	1.28E-67	17.3349728	0.263345	1.99E-66
PARL	OK	4.90E-68	17.3901621	0.262962	7.66E-67
ENSCAFG00000019501	OK	3.05E-67	17.28496915	0.262493	4.72E-66
NDUFAF2	OK	7.26E-68	17.36759654	0.262446	1.13E-66
POLR1E	OK	1.80E-67	17.31535479	0.262358	2.79E-66
MMD	OK	4.71E-69	17.52390413	0.2622	7.50E-68
LRRN3	OK	1.35E-70	17.72477728	0.262116	2.19E-69
HP1BP3	OK	5.00E-67	17.25654605	0.262033	7.71E-66
SLA	OK	5.02E-77	18.53886632	0.261172	8.98E-76
MACF1	OK	1.18E-67	17.33970489	0.260807	1.83E-66
C20H19orf38	OK	1.33E-73	18.10992454	0.26073	2.27E-72
GOLGB1	OK	1.01E-66	17.21574701	0.260611	1.55E-65
MSN	OK	1.94E-69	17.57411642	0.260596	3.12E-68
CXCL8	OK	2.30E-73	18.07970748	0.260479	3.92E-72
TYMS	OK	2.87E-66	17.15524968	0.260457	4.39E-65
ENSCAFG00000015798	OK	7.52E-70	17.62789069	0.260407	1.22E-68
PRNP	OK	6.42E-73	18.02308567	0.260358	1.08E-71
SLC4A1	OK	8.27E-67	17.22739156	0.260188	1.27E-65
VASP	OK	2.58E-67	17.29460973	0.260075	3.99E-66
SPTB	OK	4.45E-77	18.54532632	0.25958	7.98E-76
THOC2	OK	6.61E-66	17.10669611	0.259424	1.00E-64
ATIC	OK	1.79E-66	17.1827929	0.25926	2.74E-65
ARPC2	OK	7.73E-69	17.4956538	0.258874	1.23E-67
ANP32A	OK	1.32E-65	17.0665787	0.258866	1.99E-64
EIF4A3	OK	4.40E-66	17.13040632	0.258706	6.70E-65
CPLANE1	OK	1.36E-70	17.72445162	0.25862	2.20E-69
TSEN34	OK	3.78E-66	17.13933378	0.258381	5.76E-65
AATF	OK	1.93E-65	17.04424223	0.258104	2.91E-64
ENSCAFG00000049827	OK	5.57E-65	16.9821609	0.257844	8.33E-64
AASDHPPT	OK	2.31E-65	17.03375072	0.257744	3.47E-64
URI1	OK	1.82E-65	17.04775156	0.257696	2.74E-64
AGA	OK	6.62E-65	16.9719795	0.257039	9.88E-64
SELL	OK	1.06E-68	17.47792786	0.257027	1.67E-67
RBM28	OK	5.07E-65	16.9875809	0.256678	7.60E-64
NOP10	OK	8.14E-65	16.95982771	0.256625	1.21E-63
TBC1D7	OK	1.71E-66	17.18543861	0.256359	2.62E-65
PLIN2	OK	6.67E-66	17.10618048	0.256347	1.01E-64
HMGN1	OK	2.23E-64	16.90062565	0.256026	3.30E-63

ENSCAFG00000029004	OK	7.33E-64	16.83019206	0.255602	1.08E-62
MRPL15	OK	7.51E-64	16.8287943	0.255463	1.11E-62
GDE1	OK	4.15E-65	16.99930475	0.255152	6.24E-64
ENSCAFG00000043577	OK	8.29E-64	16.82293362	0.255138	1.22E-62
AK2	OK	2.13E-63	16.76683256	0.254699	3.11E-62
CENPW	OK	6.07E-64	16.84136317	0.254561	8.98E-63
SLC45A4	OK	1.03E-63	16.81009358	0.254508	1.51E-62
INCENP	OK	2.11E-63	16.7673476	0.254278	3.09E-62
TUBB4B	OK	2.84E-63	16.74991345	0.25423	4.13E-62
TAOK3	OK	1.46E-63	16.78943607	0.254125	2.14E-62
ATP6V1H	OK	1.22E-63	16.7999577	0.253898	1.79E-62
VAMP5	OK	6.04E-65	16.9773815	0.253896	9.02E-64
PDCD1	OK	2.75E-68	17.42331601	0.253864	4.32E-67
SRPK2	OK	4.12E-66	17.13421792	0.253502	6.28E-65
KIF20B	OK	6.56E-64	16.83681341	0.253445	9.68E-63
PEBP1	OK	1.02E-62	16.67372536	0.25306	1.47E-61
SNX3	OK	1.14E-62	16.66715249	0.253036	1.64E-61
APOL5	OK	1.05E-64	16.94461554	0.252892	1.57E-63
CTSC	OK	3.68E-63	16.73436114	0.252822	5.36E-62
TUFM	OK	3.75E-66	17.13979551	0.252794	5.72E-65
CCDC59	OK	6.12E-63	16.70406632	0.252699	8.87E-62
PTPRF	OK	1.72E-63	16.77960158	0.252662	2.52E-62
PSMB4	OK	2.08E-62	16.63094311	0.25255	2.99E-61
ENSCAFG00000006913	OK	2.32E-62	16.62437049	0.252409	3.33E-61
PYGL	OK	1.95E-68	17.4427999	0.251871	3.07E-67
CSK	OK	5.64E-67	17.24950243	0.251583	8.69E-66
ATP6V0E1	OK	4.33E-62	16.58698554	0.251169	6.18E-61
RB1	OK	1.57E-64	16.92117355	0.251048	2.33E-63
WDR43	OK	1.63E-62	16.64560396	0.250981	2.34E-61

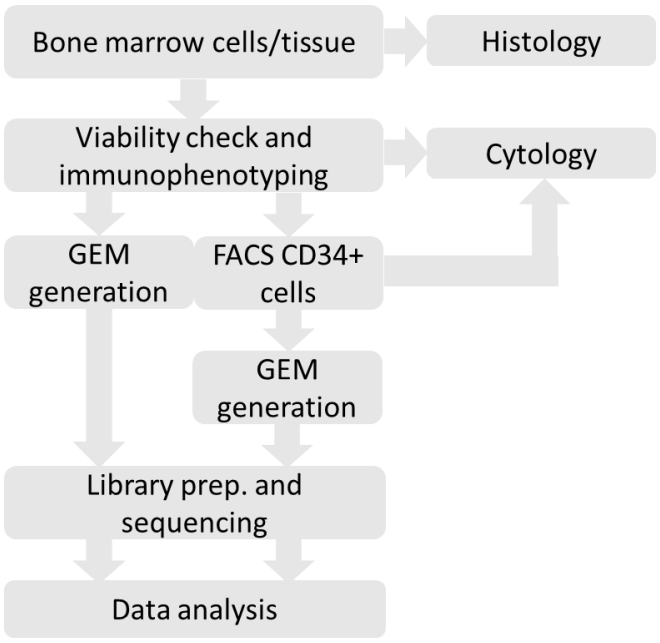

Supplemental Figure 1. Overview of sample processing for the whole bone marrow and sorted CD34+ cells.

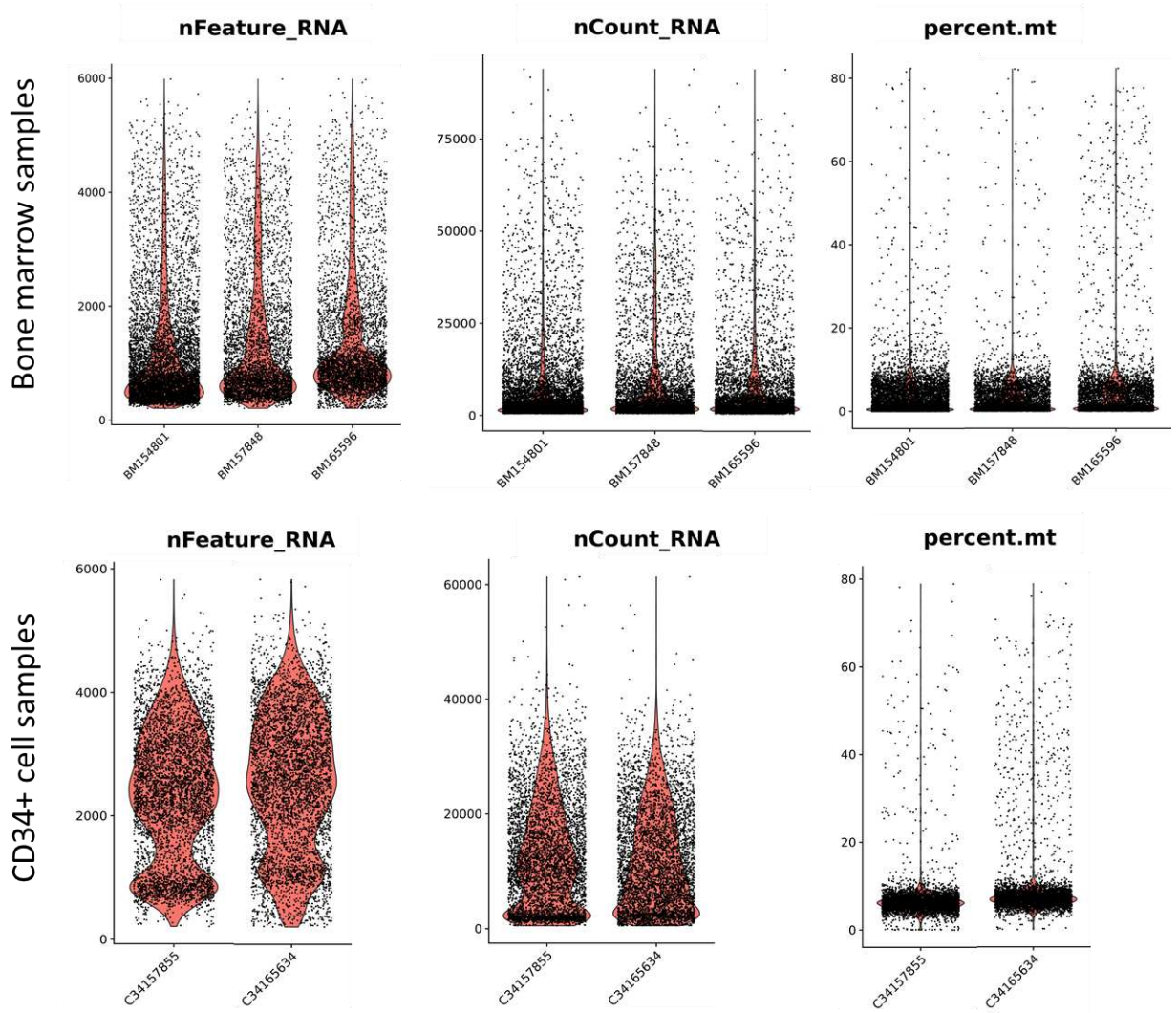

Supplemental Figure 2. Violin plots of the quality control measurements assessed prior to filtering in the bone marrow and CD34+ samples. The top and bottom row of violin plots includes all samples collected from bone marrow and the two CD34+ cell samples, respectively. number of features (nFeature_RNA), gene counts (nCount_RNA), and the percentage of mitochondrial reads (percent.mt) detected in each sample.

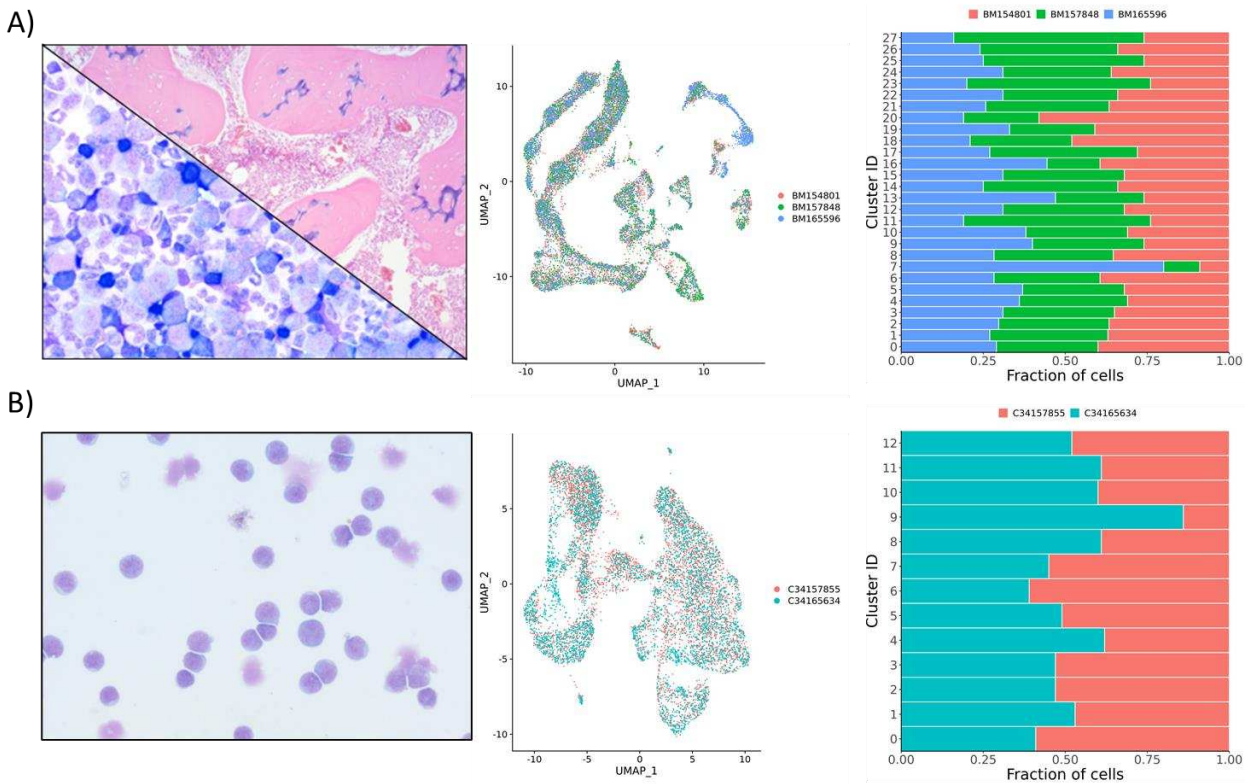

Supplemental Figure 3. Representative photomicrographic data and initial scRNA-seq clustering results from whole bone marrow and CD34+ sorted cells used to generate the single cell transcriptomic atlas. Subfigure A includes a cytologic and histologic representative images of a whole bone marrow from one dog, the distribution of each data points collected, and cell clusters are provided as a UMAP and bar plot, respectively. Cluster 7 was overrepresented in one of the samples. Subfigure B includes a representative cytologic image post FACS for CD34+ cells. The distribution of each sample data points collected, and cell clusters identified in the CD34+ cells are represented similarly as the whole bone marrow samples.

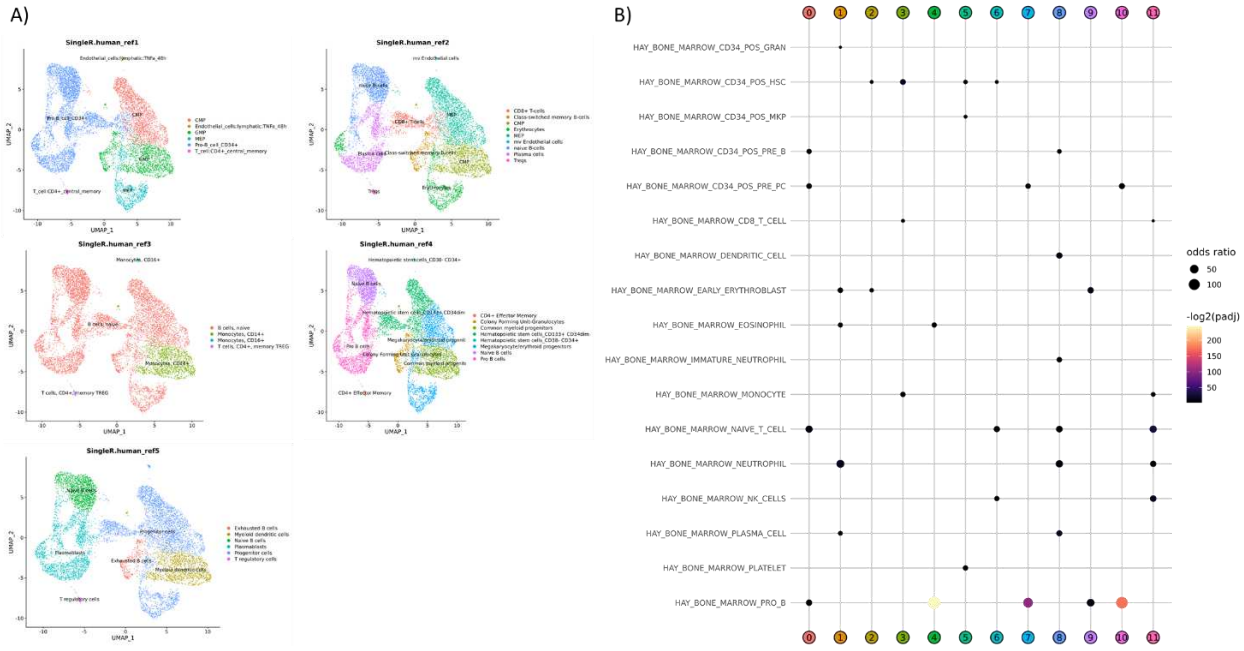

Supplemental Figure 4. Overview of cell cluster annotation results using unbiased annotation and gene set enrichment analysis from human datasets for sorted canine CD34+ cells. A) Representative UMAP plots of canine CD34+ cell samples with automated cell cluster annotations predicted using five human data references (SingleR.human_ref1-5). The cell type predicted, and the associated color scheme is displayed for each reference. B) Gene set enrichment analysis results displayed as a dot plot. The x-axis represents each cluster predicted and the y-axis represents each gene set cross-referenced. Non-significant gene sets are not displayed. No gene sets were considered enriched in cluster 12 and it is not represented. The size of the dot represents the odds ratio, and the color is illustrative of the −log2(adjusted p. value).

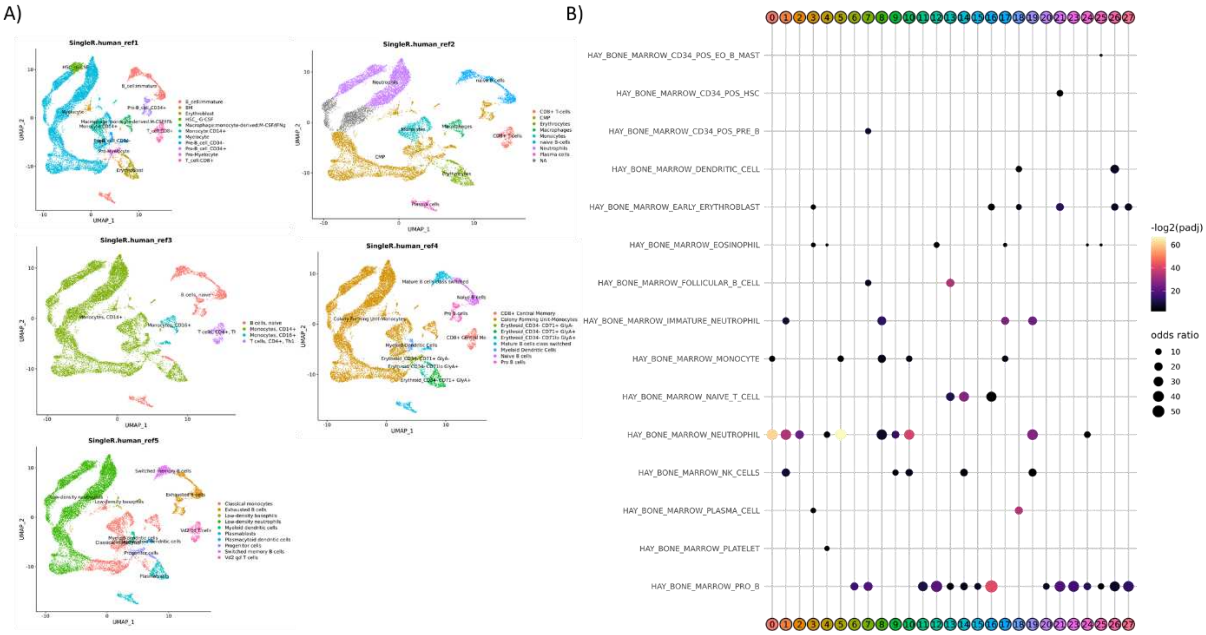

Supplemental Figure 5. Overview of cell cluster annotation results using unbiased annotation and gene set enrichment analysis from human datasets for canine whole bone marrow. A) Representative UMAP plots of canine whole bone marrow samples with automated cell cluster annotations predicted using five human data references (SingleR.human_ref1-5). The cell type predicted, and the associated color scheme is displayed for each reference. B) Gene set enrichment analysis results displayed as a dot plot. The x-axis represents each cluster predicted and the y-axis represents each gene set cross-referenced. Non-significant gene sets are not displayed. The size of the dot represents the odds ratio, and the color is illustrative of the − log2(adjusted p. value).

SUPPLEMENTARY MATERIAL FOR CHAPTER 2

Supplemental table 8: Antibody panels for canine flow cytometry immunophenotyping.

Antibody tube	**Antibody specificity and fluorochrome ‡**
Panel 1	
1	M IgG1-FITC/M IgG1-PE/M IgG1-Alexa 647/M IgG1-Alexa 700/M IgG1-PE-Alexa-750/M IgG1-Pacific Blue
2	CD3-FITC/CD25-PE/CD5-APC/CD8-Alexa 700/CD4-Pacific Blue
3	Class II MHC-FITC/CD22-PE/CD21-Alexa 647
4	Class II MHC-FITC/CD34-PE/CD5-APC/CD14-PE-Alexa 750
5	Class II MHC-FITC/CD18-PE/CD5-APC/CD14-PE-Alexa 750/CD4-Pacific Blue
6	CD5-FITC/CD45-PE/CD21-Alexa 647
Panel 2	
1	No antibodies
2	CD3-FITC/CD25-PE/CD5-APC/CD8-Alexa 700/CD4-Pacific Blue
3	CD21-Alexa 647/Class II MHC-FITC/CD34-PE
4	Class II MHC-FITC/CD18-PE/CD5-APC/CD14-Alexa 700/CD4-Pacific Blue
5	CD5-FITC/CD45-PE/CD21-Alexa 647
Abbreviation: M, Mouse	

‡ Except where noted, antibodies were purchased from Bio-Rad, Hercules, CA. Clones are as follows: CD45 = YKIX716.13, CD18 = YFC118.3 (human CD18), CD4 = YKIX302.9, CD8 = YCATE55.9, CD5 = YKIX322.3, CD21 = CA2.1D6, CD22 = RFB4 (human CD22, AbCam, Cambridge, MA), CD3 = CA17.2A12, CD14 = TUK4 (human), class II MHC = YKIX334.2, CD34 = 1H6, CD25 = P4A10 (eBioscience, San Diego, CA). All tubes contain propidium iodide for dead cell exclusion.

Supplemental Table 9: RNA concentration, 260:280 ratio(s), RNA integrity number (RIN), and total amount of RNA available for each sample.

Case ID#	Nanodrop (ng/ul)	Nanodrop 260/280	Agilent RIN	Total amount (ug)
1	595	2.06	4.9	32.7
2	253	1.96	4.4	13.9
3	390	2.03	7.3	21.5
4	205	2.01	4.1	11.3
5	99	2.12	6.6	5.4
6	2177	1.93	3.1	119.7
7	330	2.09	5.0	18.2
8	349	2.02	6.0	19.2
9	319	1.99	3.7	17.5
10	69	2.18	7.3	3.8
11	81	2.13	6.1	4.5
12	298	2.10	7.0	16.4
13	199	2.09	4.6	10.9
14	21	2.15	7.1	1.2
15	130	2.12	8.4	7.2
16	100	2.14	6.2	5.5
17	243	2.05	3.3	13.4
18	158	2.16	3.7	8.7
19	72	2.18	7.8	4.0
20	167	2.08	8.0	9.2
21	370	1.88	5.6	20.4
22	80	2.18	3.8	4.4
23	35	2.20	8.3	1.9
24	918	2.12	7.6	50.5

25	372	2.06	6.2	20.5
26	93	2.12	6.0	5.1
27	283	2.10	4.0	15.6
28	555	2.11	4.8	30.5
29	322	2.00	4.4	17.7
30	27	2.19	8.0	1.5
31	175	2.06	4.6	9.6
32	635	2.12	5.6	34.9
33	358	2.06	7.4	19.7
34	136	2.13	6.2	7.5
35	123	2.14	8.0	6.8
36	548	2.14	6.9	30.1
37	302	2.09	5.4	16.6
38	220	2.09	4.7	12.1
39	314	2.10	4.4	17.3
40	372	2.08	6.3	20.5
41	622	1.95	5.6	34.2
42	122	2.12	5.8	6.7
43	83	2.11	6.3	4.6
44	428	2.02	4.5	23.5
45	221	2.12	3.8	12.2
Control Cases:				
46	37	2.18	7.9	2.04
47	15	2.09	8.2	0.83

Supplemental Table 10: Gene list and target sequences.

Gene Symbols §	NS Probe ID	Target Sequence §	%CV ‡
ANPEP	NM_001146034.1:2238	AACTGGACCGATCACCCACAGACCCTC ACAGAACAGTACAACGAGATTAATGCC GTCAGCACCGCCTGCACTTATGGGGTTC CTAAGTGTAAGGACCTGG	316.4
CD14	XM_843653.4:0	ACTGCCTGGGGCATTGCACTCTACATTC CCTACAAGATCCTTCCTGTTATAGTCCT GGCAACATCCTTCATTGCAAAATTTCCC GGAAGGGTAGTGCATG	101.0
CD19	XM_014114517.1:1482	CTCCTTAAGCTCCTCCTGAGATCTGTAT CTGATCCTGAAATCTGGGAACCTAAGC AGACAGCGTCAACATCTGGAGCAGCAT TGCCTTGGATATGTGTAT	387.2
CD2	XM_844126.3:413	TTGAAGATTCAAGAAAAGGTCTCAACA CCTAAGATCCTCTGGAGTTGTGGCAAC CAATCCCTGACCTGTGAGATAACAAGT GGAACTGACCCTACATTAA	101.0
CD22	XM_862798.3:1905	ACGTGCGAGAGCGATGCCAACCCTCCC ATCCTCCAGTACGCCTGGTTTGACTGGA ATAACCAAAACCTCCGCCACTATGATC AGATGCTGAGATTGGATC	101.9
CD33	XM_005616249.1:1422	ATGGTTGTAAGAAGTCCCATCTCACAG GGTTGCCATGAGGATTAAAAAGAAGTG CATATGGAAAACACTCAACAGAGAGAG GTCTTGCTGCATTGTGATA	198.6
CD34	NM_001003341.1:2083	CACTGTTCTCTGGCTGAGCCTGGAACG AGACTCCAAGTTTTGAACAATGTCTTGT GTCTATGTTTGGGAGACAGCATAGGGA TGCGTGGACACATGCGTT	55.9

CD3E	NM_001003379.1:445	TAACCTTGTGGAAGGTGCTAGTAACAG AGAGCTATCTCAGAAGGAGTTTTCAGA AGTGGACGACAGTGGTTATTATGCCTG CTATGCAGATTCCATAAAG	203.0
CD5	XM_850074.4:3631	CGGGGCTCAGAGACTGTGAAAGAACCA GGTACCAAGCACAAAACATCAAGAGGC AGACCTGTTTCCTGAGACGACTCTGTAT TTACTGCCTGGAAATAAT	127.1
CD7	XM_844435.4:460	GCCAGGCCGTCACGATGGACGCCGAAG TCCAAGGCTCTGGCACCTTGCTGGTGGT GACAGACAAAGCAGCGGGCACGTACCA GGAAACTCGGCTGGTCTC	86.0
CD79A	NM_001313834.1:620	GATGGCAAAATATGAAGTTTGGGGTGG ATGCCCAGGATGACTATGAAGATGAAA ACCTTTATGAGGGCCTGAATCTGGATG ACTGCTCCATGTACGAGGA	63.0
CFD	XM_542213.6:336	GCCTGGAGGACGTGGCCGACGGGAAGG TGCGGGTGCTCCTGGGCGCGCACTCCCT GTCGCAGCCGGAGCCGTCCAAGCGCTG GTACGACGTGCTGCGGGC	236.6
CIITA	XM_005621546.2:1482	ATCGCGGAACTGGACCAGTACGTGTTC CAGGACTCCCAACTGGAGGGTCTGGGC AAAGACATTTTCATCGAGCATATAGGA TTAGAAGACATGATCAGCG	70.1
CR2	XM_005622319.1:2435	CAAAACTCATGCTTCATATGCCCACAA CGACACGGTATATTTTGCCTGCAATGCT GGCTTCATCATGAACGGCAGTCATGTG ATTCAGTGCCATACCAAT	100.3
DLA-DQA1	NM_001011726.1:441	CACATGGTTGAAGAATAGGCACTCAGT CACAGAAGGGGTTTCTGAAACCAGCTT CTTCGCCAAAGGGGATCATTCCTTCTCA AAGATCAGTTACCTCACC	209.9

DLA-DRA	NM_001011723.1:190	AGGAGACGGTGTGGCGCCTTGAAGAAT TTGGACGTTTTGCCAGCTTTGAGGCCCA GGGTGCCTTGGCCAACATAGCTGTGGA CAAAGCTAACCTTGACAC	239.9
DNTT	XM_014108823.1:737	GTCCTTCAAACTCTTTACCTCTGTGTTT GGAGTGGGACTGAAAACATCTGAGAAA TGGTTCCGGATGGGTTTCAGAACTTTGA GCAAAATAAAGTCGGAC	118.4
EEF1G	XM_848484.3:1065	CTTCCCTGAGGAGCTCACTCAGACCTTT ATGAGTTGTAACCTCATCACTGGAATGT TCCAACGGTTGGACAAGCTGAGGAAGA ATGCCTTTGCCAGTGTC	33.8
GATA3	XM_844060.1:1148	GCATGACACGCTGGAGGACTTCCCCAA GAGCAGCTCGTTCAACCCTGCCGCCCTC TCCAGACACATGTCCTCCCTCGGCCACA TTTCCCCTTTCAGCCAC	68.1
GUSB	NM_001003191.1:1362	GTCGGGATAAGAATCACCCATCTGTAG TCATGTGGTCTGTAGCCAATGAGCCCA CTTCCTTCCTGAAGCCTGCTGCTTACTA CTTCAAGACGCTGATTGC	51.2
HLA-DRB1	NM_001014768.1:414	CCTACAGTGACTGTGTATCCTACGAAG ACTCAGACCTTGCAGCATCACAACCTC CTGGTCTGCTCTGTGAATGGTTTCTATC CAGGCCACATTGAAGTCA	171.9
HPRT1	NM_001003357.2:321	GAGGCCATCACATCGTAGCCCTCTGTGT GCTCAAGGGAGGCTATAAATTCTTTGCT GACCTGCTGGATTATATCAAAGCACTG AACAGAAATAGTGATGG	29.6
IGHG	IGHG1_01.1:146	TGTGCACACCTTCCCGTCCGTCCTGCAG TCCTCAGGGCTTCACTCCCTCAGCAGCA TGGTGACAGTGCCCTCCAGCAGGTGGC CCAGCGAGACCTTCACC	133.2

IGHM	IGHM_01.1:111	TCACCTTCTCCTGGAAGTACGAGAACCT CAGTGCAATCAACAACCAGGACATTAA GACCTTCCCTTCAGTTCTGAGAGAGGG CAAGTATGTGGCGACCTC	157.0
IL3RA	XM_014111816.1:1728	ACCGATCCTGCGTCCACGGAGAAGCTC TACGAAAACCACTTCGTGATTTACAATC CCGGAAACTACGTGGCGAAACTAAAGG TGCAGGGTTTCTTCCGCA	186.1
IRF4	XM_005640152.1:1633	TCCCGTATCAGTGTCCGGTGACGTTTGG ATCCCGCGGCCACCACTGGCAGGGCCC GGCTTGTGAAAACGGTTGCCAGGTGAC AGGAACCTTTTATGCTTG	101.2
ITGAM	XM_014114359.1:2861	AATACACTGTCTTCATGGTAGTCACCAG CCATGAGGGCTCCACCAAATATCTCAA CTTCACAGCTGCGGAGAAGACTAGCCA CATTATAGAGCATTATTA	214.6
ITGAX	XM_547049.4:1965	AATTCAAACCTACAGAGATAGCCAGGT CTATATCTGAGTGTCGGGAAAAGACTT CCTCTGTCAAGGCACTGGGTGATGCCA ATGTCTGCCTTCATATTTA	187.2
ITGB2	XM_005638976.1:1507	CACCTATGACTCCTTCTGCAGTAACGGG GTGTCGCAGGTGGACCAGCCCAGAGGG GACTGCGACGGCGTCCAGATCAACGTC CCGATCACCTTCCAGGTG	66.3
KIT	NM_001003181.1:2110	GATCACGGAGAAGTGGCACTTTATAAG AACCTTCTGCATTCAAAGGAGTCTTCCT GCAGTGACAGTACTAATGAATACATGG ACATGAAACCCGGCGTTT	74.6
LGALS3	NM_001197043.1:575	GATGTTGCCTTCCACTTTAACCCACGCT TCAATGAAGACAACAAGAGAGTCATTG TTTGCAATACCAAGCTGGATAATATCTG GGGAAAGGAAGAAAGGC	169.7

LYL1	XM_014121805.1:1172	GGAGCTGGCCGAGGGTGAGTATGGGTT GGTGTGTGCATACCACCCAACAAGCCA CAAAGAGTTCATGGCAAATGTGCCATG GGCCGAGGCCGCGGAGCGC	12.0
LYZ	NM_001300876.1:167	TAATACAAGGGCTACGAACTACAATCC CGGAAGCAAAAGCACTGATTATGGGAT ATTTCAAATCAATAGCCGCTACTGGTGT AATGATGGCAAAACGCCC	255.1
MCL1	NM_001003016.1:1425	GGCCATGGAGGAGGACTTTTAGATTTA GTAAAGTTGGTAGGGTTGAAGAGACTT AATTTTCTTGTCTAGAACAGGAGAGTG GCCAGTAGCCAGGCTAGTC	121.6
MPL	XM_848349.1:998	GTGTGAAGAGGAGAAAAATCCAGGATT ACAGCCCTCCCGGTTCTCCCGCTGCCAC TTCAAGTCACGAAACGACAGCATTATT CACATCCTTGTGGAGGTG	119.1
MPO	XM_014116690.1:1183	GGTACCGCTCCTACAATGACTCGGTAG ACCCTCGCATCTCCAACGTCTTTACCAA TGCCTTCCGCTATGGCCACACCCTCATC CAACCTTTCATGTTCCG	188.9
MS4A1	NM_001048028.1:264	TTCACACGGATGTCTGTGCGCCCATCTG TATAACTATGTGGTACCCTCTCTGGGGA GGCATTATGTTCATCATTTCTGGATCAC TCCTGGCAGCAGCGGA	119.0
NPM1	NM_001252171.1:348	CCCTTGGGGGCTTTGAAATAACACCAC CTGTGGTCTTACGGTTGAAGTGTGGTTC CGGTCCTGTGCATATTAGTGGACAGCA CTTAGTAGCTGTAGAGGA	37.8
PAX5	XM_849748.4:2674	TTTTGAAATAGGGGTTCCAGGGGCCAC TATCTCTTTGCCTGGGACCTCAATTCCT TCAATAATCTCTCTTGCCAGCTCCAAGC AGCCAGGTGGAGGTCTG	97.9

POLR2A	XM_852751.4:2444	TCATTAACAACTGGCTTCTCATCGAGGG TCATACCATTGGCATTGGGGACTCCATT GCGGACTCAAAGACCTACCAGGACATT CAGAACACTATTAAGAA	28.4
PROM1	NM_001314109.1:1450	ACACCGGGGGCATCTTTCTCATGGTCG GAGTTGGAATCAGTTTCCTCTTTTGTTG GATACTGATGACCATTGTGGTGCTCAC GTTTGTCATCGGTGGAAA	60.6
RPL19	NM_001313782.1:415	TGCTCAGAAGATACCGTGAATCTAAGA AGATTGACCGCCACATGTATCATAGCC TGTACCTGAAAGTGAAGGGTAATGTGT TCAAGAACAAGCGGATTCT	23.9
SDHA	XM_535807.5:913	CCACAGGTATATATGGTGCTGGTTGTCT CATTACGGAAGGATGCCGTGGAGAGGG AGGCATTCTCATTAACAGTCAAGGCGA AAGGTTCATGGAGCGATA	20.0
SQSTM1	XM_014117639.1:655	CAGCTGCTCTTCCGACCCCAACAAACC CGATGTGGATCGGGACCCGGAGGGCAC CGCACAGGCGCTAGCTGAGCAAATGGA CAAGGTTGCCCTGGAGTCG	49.3
TRBC	Canis_TRBC.1:255	TCTGGCACAACCCGCGCAACCACTTCC GCTGCCAAGTCCAGTTCTATGGGCTCG GGGACGACGATGAGTGGAAATACGATA GAGTCAAACCCATCACCCA	101.5
TRGC2	Canis_TRGC2.1:378	CAAAGCAAAACACAGAGGTGGTAACTT TGAACCCTGCCAGTTCAAGATCTTTCAG GCCTGTCCTTAGCACTGTGGAATTTGCT GCTATTAACTCTACAGA	147.4
TRGC3	Canis_TRGC3.1:262	TATTGTCAACCACGAGAGTGATAGAGG AGGGATTAATCAAGAGATTCTTTTTCCT TCGATAAATGAAGATTTGGTAGCGAGG ATGGAATCTGATGTTGAC	85.4

TRGC8	Canis_TRGC8.1:167	TCCCAGCAGGGAGACACCGTGAAGACT AATGACACATTCATGAAATTCAGCTGG CTGACCGTGGCAAAAAAGTCAATGGCT GAAGAACAACAATGTATCA	219.2
ZYX	XM_005629733.2:33	AGCCCAGGGAGAAGGTGAGCAGTATTG ATTTGGAGATCGACTCTTTGTCCTCACT GCTGGATGACATGACCAGGAATGATCC CTTCAAATCCCGAGTGTC	76.8

§ Gene symbols and their associated target sequences are provided for the 49 genes used in this study.

‡ The coefficient of variation is provided (%CV).

Supplemental Table 11: Patient signalment, leukocyte concentration, and flow cytometry data for each case.

Case ID and Signalment				Leukocyte Count (cell/uL)	Flow Cytometry				Gene Expression Group
					Criteria for determining neoplasia				
CASE ID#	Age (years)	Breed	Sex	WBC	%CD34+	%CD5+CD3-	%CD14+MHCII-	%CD18+MHCII-CD4-CD14- (other myeloid)	
1	NR	LAB	FS	55200	35.72	25.59	0.94	3.7	1/LYMPH
2	7.4	BLGSH	MC	295000	51.68	33.71	0.90	7.6	1/LYMPH
3	10.7	KSND	MC	84600	56.63	27.81	0.07	17.2	1/LYMPH
4	11.7	BOX	MC	90480	79.67	15.6	0.01	5.89	1/LYMPH
5	14.0	MIX	MC	35380	74.85	49.72	2.11	5.6	1/LYMPH
6	10.0	GLDR	FS	92700	90.85	48.11	0.55	11.87	1/LYMPH
7	8.3	GLDR	FS	60550	26.11	27.03	0.18	1.23	1/LYMPH
8	6.7	AUS	MC	76790	40.76	18.1	0.01	1.02	1/LYMPH
9	11.6	GLDR	FS	162800	74.38	23.26	0.01	2.8	1/LYMPH
10	6.1	BMSTF	MC	45600	40.83	17.38	0.01	12.5	1/LYMPH
11	2.5	GSHEP	MC	14600	92.75	44.48	0.02	2.73	1/LYMPH
12	8.1	PWD	FS	108000	93.92	19.11	0.03	1.37	1/LYMPH
13	9.4	LAB	MC	209700	91.97	21.74	0.01	0.91	1/LYMPH

14	8.2	GLDR	NR	26900	76.04	57.5	0.13	3.9	1/LYMPH
15	8.4	MIX	FS	44600	84.71	22.29	2.89	27.09	1/LYMPH
16	8.6	LAB	FS	12300	65.98	4.12	6.55	22.1	2/MYELO
17	12.9	AUS	FS	108200	68.34	8.96	10.19	9.2	2/MYELO
18	8.3	GSHEP	MC	28900	13.11	7.41	25.69	77.3	2/MYELO
19	7.0	LAB	MC	29000	8.78	7.98	21.44	48.1	2/MYELO
20	8.7	MIX	MC	48400	70.44	6.64	1.61	21.1	2/MYELO
21	1.1	PBT	NR	212730	18.44	7.85	20.32	78.18	2/MYELO
22	11.7	MIX	MC	33800	60.96	7.22	3.14	13.2	2/MYELO
23	5.0	GLDR	MC	20550	63.67	7.58	10.87	17.9	2/MYELO
24	9.4	GSHEP	FS	55800	75.05	8.46	4.73	17.07	1/LYMPH
25	8.1	MALT	MC	49500	10.57	6.02	1.93	72.92	2/MYELO
26	10.4	LAB	FS	11300	64.34	11.92	4.47	34.2	2/MYELO
27	12.8	LBDOODLE	FS	180500	16.71	8.98	5.34	37.69	2/MYELO
28	9.0	LAB	FS	77300	39.03	11.94	52.40	89.8	2/MYELO
29	7.0	IRST	FS	99500	68.43	6.08	7.91	18	1/LYMPH
30	4.6	MIX	MC	24000	47.06	11.8	5.19	12.59	1/LYMPH
31	10.0	GLDR	FS	99580	72.41	5.93	2.48	11.1	1/LYMPH
32	11.2	MIX	FS	417220	96.87	5.3	1.08	10.61	1/LYMPH
33	8.7	GRH	MC	23000	75.11	10.45	0.42	1.9	2/MYELO
34	9.0	LAB	FS	91200	70	5.48	0.43	2.4	1/LYMPH
35	8.1	PBT	MC	112100	15.42	4.37	0.10	2.43	1/LYMPH

36	10.2	MIX	MC	224970	45.37	4.76	1.00	11.73	1/LYMPH
37	5.1	LAB	FS	283300	94.8	8.47	0.00	5.28	1/LYMPH
38	15.8	BGL	FS	298600	92	6	0.56	13.53	1/LYMPH
39	4.1	LBDOODLE	MC	53100	55.1	6.53	1.40	10.38	1/LYMPH
40	9.0	NR	M	244500	92.31	6.45	0.03	4.7	1/LYMPH
41	5.5	MIX	FS	248700	68.14	8.57	0.06	1.8	1/LYMPH
42	11.2	MIX	FS	66780	88.31	10.71	0.06	3.05	1/LYMPH
43	7.2	LAB	M	35700	62.06	9.84	0.03	0.61	1/LYMPH
44	11.6	LAB	FS	93910	40.36	15.52	5.20	8.6	1/LYMPH
45	NR	MIX	FS	251100	55.4	16.1	3.97	83.8	2/MYELO
Control Cases:									
46	3.7	BLLDENG	M	19300	#N/A	#N/A	#N/A	#N/A	#N/A
47	11.4	GLDR	MC	12500	#N/A	#N/A	#N/A	#N/A	#N/A

Abbreviations: NR: Not Reported, LAB: Labrador Retriever, BLGSH: Belgian Shepherd, KSND: Keeshond, BOX: Boxer, MIX: Mixed Breed, GLDR: Golden Retriever, AUS: Australian Shepherd, BMSTF: Bullmastiff, GSHEP: German Shepherd, PWD: Portugese Water Dog, PBT: Pit Bull Terrier, MALT: Maltese, LBDOODLE: Labradoodle, IRST: Irish Setter, GRH: Greyhound, BGL: Beagle, BLLDENG: English Bulldog, FS: Female Spayed, M: Male Intact, MC: Male Castrated, WBC: White Blood Cell, ALL: Acute lymphoid leukemia, AML: Acute myeloid leukemia, AUL: Acute unclassified leukemia, MPAL: Mixed phenotype acute leukemia

§ Flow cytometry acute leukemia lineage determined post establishment of criteria

Supplemental Table 12: Normalized Gene Counts for each group and controls. Nine genes were considered differentially expressed (FDR<0.05) and are bolded.

Gene symbol/Alternative ID (if applicable)	**Control (n=2) §**		**Group 1/LYMPH (n=14)** §		**Group 2/MYELO (n=31) §**			**p value (LYMPH vs. MYELO)**	**FDR adjusted p value (LYMPH vs. MYELO) †**
	Average	**SD**	**Average**	**SD**	**Average**	**SD**	**Log2 fold change LYMPH/MYELO ‡**		
CFD/Adipsin	**5773.74**	**1554.93**	**98.04**	**129.16**	**584.69**	**892.49**	**-2.58**	**<0.001**	**<0.001**
LGALS3/Lectin	**11801.71**	**1845.15**	**315.91**	**505.85**	**3556.81**	**4230.98**	**-3.49**	**<0.001**	**<0.001**
DNTT/TdT	**34.71**	**5.21**	**8529.96**	**6558.53**	**3259.04**	**3742.68**	**1.39**	**<0.001**	**0.030**
ITGAX/CD11c	**1509.26**	**139.71**	**186.03**	**286.44**	**1150.16**	**1693.83**	**-2.63**	**<0.001**	**0.030**
LYZ/lysozyme	**270960.03**	**59718.38**	**4080.69**	**5552.18**	**40068.01**	**88777.18**	**-3.30**	**<0.001**	**0.030**
ANPEP/CD13	**3926.25**	**898.07**	**27.52**	**15.40**	**655.57**	**1872.11**	**-4.57**	**<0.001**	**0.040**
CD79A	**1560.91**	**269.29**	**11993.06**	**5042.74**	**6669.55**	**4763.03**	**0.85**	**<0.001**	**0.040**
SQSTM1/P62	**5671.84**	**1088.47**	**2014.92**	**818.26**	**3160.42**	**1092.61**	**-0.65**	**<0.001**	**0.040**
IGHM/IgM	**8098.61**	**5661.52**	**9512.11**	**7620.33**	**3631.53**	**2916.08**	**1.39**	**<0.001**	**0.050**
TRGC8/TCR gamma	48.00	0.47	10215.63	15635.26	1376.92	3738.43	**2.89**	0.002	0.060
CD3E	2047.99	907.49	3577.09	5296.26	348.42	397.32	**3.36**	0.005	0.12
ITGAM/CD11b	12480.50	2574.10	396.08	532.76	1073.06	1325.75	**-1.44**	0.006	0.12
IGHG/IgG	4151.88	2212.11	1255.11	1366.43	469.10	513.24	**1.42**	0.007	0.13
CD2	1257.35	759.33	9198.32	7064.06	5002.32	5897.76	**0.88**	0.009	0.15
CD33	1499.98	379.95	61.13	61.00	143.96	150.18	**-1.24**	0.010	0.16
GATA3	116.74	35.00	1195.25	572.46	693.33	489.56	**0.79**	0.011	0.16
MPO/Myeloperoxidase	75.57	11.89	388.42	311.17	1747.39	2521.32	**-2.17**	0.013	0.18
CD7	74.12	16.17	93.00	71.92	49.56	39.81	**0.91**	0.019	0.25
CIITA	453.38	32.35	178.46	97.38	102.51	61.45	**0.80**	0.020	0.25

ITGB2/CD18	3497.82	291.11	1222.44	528.76	1914.71	1269.64	**-0.65**	0.026	0.31
CD34	95.65	25.06	8580.50	3664.98	5668.05	2898.79	**0.60**	0.028	0.33
HPRT1	4997.37	465.63	2684.48	758.51	3350.61	707.64	**-0.32**	0.037	0.40
CD5	710.36	345.40	368.02	349.70	315.87	537.04	**0.22**	0.054	0.57
HLA-DRB1/MHC Class II	14059.95	3040.90	1519.47	1432.67	858.09	1199.47	**0.82**	0.069	0.68
LYL1	20.00	0.00	20.00	0.00	21.76	3.43	**-0.12**	0.075	0.70
CD19	201.00	46.11	132.75	83.49	94.13	110.15	**0.50**	0.087	0.79
IL3RA/CD123	47.54	18.04	26.46	15.20	59.72	111.64	**-1.17**	0.10	0.83
ZYX/Zyxin	25552.10	8087.89	5076.27	2151.44	5724.50	1615.84	**-0.17**	0.12	0.93
CD14	54.13	16.20	35.49	43.07	27.99	16.09	**0.34**	0.89	1.00
CD22	379.11	45.51	414.19	366.39	479.06	423.58	**-0.21**	0.77	1.00
CR2/CD21	71.48	9.31	47.26	53.70	48.65	41.35	**-0.04**	0.52	1.00
DLA-DQA1/MHC Class II	22854.09	2349.05	1677.49	1739.54	861.94	715.44	**0.96**	0.16	1.00
DLA-DRA/MHC Class II	59224.78	6326.39	2973.69	2974.23	1934.45	1674.03	**0.62**	0.20	1.00
EEF1G	7557.64	167.35	18020.47	6836.67	20243.69	4148.08	**-0.17**	0.15	1.00
IRF4/MUM1	371.42	6.85	117.85	61.89	191.09	219.99	**-0.70**	0.15	1.00
KIT/CD117	56.89	17.92	9032.35	5802.56	12802.34	8241.94	**-0.50**	0.30	1.00
MCL1	59232.43	2899.15	6317.11	2421.36	7301.04	2968.60	**-0.21**	0.15	1.00
MPL/CD110	633.02	221.49	78.79	54.53	126.03	118.15	**-0.68**	0.15	1.00
MS4A1/CD20	159.95	28.24	151.22	206.57	98.03	59.42	**0.63**	0.73	1.00
NPM1	9811.09	131.22	29820.91	11161.24	34848.63	9845.82	**-0.22**	0.16	1.00
PAX5	85.19	14.60	47.09	52.60	36.83	29.14	**0.35**	0.50	1.00
POLR2A	2216.51	56.21	2789.92	715.86	2394.89	716.56	**0.22**	0.38	1.00
PROM1/CD133	82.36	21.25	23.49	8.80	25.16	11.74	**-0.10**	0.67	1.00
RPL19	59477.95	897.13	112559.05	25657.82	114153.84	23118.41	**-0.02**	0.59	1.00
SDHA	1044.70	55.32	2148.62	332.60	1925.58	260.83	**0.16**	0.60	1.00

TRBC/TCR beta	4716.21	2059.80	8022.15	9524.31	8966.43	7571.31	**-0.16**	0.59	1.00
TRGC2/TCR gamma	208.30	20.75	112.80	176.44	71.47	93.50	**0.66**	0.47	1.00
TRGC3/TCR gamma	50.04	11.07	57.39	31.39	56.35	25.45	**0.03**	0.55	1.00

§ The average of the normalized gene counts and standard deviations (SD) for each gene are provided for the control samples and the gene expression groups (Group 1/LYMPH and Group 2/MYELO).

‡ Log(2) fold changes between LYMPH vs. MYELO group are highlighted blue for decreased fold change and red for increased fold change.

† Gene list is arranged by increased FDR adjusted p values. Nine genes were considered differentially expressed (FDR<0.05) and are bolded.

Supplemental Table 13: Average normalized gene counts post-flow cytometry classification.

Gene symbol/Alternative ID (if applicable)	Controls and Flow cytometry defined acute leukemia subtypes §									
	Control (n=2)		Lymphoid (n=15)		Myeloid (n=15)		Unclassified (n=13)		Mixed Phenotype (n=2)	
B cell Associated Genes	Average	SD	Average	SD	Average	SD	Average	SD	Average	SD
CD19	201.0	46.1	131.0	88.0	118.6	128.4	97.2	69.8	57.9	37.9
CD22	379.1	45.5	407.1	358.9	561.8	421.6	302.2	256.2	802.0	665.1
CD79A	1560.9	269.3	11422.4	4966.2	6193.7	4733.2	10846.7	5851.3	8661.2	1962.3
CR2/CD21	71.5	9.3	57.1	64.5	56.4	45.7	30.8	15.7	27.2	7.2
IGHG/IgG	4151.9	2212.1	1250.2	1232.7	755.9	1300.5	542.9	393.7	1020.0	924.5
IGHM/IgM	8098.6	5661.5	8670.9	6021.9	4572.8	6535.2	7415.7	6461.6	1806.8	1350.8
MS4A1/CD20	159.9	28.2	127.1	167.3	120.5	63.9	133.3	215.9	94.0	14.7
PAX5	85.2	14.6	50.1	63.0	45.6	35.1	31.0	13.4	27.0	1.4
Myeloid Associated Genes										
ANPEP/CD13	3926.2	898.1	39.4	63.6	888.8	2224.5	37.3	32.0	323.8	303.8
CD14	54.1	16.2	42.6	51.2	30.8	20.0	20.6	2.2	31.2	11.2
CD33	1500.0	379.9	80.4	96.5	153.5	159.9	66.7	68.1	98.4	78.4
IL3RA/CD123	47.5	18.0	33.6	31.7	66.9	131.3	25.6	16.7	40.9	20.9
ITGAM/CD11b	12480.5	2574.1	294.5	257.5	1495.1	1452.4	205.0	177.5	1603.9	531.4
ITGAX/CD11c	1509.3	139.7	113.6	102.6	1524.7	1817.9	82.2	69.9	1969.2	1050.0
ITGB2/CD18	3497.8	291.1	1313.5	596.8	2044.7	1239.4	1029.6	309.9	3241.3	1397.0
LYZ/Lysozyme	270960.0	59718.4	4319.5	6620.2	53812.6	104081.5	3963.1	4621.2	25924.9	23534.7
MPL	633.0	221.5	86.3	62.0	147.7	134.5	68.5	40.8	92.1	6.0
MPO/Myeloperoxidase	75.6	11.9	408.5	336.8	1580.2	1671.8	1269.9	2873.6	518.2	383.0

NPM1	9811.1	131.2	32917.7	11429.3	35238.8	8925.9	29938.4	11082.8	20502.1	4725.9
PROM1/CD133	82.4	21.2	24.4	9.6	25.3	12.9	23.6	8.3	21.1	1.1
T Cell Associated Genes										
CD2	1257.4	759.3	8638.3	6634.6	4397.9	5755.8	7924.2	7642.2	11527.7	872.4
CD3E	2048.0	907.5	3951.1	5040.1	462.2	468.5	1499.8	4621.7	2120.4	1997.5
CD5	710.4	345.4	592.8	548.2	178.5	167.5	117.4	72.1	1159.2	654.4
CD7	74.1	16.2	94.9	63.8	49.9	27.5	63.6	79.2	115.1	24.6
LYL1	20.0	0.0	20.4	1.6	21.3	3.5	20.6	1.9	22.4	2.4
TRBC/TCR beta	4716.2	2059.8	6480.1	4449.2	8573.3	8010.4	11580.9	11913.5	2708.8	801.7
TRGC2/TCR gamma	208.3	20.8	137.4	199.6	90.9	108.9	51.6	84.8	35.6	9.4
TRGC3/TCR gamma	50.0	11.1	59.1	28.1	63.9	36.2	47.7	16.0	47.3	3.9
TRGC8/TCR gamma	48.0	0.5	12489.7	17827.2	3267.5	6127.8	2209.9	6064.4	82.5	62.5
Hematopoietic Associated Genes										
CD34	95.6	25.1	9332.2	3900.5	4520.1	2372.2	7797.0	2702.6	6451.5	112.8
CIITA	453.4	32.4	186.2	95.6	117.2	62.7	116.0	90.9	150.7	87.1
DLA-DQA1/MHC Class II	22854.1	2349.0	1599.7	1452.1	1084.6	941.1	1178.7	1760.9	978.3	588.7
DLA-DRA/MHC Class II	59224.8	6326.4	2675.9	2129.4	2412.6	1953.9	2324.3	3356.5	2205.1	1484.9
DNTT/TdT	34.7	5.2	8238.7	6465.1	2224.0	2198.4	8215.0	6323.7	2076.4	1878.4
GATA3	116.7	35.0	1157.9	394.2	654.6	438.5	1057.3	793.7	905.8	252.9
HLA-DRB1/MHC Class II	14059.9	3040.9	1553.1	1425.2	1106.8	1418.0	927.3	1208.8	936.2	724.5
IRF4/MUM1	371.4	6.9	126.0	40.9	247.6	254.0	88.2	28.1	82.1	2.8
KIT/CD117	56.9	17.9	7388.0	4079.2	8965.1	6016.0	16072.2	8054.7	17579.9	7570.1
Differentially expressed genes found in human AL										
CFD/Adipsin	5773.7	1554.9	74.9	45.6	814.0	1003.6	91.2	78.2	299.6	245.7
LGALS3/Lectin	11801.7	1845.1	251.0	213.9	4389.3	4364.4	462.0	903.0	4952.9	4558.0
MCL1	59232.4	2899.1	6835.4	2703.0	7910.0	2727.7	5730.5	2375.3	5119.5	1739.0

SQSTM1/P62	5671.8	1088.5	2282.1	954.0	3073.4	1010.8	2240.6	1203.9	3206.4	817.6
ZYX/Zyxin	25552.1	8087.9	5292.4	2132.6	6136.8	1726.1	4456.2	1584.0	6662.7	72.9

§ The average normalized gene counts and standard deviations (SD) are provided between each subtype of acute leukemia. These subtypes were determined after the flow cytometry classification scheme was generated.

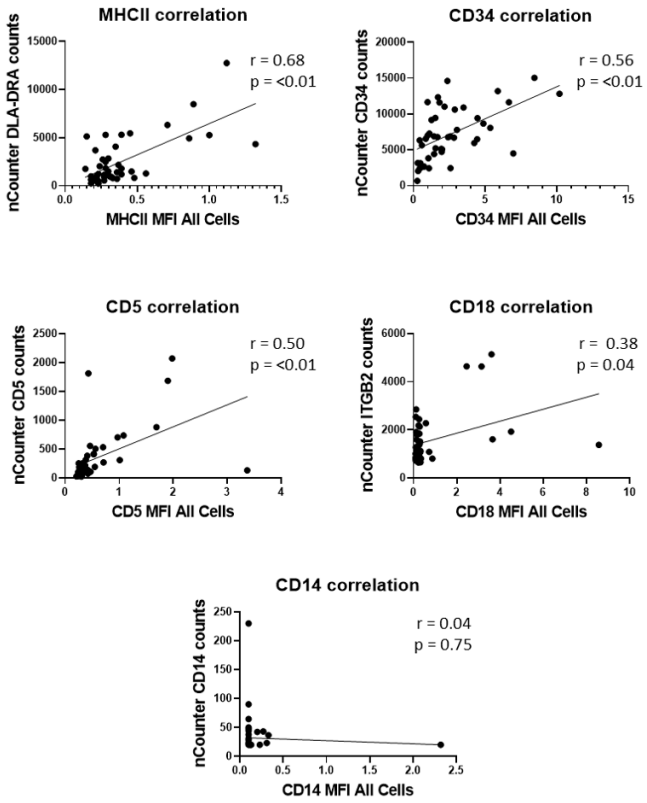

Supplemental Figure 6: Correlation between gene and protein expression. The correlation between median fluorescence intensity (MFI) measured by flow cytometry (x axis) and nCounter normalized gene counts (y axis) is shown. Pearson's correlation was used to calculate correlation and significance. r = correlation coefficient; p = p value

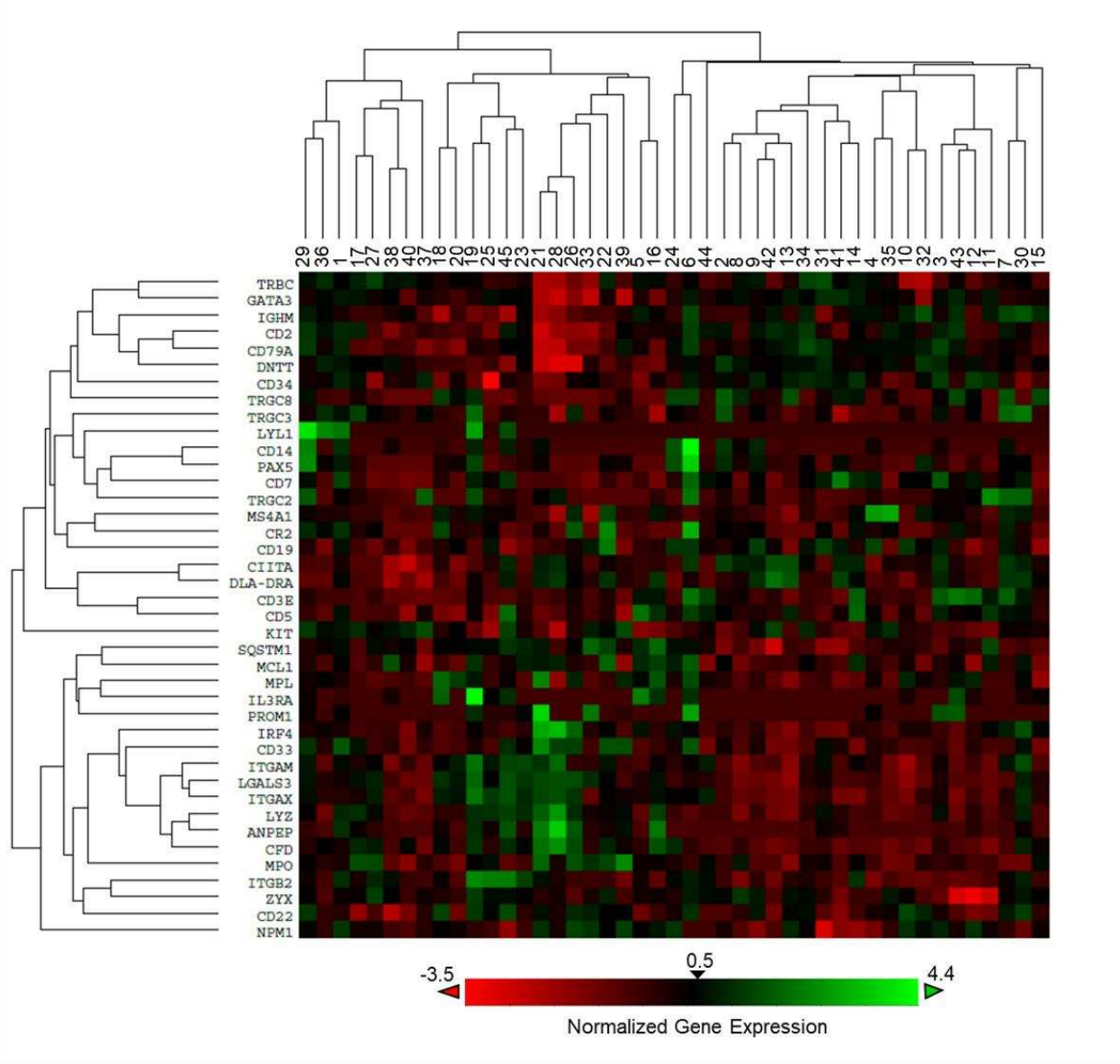

Supplemental Figure 7: Hierarchical clustering of all genes and cases: Unsupervised hierarchical clustering identified two major groups within the cases and two major gene clusters. In general, myeloid associated genes clustered together and lymphoid associated genes clustered together. Differential gene expression was used to identify significantly expressed genes.

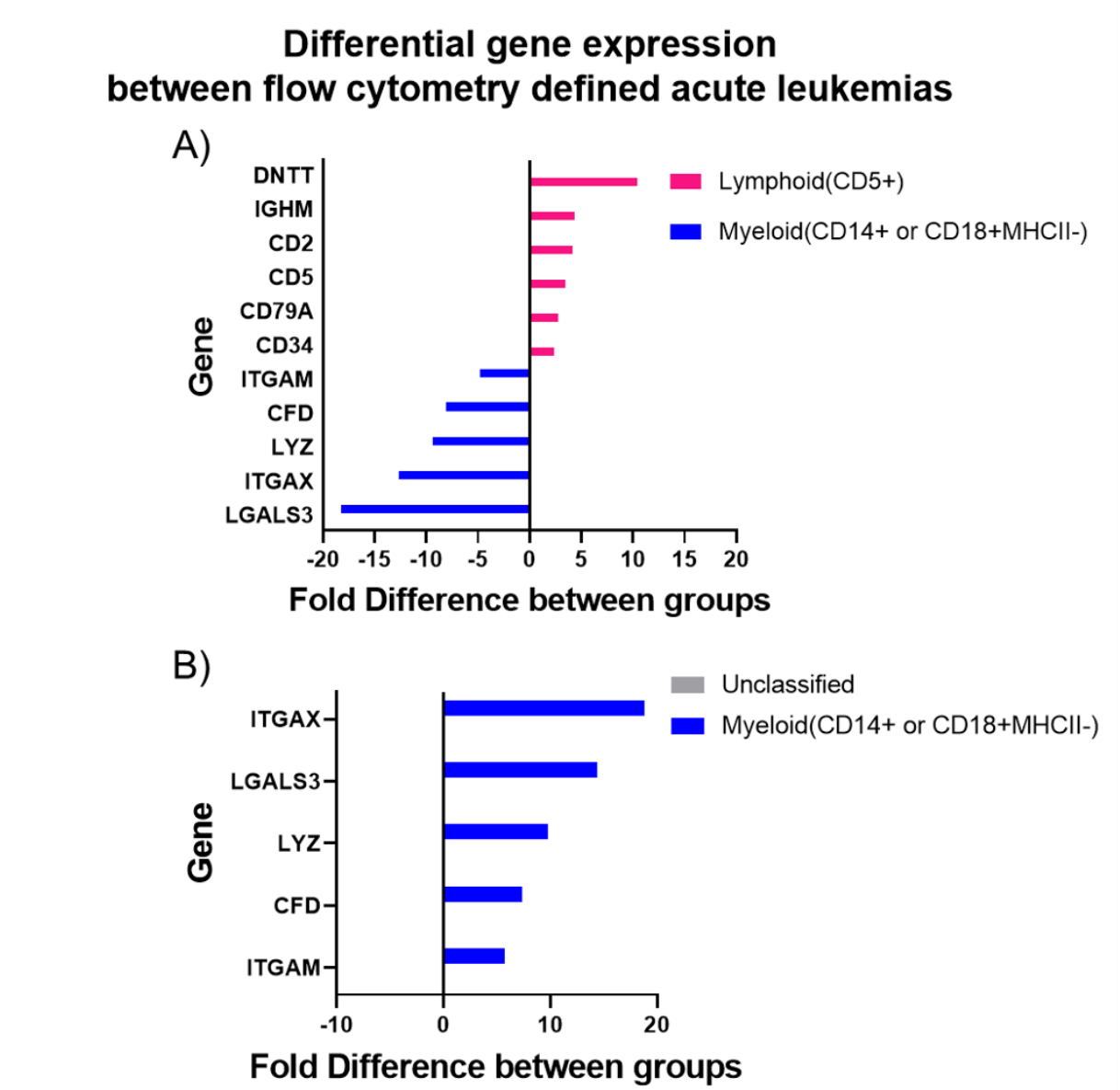

Supplemental Figure 8: Differential gene expression between flow cytometry defined acute leukemia subtypes: Acute leukemia cases were classified by flow cytometry using the newly developed flow cytometry diagnostic criteria. We then assessed differences in gene expression between flow cytometry defined acute leukemia subtypes and identified differentially expressed genes (FDR<0.05). A) Suspected lymphoid lineage acute leukemias (CD5+ neoplasms) overexpressed lymphoid associated genes and suspected myeloid lineage acute leukemias (CD14+MHCII- or CD18+MHCII-CD4- neoplasms) overexpressed myeloid associated genes, when compared to one another. B) The suspected myeloid neoplasms also overexpressed myeloid associated genes compared to unclassifiable acute leukemias. The only gene differentially expressed between suspected lymphoid acute leukemias and unclassified acute leukemias was CD5 (not shown).

SUPPLEMENTARY MATERIAL FOR CHAPTER 3

Sequencing quality control and overall coverage:

Transcriptomes of the AL cases and normal controls were sequenced to an average of 177 million reads per sample (range: 153 – 302 million). On average, 55.3 million paired end reads were assigned to the genome (Supplemental Figure 1A-1B). 65.3% mapped to protein coding regions, followed by long non-coding RNA (22.9%), small nuclear RNAs (5.6%), and various RNA molecules (cumulative percentage of other types: 6.3%, data not shown). The distribution of log-normalized and variance stabilizing transformed count data between and across samples appeared appropriate (Supplemental Figure 1C). The percentage of "protein_coding" biotypes were considered statistically different (p value < 0.05) between all groups (AL, control peripheral blood cases (BLCNTRL), and control bone marrow cases (BMCNTRL). Of the 30,951 annotated genes, 13,490 had a count per million >1 and were kept for downstream DGE analysis.

Supplemental Table 14: ROC analysis results of markers (i.e. genes) for each cAML subgroup

gene	myAUC	avg_diff	power	avg_log2FC	pct.1	pct.2	Group ID
ADGRG1	0.907	0.99291	0.814	1.432466936	1	1	0
ELK4	0.894	0.956934	0.788	1.380563418	1	1	0
RFTN1	0.893	0.778626	0.786	1.123319459	1	1	0
DDC	0.89	0.838375	0.78	1.2095193	1	1	0
SEMA4A	0.88	0.726509	0.76	1.048130631	1	1	0
CA2	0.865	0.828136	0.73	1.194747863	1	1	0
ITGA4	0.848	0.813225	0.696	1.173235305	1	1	0
CACNA1H	0.839	1.074279	0.678	1.549856924	1	1	0
CAPN2	0.163	-0.82324	0.674	-1.187681093	1	1	0
FCER1A	0.79	1.049943	0.58	1.514747341	1	0.971	0
TFPI	0.789	0.721349	0.578	1.040686109	1	0.943	0
NOTCH1	0.214	-0.85441	0.572	-1.232659883	1	1	0
ALOX15	0.785	0.912407	0.57	1.316325497	1	1	0
MMRN1	0.769	0.897063	0.538	1.294188664	1	0.971	0
WFS1	0.233	-0.73933	0.534	-1.066631087	1	1	0
FTL	0.248	-0.73135	0.504	-1.055108667	1	1	0
CPXM2	0.253	-0.84216	0.494	-1.214983944	1	1	0
APP	0.257	-0.81165	0.486	-1.170967663	1	1	0
ANPEP	0.268	-0.83292	0.464	-1.201656171	1	1	0
LRP1	0.269	-1.11361	0.462	-1.606603366	1	1	0
FN1	0.287	-1.58359	0.426	-2.284642565	1	1	0
RETN	0.287	-1.08055	0.426	-1.558902005	1	1	0
LMNA	0.291	-0.73596	0.418	-1.061765207	1	1	0
PHOX2A	0.295	-0.94166	0.41	-1.358532291	1	1	0

NFKBIA	0.297	-0.78408	0.406	-1.13118255	1	1	0
PLBD1	0.915	1.710542	0.83	2.467790307	1	1	1
FN1	0.852	1.571827	0.704	2.267667697	1	1	1
LYZ	0.863	1.550485	0.726	2.236876736	1	1	1
CRYM	0.76	1.540989	0.52	2.223177463	0.895	0.892	1
LRP1	0.909	1.51673	0.818	2.188179418	1	1	1
RETN	0.917	1.462512	0.834	2.109959476	1	1	1
PHOX2A	0.747	1.346103	0.494	1.942015745	1	1	1
ANPEP	0.922	1.261536	0.844	1.820011718	1	1	1
CSF1R	0.946	1.238411	0.892	1.786648689	1	1	1
SERPINB10	0.952	1.174476	0.904	1.694411326	1	1	1
CPXM2	0.831	1.172593	0.662	1.691694607	1	1	1
VCAN	0.855	1.172389	0.71	1.691400351	1	1	1
APP	0.881	1.171158	0.762	1.689624332	1	1	1
AP1S2	0.964	1.152158	0.928	1.662212581	1	1	1
IRF5	0.983	1.136761	0.966	1.639999559	1	1	1
TGFBI	0.871	1.110141	0.742	1.601594548	1	1	1
NLRP1	0.908	1.095436	0.816	1.580380619	1	1	1
SLC1A4	0.881	1.078819	0.762	1.556407199	1	1	1
BPI	0.873	1.036929	0.746	1.495971633	1	1	1
ANXA2	0.949	1.026479	0.898	1.480896703	1	1	1
CYBB	0.902	1.024562	0.804	1.478130868	1	1	1
CTSZ	0.932	1.021698	0.864	1.473999147	1	1	1
CAPN2	0.935	1.02154	0.87	1.473771048	1	1	1
LMNA	0.865	0.975626	0.73	1.407531347	1	1	1
PRSS57	0.9	0.947035	0.8	1.366282481	1	1	1
UNC93B1	1	0.940131	1	1.356322542	1	1	1

S100A5	0.888	0.925029	0.776	1.33453527	1	1	1
ANXA1	0.878	0.922204	0.756	1.330459807	1	1	1
ARHGAP45	0.869	0.922132	0.738	1.330354607	1	1	1
PSAP	0.844	0.883739	0.688	1.274966533	1	1	1
CTSS	0.878	0.864048	0.756	1.24655788	1	1	1
MAFB	0.882	0.858469	0.764	1.238509556	1	1	1
RHOB	0.825	0.85644	0.65	1.235582048	1	1	1
WFS1	0.872	0.84743	0.744	1.222582922	1	1	1
SMCHD1	0.853	0.845757	0.706	1.220168995	1	1	1
MPEG1	0.819	0.838353	0.638	1.209488059	1	1	1
CTTNBP2	0.812	0.83485	0.624	1.204434624	1	0.946	1
CAPG	0.917	0.832522	0.834	1.201074873	1	1	1
ABCA5	0.916	0.832508	0.832	1.201055521	1	1	1
VIM	0.93	0.829443	0.86	1.196633242	1	1	1
YBX3	0.925	0.829291	0.85	1.196413458	1	1	1
LRRK2	0.845	0.787023	0.69	1.135434597	1	1	1
ALDH3B1	0.909	0.776342	0.818	1.120024746	1	1	1
DPYD	0.811	0.77181	0.622	1.113486943	1	1	1
SULF2	0.755	0.757781	0.51	1.093246466	1	1	1
F5	0.949	0.757293	0.898	1.092542199	1	1	1
HGF	0.991	0.75449	0.982	1.088498714	1	1	1
PYCARD	0.963	0.751518	0.926	1.084211725	1	1	1
CARD9	0.881	0.751265	0.762	1.083846751	1	1	1
TNFRSF1B	0.851	0.748764	0.702	1.080237844	1	1	1
CRIP1	0.9	0.745417	0.8	1.075409389	1	1	1
MATK	0.871	0.741967	0.742	1.070432091	1	1	1
AHNAK	0.828	0.727715	0.656	1.049871339	1	1	1

PLEC	0.804	0.724843	0.608	1.045728054	1	1	1
SH2B2	0.962	0.719963	0.924	1.038687242	1	1	1
STING1	0.963	0.71757	0.926	1.035234715	1	1	1
IFI30	0.93	0.707734	0.86	1.021043929	1	1	1
FGL2	0.844	0.706444	0.688	1.019183495	1	1	1
PGD	0.892	0.702554	0.784	1.013571707	1	1	1
GATA2	0.209	-0.69603	0.582	-1.004163151	1	1	1
GPM6B	0.044	-0.70135	0.912	-1.011837086	1	1	1
LIMD1	0.041	-0.72333	0.918	-1.043551618	1	1	1
ALOX15	0.27	-0.74251	0.46	-1.071219736	1	1	1
MMRN1	0.175	-0.74998	0.65	-1.081989901	1	0.973	1
GPRASP2	0.048	-0.75385	0.904	-1.087577494	1	1	1
RBM39	0.074	-0.75543	0.852	-1.08985946	1	1	1
FCER1A	0.3	-0.75681	0.4	-1.091839058	0.947	1	1
TESPA1	0.085	-0.76405	0.83	-1.102295869	1	1	1
RFTN1	0.098	-0.77391	0.804	-1.116509107	1	1	1
EDEM1	0.067	-0.78701	0.866	-1.135416947	1	1	1
ITGA2B	0.232	-0.78725	0.536	-1.135756349	1	1	1
PIK3C2B	0.101	-0.78968	0.798	-1.139269588	1	1	1
PTPRF	0.023	-0.81283	0.954	-1.172666317	0.947	1	1
CD82	0.065	-0.81624	0.87	-1.177581354	1	1	1
RBPMS	0.006	-0.81807	0.988	-1.180230568	1	1	1
SEMA7A	0.031	-0.82606	0.938	-1.191752092	1	1	1
TRAF3IP2	0.017	-0.83169	0.966	-1.199871793	1	1	1
YTHDF1	0.023	-0.84124	0.954	-1.213646241	1	1	1
ATP2A3	0.05	-0.85373	0.9	-1.231671939	1	1	1
ELK4	0.068	-0.87706	0.864	-1.265331325	1	1	1

PLCG1	0.028	-0.89107	0.944	-1.285536451	1	1	1
CTSE	0.095	-0.89625	0.81	-1.293012886	1	1	1
ADGRG1	0.097	-0.93471	0.806	-1.348499768	1	1	1
CRYBG1	0.098	-0.94147	0.804	-1.358251559	1	1	1
CA2	0.034	-1.02884	0.932	-1.484307392	1	1	1
TFPI	0.023	-1.2358	0.954	-1.782886623	0.895	1	1
CACNA1H	0.09	-1.54463	0.82	-2.228427561	1	1	1
NOTCH1	0.803	1.147771	0.606	1.65588338	1	1	2
RBM39	0.998	1.115234	0.996	1.608943019	1	1	2
SREBF1	0.969	1.047844	0.938	1.511719108	1	1	2
RELB	0.989	0.970823	0.978	1.400601814	1	1	2
JMJD1C	0.992	0.963183	0.984	1.389578714	1	1	2
PER1	0.916	0.962744	0.832	1.388945724	1	1	2
EIF1	0.994	0.931259	0.988	1.343522446	1	1	2
ABCA1	0.953	0.895378	0.906	1.291757006	1	1	2
CSRNP1	0.998	0.877225	0.996	1.26556832	1	1	2
RSRC2	0.998	0.84141	0.996	1.213897443	1	1	2
TRA2B	0.95	0.839718	0.9	1.211457707	1	1	2
NFKB2	0.964	0.835127	0.928	1.204834265	1	1	2
CCNL1	0.959	0.818898	0.918	1.181420452	1	1	2
GPRASP2	0.817	0.818627	0.634	1.181028755	1	1	2
SFPQ	0.964	0.818188	0.928	1.180395089	1	1	2
SYTL3	0.852	0.813515	0.704	1.173653932	1	1	2
AKAP12	0.833	0.800722	0.666	1.155197557	1	1	2
PTPRE	0.908	0.794124	0.816	1.145678656	1	1	2
CNOT1	0.969	0.787048	0.938	1.135470183	1	1	2
YTHDF1	0.953	0.784055	0.906	1.131152559	1	1	2

GOLGB1	0.947	0.769134	0.894	1.109626184	1	1	2
ZBTB11	0.967	0.752511	0.934	1.085644416	1	1	2
BHLHE40	0.822	0.751013	0.644	1.083482943	1	1	2
ATG2A	0.853	0.746914	0.706	1.077568501	1	1	2
SLC3A2	0.989	0.739901	0.978	1.067451474	1	1	2
USP7	0.988	0.73447	0.976	1.059615856	1	1	2
ETF1	0.959	0.729815	0.918	1.052900266	1	1	2
YTHDF3	0.963	0.729803	0.926	1.052883741	1	1	2
PTP4A1	0.903	0.728962	0.806	1.051670545	1	1	2
BAZ2A	0.95	0.716971	0.9	1.034369886	1	1	2
ATF4	0.955	0.715341	0.91	1.032018857	1	1	2
SH3GL1	0.986	0.712626	0.972	1.028102186	1	1	2
ANKRD11	0.928	0.711979	0.856	1.027168772	1	1	2
PSME4	0.987	0.709587	0.974	1.02371753	1	1	2
CHD1	0.984	0.70914	0.968	1.023072477	1	1	2
THAP5	0.937	0.707768	0.874	1.021092767	1	1	2
SETD2	1	0.706215	1	1.01885296	1	1	2
GLUL	0.072	-0.703	0.856	-1.014210597	1	1	2
SAMD9L	0.148	-0.70901	0.704	-1.022880809	1	1	2
MYC	0.006	-0.70927	0.988	-1.023261715	1	1	2
NCKAP1L	0.006	-0.71214	0.988	-1.027394428	1	1	2
FCER2	0.22	-0.71862	0.56	-1.03674663	1	1	2
ENO1	0.072	-0.72059	0.856	-1.039596909	1	1	2
PADI3	0.275	-0.72284	0.45	-1.042833176	1	1	2
PRDX1	0.031	-0.72379	0.938	-1.044210071	1	1	2
MTHFD1	0.005	-0.72652	0.99	-1.048143467	1	1	2
ALPL	0.283	-0.7337	0.434	-1.058503846	1	1	2

RHOB	0.239	-0.73481	0.522	-1.060101617	1	1	2
TLN1	0.062	-0.73605	0.876	-1.061900293	1	1	2
TIMP2	0.038	-0.73824	0.924	-1.065049649	1	1	2
FGL2	0.052	-0.74032	0.896	-1.068054969	1	1	2
HSPA8	0.078	-0.74357	0.844	-1.072748407	1	1	2
TWF2	0.031	-0.74848	0.938	-1.079821232	1	1	2
SRGN	0.15	-0.75195	0.7	-1.084828025	1	1	2
S100A5	0.209	-0.75236	0.582	-1.085422427	1	1	2
MYO1F	0.1	-0.7624	0.8	-1.099909527	1	1	2
AP1S2	0.192	-0.76811	0.616	-1.108148901	1	1	2
SELL	0.198	-0.76992	0.604	-1.110765232	1	1	2
SLC1A4	0.175	-0.77988	0.65	-1.125133091	1	1	2
UNC93B1	0.072	-0.78284	0.856	-1.129396318	1	1	2
CAPG	0.141	-0.78878	0.718	-1.137974436	1	1	2
AHNAK	0.134	-0.80036	0.732	-1.154674936	1	1	2
PARP1	0.063	-0.84163	0.874	-1.214217941	1	1	2
F13A1	0.248	-0.8567	0.504	-1.235949874	1	1	2
RGS2	0.114	-0.86365	0.772	-1.245985365	1	1	2
SMCHD1	0.106	-0.88496	0.788	-1.276727125	1	1	2
RETN	0.286	-0.88508	0.428	-1.276904265	1	1	2
VCAN	0.219	-0.8916	0.562	-1.28630027	1	1	2
NLRP1	0.197	-0.89219	0.606	-1.287154355	1	1	2
CYBB	0.122	-0.89462	0.756	-1.290659547	1	1	2
IRF5	0.138	-0.90502	0.724	-1.305661356	1	1	2
MPEG1	0.116	-0.92276	0.768	-1.331265487	1	1	2
S100A12	0.269	-0.93126	0.462	-1.343529498	1	1	2
FLNA	0.084	-0.93602	0.832	-1.350387356	1	1	2

CARD9	0.091	-0.96454	0.818	-1.391534053	1	1	2
TGFBI	0.236	-0.96603	0.528	-1.393682375	1	1	2
CSF1R	0.159	-0.99034	0.682	-1.428751615	1	1	2
SERPINB10	0.091	-1.00732	0.818	-1.453252429	1	1	2
ANXA2	0.091	-1.03636	0.818	-1.495147445	1	1	2
NFE2	0.006	-1.08825	0.988	-1.570010785	1	1	2
PLBD1	0.197	-1.37682	0.606	-1.986338144	1	1	2
LYZ	0.208	-1.57699	0.584	-2.275117339	1	1	2

Supplemental Table 15: Differential gene set expression analysis between cAML group 0 vs. bone marrow

MSigDB Hallmark Pathway	logFC	AveExpr	t	P.Value	adj.P.Val	B
HALLMARK_BILE_ACID_METABOLISM	0.35044	-0.20008	4.911893	6.77E-06	0.000338	3.562861973
HALLMARK_PEROXISOME	0.271276	-0.21712	3.950008	0.000201	0.003975	0.353205307
HALLMARK_REACTIVE_OXYGEN_SPECIES_PATHWAY	-0.61685	-0.16233	-3.89797	0.000238	0.003975	0.190569366
HALLMARK_GLYCOLYSIS	-0.26207	-0.18243	-3.54906	0.000739	0.009233	-0.86503682
HALLMARK_HYPOXIA	-0.45044	-0.19245	-3.31167	0.001541	0.015413	-1.545885007
HALLMARK_ALLOGRAFT_REJECTION	-0.46669	-0.16034	-3.19268	0.002204	0.01557	-1.874815972
HALLMARK_COMPLEMENT	-0.47678	-0.16744	-3.1612	0.00242	0.01557	-1.9604141
HALLMARK_EPITHELIAL_MESENCHYMAL_TRANSITION	-0.43254	-0.15532	-3.0944	0.002944	0.01557	-2.139993048
HALLMARK_PROTEIN_SECRETION	-0.35724	-0.23263	-3.0924	0.002962	0.01557	-2.145349014
HALLMARK_ESTROGEN_RESPONSE_EARLY	0.275349	-0.21332	3.075168	0.003114	0.01557	-2.191191213
HALLMARK_MYC_TARGETS_V1	0.532117	-0.23076	2.940081	0.004589	0.020858	-2.544073865

HALLMARK_P53_PATHWAY	-0.28073	-0.18616	-2.84105	0.006056	0.025234	-2.795169673
HALLMARK_TNFA_SIGNALING_VIA_NFKB	-0.50952	-0.18647	-2.69254	0.009081	0.034927	-3.159242745
HALLMARK_KRAS_SIGNALING_DN	0.251791	-0.21346	2.624766	0.010876	0.037893	-3.320290408
HALLMARK_INFLAMMATORY_RESPONSE	-0.46374	-0.17119	-2.60799	0.011368	0.037893	-3.359643532
HALLMARK_APOPTOSIS	-0.29108	-0.19461	-2.54178	0.013511	0.042223	-3.512999804
HALLMARK_HEDGEHOG_SIGNALING	0.293479	-0.25277	2.396943	0.019523	0.055207	-3.837216589
HALLMARK_MYC_TARGETS_V2	0.492069	-0.12032	2.389771	0.019875	0.055207	-3.852864459
HALLMARK_PI3K_AKT_MTOR_SIGNALING	-0.20683	-0.22837	-2.25112	0.027889	0.073392	-4.147648882
HALLMARK_SPERMATOGENESIS	0.204409	-0.22459	2.228333	0.029449	0.073624	-4.194665307
HALLMARK_WNT_BETA_CATENIN_SIGNALING	0.206623	-0.23305	1.887901	0.063664	0.151581	-4.84762781
HALLMARK_PANCREAS_BETA_CELLS	-0.28857	-0.14924	-1.82695	0.072464	0.16469	-4.954458371
HALLMARK_FATTY_ACID_METABOLISM	0.13852	-0.19571	1.525314	0.132205	0.287193	-5.436117887

HALLMARK_IL2_STAT5_SIGNALING	-0.17341	-0.17911	-1.50301	0.137852	0.287193	-5.468565491
HALLMARK_COAGULATION	-0.22844	-0.18943	-1.47055	0.146408	0.292816	-5.514984162
HALLMARK_IL6_JAK_STAT3_SIGNALING	-0.24222	-0.18341	-1.42131	0.160175	0.30803	-5.583600797
HALLMARK_INTERFERON_GAMMA_RESPONSE	-0.23877	-0.19985	-1.32972	0.188425	0.348934	-5.705408912
HALLMARK_NOTCH_SIGNALING	0.139265	-0.30874	1.274025	0.207352	0.360535	-5.775723228
HALLMARK_UV_RESPONSE_DN	0.11763	-0.2056	1.269048	0.20911	0.360535	-5.781867587
HALLMARK_MTORC1_SIGNALING	-0.1507	-0.18728	-1.18404	0.240861	0.401436	-5.883286895
HALLMARK_APICAL_SURFACE	-0.13708	-0.10486	-0.99726	0.322469	0.520112	-6.082421021
HALLMARK_G2M_CHECKPOINT	-0.18325	-0.22054	-0.96003	0.340724	0.532381	-6.118169215
HALLMARK_E2F_TARGETS	-0.19696	-0.20977	-0.90993	0.366341	0.555062	-6.164195837
HALLMARK_OXIDATIVE_PHOSPHORYLATION	0.125064	-0.23442	0.841804	0.403094	0.592786	-6.222924708
HALLMARK_CHOLESTEROL_HOMEOSTASIS	0.085929	-0.21282	0.65576	0.514376	0.734822	-6.360475058

HALLMARK_ADIPOGENESIS	0.051089	-0.25165	0.607679	0.545593	0.757768	-6.390547778
HALLMARK_INTERFERON_ALPHA_RESPONSE	0.120563	-0.2059	0.52893	0.59872	0.809081	-6.434911754
HALLMARK_XENOBIOTIC_METABOLISM	0.047085	-0.23077	0.499764	0.618989	0.814459	-6.44979695
HALLMARK_TGF_BETA_SIGNALING	0.056462	-0.19917	0.436504	0.663969	0.851242	-6.479202981
HALLMARK_MYOGENESIS	-0.0405	-0.24127	-0.37785	0.706819	0.8514	-6.50293918
HALLMARK_ANDROGEN_RESPONSE	0.03861	-0.19103	0.364026	0.717062	0.8514	-6.508036965
HALLMARK_ESTROGEN_RESPONSE_LATE	0.026794	-0.22098	0.351341	0.726509	0.8514	-6.512548862
HALLMARK_KRAS_SIGNALING_UP	0.036829	-0.19727	0.343722	0.732204	0.8514	-6.515182343
HALLMARK_UV_RESPONSE_UP	0.018257	-0.26152	0.244859	0.807364	0.917459	-6.544133876
HALLMARK_MITOTIC_SPINDLE	-0.01747	-0.23514	-0.15898	0.874198	0.962416	-6.561402807
HALLMARK_DNA_REPAIR	0.015132	-0.18274	0.127718	0.898781	0.962416	-6.565866617
HALLMARK_HEME_METABOLISM	-0.015	-0.14588	-0.12025	0.904671	0.962416	-6.566789 28

HALLMARK_UNFOLDED_PROTEIN_RESPONSE	-0.01147	-0.19599	-0.09551	0.924217	0.962726	-6.569448569
HALLMARK_APICAL_JUNCTION	0.003425	-0.20733	0.033733	0.973197	0.993058	-6.573426139
HALLMARK_ANGIOGENESIS	-0.00055	-0.17685	-0.00349	0.997225	0.997225	-6.57398704

Supplemental Table 16: Differential gene set expression analysis between cAML group 1 vs. bone marrow

MSigDB Hallmark Pathway	logFC	AveExpr	t	P.Value	adj.P.Val	B
HALLMARK_PEROXISOME	0.343877	-0.21712	4.992396	5.03E-06	0.000251	3.837715748
HALLMARK_MYC_TARGETS_V1	0.85075	-0.23076	4.68677	1.54E-05	0.000385	2.771201106
HALLMARK_BILE_ACID_METABOLISM	0.31021	-0.20008	4.335218	5.37E-05	0.000895	1.584475727
HALLMARK_MYC_TARGETS_V2	0.785236	-0.12032	3.802332	0.000327	0.004087	-0.116852863
HALLMARK_ESTROGEN_RESPONSE_EARLY	0.331847	-0.21332	3.695243	0.000463	0.004632	-0.442567023
HALLMARK_EPITHELIAL_MESENCHYMAL_TRANSITION	-0.49733	-0.15532	-3.54745	0.000742	0.006187	-0.882299258
HALLMARK_HYPOXIA	-0.46383	-0.19245	-3.40011	0.001176	0.008399	-1.308812319
HALLMARK_ALLOGRAFT_REJECTION	-0.39241	-0.16034	-2.67663	0.009476	0.051738	-3.211565221
HALLMARK_FATTY_ACID_METABOLISM	0.240062	-0.19571	2.635668	0.010567	0.051738	-3.308883314
HALLMARK_OXIDATIVE_PHOSPHORYLATION	0.388618	-0.23442	2.608078	0.011365	0.051738	-3.373761774
HALLMARK_REACTIVE_OXYGEN_SPECIES_PATHWAY	-0.41385	-0.16233	-2.60751	0.011382	0.051738	-3.375100485

HALLMARK_TNFA_SIGNALING_VIA_NFKB	-0.44562	-0.18647	-2.34794	0.022043	0.081792	-3.958069981
HALLMARK_COMPLEMENT	-0.35399	-0.16744	-2.34011	0.022472	0.081792	-3.974884261
HALLMARK_INFLAMMATORY_RESPONSE	-0.41596	-0.17119	-2.33238	0.022902	0.081792	-3.991409801
HALLMARK_APICAL_SURFACE	-0.3107	-0.10486	-2.2537	0.027717	0.09239	-4.157156594
HALLMARK_PROTEIN_SECRETION	-0.25452	-0.23263	-2.19677	0.031738	0.093017	-4.274064874
HALLMARK_APOPTOSIS	-0.25184	-0.19461	-2.19267	0.032047	0.093017	-4.282396178
HALLMARK_P53_PATHWAY	-0.21545	-0.18616	-2.17398	0.033486	0.093017	-4.320152977
HALLMARK_GLYCOLYSIS	-0.15846	-0.18243	-2.13955	0.036287	0.095491	-4.388990092
HALLMARK_ADIPOGENESIS	0.178027	-0.25165	2.111288	0.038737	0.096841	-4.444796249
HALLMARK_NOTCH_SIGNALING	0.198126	-0.30874	1.807159	0.075531	0.179836	-5.003895025
HALLMARK_WNT_BETA_CATENIN_SIGNALING	0.195195	-0.23305	1.778234	0.080209	0.182294	-5.053035387
HALLMARK_XENOBIOTIC_METABOLISM	0.163505	-0.23077	1.730348	0.088483	0.192354	-5.13281462

HALLMARK_DNA_REPAIR	0.183156	-0.18274	1.541289	0.128274	0.267237	-5.428316065
HALLMARK_SPERMATOGENESIS	0.131227	-0.22459	1.426344	0.158725	0.302632	-5.592508859
HALLMARK_COAGULATION	-0.21973	-0.18943	-1.41033	0.163379	0.302632	-5.614439585
HALLMARK_UNFOLDED_PROTEIN_RESPONSE	0.169851	-0.19599	1.410188	0.163421	0.302632	-5.614635165
HALLMARK_PANCREAS_BETA_CELLS	-0.20818	-0.14924	-1.31409	0.1936	0.33996	-5.741343117
HALLMARK_IL6_JAK_STAT3_SIGNALING	-0.2228	-0.18341	-1.30347	0.197177	0.33996	-5.754826933
HALLMARK_IL2_STAT5_SIGNALING	-0.146	-0.17911	-1.26172	0.21172	0.352867	-5.806834895
HALLMARK_KRAS_SIGNALING_DN	0.117509	-0.21346	1.221358	0.226519	0.362329	-5.855577881
HALLMARK_INTERFERON_GAMMA_RESPONSE	-0.21741	-0.19985	-1.20719	0.23189	0.362329	-5.87233593
HALLMARK_CHOLESTEROL_HOMEOSTASIS	0.145197	-0.21282	1.104793	0.273467	0.414343	-5.987853286
HALLMARK_MYOGENESIS	-0.11325	-0.24127	-1.05338	0.296205	0.435595	-6.042145789
HALLMARK_HEDGEHOG_SIGNALING	0.118821	-0.25277	0.967596	0.33696	0.475674	-6.127172762

HALLMARK_PI3K_AKT_MTOR_SIGNALING	-0.08814	-0.22837	-0.95651	0.342485	0.475674	-6.137650965
HALLMARK_ANGIOGENESIS	0.133854	-0.17685	0.843768	0.402004	0.543248	-6.237526118
HALLMARK_ESTROGEN_RESPONSE_LATE	0.062639	-0.22098	0.818947	0.415916	0.547258	-6.257874629
HALLMARK_MITOTIC_SPINDLE	0.0877	-0.23514	0.795786	0.429156	0.5502	-6.276325339
HALLMARK_HEME_METABOLISM	-0.08411	-0.14588	-0.67244	0.503775	0.629718	-6.365831645
HALLMARK_UV_RESPONSE_DN	0.057886	-0.2056	0.622669	0.535758	0.653364	-6.397748881
HALLMARK_ANDROGEN_RESPONSE	0.060161	-0.19103	0.565543	0.573721	0.683001	-6.431397676
HALLMARK_INTERFERON_ALPHA_RESPONSE	0.08225	-0.2059	0.359783	0.720218	0.837462	-6.525979586
HALLMARK_APICAL_JUNCTION	0.019371	-0.20733	0.190224	0.849747	0.936559	-6.572413533
HALLMARK_E2F_TARGETS	0.038472	-0.20977	0.177213	0.859912	0.936559	-6.574795787
HALLMARK_KRAS_SIGNALING_UP	0.017233	-0.19727	0.160358	0.873114	0.936559	-6.577631341
HALLMARK_MTORC1_SIGNALING	0.0185	-0.18728	0.144918	0.88524	0.936559	-6.579980443

HALLMARK_TGF_BETA_SIGNALING	0.016517	-0.19917	0.127317	0.899097	0.936559	-6.582368691
HALLMARK_G2M_CHECKPOINT	-0.00299	-0.22054	-0.01564	0.987572	0.989011	-6.590327384
HALLMARK_UV_RESPONSE_UP	0.001034	-0.26152	0.013828	0.989011	0.989011	-6.590353 99

Supplemental Table 17: Differential gene set expression analysis between cAML group 2 vs. bone marrow

MSigDB Hallmark Pathway	logFC	AveExpr	t	P.Value	adj.P.Val	B
HALLMARK_GLYCOLYSIS	-0.35331	-0.18243	-4.74316	1.25E-05	0.000627	2.994748
HALLMARK_REACTIVE_OXYGEN_SPECIES_PATHWAY	-0.56299	-0.16233	-3.52681	0.000792	0.013513	-0.90346
HALLMARK_ESTROGEN_RESPONSE_EARLY	0.317889	-0.21332	3.519502	0.000811	0.013513	-0.92476
HALLMARK_TGF_BETA_SIGNALING	0.439852	-0.19917	3.371037	0.001286	0.015225	-1.35112
HALLMARK_HEDGEHOG_SIGNALING	0.40513	-0.25277	3.280168	0.001696	0.015225	-1.60585
HALLMARK_MYC_TARGETS_V1	0.594338	-0.23076	3.255413	0.001827	0.015225	-1.6744
HALLMARK_ALLOGRAFT_REJECTION	-0.45185	-0.16034	-3.06437	0.003213	0.022951	-2.19092
HALLMARK_EPITHELIAL_MESENCHYMAL_TRANSITION	-0.41497	-0.15532	-2.94298	0.004551	0.028445	-2.5072
HALLMARK_NOTCH_SIGNALING	0.292853	-0.30874	2.655868	0.010016	0.055643	-3.21622
HALLMARK_HYPOXIA	-0.32988	-0.19245	-2.40428	0.019168	0.095842	-3.78969
HALLMARK_COMPLEMENT	-0.35085	-0.16744	-2.30607	0.024422	0.109084	-4.00078

HALLMARK_BILE_ACID_METABOLISM	0.16273	-0.20008	2.261117	0.027228	0.109084	-4.09492
HALLMARK_PEROXISOME	0.155466	-0.21712	2.244098	0.028362	0.109084	-4.13016
HALLMARK_WNT_BETA_CATENIN_SIGNALING	0.234182	-0.23305	2.121164	0.037865	0.135231	-4.37793
HALLMARK_APICAL_SURFACE	-0.2825	-0.10486	-2.03738	0.045834	0.143741	-4.53988
HALLMARK_INFLAMMATORY_RESPONSE	-0.36516	-0.17119	-2.0358	0.045997	0.143741	-4.54288
HALLMARK_APOPTOSIS	-0.22549	-0.19461	-1.95202	0.055401	0.162943	-4.699
HALLMARK_UV_RESPONSE_DN	0.177457	-0.2056	1.897911	0.062309	0.173081	-4.79674
HALLMARK_SPERMATOGENESIS	0.170926	-0.22459	1.847183	0.069435	0.182725	-4.88616
HALLMARK_KRAS_SIGNALING_DN	0.172612	-0.21346	1.783782	0.079294	0.198234	-4.99487
HALLMARK_P53_PATHWAY	-0.17105	-0.18616	-1.71606	0.091084	0.216867	-5.1072
HALLMARK_PROTEIN_SECRETION	-0.16286	-0.23263	-1.39757	0.167164	0.379918	-5.58169
HALLMARK_INTERFERON_GAMMA_RESPONSE	-0.23987	-0.19985	-1.32428	0.190214	0.413496	-5.67804

HALLMARK_IL6_JAK_STAT3_SIGNALING	-0.21912	-0.18341	-1.2746	0.207148	0.413496	-5.74055
HALLMARK_TNFA_SIGNALING_VIA_NFKB	-0.23945	-0.18647	-1.25443	0.214336	0.413496	-5.76529
HALLMARK_COAGULATION	-0.19627	-0.18943	-1.25255	0.215018	0.413496	-5.76758
HALLMARK_IL2_STAT5_SIGNALING	-0.13801	-0.17911	-1.18584	0.240156	0.444733	-5.8466
HALLMARK_PANCREAS_BETA_CELLS	-0.18496	-0.14924	-1.16082	0.25011	0.446626	-5.87517
HALLMARK_E2F_TARGETS	-0.24703	-0.20977	-1.13136	0.262208	0.452082	-5.90807
HALLMARK_UNFOLDED_PROTEIN_RESPONSE	0.132731	-0.19599	1.09567	0.27741	0.46235	-5.94683
HALLMARK_UV_RESPONSE_UP	0.067302	-0.26152	0.894833	0.374295	0.603702	-6.14255
HALLMARK_MYC_TARGETS_V2	0.169068	-0.12032	0.813979	0.418735	0.654273	-6.21048
HALLMARK_ADIPOGENESIS	0.063809	-0.25165	0.752392	0.454628	0.688831	-6.25801
HALLMARK_PI3K_AKT_MTOR_SIGNALING	-0.06366	-0.22837	-0.68689	0.494679	0.709163	-6.30452
HALLMARK_MITOTIC_SPINDLE	0.073746	-0.23514	0.665326	0.50828	0.709163	-6.31892

HALLMARK_MTORC1_SIGNALING	-0.08269	-0.18728	-0.64405	0.521887	0.709163	-6.33268
HALLMARK_OXIDATIVE_PHOSPHORYLATION	0.095849	-0.23442	0.639569	0.524781	0.709163	-6.33553
HALLMARK_ANDROGEN_RESPONSE	0.060986	-0.19103	0.570014	0.570703	0.750925	-6.37714
HALLMARK_CHOLESTEROL_HOMEOSTASIS	0.071839	-0.21282	0.543483	0.588722	0.754772	-6.39177
HALLMARK_KRAS_SIGNALING_UP	0.056137	-0.19727	0.519384	0.60532	0.75665	-6.40445
HALLMARK_G2M_CHECKPOINT	-0.08892	-0.22054	-0.46183	0.645803	0.787564	-6.43244
HALLMARK_INTERFERON_ALPHA_RESPONSE	0.100104	-0.2059	0.435369	0.664788	0.791415	-6.44421
HALLMARK_ANGIOGENESIS	0.062977	-0.17685	0.394708	0.694397	0.807438	-6.46096
HALLMARK_DNA_REPAIR	-0.04202	-0.18274	-0.35157	0.726339	0.825385	-6.47694
HALLMARK_HEME_METABOLISM	0.036936	-0.14588	0.293595	0.770036	0.855595	-6.49552
HALLMARK_XENOBIOTIC_METABOLISM	0.025759	-0.23077	0.271039	0.78725	0.855707	-6.50185
HALLMARK_APICAL_JUNCTION	0.022935	-0.20733	0.223934	0.823536	0.863973	-6.51344

HALLMARK_MYOGENESIS	-0.02206	-0.24127	-0.204	0.839014	0.863973	-6.51768
HALLMARK_ESTROGEN_RESPONSE_LATE	-0.01493	-0.22098	-0.19414	0.846694	0.863973	-6.51963
HALLMARK_FATTY_ACID_METABOLISM	0.009269	-0.19571	0.101186	0.919726	0.919726	-6.53328

Supplemental Table 18: GSEA using hAML gene sets from pediatric and adult AML subtypes with DEG between each cAML subgroup vs. normal bone marrow

GSEA results for cAML group 0								
ID	setSize	enrichmentScore	NES	Absolute value NES	Combined NES from paired gene sets	pvalue	p.adjust	qvalues
BEAT_monoblastic.and.monocytic.leukaemia_DOWN	71	-0.30431	-1.9238	1.923799	3.745274	0.000608	0.001031	0.000136
BEAT_monoblastic.and.monocytic.leukaemia_UP	63	0.429337	1.821476	1.821476		0.00267	0.003477	0.000457
BEAT_myelomonocytic.leukaemia_DOWN	77	-0.28814	-1.83356	1.833558	3.945246	0.001203	0.001773	0.000233
BEAT_myelomonocytic.leukaemia_UP	61	0.499583	2.111688	2.111688		0.000108	0.000216	2.85E-05
BEAT_NOS_DOWN	74	-0.39318	-2.44066	2.440659	4.725193	5.57E-07	2.40E-06	3.16E-07
BEAT_NOS_UP	61	0.540475	2.284534	2.284534		7.11E-06	2.49E-05	3.28E-06
BEAT_promyelocytic.leukaemia.with.PML_RARA_DOWN	62	-0.28209	-1.7376	1.737599	3.795425	0.005722	0.00712	0.000937
BEAT_promyelocytic.leukaemia.with.PML_RARA_UP	70	0.477793	2.057826	2.057826		0.000133	0.000257	3.39E-05
BEAT_Therapy.related.myeloid.neoplasms_DOWN	61	-0.46915	-2.8976	2.897601	5.106811	2.49E-08	2.00E-07	2.63E-08

BEAT_Therapy.related.myeloid.neoplasms_UP	60	0.524118	2.20921	2.20921		1.40E-05	4.37E-05	5.75E-06
BEAT_Unknown_DOWN	76	-0.28014	-1.77833	1.778329	3.719468	0.001452	0.002085	0.000274
BEAT_Unknown_UP	67	0.453401	1.941139	1.941139		0.000562	0.000983	0.000129
BEAT_with.CBFB_MYH11_DOWN	47	0.42209	1.70166	1.70166		0.011011	0.01312	0.001726
BEAT_with.CBFB_MYH11_UP	75	0.376947	1.64948	1.64948		0.012256	0.014299	0.001881
BEAT_with.maturation_DOWN	62	-0.3066	-1.88863	1.888631	4.321141	0.001516	0.002122	0.000279
BEAT_with.maturation_UP	65	0.571996	2.43251	2.43251		3.31E-07	1.68E-06	2.22E-07
BEAT_with.minimal.differentiation_DOWN	78	-0.37185	-2.34274	2.342737	4.800826	1.45E-06	5.79E-06	7.62E-07
BEAT_with.minimal.differentiation_UP	70	0.570727	2.458089	2.458089		5.99E-08	4.19E-07	5.51E-08
BEAT_with.MLLT3_MLL_DOWN	82	-0.28527	-1.83678	1.836776	3.745406	0.001145	0.001733	0.000228
BEAT_with.MLLT3_MLL_UP	66	0.446943	1.908631	1.908631		0.000104	0.001654	0.000218
BEAT_with.mutated.CEBPA_DOWN	66	-0.26081	-1.61113	1.611113	3.811486	0.010382	0.012639	0.001663
BEAT_with.mutated.CEBPA_UP	65	0.517406	2.200356	2.200356		2.73E-05	6.95E-05	9.15E-06
BEAT_with.mutated.NPM1_DOWN	65	-0.35876	-2.22697	2.226968	4.415437	4.67E-05	0.000106	1.39E-05
BEAT_with.mutated.NPM1_UP	63	0.51584	2.18847	2.18847		3.79E-05	9.23E-05	1.21E-05

BEAT_with.myelodysplasia.related.changes_DOWN	67	-0.34055	-2.10997	2.109968	4.304794	8.89E-05	0.000184	2.43E-05
BEAT_with.myelodysplasia.related.changes_UP	64	0.515207	2.194826	2.194826		2.66E-05	6.95E-05	9.15E-06
BEAT_with.RPN1_EVI1_DOWN	75	-0.50747	-3.19406	3.194056	5.330206	2.68E-12	7.50E-11	9.87E-12
BEAT_with.RPN1_EVI1_UP	75	0.488164	2.13615	2.13615		4.73E-05	0.000106	1.39E-05
BEAT_with.RUNX1_RUNX1T1_UP	68	0.511388	2.196082	2.196082		1.90E-05	5.60E-05	7.36E-06
BEAT_without.maturation_DOWN	63	-0.50893	-3.14059	3.14059	5.394271	1.10E-10	2.05E-09	2.70E-10
BEAT_without.maturation_UP	65	0.529945	2.253681	2.253681		1.04E-05	3.42E-05	4.50E-06
TARGET_CBFA2T3_GLIS2_UP	64	0.441242	1.879732	1.879732		0.001858	0.002537	0.000334
TARGET_CBFB_MYH11_DOWN	49	0.481553	1.96784	1.96784		0.001063	0.001654	0.000218
TARGET_CBFB_MYH11_UP	67	0.419101	1.794292	1.794292		0.003712	0.004724	0.000622
TARGET_DEK_NUP214_UP	63	0.434329	1.842653	1.842653		0.002157	0.002876	0.000378
TARGET_ETS_Fusion_DOWN	73	-0.45552	-2.89948	2.89948	5.410451	2.58E-09	3.61E-08	4.75E-09
TARGET_ETS_Fusion_UP	66	0.587993	2.510971	2.510971		2.50E-08	2.00E-07	2.63E-08
TARGET_KMT2A_DOWN	64	-0.34814	-2.16016	2.160163	4.418923	5.35E-05	0.000115	1.51E-05
TARGET_KMT2A_UP	46	0.56594	2.25876	2.25876		2.63E-05	6.95E-05	9.15E-06

TARGET_No.Primary.Fusion_DOWN	74	-0.43461	-2.69778	2.69778	5.170682	1.47E-08	1.65E-07	2.17E-08
TARGET_No.Primary.Fusion_UP	60	0.586677	2.472902	2.472902		9.49E-08	5.91E-07	7.77E-08
TARGET_NOS_DOWN	79	-0.40528	-2.58	2.580001	5.585119	1.50E-07	8.40E-07	1.11E-07
TARGET_NOS_UP	49	0.735387	3.005118	3.005118		4.10E-14	2.29E-12	3.02E-13
TARGET_NUP98_KDM5A_UP	54	0.576846	2.388736	2.388736		2.48E-06	9.26E-06	1.22E-06
TARGET_NUP98_NSD1_UP	59	0.507713	2.134753	2.134753		0.000158	0.000295	3.88E-05
TARGET_RBM15_MKL1_DOWN	80	-0.37389	-2.36542	2.365419	4.308162	5.44E-07	2.40E-06	3.16E-07
TARGET_RBM15_MKL1_UP	73	0.446783	1.942743	1.942743		0.000681	0.001121	0.000148
TARGET_RUNX1_RUNX1T1_DOWN	59	0.373025	1.568437	1.568437		0.033918	0.038764	0.0051
TARGET_RUNX1_RUNX1T1_UP	63	0.487233	2.0671	2.0671		0.0002	0.000362	4.76E-05
GSEA results for cAML group 1								
ID	setSize	enrichmentScore	NES	Absolute value NES	Combined NES from paired gene sets	pvalue	p.adjust	qvalues
BEAT_monoblastic.and.monocytic.leukaemia_DOWN	67	-0.58058	-2.7684	2.768404		6.00E-09	8.40E-08	3.00E-08

BEAT_myelomonocytic.leukaemia_DOWN	71	-0.55979	-2.69672	2.696717		3.75E-09	7.00E-08	2.50E-08
BEAT_NOS_DOWN	66	-0.56342	-2.66688	2.666875	4.372953	1.66E-08	1.86E-07	6.64E-08
BEAT_NOS_UP	48	0.393579	1.706078	1.706078		0.023522	0.039917	0.014256
BEAT_promyelocytic.leukaemia.with.PML_RARA_DOWN	49	-0.50726	-2.23553	2.235527		0.000197	0.000691	0.000247
BEAT_Therapy.related.myeloid.neoplasms_DOWN	76	-0.63694	-3.08462	3.084615	4.721694	4.11E-14	2.30E-12	8.23E-13
BEAT_Therapy.related.myeloid.neoplasms_UP	52	0.372349	1.637079	1.637079		0.022917	0.039917	0.014256
BEAT_Unknown_DOWN	57	-0.51163	-2.35333	2.353334	4.075734	9.48E-06	4.08E-05	1.46E-05
BEAT_Unknown_UP	49	0.39571	1.7224	1.7224		0.01881	0.035113	0.01254
BEAT_with.CBFB_MYH11_DOWN	36	-0.53282	-2.19941	2.199941	3.952332	0.001125	0.003316	0.001184
BEAT_with.CBFB_MYH11_UP	60	0.384226	1.752923	1.752923		0.009833	0.021178	0.007564
BEAT_with.maturation_DOWN	65	-0.52831	-2.49907	2.499071		1.46E-06	8.20E-06	2.93E-06
BEAT_with.minimal.differentiation_DOWN	61	-0.5083	-2.38811	2.388112	4.007737	5.70E-06	2.84E-05	1.01E-05
BEAT_with.minimal.differentiation_UP	51	0.370934	1.619625	1.619625		0.02334	0.039917	0.014256
BEAT_with.MLLT3_MLL_DOWN	57	-0.49696	-2.28584	2.285838		2.23E-05	8.31E-05	2.97E-05

BEAT_with.mutated.CEBPA_DOWN	66	-0.51887	-2.45602	2.456016		1.18E-06	7.35E-06	2.63E-06
BEAT_with.mutated.NPM1_DOWN	60	-0.55121	-2.5811	2.581099		6.00E-07	4.20E-06	1.50E-06
BEAT_with.myelodysplasia.related.changes_DOWN	73	-0.56871	-2.77548	2.775479		2.21E-09	6.18E-08	2.21E-08
BEAT_with.RPN1_EVI1_DOWN	57	-0.57419	-2.64111	2.641106		9.45E-08	8.82E-07	3.15E-07
BEAT_with.RUNX1_RUNX1T1_DOWN	58	-0.56195	-2.61429	2.614293	4.463621	4.51E-07	3.61E-06	1.29E-06
BEAT_with.RUNX1_RUNX1T1_UP	54	0.415127	1.849328	1.849328		0.005972	0.014541	0.005193
BEAT_without.maturation_DOWN	54	-0.54504	-2.45993	2.459931		6.09E-06	2.84E-05	1.01E-05
TARGET_CBFA2T3_GLIS2_UP	45	0.422387	1.815683	1.815683		0.01093	0.022669	0.008096
TARGET_CBFB_MYH11_UP	43	0.476495	2.028192	2.028192		0.002516	0.006404	0.002287
TARGET_DEK_NUP214_DOWN	33	-0.48007	-1.95477	1.954775		0.006308	0.014718	0.005256
TARGET_DEK_NUP214_UP	47	-0.4067	-1.75263	1.752626		0.014841	0.028658	0.010235
TARGET_ETS_Fusion_DOWN	46	-0.46491	-1.98479	1.984788		0.001473	0.004126	0.001473
TARGET_KMT2A_DOWN	41	-0.51384	-2.16326	2.163262		0.000379	0.001249	0.000446

TARGET_No.Primary.Fusion_DOWN	53	-0.53285	-2.3908	2.3908		1.84E-05	7.36E-05	2.63E-05
TARGET_NOS_DOWN	52	-0.4453	-1.98953	1.989529		0.001566	0.004176	0.001491
TARGET_NUP98_NSD1_DOWN	39	-0.52687	-2.19713	2.197129		0.000503	0.001566	0.000559
TARGET_RBM15_MKL1_DOWN	45	-0.41276	-1.75858	1.758577		0.012767	0.025534	0.009119
TARGET_RUNX1_RUNX1T1_UP	47	0.438929	1.906097	1.906097		0.006833	0.015307	0.005467
GSEA results for cAML group 2								
ID	setSize	enrichmentScore	NES	Absolute value NES	Combined NES from paired gene sets	pvalue	p.adjust	qvalues
BEAT_monoblastic.and.monocytic.leukaemia_DOWN	71	-0.40258	-2.34859	2.348587	4.769464	1.68E-05	2.62E-05	1.97E-06
BEAT_monoblastic.and.monocytic.leukaemia_UP	75	0.506643	2.420877	2.420877		3.15E-06	5.51E-06	4.14E-07
BEAT_myelomonocytic.leukaemia_DOWN	76	-0.37024	-2.19005	2.190055	4.69852	6.22E-05	8.29E-05	6.23E-06
BEAT_myelomonocytic.leukaemia_UP	66	0.538981	2.508465	2.508465		1.70E-06	3.19E-06	2.40E-07

BEAT_NOS_DOWN	83	-0.47931	-2.86489	2.864891	5.624457	3.46E-10	2.15E-09	1.62E-10
BEAT_NOS_UP	66	0.592934	2.759566	2.759566		1.01E-08	4.04E-08	3.04E-09
BEAT_promyelocytic.leukaemia.with.PML_RARA_DOWN	56	-0.37704	-2.08234	2.082338	4.323173	0.000446	0.000531	4.00E-05
BEAT_promyelocytic.leukaemia.with.PML_RARA_UP	80	0.466065	2.240835	2.240835		1.09E-05	1.80E-05	1.36E-06
BEAT_Therapy.related.myeloid.neoplasms_DOWN	68	-0.47712	-2.74685	2.746853	5.399672	2.49E-08	8.21E-08	6.17E-09
BEAT_Therapy.related.myeloid.neoplasms_UP	73	0.557726	2.652819	2.652819		1.13E-07	3.00E-07	2.26E-08
BEAT_Unknown_DOWN	87	-0.43223	-2.59903	2.59903	5.100214	1.66E-08	5.81E-08	4.37E-09
BEAT_Unknown_UP	72	0.527819	2.501185	2.501185		1.51E-06	3.13E-06	2.35E-07
BEAT_with.CBFB_MYH11_DOWN	54	0.390559	1.747591	1.747591		0.015811	0.017361	0.001305
BEAT_with.CBFB_MYH11_UP	84	0.431984	2.102305	2.102305		0.000187	0.000238	1.79E-05
BEAT_with.maturation_DOWN	73	-0.37499	-2.18995	2.189951	4.896559	5.74E-05	7.84E-05	5.90E-06
BEAT_with.maturation_UP	63	0.588311	2.706608	2.706608		5.07E-08	1.50E-07	1.12E-08
BEAT_with.minimal.differentiation_DOWN	84	-0.48334	-2.89306	2.893064	5.599028	3.12E-10	2.15E-09	1.62E-10
BEAT_with.minimal.differentiation_UP	66	0.581416	2.705963	2.705963		3.39E-08	1.05E-07	7.92E-09

BEAT_with.MLLT3_MLL_DOWN	83	-0.41012	-2.45133	2.451329	4.718107	6.64E-07	1.49E-06	1.12E-07
BEAT_with.MLLT3_MLL_UP	70	0.481331	2.266778	2.266778		4.05E-05	5.85E-05	4.40E-06
BEAT_with.mutated.CEBPA_DOWN	74	-0.3239	-1.89229	1.892289	4.223818	0.001407	0.001641	0.000123
BEAT_with.mutated.CEBPA_UP	66	0.500964	2.33153	2.33153		2.93E-05	4.44E-05	3.34E-06
BEAT_with.mutated.NPM1_DOWN	68	-0.43033	-2.47746	2.477461	5.21748	1.64E-06	3.19E-06	2.40E-07
BEAT_with.mutated.NPM1_UP	73	0.576059	2.740019	2.740019		1.66E-08	5.81E-08	4.37E-09
BEAT_with.myelodysplasia.related.changes_DOWN	68	-0.41524	-2.39061	2.390609	5.010606	4.67E-06	7.92E-06	5.96E-07
BEAT_with.myelodysplasia.related.changes_UP	74	0.547662	2.619998	2.619998		2.07E-07	5.27E-07	3.97E-08
BEAT_with.RPN1_EVI1_DOWN	75	-0.56659	-3.32698	3.32698	5.752685	4.78E-14	5.35E-13	4.02E-14
BEAT_with.RPN1_EVI1_UP	79	0.50422	2.425705	2.425705		1.89E-06	3.41E-06	2.57E-07
BEAT_with.RUNX1_RUNX1T1_DOWN	77	-0.30712	-1.83227	1.832268	4.408661	0.004424	0.004967	0.000373
BEAT_with.RUNX1_RUNX1T1_UP	71	0.54491	2.576393	2.576393		3.29E-07	7.67E-07	5.77E-08
BEAT_without.maturation_DOWN	72	-0.51044	-2.98754	2.987543	5.654112	4.57E-10	2.56E-09	1.92E-10
BEAT_without.maturation_UP	72	0.562719	2.666569	2.666569		5.90E-08	1.65E-07	1.24E-08

TARGET_CBFA2T3_GLIS2_DOWN	63	-0.40399	-2.27759	2.277586	4.815194	4.38E-05	6.13E-05	4.61E-06
TARGET_CBFA2T3_GLIS2_UP	66	0.545243	2.537608	2.537608		9.66E-07	2.08E-06	1.56E-07
TARGET_CBFB_MYH11_DOWN	57	0.411188	1.862599	1.862599	4.053996	0.004435	0.004967	0.000373
TARGET_CBFB_MYH11_UP	65	0.473852	2.191397	2.191397		0.000198	0.000246	1.85E-05
TARGET_DEK_NUP214_DOWN	74	-0.3641	-2.12709	2.127093	4.269986	0.00012	0.000156	1.17E-05
TARGET_DEK_NUP214_UP	66	0.460432	2.142893	2.142893		0.000296	0.00036	2.71E-05
TARGET_ETS_Fusion_DOWN	84	-0.6221	-3.72362	3.723619	6.705986	1.33E-20	7.45E-19	5.60E-20
TARGET_ETS_Fusion_UP	68	0.635668	2.982367	2.982367		4.73E-11	3.78E-10	2.84E-11
TARGET_KMT2A_DOWN	66	-0.41524	-2.36597	2.365969	5.205858	1.29E-05	2.07E-05	1.55E-06
TARGET_KMT2A_UP	49	0.650492	2.839888	2.839888		5.72E-09	2.67E-08	2.01E-09
TARGET_No.Primary.Fusion_DOWN	87	-0.54744	-3.29179	3.29179	6.197004	5.62E-15	7.87E-14	5.92E-15
TARGET_No.Primary.Fusion_UP	62	0.632939	2.905214	2.905214		5.26E-10	2.68E-09	2.01E-10
TARGET_NOS_DOWN	94	-0.53371	-3.281	3.280996	6.658649	3.38E-15	6.30E-14	4.74E-15
TARGET_NOS_UP	52	0.760175	3.377653	3.377653		7.68E-17	2.15E-15	1.62E-16
TARGET_NUP98_KDM5A_UP	59	0.608405	2.783063	2.783063		9.13E-09	3.93E-08	2.96E-09

TARGET_NUP98_NSD1_UP	57	0.501924	2.273616	2.273616		4.08E-05	5.85E-05	4.40E-06
TARGET_RBM15_MKL1_DOWN	87	-0.4938	-2.96924	2.969241	5.465962	1.30E-11	1.22E-10	9.15E-12
TARGET_RBM15_MKL1_UP	69	0.52929	2.496722	2.496722		1.71E-06	3.19E-06	2.40E-07
TARGET_RUNX1_RUNX1T1_DOWN	62	0.366776	1.683518	1.683518		0.024845	0.026757	0.002012
TARGET_RUNX1_RUNX1T1_UP	70	0.546207	2.572307	2.572307		2.17E-07	5.29E-07	3.98E-08

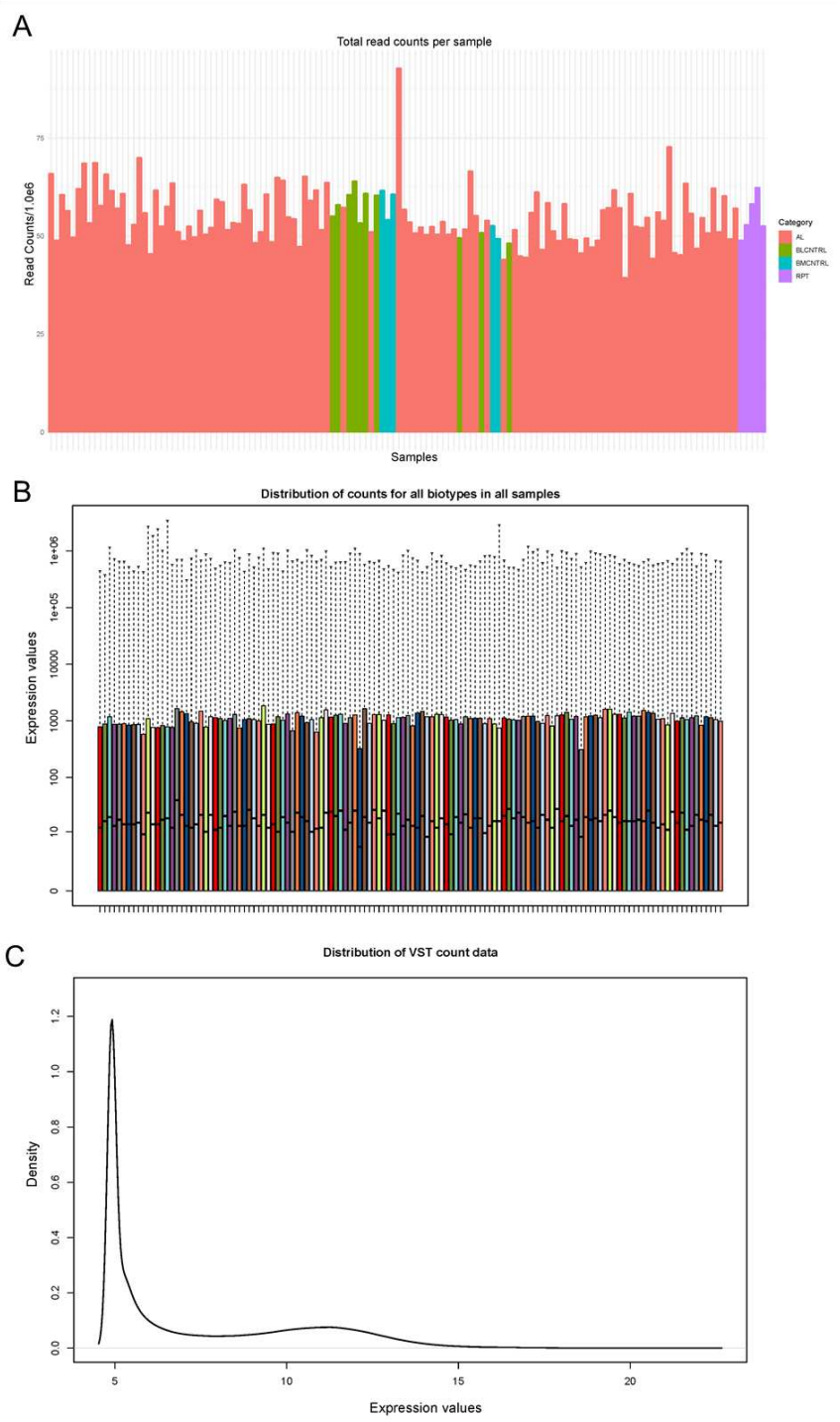

Supplemental Figure 9: Overview of gene counts acquired in the canine acute leukemia, peripheral blood and bone marrow control samples. A) Bar plot showing the total read counts within each sample. The color of the bar corresponds to the sample type. B) Bar plot of the distribution of gene counts for all gene biotypes in all samples. C) Line graph representing the distribution of the variance stabilizing transformed gene counts in all samples. Abbreviations: AL, Acute leukemia; BLCNTRL, blood control; BMCNTRL, Bone marrow control; RPT, technical replicate; Variance stabilizing transformation, VST.

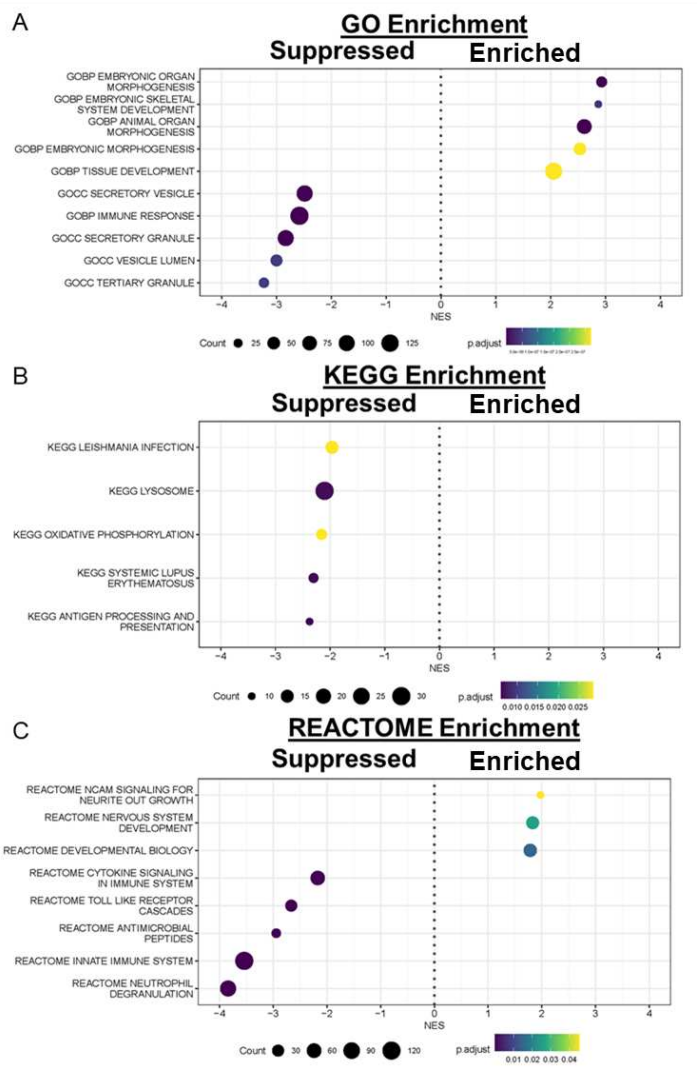

Supplemental Figure 10: Gene set enrichment analysis results using DEG between the entire canine acute leukemia cohort versus the bone marrow control samples. Each dot represents a A) Gene ontology, B) KEGG, or C) REACTOME gene set enriched in the acute leukemia group. The top 5 up (enriched) and down (suppressed) gene sets with the highest and lowest normalized enrichment scores are shown. The size of each dot corresponds to the gene count, and the color of each dot corresponds to the adjusted p-value.

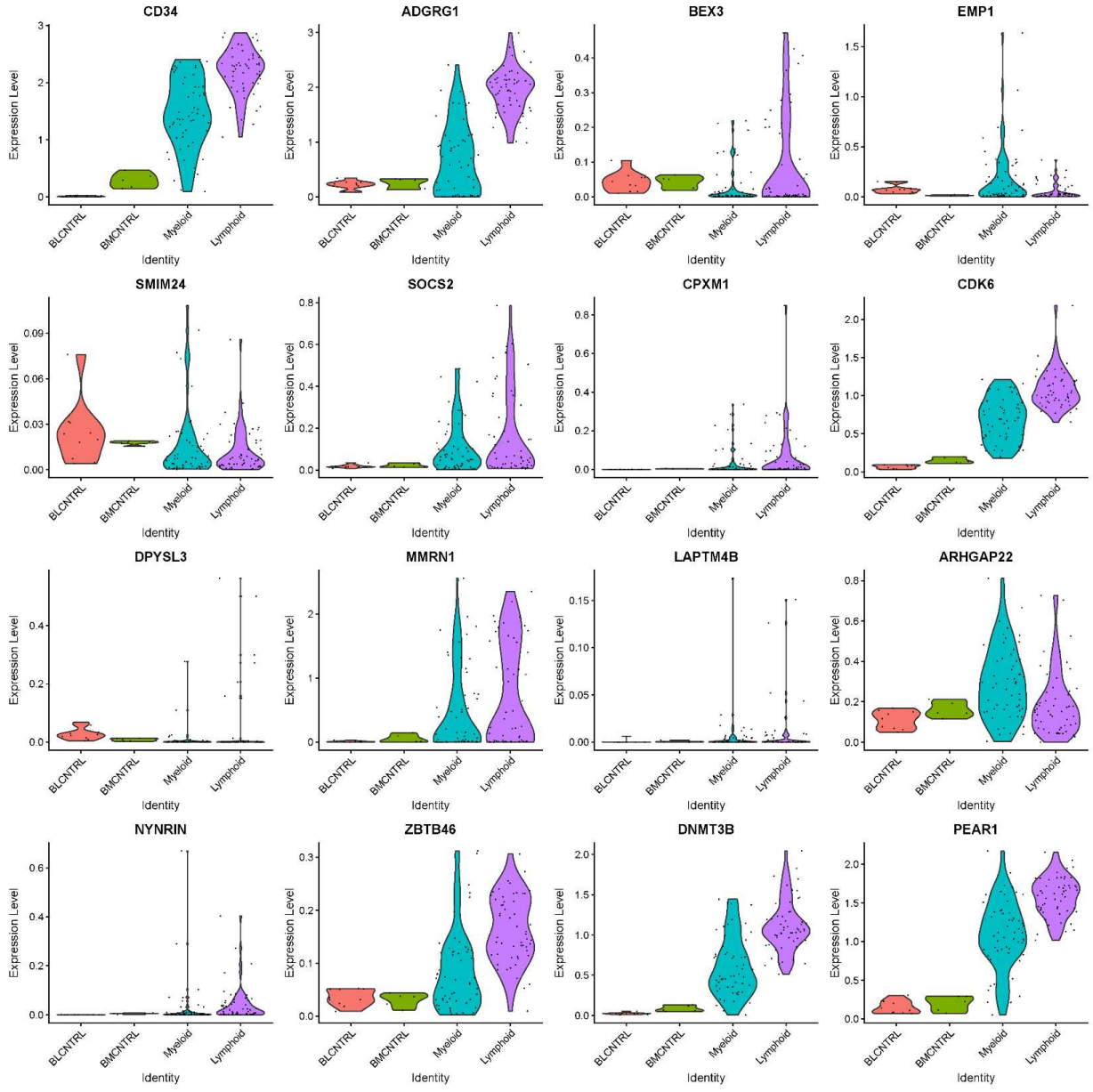

Supplemental Figure 11: Canine acute myeloid leukemia samples overexpress genes associated with myeloid leukemic stem cells and genes correlative with a poor prognosis in hAML. 15 of the 17 genes in the 17-gene LSC panel had a corresponding gene symbol in the dog and are shown. The cAML subgroup overexpressed CD34, ADGRG1, EMP1, SOCS2, MMRN1, ZBTB46, and DNMT3B relative to the BMCNTRL (bone marrow controls). PEAR1, recently shown to be associated with poor prognosis in hAML patients, was also overexpressed in the cAML group.

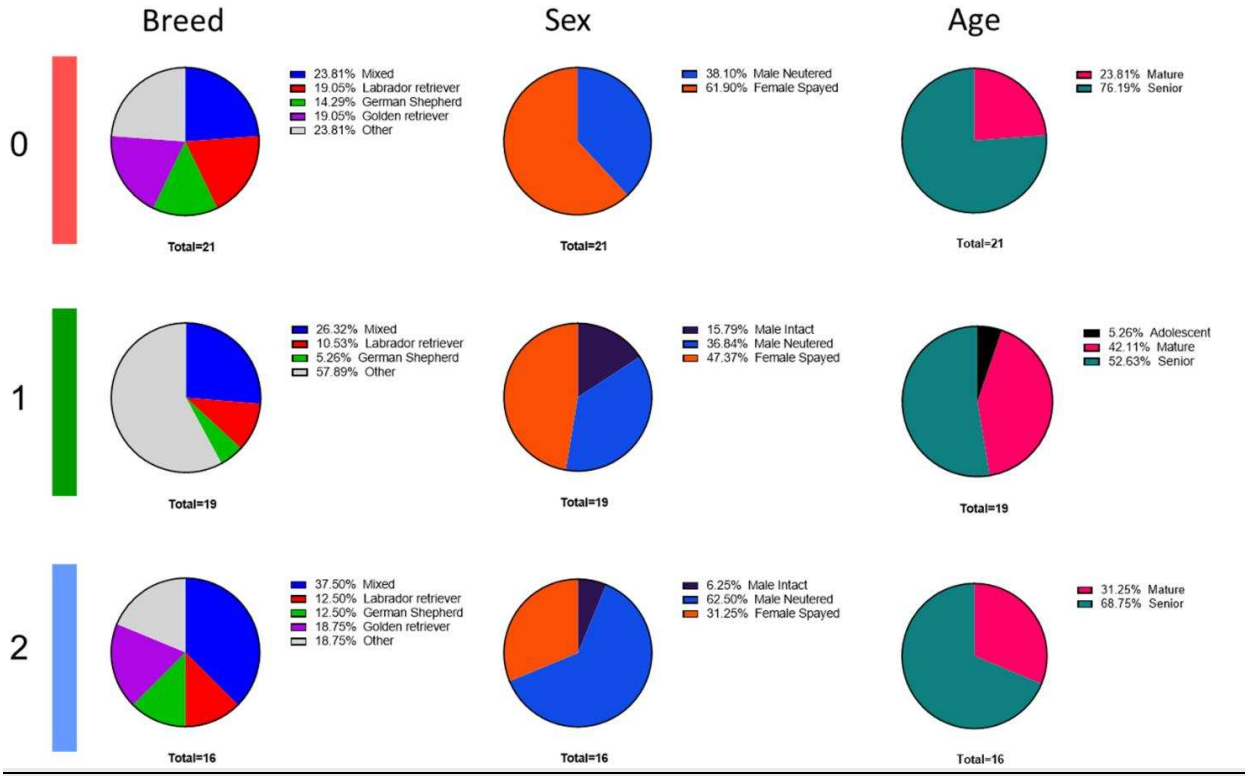

Supplemental Figure 12: Overview of the breed, sex, and age distribution between the predicted cAML subgroups. Pie charts and associated proportions are shown for the top four most common breeds, the sex, and age group in each cAML subgroup. Age groups were defined as adolescent (6 months - 2 years old), Mature (2 – 7 years old), and Senior (>7 years old). The cAML groups 0, 1, and 2, are identified to the left and by their corresponding-colored bar.

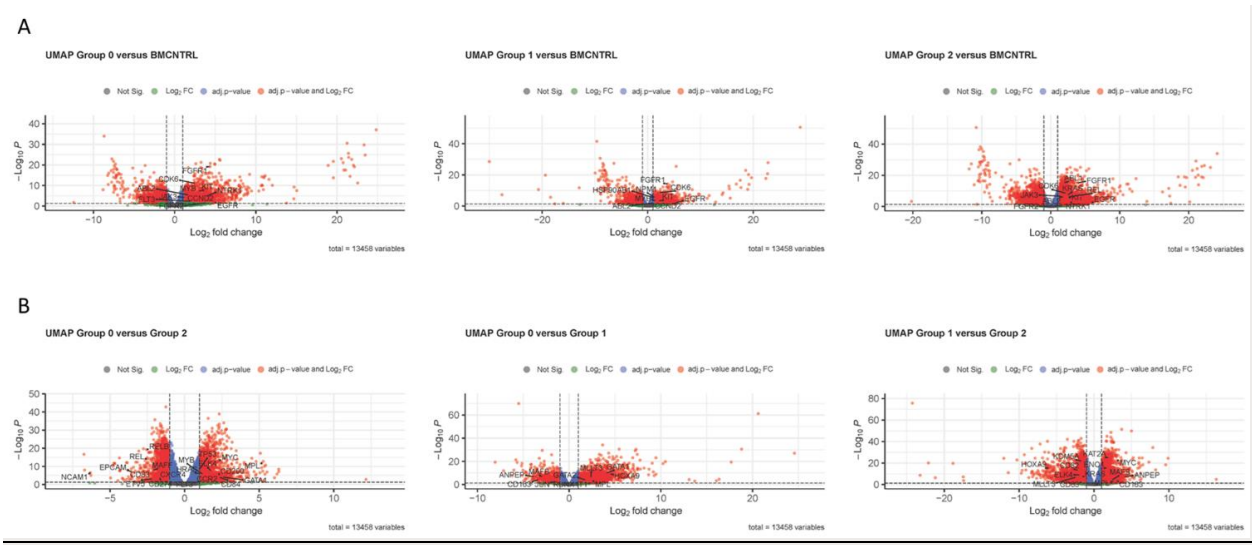

Supplemental Figure 13: cAML subgroups overexpress oncogenes involved in RAS and PI3K/AKT signaling, and markers implicated in hAML pathogenesis. A) The volcano plots shown are highlighting select genes in the RAS or PI3K/AKT signaling pathway that are overexpressed in each cAML subgroup compared to normal bone marrow (BMCNTRL). Additionally, *NPM1* overexpression was a unique feature identified in UMAP group 1. B) Volcano plots highlighting unique markers that have been implicated in the pathogenesis in subtypes of hAML and are considered differentially expressed between cAML subgroups when evaluated as standard pairwise comparisons. Abbreviations: Sig, Significant; adj., adjusted; FC, fold change.

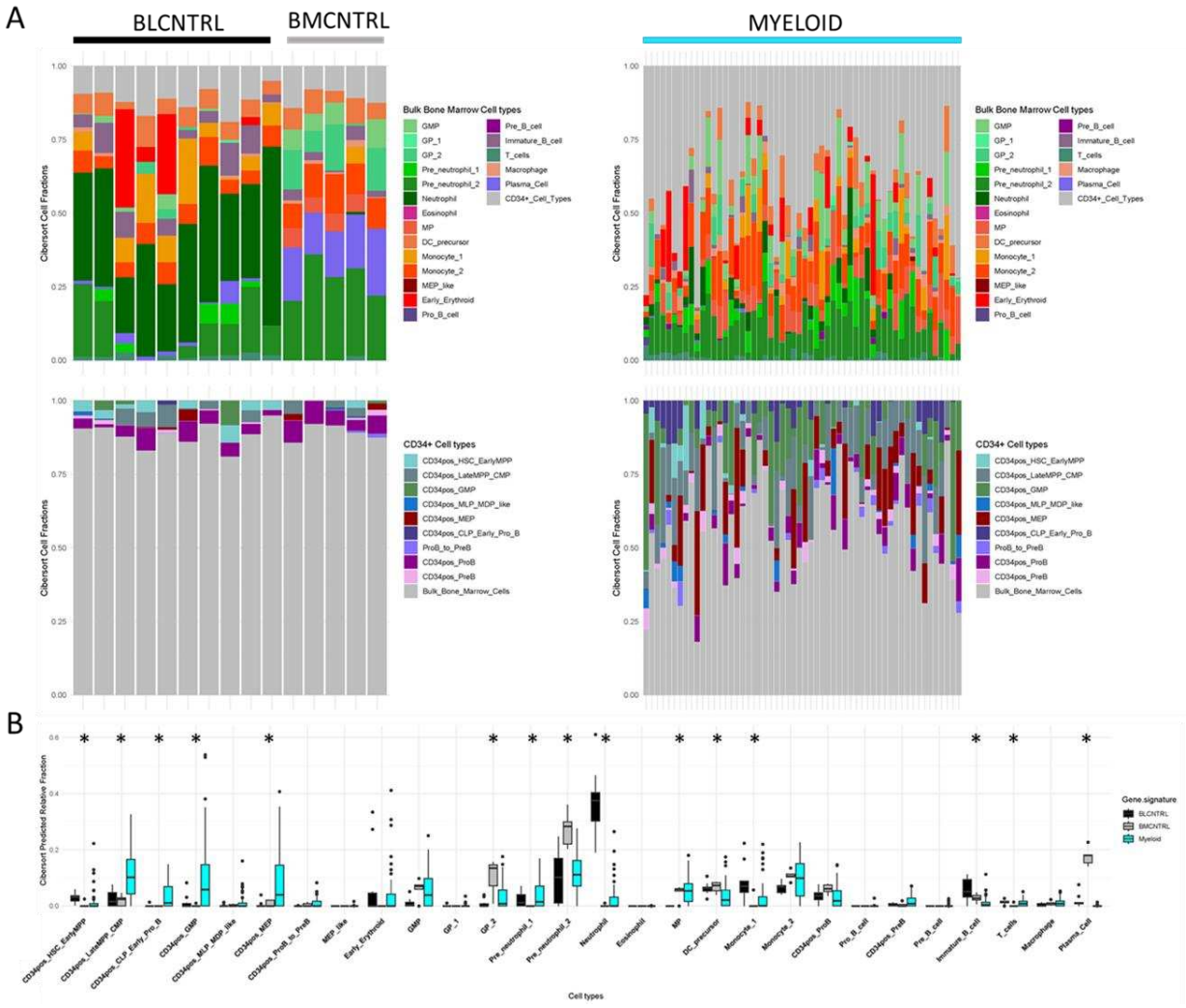

Supplemental Figure 14: Imputed cell fractions in controls and myeloid (cAML) samples. A) Bar plots representing the proportion of cell types predicted in each sample type denoted by the bar above the plot. Although the predicted cell fractions were computed altogether for each sample, the bar plots are broken down by cell types predicted using the whole bone marrow or sorted CD34+ data set (bottom) to highlight the aberrant cell populations identified in the myeloid samples. B) Boxplot of the predicted relative fractions of cell types across each sample type denoted by gene signature group. The * at the top represents statistical significance and p value < 0.05 using a Kruskal-Wallis test. Abbreviations: HSC, Hematopoietic stem cell; pos, positive, GMP, Granulocyte-monocyte precursor; MPP, Multipotent progenitor; MEP, Megakaryocytic-erythroid progenitor; CLP, Common lymphoid progenitor; MLP, Multi-lymphoid progenitor; MDP, Monocyte-dendritic precursor; GP, Granulocyte precursor; MP, Monocyte precursor; DC, Dendritic cell; MLP, Multi-lymphoid progenitor.

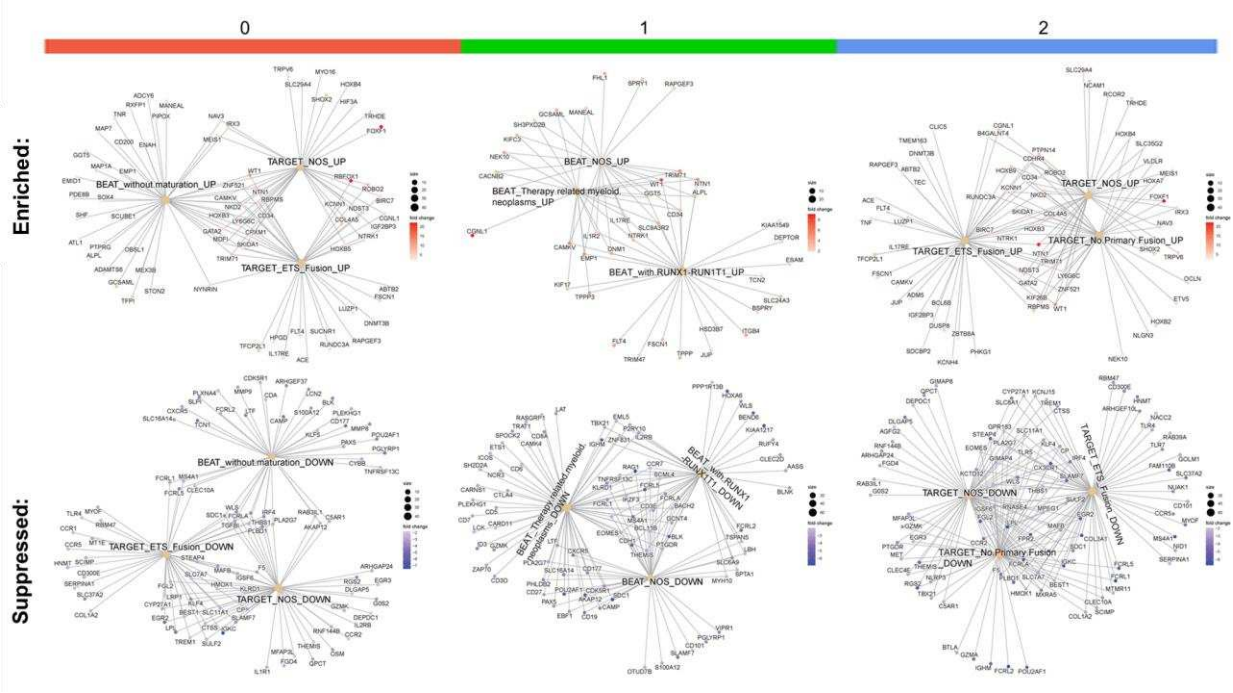

Supplemental Figure 15: Leading edge analysis results of genes shared and unique in each hAML gene set and over- or under-expressed in the cAML subgroups. Category net plots using of the top 3 (highest combined normalized enrichment score) hAML gene sets enriched or suppressed in each cAML subgroup. The enriched and suppressed gene sets are displayed on top and bottom, respectively. The size of the center dot corresponds to the gene count and the color of the dots with gene symbols correlates with the fold change of gene expression found in that cAML subgroup. The cAML groups 0, 1, and 2, are identified to the left and by their corresponding-colored bar. The category net plots reveal overlapping and unique genes enriched in our cAML subgroups and shared with the hAML gene sets.

SUPPLEMENTARY MATERIAL FOR CHAPTER 4

Supplemental Table 19: Metadata for each sample

Tumor Sample Barcode	Sample type	UMAP.Group	Flow_subtype[δ]	Age	Breed	Sex
M105453	AML	GRP_2	CD14+	7.6	GLDR	M
M106053	AML	GRP_1	CD14+	2.8	GSHEP	M
M118542	AML	GRP_NA	CD18+	9.5	GLDR	F
M119591	AML	GRP_0	CD18+	8.3	GSHEP	F
M120378	AML	GRP_1	CD14+	8	LAB	F
M120399	AML	GRP_0	CD14+	6	GLDR	M
M69860	AML	GRP_1	CD18+	7	LAB	M
M71281	AML	GRP_2	CD14+	5	GLDR	M
M71335	AML	GRP_2	CD14+	9.4	GSHEP	F
M71609	AML	GRP_0	CD14+	10.4	LAB	F
M52097	AML	GRP_0	CD14+CD5+	11.6	LAB	F
L52744	AML	GRP_2	CD5+	14	MIX	M
L53739	AML	GRP_2	CD5+	10	MIX	F
M58697	AML	GRP_0	CD14+	8.1	MIX	F
U69959	AML	GRP_1	Lin-	4.1	LBDOODLE	M
M69965	AML	GRP_1	CD14+	8.7	MIX	M
M70848	AML	GRP_1	CD14+	11.7	MIX	M
M71679	AML	GRP_1	CD14+	12.8	LBDOODLE	F
M73441	AML	GRP_0	CD14+	9	LAB	F
M71593	AML	GRP_2	CD18+	8.1	MALT	M
M58698	AML	GRP_0	CD14+	3	JKR	F
M99876	AML	GRP_1	CD14+	9.2	MIX	M
L105735	AML	GRP_0	CD5+	7.5	MIX	F
L105585	AML	GRP_2	CD5+	6.5	GLDR	F
L71592	AML	GRP_0	CD5+	9.6	GSHEP	F

M101740	AML	GRP_0	CD14+	11.4	AUS	F
M103733	AML	GRP_1	CD14+	1.9	BOST	F
L107858	AML	GRP_2	CD5+	6.8	MIX	M
M108089	AML	GRP_1	CD14+	3.8	CHOW	F
M108735	AML	GRP_1	CD18+	8.9	MIX	F
L114148	AML	GRP_2	CD5+	13.2	MIX	F
L114182	AML	GRP_0	CD5+	13.7	MIX	F
M114337	AML	GRP_1	CD14+	8.2	MIX	F
M114677	AML	GRP_1	CD14+	8.4	BELMAL	M
M115951	AML	GRP_0	CD18+	13	GLDR	M
L110446	AML	GRP_0	CD5+	7.1	GLDR	M
M113164	AML	GRP_1	CD14+	3.6	WHTERR	F
M120398	AML	GRP_1	CD14+	2	DOB	F
M120486	AML	GRP_2	CD18+	7.6	MIX	M
M120655	AML	GRP_0	CD18+	6	CHES	M
M121047	AML	GRP_2	CD14+	5.6	MIX	M
M121064	AML	GRP_1	CD14+	4.6	AKT	M
M121010	AML	GRP_2	CD14+	7.6	AUS	M
M122308	AML	GRP_2	CD14+	10	NEWFIE	M

δ Immunophenotype of neoplastic cells at the time of sample submission

Abbreviations: NA: not available; LAB: Labrador retriever, BOST: Boston terrier, MIX: Mixed breed, GLDR: Golden retriever, AUS: Australian shepherd, GSHEP: German shepherd, MALT: Maltese, LBDOODLE: Labradoodle, CHOW: Chow Chow, JKR: Jack Russell Terrier, AKT: Akita, NEWFIE: Newfoundland, CHES: Chesapeake Bay Retriever, DOB: Doberman Pinscher, WHTERR: Soft-coated Wheaten Terrier, BELMAL: Belgian Malinois, F: Female, M: Male, AML: Acute myeloid leukemia

Supplemental Table 20: Filtered variants identified across 44 cAML samples

Sample ID	Gene Symbol	Chromosome	Start Position	End Position	Liftover Human (hg38) Position	Variant Classification	Reference Allele	Tumor Allele 1	Tumor Allele 2	VAF	HGV Sp Short	Exon #	SIFT	IMPACT
M99876	ABL1	9	53121211	53121211	chr9:130884921-130884921	Missense_Mutation	C	C	A	0.033	p.R896S	11/11	deleterious_low_confidence(0)	MODERATE
M99876	ABL1	9	53132823	53132823	chr9:130872213-130872213	Missense_Mutation	C	C	A	0.075	p.G322C	5/11	deleterious(0)	MODERATE
M99876	ACSL3	37	28909130	28909130	chr2:222916463-222916463	Missense_Mutation	G	G	T	0.075	p.A175S	4/16	tolerated(0.25)	MODERATE
M108089	ACVR2A	19	49642162	49642162	chr2:147844734-147844734	Missense_Mutation	C	C	T	0.833	p.A315V	1/9	tolerated_low_confidence(0.05)	MODERATE

M73441	AFDN	1	55513342	55513342	chr6:167947942-167947942	Nonsense_Mutation	G	G	T	0.081	p.E1174*	27/33		HIGH
M99876	AFDN	1	55444229	55444229	chr6:167875454-167875454	Missense_Mutation	G	G	T	0.077	p.R192M	4/1	deleterious(0)	MODERATE
M99876	AFDN	1	55487969	55487969	chr6:167917135-167917135	Missense_Mutation	C	C	A	0.063	p.P830Q	19/33	tolerated(0.69)	MODERATE
M99876	AFDN	1	55488002	55488002	chr6:167917168-167917168	Nonsense_Mutation	C	C	A	0.049	p.S841*	19/33		HIGH
M99876	AFDN	1	55517111	55517111	chr6:167951579-167951579	Missense_Mutation	G	G	T	0.086	p.A1367S	29/33	tolerated_low_confidence(0.63)	MODERATE
M103733	AFF1	32	10599666	10599666	chr4:87108209-	Missense_Mutation	C	C	T	0.13	p.A483V	11/21	deleterious(0.03)	MODERATE

					87108209									
M99876	AFF1	32	10540653	10540653	chr4:87047017-87047017	Missense_Mutation	C	C	A	0.063	p.P162Q	4/21	tolerated(0.09)	MODERATE
M73441	AFF3	10	43111160	43111160	chr2:99551398-99551398	Missense_Mutation	G	G	T	0.25	p.K81N	24/46	deleterious_low_confidence(0.04)	MODERATE
M99876	AFF3	10	43245884	43245884	chr2:99402915-99402915	Nonsense_Mutation	G	G	T	0.088	p.E1215*	43/46		HIGH
M108735	AKAP9	14	17629656	17629656	chr7:91995777-91995777	Nonsense_Mutation	G	G	T	0.25	p.E294*	7/1		HIGH
M122308	AKAP9	14	17714518	17714518	chr7:92083438-92083438	Missense_Mutation	G	G	A	0.406	p.S2825N	34/50	tolerated(0.78)	MODERATE

M99876	AKAP9	14	17653058	17653058	chr7:92022865-92022865	Missense_Mutation	A	A	G	0.222	p.K1341R	14/50	tolerated(0.08)	MODERATE
M99876	AKAP9	14	17715346	17715346	chr7:92084664-92084664	Missense_Mutation	C	C	A	0.246	p.H2906N	35/50	tolerated(0.22)	MODERATE
M99876	AKAP9	14	17730906	17730906	chr7:92099783-92099783	Nonsense_Mutation	G	G	T	0.075	p.E3619*	45/50		HIGH
L105735	AKT2	1	1.13E+08	1.13E+08	chr19:40233703-40233703	Missense_Mutation	G	G	A	0.282	p.A519T	13/13		MODERATE
M73441	ANK1	16	23898152	23898152	chr8:41723629-41723629	Missense_Mutation	G	G	A	0.049	p.G232D	6/1	tolerated(0.4)	MODERATE
L114148	APC	3	322882	322882	chr5:112754985-112754985	Missense_Mutation	T	T	C	0.326	p.N32S	1/16	tolerated(0.64)	MODERATE

M115951	ARHGAP26	2	37626747	37626747	chr5:142769949-142769949	Missense_Mutation	C	C	T	0.333	p.S17L	1/19		MODERATE
M73441	ARHGAP26	2	37626892	37626893	chr5:142770104-142770105	Missense_Mutation	GC	GC	AA	0.333	p.Q66K	1/19		MODERATE
M73441	ARHGAP35	1	1.09E+08	1.09E+08	chr19:46921665-46921665	Missense_Mutation	C	C	A	0.044	p.R998L	1/8	tolerated(0.07)	MODERATE
M121010	ARHGAP5	8	11261532	11261532	chr14:32152449-32152449	Missense_Mutation	C	C	A	0.68	p.H1369N	5/6	tolerated(0.32)	MODERATE
M58697	ARHGAP5	8	11260834	11260835	chr14:32150033-32150034	Frame_Shift_Ins	-	-	AAATCCCGGATAAACAGAACGTCTTCATGCATTGA	0.196	p.V1381Kfs*12			HIGH

									AAGAAATTGTTAAGAAATTTCATCCT					
M99876	ARHGAP5	8	11205678	11205678	chr14:32091484-32091484	Missense_Mutation	C	C	A	0.078	p.A272E	1/6	deleterious(0)	MODERATE
M99876	ARHGAP5	8	11205776	11205776	chr14:32091582-32091582	Nonsense_Mutation	G	G	T	0.119	p.E305*	1/6		HIGH
L110446	ARHGEF10L	2	80642436	80642436	NA	Missense_Mutation	G	G	T	0.4	p.P1363T	31/31		MODERATE
M108089	ARHGEF10L	2	80642904	80642904	chr1:177734030-177734030	Missense_Mutation	T	T	C	0.4	p.K1207E	31/31	tolerated_low_confidence(0.05)	MODERATE

M108735	ARHGEF10L	2	80642420	80642420	chr1:177349911-177349911	Missense_Mutation	G	G	T	0.333	p.P1368Q	31/31		MODERATE
M114337	ARHGEF10L	2	80642885	80642885	chr1:177340049-177340049	Missense_Mutation	G	G	A	0.333	p.T1213M	31/31	tolerated_low_confidence(0.12)	MODERATE
M122308	ARHGEF10L	2	80642633	80642633	chr1:177343359-177343359	Missense_Mutation	T	T	C	0.333	p.K1297R	31/31		MODERATE
M122308	ARHGEF10L	2	80642817	80642817	chr1:177341332-177341332	Missense_Mutation	C	C	T	0.282	p.G1236R	31/31	deleterious_low_confidence(0.01)	MODERATE
M99876	ARHGEF10L	2	80642427	80642427	NA	Nonsense_Mutation	C	C	A	0.333	p.G1366*	31/31		HIGH
M121064	ARHGEF12	5	13557790	13557790	chr11:120446461-	Missense_Mutation	C	C	T	0.418	p.M468I	17/41	tolerated(0.11)	MODERATE

					12044 6461									
M586 98	ARH GEF1 2	5	13525 445	13525 445	chr11: 12048 1308- 12048 1308	Misse nse_ Mutati on	G	G	A	0.169	p.T14 28M	39/41	delete rious_ low_c onfide nce(0)	MOD ERAT E
M716 09	ARID 1B	1	46792 713	46792 713	chr6:1 57201 360- 15720 1360	Misse nse_ Mutati on	C	C	A	0.649	p.T87 9K	19/22	tolerat ed(0.0 6)	MOD ERAT E
M998 76	ARID 1B	1	46727 681	46727 681	chr6:1 57133 088- 15713 3088	Misse nse_ Mutati on	G	G	T	0.099	p.G48 V	8/22	delete rious_ low_c onfide nce(0. 02)	MOD ERAT E
M120 486	ARID 2	27	84274 44	84274 44	chr12: 45893 717- 45893 717	Misse nse_ Mutati on	G	G	A	0.286	p.R18 26C	21/22	delete rious(0)	MOD ERAT E
M734 41	ARID 2	27	84648 18	84648 18	chr12: 45848 843- 45848 843	Misse nse_ Mutati on	C	C	A	0.105	p.A53 0S	13/22	tolerat ed(0.1 2)	MOD ERAT E

M69965	ASPSCR1	9	330679	330679	NA	Missense_Mutation	C	C	A	0.25	p.R93L	1/15	tolerated_low_confidence(0.12)	MODERATE
L105585	ASXL1	24	21800097	21800098	chr20:32434638-32434639	Frame_Shift_Ins	-	-	G	0.53	p.G1283Wfs*12	18/18		HIGH
M99876	ASXL1	24	21686439	21686439	chr20:32309862-32309862	Missense_Mutation	G	G	T	0.047	p.D29Y	2/18	deleterious_low_confidence(0.03)	MODERATE
M99876	ASXL1	24	21795018	21795018	chr20:32429933-32429933	Missense_Mutation	G	G	T	0.091	p.G837C	13/18	deleterious_low_confidence(0)	MODERATE
M52097	ASXL2	17	19999343	19999343	chr2:25845482-25845482	Missense_Mutation	T	T	C	0.286	p.S47G	2/13	deleterious(0.02)	MODERATE
M73441	ASXL2	17	19947106	19947106	chr2:25767680-	Missense_	C	C	A	0.111	p.Q232H	7/13	tolerated(0.13)	MODERATE

					25767680	Mutation								
M99876	ASXL2	17	19923397	19923397	chr2:25742876-25742876	Missense_Mutation	C	C	A	0.062	p.S1168I	12/13	deleterious(0.04)	MODERATE
L114148	ATIC	37	22424209	22424209	chr2:215318201-215318201	Missense_Mutation	G	G	A	0.301	p.R64H	3/16	deleterious(0)	MODERATE
M120398	ATM	5	24202732	24202732	chr11:108332821-108332821	Missense_Mutation	C	C	T	0.397	p.M2616I	54/64	tolerated(0.36)	MODERATE
M99876	ATM	5	24199673	24199673	chr11:108334976-108334976	Missense_Mutation	G	G	A	0.243	p.P2673L	56/64	deleterious(0.04)	MODERATE
M99876	ATM	5	24272836	24272836	chr11:108246963-108246963	Splice_Site	C	C	A	0.2	p.X3011_splice			HIGH

M122308	ATP1A1	17	53817215	53817215	chr1:116372681-116372681	Missense_Mutation	C	C	T	0.333	p.A100V	2/24	tolerated_low_confidence(0.1)	MODERATE
L110446	ATP2B3	X	1.21E+08	1.21E+08	chrX:153536278-153536278	Missense_Mutation	T	T	C	0.286	p.F11L	1/20	deleterious_low_confidence(0.02)	MODERATE
L71592	ATP2B3	X	1.21E+08	1.21E+08	chrX:153556211-153556211	Missense_Mutation	C	C	T	0.358	p.R741C	12/20	deleterious(0.02)	MODERATE
M73441	ATR	23	38203416	38203416	chr3:142549496-142549496	Missense_Mutation	C	C	A	0.329	p.A1055S	15/47	tolerated(0.13)	MODERATE
M99876	ATR	23	38147503	38147503	chr3:142466452-142466452	Nonsense_Mutation	C	C	A	0.115	p.E2260*	40/47		HIGH
M99876	ATR	23	38150580	38150580	chr3:142469558-	Missense_Mutation	C	C	A	0.057	p.D2114Y	38/47	deleterious(0.01)	MODERATE

					142469558									
M121010	ATRX	X	59987504	59987504	chrX:77681811-77681811	Missense_Mutation	C	C	G	0.957	p.V1151L	9/1	tolerated_low_confidence(0.28)	MODERATE
M121010	ATRX	X	59989105	59989105	chrX:77683403-77683403	Missense_Mutation	G	G	A	0.972	p.S617F	9/1	deleterious_low_confidence(0.03)	MODERATE
M121047	ATRX	X	59987246	59987246	chrX:77681556-77681556	Missense_Mutation	C	C	T	0.952	p.V1237M	9/1	tolerated(0.31)	MODERATE
M73441	ATRX	X	59956858	59956858	chrX:77663382-77663382	Missense_Mutation	C	C	A	0.088	p.V1377L	12/1	tolerated(0.07)	MODERATE
M99876	ATRX	X	59775804	59775804	chrX:77508600-77508600	Missense_Mutation	C	C	T	0.12	p.M2407I	35/35	tolerated(0.06)	MODERATE

M99876	ATRX	X	59860702	59860702	chrX:77599797-77599797	Missense_Mutation	C	C	A	0.25	p.M1903I	24/35	tolerated(0.05)	MODERATE
L105735	AXIN1	6	40215809	40215809	chr16:290821-290821	Missense_Mutation	G	G	A	0.333	p.G879D	10/10		MODERATE
M121064	AXIN1	6	40215887	40215887	chr16:290747-290747	Missense_Mutation	C	C	G	0.254	p.S905C	10/10		MODERATE
M73441	AXIN1	6	40215714	40215714	chr16:290954-290954	Missense_Mutation	A	A	C	0.286	p.R847S	10/10		MODERATE
M99876	AXIN2	9	14587456	14587456	chr17:65530050-65530050	Nonsense_Mutation	G	G	T	0.072	p.E820*	11/11		HIGH
M99876	BARD1	37	21995510	21995510	chr2:214781347-214781347	Missense_Mutation	C	C	A	0.333	p.R135L	4/11	tolerated(0.13)	MODERATE

M58698	BAZ1A	8	13612382	13612382	chr14:34764841-34764841	Missense_Mutation	A	A	T	0.683	p.S1214R	22/26	deleterious_low_confidence(0)	MODERATE
L110446	BCL11B	8	67624151	67624152	chr14:99175525-99175526	Frame_Shift_Ins	-	-	TTGAA	0.386	p.K437Nfs*40	5/5		HIGH
M101740	BCL11B	8	67624219	67624220	chr14:99175593-99175594	Frame_Shift_Ins	-	-	G	0.456	p.G415Rfs*493	5/5		HIGH
M115951	BCL11B	8	67624219	67624220	chr14:99175593-99175594	Frame_Shift_Ins	-	-	G	0.404	p.G415Rfs*493	5/5		HIGH
M120486	BCL11B	8	67673679	67673680	chr14:99231437-99231438	Frame_Shift_Ins	-	-	G	0.727	p.L183Pfs*12	4/5		HIGH
M120655	BCL11B	8	67624107	67624107	chr14:99175481-99175481	Missense_Mutation	T	T	A	0.303	p.E452V	5/5	deleterious(0)	MODERATE

M120655	BCL11B	8	67624114	67624114	chr14:99175488-99175488	Frame_Shift_Del	T	T	-	0.307	p.T450Rfs*25	5/5		HIGH
M52097	BCL11B	8	67624219	67624220	chr14:99175593-99175594	Frame_Shift_Ins	-	-	G	0.457	p.G415Rfs*493	5/5		HIGH
M69860	BCL11B	8	67623658	67623659	chr14:99175080-99175081	Frame_Shift_Ins	-	-	CTTGG	0.418	p.A602Pfs*146	5/5		HIGH
M70848	BCL11B	8	67713768	67713768	chr14:99271160-99271160	Splice_Site	C	C	G	0.351	p.X20_splice			HIGH
M71281	BCL11B	8	67623996	67623997	chr14:99175370-99175371	Frame_Shift_Ins	-	-	CGTCG	0.047	p.D489Afs*76	5/5		HIGH
M71679	BCL11B	8	67624214	67624215	chr14:99175588-99175589	Frame_Shift_Ins	-	-	C	0.425	p.T417Hfs*491	5/5		HIGH

M99876	BCL11B	8	67624662	67624662	chr14:99176036-99176036	Frame_Shift_Del	G	G	-	0.42	p.P267Rfs*14	5/5		HIGH
M69965	BCL3	1	1.11E+08	1.11E+08	chr19:44757713-44757713	Missense_Mutation	A	A	G	0.095	p.L419P	7/7	deleterious_low_confidence(0)	MODERATE
M99876	BCL3	1	1.11E+08	1.11E+08	chr19:44756233-44756233	Missense_Mutation	G	G	T	0.073	p.P263T	4/7	deleterious_low_confidence(0.01)	MODERATE
M99876	BCLAF1	1	28870945	28870945	chr6:136276474-136276474	Missense_Mutation	C	C	A	0.053	p.D351Y	5/12	deleterious(0)	MODERATE
M108089	BCOR	X	34624829	34624829	chrX:40055509-40055509	Missense_Mutation	G	G	A	0.419	p.L1537F	11/15	deleterious(0.04)	MODERATE
M99876	BCOR	X	34633161	34633161	chrX:40064549-	Nonsense_Mutation	C	C	A	0.12	p.E1100*	6/15		HIGH

					40064549								
M99876	BCOR	X	34633166	34633166	chrX:40064554-40064554	Missense_Mutation	G	G	T	0.119	p.P1098Q	6/15	tolerated(0.14)	MODERATE
L105735	BCORL1	X	1.01E+08	1.01E+08	chrX:130013665-130013667	In_Frame_Del	CGG	CGG	-	0.156	p.A299del	4/14		MODERATE
L105735	BCORL1	X	1.01E+08	1.01E+08	chrX:130013668-130013669	Frame_Shift_Ins	-	-	AT	0.156	p.P300Ffs*18	4/14		HIGH
M122308	BCORL1	X	1.01E+08	1.01E+08	chrX:130013508-130013509	Frame_Shift_Ins	-	-	A	0.791	p.P246Hfs*26	4/14		HIGH
M122308	BCORL1	X	1.01E+08	1.01E+08	chrX:130013509-130013509	Missense_Mutation	C	C	G	0.791	p.P246R	4/14	deleterious_low_confidence(0.01)	MODERATE

M71679	BCORL1	X	1.01E+08	1.01E+08	chrX:130015844-130015844	Missense_Mutation	T	T	A	0.952	p.D1024E	4/14	tolerated(0.43)	MODERATE
M71679	BCORL1	X	1.01E+08	1.01E+08	chrX:130016209-130016209	Missense_Mutation	C	C	G	0.937	p.P1149R	4/14	tolerated(1)	MODERATE
M99876	BCORL1	X	1.01E+08	1.01E+08	chrX:130015926-130015926	Nonsense_Mutation	G	G	T	0.098	p.E1052*	4/14		HIGH
M99876	BCORL1	X	1.01E+08	1.01E+08	chrX:130025229-130025229	Missense_Mutation	C	C	A	0.115	p.Q1313K	7/14	tolerated(0.17)	MODERATE
M73441	BIRC3	5	29336469	29336469	chr11:102325281-102325281	Missense_Mutation	G	G	T	0.047	p.R258S	1/7	deleterious(0)	MODERATE
M99876	BIRC6	17	25752434	25752434	chr2:32510573-32510573	Missense_Mutation	G	G	T	0.088	p.D3349Y	53/74	deleterious(0)	MODERATE

M99876	BIRC6	17	25841010	25841010	chr2:32611483-32611483	Missense_Mutation	G	G	T	0.103	p.E4686D	73/74	deleterious(0)	MODERATE
M101740	BMPR1A	4	34569377	34569377	chr10:86912268-86912268	Missense_Mutation	C	C	T	0.572	p.R187C	7/12	tolerated(0.06)	MODERATE
M122308	BMPR1A	4	34551910	34551910	chr10:86890088-86890088	Missense_Mutation	G	G	A	0.465	p.G32S	3/12	tolerated_low_confidence(0.09)	MODERATE
M99876	BMPR1A	4	34576870	34576870	chr10:86921555-86921555	Missense_Mutation	G	G	T	0.083	p.R401L	10/12	deleterious(0)	MODERATE
M73441	BRCA1	9	19986741	19986741	chr17:43093121-43093121	Missense_Mutation	C	C	A	0.046	p.L845M	10/23	tolerated(0.13)	MODERATE
M101740	BRCA2	25	7777437	7777437	chr13:32332667-	Missense_Mutation	C	C	T	0.62	p.D388N	10/27	deleterious(0.02)	MODERATE

					32332667									
M108735	BRCA2	25	7771723	7771723	chr13:32340005-32340005	Missense_Mutation	T	T	C	0.4	p.T1910A	11/27	tolerated(0.1)	MODERATE
M121064	BRCA2	25	7761258	7761258	chr13:32354874-32354874	Missense_Mutation	G	G	A	0.464	p.R2358W	14/27	deleterious(0.02)	MODERATE
M69965	BRCA2	25	7771953	7771953	chr13:32339796-32339796	Missense_Mutation	G	G	A	0.44	p.A1833V	11/27	tolerated(0.63)	MODERATE
M73441	BRCA2	25	7787768	7787768	chr13:32325119-32325119	Missense_Mutation	C	C	A	0.064	p.M114I	4/27	tolerated(0.09)	MODERATE
M99876	BRCA2	25	7760304	7760304	chr13:32356505-32356505	Missense_Mutation	G	G	T	0.053	p.P2524T	15/27	deleterious(0)	MODERATE

M99876	BRCA2	25	7770633	7770633	chr13:32341122-32341122	Missense_Mutation	C	C	A	0.04	p.C2273F	11/27	deleterious(0)	MODERATE
M99876	BRCA2	25	7770765	7770765	chr13:32340990-32340990	Missense_Mutation	C	C	A	0.73	p.C2229F	11/27	tolerated(0.35)	MODERATE
M101740	BRD3	9	50293226	50293226	chr9:134034754-134034754	Missense_Mutation	C	C	T	0.352	p.R673Q	11/12	deleterious(0.04)	MODERATE
M73441	BRD3	9	50297490	50297490	chr9:134040086-134040086	Missense_Mutation	G	G	T	0.286	p.Q533K	9/12	tolerated(0.79)	MODERATE
M99876	BRD3	9	50297492	50297492	chr9:134040088-134040088	Missense_Mutation	G	G	T	0.333	p.A532D	9/12	tolerated(0.58)	MODERATE
M99876	BRD3	9	50297527	50297527	chr9:134040123-134040123	Missense_Mutation	C	C	A	0.4	p.E520D	9/12	tolerated(0.36)	MODERATE

M99876	BRIP1	9	34958264	34958264	chr17:61716003-61716003	Missense_Mutation	C	C	A	0.099	p.R813S	16/21	tolerated(0.59)	MODERATE
M99876	BTK	X	75277936	75277936	chrX:101357551-101357551	Missense_Mutation	G	G	T	0.077	p.Q407K	13/19	tolerated(0.6)	MODERATE
M99876	BUB1B	30	7401048	7401048	chr15:40210210-40210210	Missense_Mutation	G	G	T	0.1	p.K796N	19/24	deleterious(0.02)	MODERATE
M99876	CAMTA1	5	61398362	61398362	chr1:77324778-77324778	Missense_Mutation	G	G	T	0.065	p.R982L	12/23	deleterious(0.01)	MODERATE
M121064	CARD11	6	14328477	14328477	chr7:29101444-29101444	Missense_Mutation	G	G	T	0.464	p.A1056S	24/25	tolerated(0.11)	MODERATE
M99876	CBFA2T3	5	64463747	64463747	chr16:88941356-88941356	Missense_Mutation	G	G	T	0.333	p.G270C	1/12	deleterious_low_confidence(0)	MODERATE

M113164	CBL	5	14658505	14658505	NA	Missense_Mutation	T	T	G	0.333	p.K11T	1/17		MODERATE
M121010	CBL	5	14624444	14624444	chr11:11927 8256-11927 8256	Missense_Mutation	A	A	G	0.125	p.C392R	8/17	deleterious(0)	MODERATE
M121047	CBL	5	14624444	14624444	chr11:11927 8256-11927 8256	Missense_Mutation	A	A	G	0.454	p.C392R	8/17	deleterious(0)	MODERATE
M121047	CBL	5	14676864	14676864	chr11:11920 6462-11920 6462	Frame_Shift_Del	G	G	-	0.464	p.G16Afs*12	1/18		HIGH
M58698	CBL	5	14624520	14624520	chr11:11927 8180-11927 8180	Missense_Mutation	T	T	G	0.586	p.L366F	8/17	deleterious(0)	MODERATE
M71593	CBL	5	14624444	14624444	chr11:11927 8256-11927 8256	Missense_Mutation	A	A	G	0.899	p.C392R	8/17	deleterious(0)	MODERATE

M99876	CBL	5	146240002	146240002	chr11:119278708-119278708	Missense_Mutation	C	C	A	0.053	p.A472S	9/17	tolerated(0.67)	MODERATE
M108089	CBLB	33	112801138	112801143	chr3:105670240-105670245	In_Frame_Del	TGAAGG	TGAAGG	-	0.386	p.P915_S916del	19/20		MODERATE
M108735	CBLB	33	112801138	112801143	chr3:105670240-105670245	In_Frame_Del	TGAAGG	TGAAGG	-	0.455	p.P915_S916del	19/20		MODERATE
M99876	CBLB	33	113621118	113621118	chr3:105751462-105751462	Missense_Mutation	C	C	A	0.329	p.Q262H	6/20	deleterious(0)	MODERATE
L52744	CCND1	18	48515779	48515779	chr11:69636917-69636917	Missense_Mutation	G	G	T	0.25	p.P76H	1/5	deleterious(0.02)	MODERATE
M114677	CCND1	18	48515966	48515966	chr11:69636731-69636731	Missense_Mutation	C	C	A	0.286	p.A14S	1/5	tolerated_low_confidenc	MODERATE

													e(0.46)	
M58698	CCND1	18	48515948	48515948	chr11:69636749-69636749	Missense_Mutation	C	C	T	0.754	p.A20T	1/5	deleterious_low_confidence(0)	MODERATE
M70848	CCND1	18	48509683	48509683	chr11:69643032-69643032	Missense_Mutation	A	A	C	0.105	p.V103G	2/5	deleterious(0)	MODERATE
M70848	CCND1	18	48509686	48509686	chr11:69643029-69643029	Splice_Site	T	T	G	0.111	p.X103_splice			HIGH
M108089	CCND3	12	10595363	10595363	chr6:41936422-41936422	Missense_Mutation	A	A	C	0.333	p.L350V	5/5	deleterious_low_confidence(0)	MODERATE
M121010	CCND3	12	10595272	10595272	chr6:41936331-41936331	Missense_Mutation	G	G	C	0.333	p.A380G	5/5		MODERATE

M101740	CDC73	38	58061 00	58061 00	NA	Missense_Mutation	C	C	A	0.4	p.R505L	16/16		MODERATE
M99876	CDH1	5	80784 451	80784 451	chr16:68801870-68801870	Missense_Mutation	G	G	T	0.222	p.H126N	3/16	tolerated(0.2)	MODERATE
M120655	CDKN1A	12	57467 83	57467 83	chr6:36678527-36678527	Missense_Mutation	G	G	A	0.337	p.C74Y	1/2		MODERATE
M99876	CDKN1A	12	57466 86	57466 86	chr6:36678453-36678453	Missense_Mutation	G	G	T	0.286	p.G42W	1/2		MODERATE
M52097	CDKN1B	27	33611 784	33611 785	chr12:12718921-12718922	Frame_Shift_Ins	-	-	AAGCCCCT	0.599	p.L193Afs*?	2/2		HIGH
M99876	CHD4	27	38431 476	38431 476	chr12:6583215-6583215	Missense_Mutation	G	G	T	0.041	p.G1348V	26/39	tolerated(0.2)	MODERATE

M99876	CHD4	27	38434614	38434614	chr12:65781128-65781128	Missense_Mutation	C	C	A	0.075	p.S1710Y	36/39	deleterious(0)	MODERATE
M108735	CIC	1	1.12E+08	1.12E+08	chr19:42274043-42274043	Missense_Mutation	G	G	T	0.4	p.H737N	2/21	deleterious_low_confidence(0.02)	MODERATE
M120486	CIC	1	1.12E+08	1.12E+08	chr19:42273518-42273518	Missense_Mutation	A	A	G	0.333	p.S562P	2/21	deleterious(0.02)	MODERATE
M120655	CIC	1	1.12E+08	1.12E+08	chr19:42273069-42273069	Missense_Mutation	G	G	A	0.286	p.P412L	2/21	deleterious_low_confidence(0.01)	MODERATE
M71679	CIC	1	1.12E+08	1.12E+08	chr19:42272973-42272973	Missense_Mutation	C	C	A	0.282	p.C380F	2/21	tolerated_low_confidence(0.09)	MODERATE

M99876	CIC	1	1.12E+08	1.12E+08	chr19:42273810-42273810	Missense_Mutation	G	G	T	0.333	p.P659Q	2/21	deleterious_low_confidence(0.01)	MODERATE
M99876	CIC	1	1.12E+08	1.12E+08	chr19:42273582-42273582	Missense_Mutation	G	G	T	0.286	p.A583D	2/21	deleterious(0)	MODERATE
M99876	CIC	1	1.12E+08	1.12E+08	chr19:42273560-42273560	Nonsense_Mutation	C	C	A	0.286	p.E576*	2/21		HIGH
M99876	CIC	1	1.12E+08	1.12E+08	chr19:42273192-42273192	Missense_Mutation	G	G	T	0.286	p.A453D	2/21	deleterious(0.01)	MODERATE
M99876	CIC	1	1.12E+08	1.12E+08	chr19:42272704-42272704	Missense_Mutation	C	C	A	0.286	p.Q291H	2/21	tolerated_low_confidence(0.23)	MODERATE
M70848	CIITA	6	31781419	31781419	chr16:10915578-	Missense_	G	G	A	0.625	p.S1042L	14/20	deleterious(0)	MODERATE

					10915578	Mutation								
M99876	CIITA	6	31821030	31821030	chr16:10866505-10866505	Missense_Mutation	C	C	A	0.4	p.L72F	1/20	deleterious(0.05)	MODERATE
M58697	CLIP1	26	7045416	7045417	chr12:122328323-122328324	Frame_Shift_Ins	-	-	CAGGTATTGTGGTCCCGCCGCACCATTGTGCGCCGTAGCGGCCCGAGCGGGTCGCGGTCCTCGCGGGAGCCCGAGC	0.136	p.E992Vfs*32	16/27		HIGH

									CCA CCC					
M99876	CLTC	9	34173948	34173948	chr17:59685114-59685114	Missense_Mutation	G	G	T	0.271	p.R1498L	29/33	deleterious(0.05)	MODERATE
M99876	CLTCL1	26	29959123	29959123	chr22:19229887-19229887	Missense_Mutation	G	G	T	0.056	p.G578V	11/1	deleterious(0)	MODERATE
M99876	CLTCL1	26	29988814	29988814	chr22:19199797-19199797	Missense_Mutation	G	G	T	0.072	p.Q1270H	24/32	deleterious(0.05)	MODERATE

M58698	CNBP	20	29262 86	29263 83	chr3:1 29171 541- 12917 1635	Splice _Site	AGG TATT TTTG TCG AAT AAA AAA TTTT GAA GTG CTTC AGT ATCT ATTA GTGT CAA GAC TGGT CTA ATTA GCC AAA TTCT TTTT GTTT CTGC CCA AAA T	AGG TATT TTTG TCG AAT AAA AAA TTTT GAA GTG CTTC AGT ATCT ATTA GTGT CAA GAC TGGT CTA ATTA GCC AAA TTCT TTTT GTTT CTGC CCA AAA T	-	0.222	p.X42 _splic e	2/5		HIGH
M99876	CNBP	20	29264 33	29264 33	chr3:1 29171 491-	Misse nse_	G	G	T	0.086	p.G58 C	3/5	delete rious(0)	MOD ERAT E

					129171491	Mutation								
M99876	CNBP	20	29282 77	29282 77	chr3:129170509-129170509	Missense_Mutation	C	C	A	0.051	p.R160S	5/5	tolerated(0.12)	MODERATE
M99876	CNOT3	1	1.03E+08	1.03E+08	chr19:54152626-54152626	Missense_Mutation	C	C	A	0.099	p.R635L	14/16	deleterious(0)	MODERATE
M99876	CNTNAP2	16	42083 44	42083 44	chr7:146116949-146116949	Missense_Mutation	C	C	A	0.286	p.A25S	1/24	tolerated(0.93)	MODERATE
L105585	CNTRL	11	74120 055	74120 055	chr9:121135983-121135983	Splice_Site	G	G	T	0.282	p.X735_splice			HIGH
M101740	CNTRL	11	74156 305	74156 305	chr9:121177432-121177432	Missense_Mutation	G	G	A	0.4	p.G2500S	42/42		MODERATE

M71281	CNTRL	11	74155828	74155828	NA	Missense_Mutation	G	G	A	0.373	p.R2391Q	41/42		MODERATE
M73441	CNTRL	11	74156324	74156324	chr9:121177451-121177451	Missense_Mutation	C	C	A	0.282	p.P2506Q	42/42		MODERATE
M99876	COL1A1	9	26199834	26199834	chr17:50201508-50201508	Missense_Mutation	G	G	T	0.222	p.F2L	1/1	tolerated_low_confidence(0.11)	MODERATE
M114337	COL3A1	36	30536595	30536595	NA	Missense_Mutation	G	G	T	0.282	p.D1484Y	52/52		MODERATE
M121010	COL3A1	36	30509443	30509443	chr2:188995050-188995050	Frame_Shift_Del	C	C	-	0.137	p.A487Dfs*49	21/52		HIGH
M121064	COL3A1	36	30498688	30498688	chr2:188984799-188984799	Missense_Mutation	C	C	A	0.403	p.A40E	2/1	tolerated(0.31)	MODERATE

M99876	COL3A1	36	30507924	30507924	chr2:188993424-188993424	Nonsense_Mutation	G	G	T	0.149	p.G372*	16/52		HIGH
M99876	COL3A1	36	30512609	30512609	chr2:188998675-188998675	Missense_Mutation	G	G	T	0.061	p.G660V	29/52	deleterious(0)	MODERATE
M121064	CREB1	37	15977329	15977329	chr2:207596915-207596915	Nonsense_Mutation	G	G	T	0.291	p.E295*	8/8		HIGH
L114148	CREBBP	6	37526532	37526532	chr16:3736714-3736714	Missense_Mutation	T	T	C	0.429	p.L1502P	27/31	deleterious(0)	MODERATE
L52744	CREBBP	6	37490898	37490898	chr16:3782726-3782726	Nonsense_Mutation	C	C	T	0.886	p.Q511*	6/1		HIGH
M118542	CREBBP	6	37530378	37530379	chr16:3731299-3731300	Frame_Shift_Ins	-	-	CTGTG	0.354	p.M1694Cfs*55	30/31		HIGH

M71335	CREBBP	6	37481568	37481568	chr16:3793446-3793446	Nonsense_Mutation	C	C	T	0.282	p.R386*	4/1		HIGH
M73441	CREBBP	6	37527024	37527024	chr16:3736045-3736045	Missense_Mutation	G	G	T	0.08	p.E1576D	28/31	tolerated(0.14)	MODERATE
M73441	CREBBP	6	37532564	37532564	chr16:3729339-3729339	Missense_Mutation	C	C	A	0.045	p.P1906Q	31/31	deleterious(0.02)	MODERATE
M99876	CREBBP	6	37490710	37490710	chr16:3782914-3782914	Missense_Mutation	C	C	A	0.119	p.S448Y	6/1	tolerated(0.12)	MODERATE
M69965	CRNKL1	24	3306051	3306051	chr20:20040733-20040733	Missense_Mutation	C	C	G	0.473	p.Q461E	10/14	tolerated(0.13)	MODERATE
M121064	CRTC1	20	44328581	44328581	chr19:18768630-18768630	Missense_Mutation	G	G	A	0.625	p.P406L	11/15	tolerated_low_confidenc	MODERATE

													e(0.93)	
M108735	CRTC3	3	53567300	53567300	chr15:90638513-90638513	Missense_Mutation	G	G	T	0.3	p.P421Q	11/14	tolerated(0.08)	MODERATE
L114148	CSMD3	13	13398000	13398000	chr8:113278645-113278645	Missense_Mutation	C	C	T	0.349	p.R154H	3/1	tolerated(0.6)	MODERATE
M69965	CSMD3	13	12769535	12769535	chr8:112638750-112638750	Missense_Mutation	G	G	A	0.547	p.R1158C	21/71	deleterious(0)	MODERATE
M73441	CSMD3	13	12628238	12628238	chr8:112472614-112472614	Missense_Mutation	G	G	T	0.083	p.S1791Y	32/71	tolerated(1)	MODERATE
M99876	CSMD3	13	12473844	12473844	chr8:112306019-112306019	Missense_Mutation	G	G	T	0.056	p.P2687T	51/71	deleterious(0.03)	MODERATE

M99876	CSMD3	13	12473856	12473856	chr8:112306031-112306031	Missense_Mutation	G	G	T	0.059	p.H2683N	51/71	tolerated(0.6)	MODERATE
M99876	CSMD3	13	12474017	12474017	chr8:112306192-112306192	Missense_Mutation	G	G	T	0.22	p.A2629E	51/71	deleterious(0)	MODERATE
L114182	CTCF	5	81833602	81833603	chr16:67611442-67611443	Frame_Shift_Ins	-	-	T	0.133	p.T204Nfs*24	2/11		HIGH
M120399	CTCF	5	81825464	81825464	chr16:67620743-67620743	Missense_Mutation	G	G	A	0.115	p.P378L	5/11	deleterious(0)	MODERATE

L114182	CTNNA1	11	26346481	26346482	chr5:138827719-138827720	Splice_Site	-	-	CTGGACGTAAAGAAAGAAGTGATGCACTCAATTCTGCCATAGATAAAATGACCAAGAAGACAAGGGAC	0.403	p.X366_splice			HIGH

L114182	CTNNA1	11	26456768	26456875	chr5:138930654-138930828	Splice_Site	GGTGAGCTGCGCCGCCTGGGTGCCCACCCTGTGCTCCGCGGCCGGCCCCTTCTTCCCCTTCACCGTCAGCACACAGTGATCTTTGCTCTCTTTGTCA	GGTGAGCTGCGCCGCCTGGGTGCCCACCCTGTGCTCCGCGGCCGGCCCCTTCTTCCCCTTCACCGTCAGCACACAGTGATCTTTGCTCTCTTTGTCA	-	0.096	p.X743_splice	15/18		HIGH

M120655	CTNNA1	11	26456768	26456875	chr5:138930654-138930828	Splice_Site	GGTGAGCTGCGCCGCCTGGGTGCCACCCTGTGCTCCGCGGCCGGCCCCTTCTTCCCCTTCACCGTCAGCACACAGTGATCTTTGCTCTCTTTGTCA	GGTGAGCTGCGCCGCCTGGGTGCCACCCTGTGCTCCGCGGCCGGCCCCTTCTTCCCCTTCACCGTCAGCACACAGTGATCTTTGCTCTCTTTGTCA	-	0.081	p.X743_splice	15/18		HIGH

M99876	CTNNA1	11	26458669	26458669	chr5:138934045-138934045	Missense_Mutation	C	C	A	0.077	p.P905T	18/18	deleterious(0)	MODERATE
U69959	CTNNA1	11	26456768	26456875	chr5:138930654-138930828	Splice_Site	GGTGAGCTGCGCCGCCCTGGGTGCCGGCCCACCCTGTGCTCCGCGGCCGGCCCCTTCTTCCCCTTCACCGTCAGCCACACAGTGAT	GGTGAGCTGCGCCGCCCTGGGTGCCGGCCCACCCTGTGCTCCGCGGCCGGCCCCTTCTTCCCCTTCACCGTCAGCCACACAGTGAT	-	0.096	p.X743_splice	15/18		HIGH

							GCTCTCTTTTGTCA	GCTCTCTTTTGTCA						
M99876	CTNNA2	17	43578999	43578999	chr2:80555842-80555842	Missense_Mutation	C	C	A	0.066	p.G564C	12/19	tolerated(0.16)	MODERATE
L114148	CTNND2	34	3046699	3046700	chr5:113851154-113851155	Missense_Mutation	GT	GT	CG	0.173	p.F232V	7/23		MODERATE
M121064	CTNND2	34	3309167	3309167	chr5:111109 35-	Missense_	G	G	A	0.572	p.G792S	14/23	tolerated(0.57)	MODERATE

					11110935	Mutation								
L53739	CUL3	25	37733627	37733627	chr2:224474327-224474327	Missense_Mutation	T	T	G	0.286	p.K720T	15/15	deleterious(0)	MODERATE
M120378	CUL3	25	37739943	37739943	chr2:224482038-224482038	Missense_Mutation	A	A	C	0.05	p.V606G	13/15	tolerated(0.18)	MODERATE
M99876	CYLD	2	64621674	64621674	chr16:50749739-50749739	Missense_Mutation	G	G	T	0.085	p.P14H	2/18	deleterious_low_confidence(0.01)	MODERATE
L114148	DAXX	12	2759228	2759228	chr6:33321822-33321822	Missense_Mutation	T	T	C	0.333	p.Q35R	2/8	tolerated(1)	MODERATE
M99876	DCC	1	21823469	21823469	chr18:53499430-53499430	Missense_Mutation	C	C	A	0.052	p.S1313I	26/28	deleterious(0.01)	MODERATE

M99876	DCTN1	17	48755065	48755065	chr2:74365155-74365155	Missense_Mutation	G	G	T	0.11	p.S1039I	26/32	tolerated(0.15)	MODERATE
M99876	DCTN1	17	48756886	48756886	chr2:74363415-74363415	Missense_Mutation	G	G	T	0.222	p.G1075V	28/32	tolerated(0.48)	MODERATE
M99876	DDR2	38	20036007	20036007	chr1:162755688-162755688	Missense_Mutation	G	G	T	0.077	p.P208Q	6/17	deleterious(0)	MODERATE
M99876	DDX10	5	23890740	23890740	chr11:108706776-108706776	Missense_Mutation	G	G	T	0.182	p.P421T	10/18	deleterious(0)	MODERATE
L114148	DDX3X	X	35769160	35769160	chrX:41343775-41343775	Missense_Mutation	A	A	C	0.568	p.S240R	8/17	deleterious(0)	MODERATE
M120398	DGCR8	26	29251643	29251648	chr22:20090116-20090121	In_Frame_Del	AACTCC	AACTCC	-	0.44	p.L388_E389del	5/14		MODERATE

M99876	DGCR8	26	29255674	29255674	chr22:20086126-20086126	Missense_Mutation	C	C	A	0.069	p.G55C	2/14	deleterious_low_confidence(0)	MODERATE
M108089	DICER1	8	63980973	63980973	chr14:95096597-95096597	Missense_Mutation	A	A	C	0.345	p.D1442E	22/27	tolerated_low_confidence(0.11)	MODERATE
M73441	DICER1	8	64016010	64016010	chr14:95133345-95133345	Missense_Mutation	A	A	T	0.167	p.H38Q	1/27	deleterious(0.01)	MODERATE
M73441	DICER1	8	64016017	64016018	chr14:95133352-95133353	Missense_Mutation	GC	GC	TT	0.167	p.A36K	1/27	tolerated(0.41)	MODERATE
M99876	DICER1	8	63988580	63988580	chr14:95104106-95104106	Missense_Mutation	C	C	A	0.115	p.G1097V	20/27	deleterious(0)	MODERATE
M121047	DNAJB1	20	48121500	48121500	chr19:14527816-	Missense_Mutation	T	T	C	0.333	p.V41A	1/3	tolerated(1)	MODERATE

					14527816									
M71593	DNM2	20	50420117	50420117	chr19:10803646-10803646	Missense_Mutation	A	A	G	0.286	p.Y501H	13/22	tolerated(0.54)	MODERATE
M115951	DNMT3A	17	19504277	19504277	chr2:25247692-25247692	Missense_Mutation	A	A	G	0.333	p.W290R	6/21	deleterious(0)	MODERATE
M73441	DNMT3A	17	19504328	19504328	chr2:25247743-25247743	Missense_Mutation	G	G	A	0.286	p.R273W	6/21	deleterious(0)	MODERATE
M99876	DNMT3A	17	19504300	19504300	chr2:25247715-25247715	Missense_Mutation	C	C	A	0.4	p.W282L	6/21	deleterious(0.03)	MODERATE

M120655	EBF1	4	51731054	51731055	chr5:158731069-158731070	Frame_Shift_Ins	-	-	GGTCAGGATACTTCTTTTTTTTTTTGTTTGTTTTTGTTTTTTTTTTTTTTTT	0.255		11/16		HIGH
M52097	EIF1AX	X	16090837	16090837	chrX:20133970-20133970	Missense_Mutation	T	T	C	0.286	p.L84P	3/6	deleterious(0)	MODERATE
L114148	EIF4A2	34	19408119	19408119	chr3:186854393-186854393	Missense_Mutation	C	C	T	0.339	p.H151Y	3/3	deleterious(0)	MODERATE
M73441	EIF4A2	34	19406627	19406627	chr3:186853075-	Missense_Mutation	C	C	T	0.166	p.A15V	2/3	tolerated(0.6)	MODERATE

					18685 3075								
M114 677	ELF4	X	1.01E +08	1.01E +08	chrX: 13007 1199- 13007 1199	Frame _Shift _Del	G	G	-	0.941	p.A21 8Gfs* 44	7/9		HIGH
M713 35	ELF4	X	1.01E +08	1.01E +08	chrX: 13007 1146- 13007 1147	Frame _Shift _Ins	-	-	T	0.287	p.E23 6Rfs* 25	7/9		HIGH
M998 76	ELF4	X	1.01E +08	1.01E +08	chrX: 13007 2283- 13007 2283	Nonse nse_ Mutati on	C	C	A	0.078	p.E16 0*	5/9		HIGH
M119 591	ELL	20	44494 917	44494 917	chr19: 18543 540- 18543 540	Misse nse_ Mutati on	G	G	T	0.213	p.R31 L	1/10	tolerat ed_lo w_con fidenc e(0.11)	MOD ERAT E
M121 064	ELL	20	44500 416	44500 416	chr19: 18537 665- 18537 665	Misse nse_ Mutati on	G	G	A	0.538	p.R33 9H	7/10	tolerat ed(0.2 2)	MOD ERAT E

M99876	ELL	20	44498842	44498842	chr19:18539631-18539631	Missense_Mutation	C	C	A	0.079	p.Q173K	4/10	tolerated(0.89)	MODERATE
M73441	ELN	6	6304242	6304242	chr7:74063695-74063695	Missense_Mutation	C	C	A	0.25	p.G486C	24/27	deleterious_low_confidence(0)	MODERATE
M99876	ELN	6	6331279	6331279	chr7:74028233-74028233	Missense_Mutation	G	G	T	0.286	p.L16I	1/27	deleterious_low_confidence(0)	MODERATE
M99876	ELN	6	6331282	6331282	chr7:74028230-74028230	Missense_Mutation	G	G	C	0.286	p.L15V	1/27	deleterious_low_confidence(0)	MODERATE
M99876	EML4	17	33862980	33862980	chr2:42264705-42264705	Splice_Site	G	G	T	0.247	p.X228_splice			HIGH
M108735	EP300	10	24079851	24079851	chr22:41176827-41176827	Nonsense_Mutation	C	C	A	0.107	p.E1683*	30/30		HIGH

M73441	EP300	10	24113185	24113185	chr22:41141115-41141115	Missense_Mutation	C	C	A	0.084	p.R650M	10/30	deleterious(0.02)	MODERATE
M99876	EPS15	15	9856331	9856331	chr1:51406015-51406015	Missense_Mutation	G	G	T	0.078	p.A512S	15/24	tolerated(0.66)	MODERATE
M121064	ERBB2	9	22769291	22769291	chr17:39717481-39717481	Splice_Site	C	C	T	0.399	p.X636_splice			HIGH
M108735	ERBB3	10	412960	412960	chr12:56087834-56087834	Missense_Mutation	G	G	A	0.286	p.C218Y	6/29	deleterious(0)	MODERATE
M108735	ERBB3	10	413041	413041	chr12:56087915-56087915	Splice_Site	T	T	C	0.333	p.X244_splice			HIGH
M120655	ERBB3	10	412060	412060	chr12:56086580-56086580	Missense_Mutation	C	C	A	0.286	p.H157Q	4/29	deleterious(0.03)	MODERATE

M121010	ERBB3	10	413008	413008	chr12:56087882-56087882	Missense_Mutation	G	G	T	0.4	p.G234V	6/29	deleterious(0)	MODERATE
M122308	ERBB3	10	410684	410684	chr12:56083874-56083874	Missense_Mutation	G	G	A	0.329	p.G69E	2/1	tolerated(1)	MODERATE
M70848	ERBB3	10	412988	412988	chr12:56087862-56087862	Nonsense_Mutation	C	C	A	0.286	p.C227*	6/29		HIGH
M99876	ERBB3	10	412023	412023	chr12:56086543-56086543	Missense_Mutation	G	G	T	0.25	p.G145V	4/29	deleterious(0)	MODERATE
M73441	ERBB4	37	19040923	19040923	chr2:211387000-211387000	Missense_Mutation	G	G	A	0.556	p.R1128C	28/29	deleterious(0.02)	MODERATE
M73441	ERBB4	37	19041864	19041864	chr2:211387973-211387973	Missense_Mutation	G	G	T	0.054	p.P1068H	27/29	tolerated(0.12)	MODERATE

M120398	ERCC2	1	1.1E+08	1.1E+08	chr19:45353191-45353191	Missense_Mutation	A	A	G	0.548	p.M610V	18/18	tolerated(1)	MODERATE
M99876	ERCC2	1	1.1E+08	1.1E+08	chr19:45352932-45352932	Missense_Mutation	G	G	T	0.2	p.S691I	18/18	deleterious_low_confidence(0)	MODERATE
M121064	ETV4	9	19716289	19716289	chr17:43545310-43545310	Missense_Mutation	A	A	T	0.411	p.M40L	3/14	tolerated(0.43)	MODERATE
M99876	ETV4	9	19726320	19726320	chr17:43532755-43532755	Missense_Mutation	C	C	A	0.115	p.Q239K	8/14	tolerated(0.93)	MODERATE
M58697	ETV5	34	18788925	18788925	chr3:186109080-186109080	Missense_Mutation	G	G	T	0.333	p.S27R	1/13		MODERATE
L110446	EWSR1	26	22594342	22594342	chr22:29288779-29288779	Missense_Mutation	G	G	A	0.333	p.G329R	9/18	tolerated(0.64)	MODERATE

M101740	EWSR1	26	22594324	22594324	chr22:29288761-29288761	Missense_Mutation	C	C	T	0.333	p.R323W	9/18	tolerated(0.11)	MODERATE
M108089	EWSR1	26	22606455	22606455	chr22:29298783-29298783	Missense_Mutation	C	C	G	0.286	p.R495G	15/18	tolerated(0.33)	MODERATE
M115951	EWSR1	26	22594274	22594274	chr22:29288711-29288711	Missense_Mutation	G	G	T	0.333	p.R306L	9/18	tolerated(0.67)	MODERATE
M120655	EWSR1	26	22594294	22594294	chr22:29288731-29288731	Missense_Mutation	T	T	C	0.333	p.F313L	9/18	tolerated(0.19)	MODERATE
M71679	EWSR1	26	22589411	22589411	chr22:29278171-29278171	Missense_Mutation	C	C	T	0.4	p.A129V	6/18	deleterious(0)	MODERATE
L107858	EZH2	16	1991694	1991694	chr7:148807678-148807678	Missense_Mutation	G	G	A	0.429	p.V833M	22/22	deleterious(0)	MODERATE

M121064	EZR	1	48161827	48161827	chr6:158767451-158767451	Missense_Mutation	G	G	T	0.396	p.A469D	12/13	tolerated(0.15)	MODERATE
M73441	FAM131B	16	6335864	6335864	chr7:143360183-143360183	Missense_Mutation	G	G	T	0.063	p.G27V	1/7	deleterious_low_confidence(0)	MODERATE
M70848	FAM135B	13	33418762	33418762	chr8:138152673-138152673	Missense_Mutation	C	C	T	0.381	p.R600H	12/19	tolerated(0.56)	MODERATE
M73441	FANCA	5	63792736	63792736	chr16:89792476-89792476	Missense_Mutation	C	C	A	0.059	p.R357S	12/1	deleterious(0.01)	MODERATE
M101740	FANCF	21	44255199	44255199	NA	Missense_Mutation	C	C	T	0.579	p.A474T	1/1		MODERATE
M99876	FANCG	11	51658321	51658321	chr9:350786611-350786611	Nonsense_Mutation	C	C	A	0.037	p.E285*	3/14		HIGH

M103733	FAS	26	38738528	38738528	NA	Missense_Mutation	G	G	T	0.333	p.E306D	1/10		MODERATE
M114677	FAS	26	38738497	38738497	NA	Missense_Mutation	C	C	A	0.333	p.A296E	1/10		MODERATE
M58697	FAS	26	38738236	38738236	NA	Missense_Mutation	C	C	G	0.75	p.P209R	1/10		MODERATE
M99876	FAS	26	38738239	38738239	NA	Missense_Mutation	C	C	T	0.214	p.A210V	1/10		MODERATE
M99876	FAS	26	38738377	38738377	NA	Missense_Mutation	C	C	A	0.222	p.A256D	1/10		MODERATE
M70848	FAT1	16	44212626	44212626	chr4:186618854-186618854	Missense_Mutation	G	G	A	0.378	p.A2601T	10/29	tolerated(0.29)	MODERATE
M71679	FAT1	16	44213596	44213596	chr4:186617884-	Missense_Mutation	C	C	T	0.438	p.T2924M	10/29	tolerated(0.11)	MODERATE

					18661 7884									
M998 76	FAT1	16	44221 410	44221 410	chr4:1 86609 315-18660 9315	Misse nse_ Mutati on	G	G	T	0.105	p.M33 84I	16/29	tolerat ed(0.6)	MOD ERAT E
M115 951	FAT3	21	78010 32	78010 32	chr11: 92798 426-92798 426	Misse nse_ Mutati on	T	T	A	0.422	p.S18 28C	10/28	tolerat ed(0.1 8)	MOD ERAT E
M734 41	FAT3	21	77367 75	77367 75	chr11: 92867 187-92867 187	Misse nse_ Mutati on	G	G	T	0.197	p.S40 58R	22/28	tolerat ed(0.0 8)	MOD ERAT E
M734 41	FAT3	21	77638 72	77638 72	chr11: 92837 670-92837 670	Misse nse_ Mutati on	C	C	A	0.102	p.G34 34V	17/28	tolerat ed(0.0 5)	MOD ERAT E
L1078 58	FAT4	19	15159 841	15159 841	chr4:1 25490 849-12549 0849	Misse nse_ Mutati on	G	G	A	0.463	p.P46 77L	17/17	delete rious(0.01)	MOD ERAT E

M121010	FAT4	19	15255302	15255302	chr4:125398868-125398868	Missense_Mutation	C	C	T	0.385	p.G1754S	2/17	tolerated(0.15)	MODERATE
M71281	FAT4	19	15330763	15330763	chr4:125317694-125317694	Missense_Mutation	C	C	T	0.165	p.R428H	1/17	deleterious(0)	MODERATE
M71593	FAT4	19	15159132	15159133	chr4:125491557-125491558	Frame_Shift_Ins	-	-	C	0.473	p.A4914Cfs*2	17/17		HIGH
M122308	FBLN2	20	3875019	3875019	chr3:135704420-135704420	Missense_Mutation	C	C	T	0.333	p.P22L	1/17	tolerated(0.38)	MODERATE
M99876	FBLN2	20	3932447	3932447	chr3:136364465-136364465	Missense_Mutation	G	G	T	0.027	p.G1076C	16/17	deleterious(0)	MODERATE
L52744	FBXW7	15	50416501	50416501	chr4:152535372-152535372	Missense_Mutation	C	C	T	0.286	p.G232D	1/3	deleterious_low_confidence(0)	MODERATE

L53739	FBXW7	15	50416414	50416414	chr4:152535284-152535284	Missense_Mutation	C	C	A	0.334	p.G261V	1/3	deleterious_low_confidence(0)	MODERATE
L53739	FBXW7	15	50416963	50416964	chr4:152535835-152535836	In_Frame_Ins	-	-	GGCTCC	0.426	p.S77_P78insRS	1/3		MODERATE
M121047	FBXW7	15	50416919	50416919	chr4:152535790-152535790	Missense_Mutation	T	T	C	0.329	p.R93G	1/3	tolerated_low_confidence(0.68)	MODERATE
M122308	FBXW7	15	50416777	50416777	chr4:152535647-152535647	Missense_Mutation	G	G	T	0.333	p.T140K	1/3	deleterious_low_confidence(0)	MODERATE
M69965	FBXW7	15	50416963	50416964	chr4:152535835-152535836	In_Frame_Ins	-	-	GGCTCC	0.28	p.S77_P78insRS	1/3		MODERATE
M73441	FBXW7	15	50417168	50417168	chr4:152536052-	Missense_Mutation	C	C	A	0.286	p.D10Y	1/3	deleterious_low_c	MODERATE

					15253 6052								onfide nce(0)	
M998 76	FBX W7	15	50189 324	50189 324	chr4:1 52322 904-15232 2904	Misse nse_ Mutati on	C	C	A	0.029	p.D74 8Y	11/11	delete rious(0)	MOD ERAT E
M998 76	FBX W7	15	50282 320	50282 320	chr4:1 52411 830-15241 1830	Misse nse_ Mutati on	G	G	T	0.049	p.Q34 K	1/11	delete rious_ low_c onfide nce(0)	MOD ERAT E
M121 064	FCRL 4	7	40653 450	40653 450	chr1:1 57586 201-15758 6201	Misse nse_ Mutati on	G	G	A	0.55	p.A36 1T	6/12	tolerat ed(0.0 7)	MOD ERAT E
M998 76	FEN1	18	54681 769	54681 769	chr11: 61796 495-61796 495	Misse nse_ Mutati on	C	C	A	0.09	p.R37 8S	1/1	delete rious(0.01)	MOD ERAT E
M998 76	FEN1	18	54682 383	54682 383	chr11: 61795 881-61795 881	Misse nse_ Mutati on	C	C	A	0.1	p.A17 4S	1/1	delete rious(0.01)	MOD ERAT E

M99876	FES	3	53351618	53351618	chr15:90889922-90889922	Missense_Mutation	C	C	A	0.071	p.D335Y	8/19	deleterious(0)	MODERATE
M99876	FES	3	53356058	53356058	chr15:90885078-90885078	Missense_Mutation	C	C	A	0.396	p.Q11H	2/19	deleterious(0.02)	MODERATE
L71592	FGFR3	3	62315053	62315053	chr4:180296969-18029969	Missense_Mutation	G	G	T	0.4	p.S317Y	6/16	deleterious(0)	MODERATE
M114337	FGFR3	3	62309037	62309037	NA	Missense_Mutation	G	G	T	0.4	p.Q754K	16/16	tolerated(0.12)	MODERATE
M52097	FGFR3	3	62308920	62308920	NA	Missense_Mutation	G	G	T	0.4	p.Q793K	16/16		MODERATE
M71593	FGFR3	3	62308497	62308497	NA	Missense_Mutation	C	C	A	0.333	p.A934S	16/16		MODERATE

M73441	FGFR3	3	62308400	62308400	chr4:180934-180934	Missense_Mutation	G	G	A	0.4	p.P966L	16/16		MODERATE
M73441	FGFR3	3	62308635	62308635	chr4:180914-180914	Missense_Mutation	G	G	T	0.25	p.P888T	16/16		MODERATE
M99876	FGFR3	3	62316219	62316219	chr4:180184-180184	Missense_Mutation	G	G	T	0.062	p.P238Q	5/16	deleterious(0.02)	MODERATE
M99876	FIP1L1	13	46025980	46025980	chr4:53389834-53389834	Missense_Mutation	C	C	A	0.125	p.L118I	9/21	deleterious(0.02)	MODERATE
M121064	FKBP9	14	45067775	45067775	chr7:33005324-33005324	Missense_Mutation	C	C	G	0.971	p.D530E	10/10	tolerated(0.08)	MODERATE
M58698	FLCN	5	42178998	42178998	chr17:17232829-17232829	Missense_Mutation	G	G	T	0.333	p.L147F	2/13	deleterious_low_confide	MODERATE

													nce(0.05)	
M58697	FLI1	5	58430452	58430452	chr11:128810959-128810959	Missense_Mutation	C	C	T	0.355	p.V461M	10/10	tolerated(0.54)	MODERATE
L114148	FLNA	X	1.22E+08	1.22E+08	chrX:154366194-154366194	Missense_Mutation	T	T	C	0.255	p.I420T	8/1	deleterious(0)	MODERATE
M118542	FLNA	X	1.22E+08	1.22E+08	chrX:154365154-154365154	Missense_Mutation	G	G	A	0.058	p.G558D	10/1	deleterious(0.01)	MODERATE
M99876	FLNA	X	1.22E+08	1.22E+08	chrX:154351004-154351004	Missense_Mutation	C	C	A	0.043	p.A2354E	44/48	tolerated(0.05)	MODERATE
M99876	FLNA	X	1.22E+08	1.22E+08	chrX:154348929-154348929	Missense_Mutation	G	G	T	0.11	p.D2621Y	48/48	deleterious(0)	MODERATE

L53739	FLT3	25	11643622	11643623	chr13:28037273-28037274	Missense_Mutation	GC	GC	CT	0.09	p.C388S	10/24	deleterious(0.01)	MODERATE
M101740	FLT3	25	11650270	11650270	chr13:28028204-28028204	Missense_Mutation	A	A	C	0.622	p.N657T	16/24	deleterious(0)	MODERATE
M121047	FLT3	25	11646088	11646089	chr13:28034149-28034150	In_Frame_Ins	-	-	CTACATTGATTTCAGAGAATATGA	0.423	p.Y578_E579insDYIDFREY	14/24		MODERATE
M71679	FLT3	25	11650282	11650282	chr13:28028192-28028192	Missense_Mutation	C	C	T	0.464	p.A661V	16/24	deleterious(0)	MODERATE
M99876	FLT3	25	11650294	11650294	chr13:28028180-28028180	Nonsense_Mutation	C	C	A	0.048	p.S665*	16/24		HIGH
M73441	FLT4	11	11765 95	11765 95	chr5:180611382-	Missense_	C	C	A	0.128	p.A1247D	27/31	tolerated(0.47)	MODERATE

					18061 1382	Mutation								
M716 79	FOX A1	8	16079 666	16079 666	chr14: 37591 951- 37591 951	Misse nse_ Mutation	C	C	G	0.625	p.G45 0A	3/3	tolerat ed_lo w_con fidenc e(0.12)	MOD ERAT E
M734 41	FOX A1	8	16083 695	16083 695	chr14: 37595 730- 37595 730	Misse nse_ Mutation	G	G	T	0.4	p.A38 E	1/3	delete rious_ low_c onfide nce(0)	MOD ERAT E
L1104 46	FOXP 1	20	21004 173	21004 173	chr3:7 09721 52- 70972 152	Misse nse_ Mutation	A	A	G	0.333	p.H52 0R	13/16	delete rious(0)	MOD ERAT E
M713 35	FOXP 1	20	21009 973	21009 973	chr3:7 09659 42- 70965 942	Misse nse_ Mutation	A	A	G	0.474	p.T62 9A	15/16	tolerat ed(0.6 7)	MOD ERAT E
M998 76	FOXP 1	20	20788 568	20788 568	chr3:7 11982 57- 71198 257	Misse nse_ Mutation	C	C	A	0.073	p.P42 Q	1/16	tolerat ed_lo w_con fidenc e(0.09)	MOD ERAT E

L105585	FSTL3	20	57884159	57884159	chr19:676437-676437	Missense_Mutation	G	G	A	0.282	p.A5V	1/5	tolerated_low_confidence(0.23)	MODERATE
M99876	FSTL3	20	57884094	57884094	chr19:676502-676502	Missense_Mutation	C	C	A	0.25	p.V27L	1/5	tolerated(0.31)	MODERATE
M99876	GAS7	5	34340118	34340118	chr17:9917858-9917858	Missense_Mutation	G	G	T	0.333	p.P401T	13/13	tolerated_low_confidence(0.06)	MODERATE
L71592	GATA2	20	2479017	2479018	chr3:128485943-128485944	Frame_Shift_Ins	-	-	GGGG	0.063	p.D219Pfs*3	3/7		HIGH
M105453	GATA2	20	2476823	2476823	chr3:128483903-128483903	Missense_Mutation	A	A	C	0.455	p.M325R	4/7	deleterious(0)	MODERATE
M119591	GATA2	20	2479055	2479056	chr3:128485981-	Frame_Shift_Ins	-	-	C	0.277	p.E206Gfs*15	3/7		HIGH

					12848 5982									
M699 65	GAT A2	20	24788 06	24788 06	chr3:1 28485 732-12848 5732	Misse nse_ Mutati on	C	C	A	0.149	p.C28 9F	3/7	tolerat ed(0.2 2)	MOD ERAT E
M708 48	GAT A2	20	24790 55	24790 56	chr3:1 28485 981-12848 5982	Frame _Shift _Ins	-	-	C	0.403	p.E20 6Gfs* 15	3/7		HIGH
M715 93	GAT A2	20	24790 55	24790 56	chr3:1 28485 981-12848 5982	Frame _Shift _Ins	-	-	C	0.413	p.E20 6Gfs* 15	3/7		HIGH
M716 79	GAT A2	20	24790 55	24790 56	chr3:1 28485 981-12848 5982	Frame _Shift _Ins	-	-	C	0.577	p.E20 6Gfs* 15	3/7		HIGH
L1055 85	GAT A3	2	28074 307	28074 308	chr10: 80695 59-80695 60	Frame _Shift _Ins	-	-	G	0.457	p.V33 8Rfs* 3	4/5		HIGH
M734 41	GLI1	10	15688 95	15688 95	chr12: 57463 914-	Nonse nse_	G	G	A	0.222	p.W36 *	3/12		HIGH

					57463914	Mutation								
M99876	GLI1	10	157015 3	157015 3	chr12:57465251-57465251	Missense_Mutation	G	G	T	0.167	p.C210F	5/12	deleterious(0.04)	MODERATE
M73441	GMPS	23	49698491	49698491	chr3:156019837-156019837	Missense_Mutation	G	G	T	0.4	p.G786W	17/18	deleterious_low_confidence(0.01)	MODERATE
M73441	GMPS	23	49698518	49698518	chr3:156019864-156019864	Missense_Mutation	A	A	C	0.333	p.K795Q	17/18	deleterious_low_confidence(0)	MODERATE
M99876	GNAS	24	43657210	43657210	chr20:58909825-58909825	Missense_Mutation	C	C	A	0.167	p.P245Q	9/13	deleterious(0.01)	MODERATE
M99876	GNAS	24	43657213	43657213	chr20:58909828-58909828	Missense_Mutation	C	C	A	0.167	p.P246H	9/13	deleterious(0.02)	MODERATE

M73441	GOLGA5	8	18857 67	18857 67	chr14: 92809 338-92809 338	Missense_ Mutation	G	G	T	0.103	p.V271F	4/14	tolerated(0.05)	MODERATE
M99876	GOLGA5	8	19040 66	19040 66	chr14: 92835 558-92835 558	Splice_Site	G	G	T	0.087	p.X667_splice			HIGH
M73441	GPC3	X	1.05E +08	1.05E +08	chrX: 13386 4204-13386 4204	Missense_ Mutation	G	G	T	0.333	p.H115N	3/9	tolerated_low_confidence(0.12)	MODERATE
M99876	GPC3	X	1.05E +08	1.05E +08	chrX: 13395 3163-13395 3163	Missense_ Mutation	C	C	A	0.079	p.R75I	2/9	deleterious(0)	MODERATE
M99876	GPC5	22	43195 292	43195 292	chr13: 92144 935-92144 935	Missense_ Mutation	G	G	T	0.25	p.G502C	7/8	deleterious(0.03)	MODERATE
M99876	GPHN	8	40930 446	40930 446	chr14: 66879 978-	Missense_ Mutation	G	G	T	0.056	p.A125S	6/25	tolerated(0.37)	MODERATE

					66879978									
M106053	GRIN2A	6	32667673	32667673	chr16:97643624-97643624	Missense_Mutation	C	C	T	0.067	p.P1074S	12/12	tolerated(0.61)	MODERATE
M120486	GRIN2A	6	32303123	32303123	chr16:10180409-10180409	Translation_Start_Site	G	G	A	0.333	p.M1?	1/12	deleterious_low_confidence(0)	HIGH
M99876	GRIN2A	6	32667103	32667103	chr16:97648894-97648894	Missense_Mutation	G	G	T	0.115	p.D884Y	12/12	deleterious(0)	MODERATE

M114337	GRM3	14	12999934	12999935	NA	Frame_Shift_Ins	-	-	TGTTCGTGGTGAACGCCGTGTACGCCATGGCGCAGCCCTGCACAAAATGCAGCGCACCTCTGCCCCAACACCACCAGCTCTGCGACGCGATGAAGATCCTG	0.968	p.*391Mfs*81	2/5		HIGH

									GAC GG					
M120 378	GRM 3	14	12980 514	12980 514	chr7:8 67653 36-86765 336	Misse nse_ Mutati on	G	G	A	0.035	p.R64 Q	1/5	tolerat ed(0.1 2)	MOD ERAT E
M734 41	HIF1 A	8	36649 357	36649 357	chr14: 61738 158-61738 158	Nonse nse_ Mutati on	G	G	T	0.107	p.E44 1*	10/15		HIGH

M99876	HIF1A	8	36651152	36651152	chr14:61740812-61740812	Missense_Mutation	C	C	A	0.047	p.Q573K	12/15	deleterious(0)	MODERATE
M73441	HIP1	6	7115542	7115542	chr7:75738844-75738844	Missense_Mutation	G	G	T	0.286	p.A26E	1/1	tolerated(0.46)	MODERATE
M99876	HNF1A	26	16818048	16818048	chr12:120993567-120993567	Missense_Mutation	G	G	T	0.088	p.D192Y	3/10	deleterious(0)	MODERATE
M99876	HNF1A	26	16822393	16822393	chr12:120999270-120999270	Missense_Mutation	C	C	A	0.049	p.L502I	8/10	tolerated(0.08)	MODERATE
M99876	HNF1A	26	16822648	16822648	chr12:120999532-120999532	Missense_Mutation	C	C	A	0.036	p.P565Q	9/10	tolerated_low_confidence(0.06)	MODERATE
M58697	HOXA13	14	40374271	40374271	chr7:27199191-	Missense_Mutation	G	G	A	0.299	p.A297V	1/2	tolerated(0.06)	MODERATE

					27199191									
M99876	HOXA13	14	40374820	40374820	chr7:27199737-27199737	Missense_Mutation	G	G	T	0.333	p.P114Q	1/2	tolerated(0.28)	MODERATE
L110446	HSP90AA1	8	70094840	70094840	chr14:102084726-102084726	Missense_Mutation	A	A	T	0.333	p.F122L	2/8	deleterious_low_confidence(0.02)	MODERATE
M99876	HSP90AB1	12	12660058	12660058	chr6:44248680-44248680	Missense_Mutation	C	C	A	0.115	p.F17L	1/11	deleterious(0)	MODERATE
M121010	IDH1	37	16524295	16524295	chr2:208248389-208248389	Missense_Mutation	G	G	A	0.137	p.R132C	4/10	deleterious_low_confidence(0.03)	MODERATE
M103733	IDH2	3	53087478	53087478	NA	Missense_Mutation	C	C	T	0.811	p.D7N	1/11	tolerated_low_confidence(0.7)	MODERATE

M99876	IDH2	3	53070781	53070781	chr15:90084332-90084332	Missense_Mutation	G	G	T	0.25	p.F421L	12/12	deleterious_low_confidence(0.01)	MODERATE
M52097	IKBKB	16	23362904	23362904	NA	Missense_Mutation	C	C	A	0.333	p.A734S	21/21	tolerated_low_confidence(0.26)	MODERATE
M99876	IKBKB	16	23372877	23372877	chr8:42316886-42316886	Missense_Mutation	C	C	A	0.096	p.Q369H	11/21	deleterious(0.03)	MODERATE
M99876	IKBKB	16	23404350	23404350	chr8:42290223-42290223	Missense_Mutation	C	C	A	0.079	p.D90Y	4/21	deleterious(0)	MODERATE
L52744	IKZF1	18	17329902	17329902	chr7:50382602-50382602	Missense_Mutation	C	C	T	0.457	p.R218W	5/10	deleterious_low_confidence(0)	MODERATE
L53739	IKZF1	18	17329984	17329985	chr7:50382684-	Frame_Shift_Ins	-	-	A	0.262	p.G246Rfs*10	5/10		HIGH

					50382685									
L71592	IKZF1	18	1732993	1732993	chr7:50382693-50382693	Missense_Mutation	T	T	C	0.092	p.L248P	5/10	deleterious_low_confidence(0)	MODERATE
M105453	IKZF1	18	1733001	1733001	chr7:50382701-50382701	Missense_Mutation	C	C	G	0.279	p.H251D	5/10	deleterious_low_confidence(0)	MODERATE
M115951	IKZF1	18	1727531	1727532	chr7:50376708-50376709	Frame_Shift_Ins	-	-	TTTAA	0.435	p.P169Ffs*7	4/10		HIGH
M120399	IKZF1	18	1749570	1749570	chr7:50400468-50400468	Nonsense_Mutation	C	C	A	0.297	p.C523*	8/10		HIGH
M120486	IKZF1	18	1732897	1732897	chr7:50382597-50382597	Missense_Mutation	T	T	C	0.257	p.L216P	5/10	deleterious_low_confidence(0)	MODERATE

M120655	IKZF1	18	17329768	17329768	chr7:50382668-50382668	Missense_Mutation	C	C	T	0.259	p.R240W	5/10	deleterious_low_confidence(0)	MODERATE
M121047	IKZF1	18	17490441	17490442	chr7:50399939-50399940	Frame_Shift_Ins	-	-	G	0.438	p.P348Afs*13	8/10		HIGH
M122308	IKZF1	18	17329764	17329767	chr7:50382664-50382667	Frame_Shift_Del	CCGC	CCGC	-	0.384	p.R239Gfs*9	5/10		HIGH
M122308	IKZF1	18	17329772	17329774	chr7:50382672-50382674	In_Frame_Del	GGG	GGG	-	0.391	p.R241_D242delinsH	5/10		MODERATE
M52097	IKZF1	18	17329775	17329776	chr7:50382675-50382676	In_Frame_Ins	-	-	AAT	0.417	p.D242delinsEI	5/10		MODERATE
M52097	IKZF1	18	17329776	17329776	chr7:50382676-50382676	Missense_Mutation	C	C	G	0.417	p.D242E	5/10	deleterious_low_confidence(0)	MODERATE

M58697	IKZF1	18	1732968	1732968	chr7:50382668-50382668	Missense_Mutation	C	C	T	0.433	p.R240W	5/10	deleterious_low_confidence(0)	MODERATE
M70848	IKZF1	18	1676694	1676707	chr7:50319096-50319109	Splice_Site	TTTCAGGTGAGACC	TTTCAGGTGAGACC	-	0.295	p.X69_splice	2/10		HIGH
M70848	IKZF1	18	1683882	1683883	chr7:50327674-50327675	Frame_Shift_Ins	-	-	T	0.341	p.G83Wfs*3	3/10		HIGH
M99876	IKZF1	18	1732993	1732993	chr7:50382693-50382693	Missense_Mutation	T	T	C	0.528	p.L248P	5/10	deleterious_low_confidence(0)	MODERATE
M121010	IL21R	6	19196595	19196595	chr16:27430084-27430084	Missense_Mutation	C	C	T	0.4	p.G5R	2/9	tolerated(0.11)	MODERATE
M122308	IL21R	6	19188326	19188326	chr16:27442970-27442970	Missense_Mutation	A	A	G	0.397	p.S121P	5/9	tolerated(0.12)	MODERATE

M99876	IL21R	6	19188203	19188203	chr16:27443102-27443102	Missense_Mutation	G	G	T	0.071	p.R162S	5/9	deleterious(0.02)	MODERATE
U69959	IL21R	6	19188203	19188203	chr16:27443102-27443102	Missense_Mutation	G	G	A	0.372	p.R162C	5/9	deleterious(0)	MODERATE
M71679	IRS4	X	82292016	82292016	chrX:108735985-108735985	Missense_Mutation	G	G	T	0.8	p.H120Q	1/2	tolerated(0.06)	MODERATE
M99876	IRS4	X	82290328	82290328	chrX:108734312-108734312	Missense_Mutation	C	C	A	0.07	p.S683I	1/2	tolerated_low_confidence(0.23)	MODERATE
M99876	IRS4	X	82290389	82290389	chrX:108734370-108734370	Missense_Mutation	C	C	A	0.061	p.A663S	1/2	tolerated_low_confidence(0.09)	MODERATE
M106053	ITGAV	36	28804043	28804043	chr2:186588868-	Missense_	G	G	A	0.4	p.A11T	1/30		MODERATE

					18658 8868	Mutation								
M998 76	ITGA V	36	28837 998	28837 998	chr2:1 86625 523-18662 5523	Misse nse_ Mutation	G	G	T	0.063	p.E13 9D	4/30	tolerat ed(1)	MOD ERAT E
M120 655	JAK2	1	93419 708	93419 708	chr9:5 07748 3-50774 83	Misse nse_ Mutation	G	G	T	0.333	p.G90 7V	21/31	delete rious(0)	MOD ERAT E
M114 677	KAT6 A	16	23713 304	23713 305	chr8:4 19331 95-41933 196	Frame _Shift _Ins	-	-	A	0.118	p.Q16 77Pfs *47	19/20		HIGH
M998 76	KAT6 A	16	23705 771	23705 771	chr8:4 19413 68-41941 368	Misse nse_ Mutation	C	C	T	0.288	p.T84 0I	16/20	tolerat ed_lo w_con fidenc e(0.2)	MOD ERAT E
M119 591	KDM 5A	27	42371 961	42371 961	chr12: 29316 2-29316 2	Misse nse_ Mutation	C	C	T	0.466	p.S14 85N	29/31	tolerat ed(0.1 5)	MOD ERAT E
L5373 9	KDM 5C	X	44941 808	44941 808	chrX: 53201 708-	Nonse nse_	C	C	T	0.435	p.R63 5*	14/26		HIGH

					53201708	Mutation								
M115951	KDM5C	X	44935164	44935164	chrX:53210460-53210460	Missense_Mutation	T	T	C	0.787	p.L567P	12/26	deleterious(0)	MODERATE
M118542	KDM5C	X	44945572	44945573	chrX:53199137-53199138	In_Frame_Ins	-	-	GAGGCTTTC	0.965	p.A696_E698dup	15/26		MODERATE
M119591	KDM5C	X	44935056	44935056	chrX:53210568-53210568	Missense_Mutation	C	C	T	0.426	p.P531L	12/26	deleterious(0)	MODERATE
M120399	KDM5C	X	44947703	44947728	chrX:53196947-53196972	Frame_Shift_Del	GGGCTACTGCAGTCCCTTTTGGAGAG	GGGCTACTGCAGTCCCTTTTGGAGAG	-	0.75	p.L900Afs*9	19/26		HIGH
M52097	KDM5C	X	44935142	44935142	chrX:53210482-53210482	Nonsense_Mutation	C	C	T	0.973	p.Q560*	12/26		HIGH

M73441	KDM5C	X	44949950	44949953	chrX:53194618-53194621	Frame_Shift_Del	TCTG	TCTG	-	0.454	p.C1190Gfs*73	23/26		HIGH
L107858	KDM6A	X	38927047	38927048	chrX:45082790-45082791	Splice_Site	-	-	T	0.762	p.X1147_splice			HIGH
L53739	KDM6A	X	38924548	38924548	chrX:45079223-45079223	Nonsense_Mutation	C	C	T	0.295	p.Q1058*	21/30		HIGH
M114337	KDM6A	X	38957348	38957348	chrX:45110125-45110125	Missense_Mutation	G	G	A	0.601	p.R1403Q	29/30	tolerated(0.59)	MODERATE
M118542	KDM6A	X	38927639	38927668	chrX:45083523-45083552	In_Frame_Del	AAATCTTCTAAGCCACGTTGGTCATACCAT	AAATCTTCTAAGCCACGTTGGTCATACCAT	-	0.93	p.N1169_I1178del	24/30		MODERATE

M122308	KDM6A	X	38927628	38927629	chrX:45083512-45083513	Nonsense_Mutation	GT	GT	TG	0.715	p.V1165*	24/30		HIGH
M71281	KDM6A	X	38927574	38927574	chrX:45083458-45083458	Splice_Site	A	A	G	0.956	p.X1147_splice			HIGH
M71335	KDM6A	X	38927628	38927629	chrX:45083512-45083513	Frame_Shift_Ins	-	-	TTTATCTCTC	0.857	p.S1166Yfs*40	24/30		HIGH
M99876	KEAP1	20	50653297	50653297	chr19:10499955-10499955	Missense_Mutation	G	G	T	0.044	p.A27S	2/6	tolerated(0.22)	MODERATE
M99876	KEAP1	20	50653573	50653573	chr19:10499679-10499679	Missense_Mutation	G	G	T	0.065	p.G119C	2/6	deleterious(0.04)	MODERATE
M69965	KIAA1549	16	9753786	9753787	NA	In_Frame_Ins	-	-	AGCAGC	0.555	p.S347_S348dup	2/20		MODERATE

M99876	KIAA1549	16	9754634	9754634	chr7:138917755-138917755	Missense_Mutation	C	C	A	0.062	p.A624D	2/20	deleterious_low_confidence(0.03)	MODERATE
M99876	KIF5B	2	14857370	14857370	chr10:32034701-32034701	Missense_Mutation	G	G	T	0.077	p.R367L	11/26	deleterious(0.02)	MODERATE
L105735	KIT	13	47184335	47184335	chr4:54733155-54733155	Missense_Mutation	A	A	T	0.237	p.D815V	17/21	deleterious(0)	MODERATE
L114182	KIT	13	47184335	47184335	chr4:54733155-54733155	Missense_Mutation	A	A	T	0.652	p.D815V	17/21	deleterious(0)	MODERATE
M120378	KIT	13	47184354	47184354	chr4:54733174-54733174	Missense_Mutation	T	T	G	0.095	p.N821K	17/21	deleterious(0)	MODERATE
M120399	KIT	13	47184334	47184335	chr4:54733154-	Missense_Mutation	GA	GA	TT	0.63	p.D815F	17/21	deleterious(0)	MODERATE

					54733155									
U69959	KIT	13	47178591	47178591	chr4:54727495-54727495	Missense_Mutation	T	T	C	0.602	p.L575P	11/21	deleterious(0.02)	MODERATE
U69959	KIT	13	47184337	47184337	chr4:54733157-54733157	Missense_Mutation	A	A	C	0.536	p.I816L	17/21	deleterious(0)	MODERATE
M122308	KLF4	11	62885053	62885055	NA	In_Frame_Del	CCG	CCG	-	0.576	p.G175del	4/6		MODERATE
L114148	KLK2	1	1.06E+08	1.06E+08	chr19:50858015-50858015	Missense_Mutation	G	G	T	0.635	p.P131T	1/4	deleterious_low_confidence(0)	MODERATE
L52744	KMT2A	5	15259920	15259921	chr11:118481777-118481778	Frame_Shift_Del	AC	AC	-	0.418	p.V1090Wfs*26	6/1		HIGH
M58698	KMT2A	5	15237636	15237636	chr11:118505904-	Missense_Mutation	C	C	T	0.929	p.A3193T	26/35	tolerated_low_confidenc	MODERATE

					11850 5904								e(0.13)	
M586 98	KMT 2A	5	15237 940	15237 940	chr11: 11850 5600- 11850 5600	Misse nse_ Mutati on	T	T	G	0.875	p.K30 91N	26/35	delete rious_ low_c onfide nce(0)	MOD ERAT E
M734 41	KMT 2A	5	15259 973	15259 973	chr11: 11848 1725- 11848 1725	Misse nse_ Mutati on	C	C	A	0.047	p.K10 72N	6/1	delete rious_ low_c onfide nce(0. 01)	MOD ERAT E
M998 76	KMT 2A	5	15230 897	15230 897	chr11: 11851 2023- 11851 2023	Misse nse_ Mutati on	G	G	T	0.051	p.A35 65E	30/35	tolerat ed(0.4)	MOD ERAT E
M998 76	KMT 2A	5	15240 508	15240 508	chr11: 11850 3029- 11850 3029	Misse nse_ Mutati on	C	C	A	0.052	p.R22 35S	26/35	delete rious_ low_c onfide nce(0)	MOD ERAT E
M998 76	KMT 2A	5	15267 101	15267 101	chr11: 11847 2809- 11847 2809	Misse nse_ Mutati on	C	C	A	0.059	p.Q40 7H	2/1	delete rious_ low_c onfide	MOD ERAT E

													nce(0.02)	
L105735	KMT2D	27	5528193	5528193	chr12:49049200-49049200	Missense_Mutation	C	C	T	0.323	p.P1408S	12/1		MODERATE
L114182	KMT2D	27	5549133	5549134	chr12:49026590-49026591	Frame_Shift_Ins	-	-	TT	0.429	p.K5332Sfs*21	47/52		HIGH
L52744	KMT2D	27	5543118	5543119	chr12:49033113-49033113	Frame_Shift_Ins	-	-	C	0.437	p.Q4052Pfs*159	38/52		HIGH
M108089	KMT2D	27	5539458	5539459	chr12:49037536-49037537	In_Frame_Ins	-	-	CAGCAG	0.572	p.Q3463_Q3464dup	33/52		MODERATE
M73441	KMT2D	27	5537147	5537147	chr12:49039828-49039828	Missense_Mutation	C	C	A	0.057	p.P2820T	30/52		MODERATE

M73441	KMT2D	27	5539333	5539333	chr12:49037662-49037662	Nonsense_Mutation	G	G	T	0.043	p.E3411*	33/52		HIGH
L110446	KRAS	27	22258700	22258700	chr12:25250004-25250004	Missense_Mutation	G	G	A	0.333	p.E68K	1/6	deleterious_low_confidence(0)	MODERATE
M106053	KRAS	27	22261798	22261798	chr12:25245350-25245350	Missense_Mutation	G	G	A	0.38	p.G106D	2/6	deleterious_low_confidence(0)	MODERATE
M108089	KRAS	27	22261801	22261801	chr12:25245347-25245347	Missense_Mutation	G	G	A	0.148	p.G107D	2/6	deleterious_low_confidence(0.03)	MODERATE
M115951	KRAS	27	22261798	22261798	chr12:25245350-25245350	Missense_Mutation	G	G	T	0.527	p.G106V	2/6	deleterious_low_confidence(0)	MODERATE
M118542	KRAS	27	22261801	22261801	chr12:25245347-	Missense_Mutation	G	G	A	0.469	p.G107D	2/6	deleterious_low_confide	MODERATE

					25245347								nce(0.03)	
M119591	KRAS	27	22261798	22261798	chr12:25245350-25245350	Missense_Mutation	G	G	A	0.269	p.G106D	2/6	deleterious_low_confidence(0)	MODERATE
M120398	KRAS	27	22261798	22261798	chr12:25245350-25245350	Missense_Mutation	G	G	A	0.083	p.G106D	2/6	deleterious_low_confidence(0)	MODERATE
M120486	KRAS	27	22277968	22277969	chr12:25227343-25227344	Missense_Mutation	TC	TC	AA	0.325	p.Q155K	3/6		MODERATE
M70848	KRAS	27	22261801	22261801	chr12:25245347-25245347	Missense_Mutation	G	G	A	0.439	p.G107D	2/6	deleterious_low_confidence(0.03)	MODERATE
M99876	KTN1	8	31412451	31412451	chr14:55637202-55637202	Missense_Mutation	G	G	T	0.247	p.L657F	11/1	deleterious(0)	MODERATE

L107858	LARP4B	2	34096761	34096761	chr10:82954 2-82954 2	Missense_Mutation	G	G	T	0.333	p.G324V	11/18	deleterious(0.02)	MODERATE
L110446	LARP4B	2	34117376	34117376	chr10:81495 5-81495 5	Missense_Mutation	G	G	T	0.329	p.C595F	16/18	tolerated(0.39)	MODERATE
L114182	LARP4B	2	34100411	34100411	chr10:82513 5-82513 5	Missense_Mutation	A	A	G	0.333	p.K473E	13/18	tolerated(0.27)	MODERATE
L114182	LARP4B	2	34118762	34118762	chr10:81315 3-81315 3	Missense_Mutation	T	T	C	0.4	p.S655P	18/18	tolerated(0.24)	MODERATE
M101740	LARP4B	2	34118766	34118766	chr10:81314 9-81314 9	Missense_Mutation	C	C	T	0.4	p.P656L	18/18	tolerated(0.33)	MODERATE
M108089	LARP4B	2	34118915	34118915	chr10:81298 5-81298 5	Missense_Mutation	C	C	A	0.286	p.P706T	18/18	tolerated(0.06)	MODERATE

M122308	LARP4B	2	34117267	34117267	chr10:815064-815064	Missense_Mutation	A	A	G	0.4	p.N559D	16/18	tolerated(0.08)	MODERATE
M73441	LARP4B	2	34095144	34095144	chr10:830878-830878	Missense_Mutation	G	G	A	0.4	p.D285N	9/18	deleterious(0)	MODERATE
M113164	LATS2	25	17159339	17159339	chr13:20988195-20988195	Missense_Mutation	G	G	A	0.058	p.E524K	3/7	tolerated_low_confidence(0.1)	MODERATE
M99876	LCK	2	68947011	68947011	chr1:32276672-32276672	Missense_Mutation	C	C	A	0.091	p.A284S	9/13	tolerated(0.07)	MODERATE
M99876	LCK	2	68948813	68948813	chr1:32275061-32275061	Nonsense_Mutation	C	C	A	0.083	p.E86*	4/13		HIGH
M99876	LCP1	22	5005867	5005867	chr13:46183952-46183952	Missense_Mutation	C	C	T	0.286	p.A63V	2/18		MODERATE

L105585	LEF1	32	28580490	28580490	chr4:108114368-108114368	Missense_Mutation	C	C	A	0.286	p.W192C	4/12	tolerated(0.18)	MODERATE
M70848	LHFPL6	25	1804026	1804026	chr13:39343943-39343943	Missense_Mutation	C	C	A	0.333	p.P216Q	5/5	deleterious_low_confidence(0.01)	MODERATE
L107858	LMNA	7	41508836	41508836	chr1:156421093-156421093	Missense_Mutation	C	C	A	0.4	p.G637C	12/12	deleterious_low_confidence(0)	MODERATE
M103733	LMNA	7	41508903	41508903	chr1:156421025-156421025	Missense_Mutation	C	C	A	0.333	p.K614N	12/12	tolerated_low_confidence(0.18)	MODERATE
M73441	LMNA	7	41508598	41508598	chr1:156421349-156421349	Missense_Mutation	C	C	A	0.286	p.G716V	12/12		MODERATE
M99876	LRIG3	10	2735991	2735991	chr12:58883581-	Missense_	C	C	A	0.119	p.D386Y	11/19	deleterious(0.04)	MODERATE

					58883581	Mutation								
M11854 2	LRP1B	19	43249380	43249380	chr2:140923070-140923070	Missense_Mutation	G	G	A	0.46	p.R1072C	21/91	deleterious(0)	MODERATE
M70848	LRP1B	19	43249445	43249445	chr2:140923135-140923135	Missense_Mutation	G	G	A	0.3	p.P1050L	21/91	deleterious(0.04)	MODERATE
M99876	LRP1B	19	42684678	42684678	chr2:140315033-140315033	Missense_Mutation	C	C	A	0.052	p.R4236M	83/91	deleterious(0.01)	MODERATE
M99876	LRP1B	19	43782282	43782282	chr2:141480508-141480508	Nonsense_Mutation	G	G	T	0.119	p.C77*	3/1		HIGH
M99876	MACC1	14	34209080	34209080	chr7:20159652-20159652	Missense_Mutation	G	G	T	0.072	p.P237T	3/5	deleterious(0)	MODERATE

L71592	MAF	5	71966016	71966016	chr16:79599416-79599416	Missense_Mutation	G	G	A	0.4	p.V163M	2/4	tolerated_low_confidence(0.11)	MODERATE
M101740	MAF	5	71966143	71966143	chr16:79599292-79599292	Missense_Mutation	G	G	T	0.286	p.G205V	2/4	tolerated(0.29)	MODERATE
M114337	MAF	5	71966668	71966668	chr16:79598784-79598784	Splice_Site	G	G	T	0.4	p.X379_splice			HIGH
M120398	MAF	5	71966014	71966014	chr16:79599418-79599418	Missense_Mutation	C	C	A	0.4	p.A162D	2/4	tolerated_low_confidence(0.07)	MODERATE
M120486	MAF	5	71966453	71966453	chr16:79598999-79598999	Missense_Mutation	G	G	T	0.333	p.A308S	3/4	deleterious(0)	MODERATE
M99876	MAF	5	71966394	71966394	chr16:79599058-	Missense_	G	G	T	0.187	p.S288I	3/4	deleterious(0)	MODERATE

					79599058	Mutation								
M115951	MAFB	24	28774570	28774570	chr20:40690295-40690295	Missense_Mutation	G	G	A	0.333	p.P127S	1/2	deleterious_low_confidence(0.01)	MODERATE
M120655	MAFB	24	28774587	28774587	chr20:40690312-40690312	Missense_Mutation	T	T	C	0.286	p.H121R	1/2	deleterious_low_confidence(0)	MODERATE
M121064	MAFB	24	28774740	28774740	NA	Missense_Mutation	G	G	T	0.333	p.P70H	1/2	deleterious_low_confidence(0.01)	MODERATE
M99876	MAFB	24	28771949	28771949	chr20:40687884-40687884	Missense_Mutation	G	G	T	0.039	p.L275M	2/2	tolerated_low_confidence(0.2)	MODERATE
M99876	MAFB	24	28774853	28774853	chr20:40690555-40690555	Missense_Mutation	G	G	T	0.286	p.F32L	1/2		MODERATE

M108089	MALT1	1	17383033	17383033	chr18:58709525-58709525	Missense_Mutation	G	G	T	0.25	p.P199Q	5/17	deleterious(0.03)	MODERATE
M99876	MALT1	1	17403560	17403560	chr18:58681336-58681336	Nonsense_Mutation	C	C	A	0.222	p.G56*	2/17		HIGH
L52744	MAML2	21	5057027	5057028	chr11:96092201-96092202	In_Frame_Ins	-	-	GCCACC	0.442	p.P615_P616dup	3/6		MODERATE
M119591	MAML2	21	5057027	5057028	chr11:96092201-96092202	In_Frame_Ins	-	-	GCCACC	0.956	p.P615_P616dup	3/6		MODERATE
M71335	MAML2	21	5057027	5057028	chr11:96092201-96092202	In_Frame_Ins	-	-	GCCACC	0.972	p.P615_P616dup	3/6		MODERATE
M71609	MAML2	21	5057027	5057028	chr11:96092201-96092202	In_Frame_Ins	-	-	GCCACC	0.618	p.P615_P616dup	3/6		MODERATE

M69965	MAP2K2	20	55483545	55483545	chr19:40969035-40969035	Missense_Mutation	C	C	A	0.246	p.A402E	8/8		MODERATE
M73441	MAP3K1	2	43985673	43985673	chr5:56881181-56881181	Missense_Mutation	C	C	A	0.039	p.L921I	13/21	deleterious(0.05)	MODERATE
M99876	MECOM	34	33807475	33807475	chr3:169143697-169143697	Splice_Site	C	C	A	0.073	p.X170_splice			HIGH
L107858	MED12	X	55505590	55505590	chrX:71137564-71137564	Nonsense_Mutation	C	C	T	0.765	p.Q1919*	41/43		HIGH
L110446	MED12	X	55504491	55504492	chrX:71136469-71136470	Frame_Shift_Ins	-	-	CT	0.667	p.E1741Wfs*19	38/43		HIGH
L114148	MED12	X	55505275	55505275	chrX:71137246-71137246	Nonsense_Mutation	C	C	T	0.579	p.R1872*	40/43		HIGH

L114182	MED12	X	55498452	55498452	chrX:71129358-71129358	Missense_Mutation	T	T	C	0.461	p.L1208P	27/43	deleterious(0)	MODERATE
L53739	MED12	X	55488992	55488992	chrX:71119879-71119879	Splice_Site	T	T	G	0.421	p.X132_splice			HIGH
M101740	MED12	X	55492015	55492015	chrX:71123170-71123170	Missense_Mutation	C	C	T	0.718	p.R522C	12/1	deleterious(0)	MODERATE
M115951	MED12	X	55504572	55504573	chrX:71136550-71136551	Frame_Shift_Ins	-	-	C	0.942	p.K1769Qfs*3	38/43		HIGH
M118542	MED12	X	55504572	55504573	chrX:71136550-71136551	Frame_Shift_Ins	-	-	C	0.889	p.K1769Qfs*3	38/43		HIGH
M119591	MED12	X	55487847	55487847	chrX:71118767-71118767	Frame_Shift_Del	G	G	-	0.721	p.I6Sfs*2	2/1		HIGH

M120399	MED12	X	55499134	55499134	chrX:71130034-71130034	Splice_Site	G	G	A	0.697	p.X1291_splice			HIGH
M120486	MED12	X	55488588	55488588	chrX:71119478-71119478	Splice_Site	G	G	A	0.667	p.X68_splice			HIGH
M120655	MED12	X	55497497	55497497	chrX:71128441-71128441	Splice_Site	G	G	A	0.608	p.X1119_splice			HIGH
M121010	MED12	X	55491378	55491379	chrX:71122524-71122525	Nonsense_Mutation	-	-	TGAGATTACGTAATGATGGGAACT	0.357	p.I425_E426insT*	10/1		HIGH
M122308	MED12	X	55491939	55491939	chrX:71123094-71123094	Splice_Site	G	G	T	0.735	p.X497_splice			HIGH

M52097	MED12	X	55498774	55498774	chrX:71129678-71129678	Splice_Site	A	A	C	0.864	p.X1232_splice			HIGH
M58697	MED12	X	55492015	55492015	chrX:71123170-71123170	Missense_Mutation	C	C	T	0.441	p.R522C	12/1	deleterious(0)	MODERATE
M69965	MED12	X	55505356	55505356	chrX:71137330-71137330	Nonsense_Mutation	C	C	T	0.931	p.R1899*	40/43		HIGH
M70848	MED12	X	55504572	55504573	chrX:71136550-71136551	Frame_Shift_Ins	-	-	C	0.808	p.K1769Qfs*3	38/43		HIGH
M71281	MED12	X	55496025	55496025	chrX:71126973-71126973	Missense_Mutation	T	T	C	0.865	p.L898P	21/43	deleterious(0)	MODERATE
M71335	MED12	X	55504593	55504594	chrX:71136571-71136572	Frame_Shift_Ins	-	-	GGCC	0.841	p.A1775Rfs*53	38/43		HIGH

M71593	MED12	X	55504535	55504536	chrX:71136513-71136514	Frame_Shift_Ins	-	-	T	0.772	p.P1755Sfs*7	38/43		HIGH
M71593	MED12	X	55504537	55504537	chrX:71136515-71136515	Missense_Mutation	C	C	T	0.771	p.P1755S	38/43	tolerated(0.06)	MODERATE
M71679	MED12	X	55505371	55505372	chrX:71137345-71137346	Frame_Shift_Ins	-	-	CCGTG	0.93	p.Q1907Cfs*26	40/43		HIGH
M99876	MED12	X	55491986	55491986	chrX:71123141-71123141	Missense_Mutation	C	C	A	0.111	p.A512D	12/1	deleterious(0)	MODERATE
M99876	MED12	X	55492770	55492770	chrX:71123709-71123709	Missense_Mutation	C	C	A	0.222	p.A579D	13/43	deleterious(0)	MODERATE
M99876	MED12	X	55499139	55499139	chrX:71130039-71130039	Nonsense_Mutation	G	G	A	0.957	p.W1292*	29/43		HIGH

M58697	MGMT	28	38204665	38204665	chr10:129536295-129536295	Missense_Mutation	C	C	T	0.526	p.P15S	1/5	deleterious(0)	MODERATE
M120398	MN1	26	21258833	21258833	chr22:27798375-27798375	Missense_Mutation	G	G	T	0.222	p.S712R	2/3	deleterious_low_confidence(0.02)	MODERATE
M121010	MN1	26	21258760	21258760	chr22:27798305-27798305	Missense_Mutation	G	G	A	0.563	p.P737S	2/3	deleterious_low_confidence(0)	MODERATE
M99876	MN1	26	21258833	21258833	chr22:27798375-27798375	Missense_Mutation	G	G	T	0.097	p.S712R	2/3	deleterious_low_confidence(0.02)	MODERATE
M114677	MPL	15	16815461	16815461	NA	Nonsense_Mutation	C	C	A	0.4	p.G481*	9/9		HIGH
M99876	MTOR	2	84862055	84862055	chr1:112123 80-	Missense_Mutation	C	C	A	0.056	p.Q1262K	24/59	tolerated(0.37)	MODERATE

					11212380									
M106053	MUC1	7	42340858	42340858	chr1:155192085-155192085	Missense_Mutation	C	C	T	0.4	p.P32L	2/8	deleterious(0.01)	MODERATE
M113164	MUC1	7	42341119	42341119	chr1:155191824-155191824	Missense_Mutation	G	G	T	0.254	p.S119I	2/8	tolerated(0.17)	MODERATE
M58697	MUC1	7	42340941	42340941	chr1:155191997-155191997	Missense_Mutation	C	C	A	0.333	p.L60M	2/8	tolerated(0.14)	MODERATE
M113164	MUC4	33	29064287	29064287	chr3:195749010-195749010	Missense_Mutation	C	C	T	0.335	p.R1024H	22/24	tolerated(1)	MODERATE
M71593	MUTYH	15	15024617	15024618	chr1:45331751-45331752	Frame_Shift_Ins	-	-	C	0.401	p.R547Qfs*52	16/20		HIGH

M99876	MYB	1	27917327	27917327	chr6:135190333-135190333	Missense_Mutation	G	G	T	0.166	p.K171N	5/16	deleterious(0)	MODERATE
M73441	MYH11	6	28137830	28137830	chr16:15735559-15735559	Missense_Mutation	C	C	A	0.102	p.Q1112K	27/42	tolerated(0.43)	MODERATE
M73441	MYH11	6	28204788	28204788	chr16:15624769-15624769	Missense_Mutation	G	G	T	0.035	p.R759L	9/26	deleterious(0)	MODERATE
M73441	MYH11	6	28225455	28225455	chr16:15600417-15600417	Missense_Mutation	C	C	A	0.25	p.A1885E	41/41	tolerated_low_confidence(1)	MODERATE
M99876	MYH11	6	28136193	28136193	chr16:15737501-15737501	Missense_Mutation	C	C	A	0.081	p.L1088I	26/42	deleterious(0.01)	MODERATE
M99876	MYH11	6	28197270	28197270	chr16:15636301-15636301	Missense_Mutation	G	G	T	0.11	p.K62N	2/26	deleterious_low_confidence(0)	MODERATE

M73441	MYH9	10	28112965	28112965	chr22:36293457-36293457	Missense_Mutation	C	C	A	0.096	p.Q1344K	30/41	tolerated(0.14)	MODERATE
M121064	MYO5A	30	17939726	17939726	chr15:52248780-52248780	Missense_Mutation	C	C	G	0.562	p.E401Q	12/1	tolerated(0.06)	MODERATE
M99876	MYO5A	30	18063683	18063683	chr15:52384221-52384221	Missense_Mutation	C	C	A	0.081	p.K649N	17/43	deleterious(0.01)	MODERATE
M99876	N4BP2	3	72387644	72387644	chr4:40120513-40120513	Missense_Mutation	G	G	T	0.068	p.A801D	7/17	deleterious(0.01)	MODERATE
M73441	NAB2	10	123089	123089	chr12:57093690-57093690	Missense_Mutation	G	G	T	0.333	p.R487M	6/6		MODERATE
M99876	NAB2	10	122899	122899	chr12:57091757-57091757	Missense_Mutation	C	C	A	0.041	p.P206Q	2/6	tolerated(0.07)	MODERATE

M108089	NBEA	25	5387896	5387896	chr13:35109299-35109299	Missense_Mutation	C	C	T	0.362	p.V570I	12/1	tolerated(0.19)	MODERATE
M108735	NBEA	25	5536931	5536936	chr13:34942910-34942915	In_Frame_Del	CCGCCT	CCGCCT	-	0.463	p.G44_G45del	1/1		MODERATE
M115951	NBEA	25	5454381	5454381	chr13:35044963-35044963	Missense_Mutation	C	C	A	0.356	p.M187I	3/1	tolerated(0.1)	MODERATE
M120378	NBEA	25	4861724	4861724	chr13:35667392-35667392	Missense_Mutation	T	T	G	0.621	p.H2831P	56/58	deleterious(0)	MODERATE
M122308	NBEA	25	5386474	5386474	chr13:35110941-35110941	Missense_Mutation	A	A	T	0.453	p.N661K	13/58	deleterious(0.01)	MODERATE
M69860	NBEA	25	4983487	4983487	chr13:35550522-35550522	Missense_Mutation	C	C	T	0.107	p.E2214K	41/58	deleterious(0)	MODERATE

M73441	NBEA	25	5340300	5340300	chr13:35164378-35164378	Missense_Mutation	C	C	A	0.202	p.D1374Y	24/58	deleterious(0)	MODERATE
M73441	NBEA	25	5438449	5438449	chr13:35056120-35056120	Missense_Mutation	G	G	T	0.091	p.N367K	7/1	deleterious(0)	MODERATE
M99876	NBEA	25	5102079	5102079	chr13:35432328-35432328	Missense_Mutation	C	C	A	0.051	p.R2083L	38/58	deleterious(0)	MODERATE
L110446	NBN	29	35477352	35477352	chr8:89984459-89984459	Missense_Mutation	G	G	A	0.334	p.R35W	1/15		MODERATE
L114182	NBN	29	35477069	35477069	NA	Missense_Mutation	A	A	G	0.286	p.L129P	1/15		MODERATE
M106053	NBN	29	35477366	35477366	chr8:89984473-89984473	Missense_Mutation	G	G	T	0.4	p.A30E	1/15		MODERATE

M121047	NBN	29	35477444	35477444	chr8:89984551-89984551	Missense_Mutation	A	A	G	0.4	p.L4P	1/15		MODERATE
M73441	NCOA1	17	19083378	19083378	chr2:24726595-24726595	Missense_Mutation	C	C	A	0.046	p.P869Q	11/18	deleterious(0.01)	MODERATE
M99876	NCOR2	26	5481644	5481644	chr12:124340034-124340034	Missense_Mutation	G	G	A	0.307	p.V1891M	37/47	tolerated(0.19)	MODERATE
M99876	NCOR2	26	5485280	5485280	chr12:124335280-124335280	Missense_Mutation	G	G	T	0.097	p.G2093V	40/47	deleterious(0)	MODERATE
L52744	NDRG1	13	29732841	29732841	chr8:133284330-133284330	Splice_Site	C	C	T	0.415	p.X203_splice			HIGH
M115951	NF1	9	41614682	41614682	chr17:31229061-31229061	Nonsense_Mutation	G	G	A	0.388	p.R761*	21/58		HIGH

M120486	NF1	9	41611395	41611395	chr17:31232764-31232764	Missense_Mutation	T	T	C	0.411	p.T1072A	26/58	tolerated(0.75)	MODERATE
M52097	NF1	9	41516537	41516537	chr17:31326184-31326184	Nonsense_Mutation	C	C	A	0.909	p.E1679*	37/58		HIGH
M70848	NF1	9	41582574	41582574	chr17:31261710-31261710	Splice_Site	C	C	A	0.317	p.X1471_splice			HIGH
M99876	NF1	9	41515593	41515593	chr17:31327803-31327803	Missense_Mutation	G	G	T	0.431	p.A1803E	38/58	deleterious(0)	MODERATE
M114337	NFATC2	24	37770000	37770000	chr20:51562639-51562639	Missense_Mutation	C	C	A	0.396	p.Q184H	1/10	deleterious_low_confidence(0)	MODERATE
M73441	NFATC2	24	37733932	37733932	chr20:51523116-51523116	Missense_Mutation	C	C	A	0.052	p.W536C	2/10	deleterious(0)	MODERATE

M69860	NFIB	11	34799882	34799882	chr9:14307165-14307165	Missense_Mutation	C	C	T	0.467	p.R125H	2/12	deleterious(0)	MODERATE
L71592	NIN	8	27153086	27153086	chr14:50778789-50778789	Missense_Mutation	G	G	A	0.443	p.R148C	4/29	deleterious(0.05)	MODERATE
M106053	NIN	8	27134575	27134575	chr14:50758275-50758275	Missense_Mutation	G	G	T	0.38	p.L917M	16/29	deleterious(0)	MODERATE
M99876	NIN	8	27139567	27139567	chr14:50763928-50763928	Missense_Mutation	G	G	T	0.077	p.L555M	13/29	deleterious(0)	MODERATE
L110446	NOTCH1	9	49016945	49016961	chr9:136496384-136496400	Frame_Shift_Del	GGTGCCAGTGGCCTGGC	GGTGCCAGTGGCCTGGC	-	0.406	p.S2458Hfs*62	34/34		HIGH
L53739	NOTCH1	9	49016944	49016960	chr9:136496385-	Frame_Shift_Del	GGGTGCCAGTGGC	GGGTGCCAGTGGC	-	0.244	p.L2455Ffs*65	34/34		HIGH

					136496401		CTG G	CTG G						
M120399	NOTCH1	9	49016863	49016864	chr9:136496481-136496482	Frame_Shift_Ins	-	-	G	0.323	p.V2430Gfs*96	34/34		HIGH
M122308	NOTCH1	9	49016863	49016864	chr9:136496481-136496482	Frame_Shift_Ins	-	-	CTGAT	0.316	p.G2429Lfs*4	34/34		HIGH
L105585	NRAS	17	52418151	52418151	chr1:114716124-114716124	Missense_Mutation	C	C	G	0.4	p.G13R	2/7	deleterious(0)	MODERATE
L107858	NRAS	17	52418154	52418154	chr1:114716127-114716127	Missense_Mutation	C	C	T	0.859	p.G12S	2/7	deleterious(0.03)	MODERATE
L114148	NRAS	17	52418151	52418151	chr1:114716124-114716124	Missense_Mutation	C	C	G	0.252	p.G13R	2/7	deleterious(0)	MODERATE

L52744	NRAS	17	52415853	52415853	chr1:114713908-114713908	Missense_Mutation	T	T	G	0.956	p.Q61P	3/7	deleterious(0)	MODERATE
L53739	NRAS	17	52418151	52418151	chr1:114716124-114716124	Missense_Mutation	C	C	G	0.182	p.G13R	2/7	deleterious(0)	MODERATE
M103733	NRAS	17	52418154	52418154	chr1:114716127-114716127	Missense_Mutation	C	C	T	0.417	p.G12S	2/7	deleterious(0.03)	MODERATE
M108089	NRAS	17	52418153	52418153	chr1:114716126-114716126	Missense_Mutation	C	C	T	0.176	p.G12D	2/7	deleterious(0)	MODERATE
M108735	NRAS	17	52415854	52415854	chr1:114713909-114713909	Missense_Mutation	G	G	T	0.4	p.Q61K	3/7	deleterious(0.01)	MODERATE
M113164	NRAS	17	52418151	52418151	chr1:114716124-114716124	Missense_Mutation	C	C	G	0.26	p.G13R	2/7	deleterious(0)	MODERATE

M114337	NRAS	17	52418151	52418151	chr1:114716124-114716124	Missense_Mutation	C	C	G	0.363	p.G13R	2/7	deleterious(0)	MODERATE
M114677	NRAS	17	52415853	52415853	chr1:114713908-114713908	Missense_Mutation	T	T	C	0.14	p.Q61R	3/7	tolerated(0.06)	MODERATE
M114677	NRAS	17	52418153	52418153	chr1:114716126-114716126	Missense_Mutation	C	C	T	0.387	p.G12D	2/7	deleterious(0)	MODERATE
M121064	NRAS	17	52415853	52415853	chr1:114713908-114713908	Missense_Mutation	T	T	C	0.336	p.Q61R	3/7	tolerated(0.06)	MODERATE
M122308	NRAS	17	52415853	52415853	chr1:114713908-114713908	Missense_Mutation	T	T	C	0.416	p.Q61R	3/7	tolerated(0.06)	MODERATE
M58697	NRAS	17	52415848	52415849	chr1:114713903-114713904	Frame_Shift_Ins	-	-	AGGAGAG	0.304	p.E63Lfs*3	3/7		HIGH

M58697	NRAS	17	52415849	52415850	chr1:114713904-114713905	Frame_Shift_Ins	-	-	TA	0.304	p.E62Dfs*7	3/7		HIGH
M69860	NRAS	17	52418151	52418151	chr1:114716124-114716124	Missense_Mutation	C	C	G	0.88	p.G13R	2/7	deleterious(0)	MODERATE
M69965	NRAS	17	52418153	52418153	chr1:114716126-114716126	Missense_Mutation	C	C	T	0.94	p.G12D	2/7	deleterious(0)	MODERATE
M71281	NRAS	17	52415852	52415852	chr1:114713907-114713907	Missense_Mutation	T	T	G	0.868	p.Q61H	3/7	deleterious(0)	MODERATE
M71609	NRAS	17	52418153	52418153	chr1:114716126-114716126	Missense_Mutation	C	C	T	0.399	p.G12D	2/7	deleterious(0)	MODERATE
M73441	NRAS	17	52418151	52418151	chr1:114716124-114716124	Missense_Mutation	C	C	G	0.314	p.G13R	2/7	deleterious(0)	MODERATE

L114148	NRG1	16	32771846	32771847	chr8:31640508-31640509	Nonsense_Mutation	CA	CA	TT	0.4	p.L29*	1/13		HIGH
L114182	NRG1	16	32771655	32771655	chr8:31640700-31640700	Missense_Mutation	T	T	G	0.8	p.E93A	1/13	deleterious(0.01)	MODERATE
M103733	NRG1	16	32771859	32771859	chr8:31640496-31640496	Missense_Mutation	T	T	C	0.286	p.K25R	1/13	tolerated(0.83)	MODERATE
M113164	NRG1	16	32771660	32771660	chr8:31640695-31640695	Missense_Mutation	C	C	A	0.286	p.K91N	1/13	deleterious(0)	MODERATE
M69965	NRG1	16	32771905	32771905	chr8:31640453-31640453	Missense_Mutation	C	C	A	0.333	p.D10Y	1/13	tolerated_low_confidence(0.1)	MODERATE
M73441	NRG1	16	32771931	32771931	chr8:31640427-31640427	Translation_Start_Site	G	G	T	0.222	p.A1?	1/13	tolerated_low_confidenc	HIGH

													e(0.06)	
M122308	NSD1	4	36063502	36063502	chr5:177295091-177295091	Missense_Mutation	C	C	T	0.204	p.G2577S	22/22	deleterious_low_confidence(0.03)	MODERATE
M99876	NSD1	4	36103319	36103319	chr5:177248213-177248213	Missense_Mutation	G	G	T	0.054	p.S1511R	10/22	deleterious(0)	MODERATE
M99876	NSD1	4	36103326	36103326	chr5:177248206-177248206	Missense_Mutation	G	G	T	0.042	p.A1509D	10/22	deleterious(0.04)	MODERATE
M99876	NSD1	4	36111522	36111523	chr5:177238235-177238236	Splice_Site	CT	CT	AA	0.068	p.X1312_splice			HIGH
M99876	NSD2	3	62184918	62184918	chr4:195351818-195351818	Missense_Mutation	A	A	G	0.222	p.S757P	11/21	deleterious(0)	MODERATE

M99876	NSD3	16	27219233	27219233	chr8:38276301-38276301	Missense_Mutation	C	C	A	0.08	p.P1356Q	22/23	deleterious(0)	MODERATE
M52097	NTRK3	3	51138900	51138900	chr15:87877084-87877084	Missense_Mutation	G	G	A	0.4	p.R779W	19/19	deleterious(0)	MODERATE
M71609	NTRK3	3	51166504	51166504	chr15:87908532-87908532	Missense_Mutation	A	A	G	0.333	p.V685A	16/19	tolerated_low_confidence(0.62)	MODERATE
M99876	NTRK3	3	51512676	51512676	chr15:88255239-88255239	Missense_Mutation	G	G	T	0.333	p.P34T	1/19	tolerated_low_confidence(0.11)	MODERATE
M99876	NUMA1	21	26069786	26069786	chr11:72009310-72009310	Missense_Mutation	G	G	T	0.073	p.Q1601H	16/25	deleterious(0)	MODERATE
M99876	NUP214	9	52895908	52895908	chr9:131178350-	Missense_	G	G	T	0.075	p.P1108H	25/38	deleterious(0)	MODERATE

					131178350	Mutation								
L107858	PABPC1	13	25662240	25662240	chr8:100705674-100705674	Splice_Site	C	C	A	0.25	p.X535_splice			HIGH
M99876	PABPC1	13	25762794	25762794	chr8:100717816-100717816	Missense_Mutation	C	C	A	0.076	p.A154S	3/14	tolerated(0.09)	MODERATE
M99876	PAFAH1B2	5	16447023	16447023	chr11:117145213-117145213	Missense_Mutation	G	G	T	0.4	p.Q41K	1/7	tolerated_low_confidence(0.59)	MODERATE
M71593	PALB2	6	22237401	22237401	chr16:23603578-23603578	Missense_Mutation	A	A	G	0.946	p.T1318A	13/13	tolerated(0.05)	MODERATE
M99876	PALB2	6	22218830	22218830	chr16:23630410-23630410	Missense_Mutation	G	G	T	0.071	p.A737S	5/13	tolerated(0.27)	MODERATE

M99876	PAX3	37	28366741	28366741	chr2:222221318-222221318	Missense_Mutation	G	G	T	0.115	p.H318N	5/8	tolerated(0.08)	MODERATE
M58698	PAX5	11	53376505	53376505	chr9:37020736-37020736	Missense_Mutation	G	G	A	0.245	p.R38C	2/9	deleterious(0)	MODERATE
M73441	PBRM1	20	37147896	37147896	chr3:52644774-52644774	Frame_Shift_Del	A	A	-	0.698	p.I300Yfs*4	11/1		HIGH
M73441	PCM1	16	41226893	41226893	chr8:17938929-17938929	Missense_Mutation	G	G	A	0.359	p.A178T	5/1	deleterious(0.02)	MODERATE
M108735	PDE4DIP	17	57135961	57135961	chr1:120197111-120197111	Nonsense_Mutation	C	C	A	0.333	p.C77*	1/1		HIGH
M120655	PDE4DIP	17	57173655	57173655	chr1:120232908-120232908	Missense_Mutation	C	C	A	0.309	p.P44T	1/1		MODERATE

M121047	PDE4DIP	17	57136022	57136022	chr1:120197202-120197202	Missense_Mutation	C	C	A	0.396	p.P98T	1/1	tolerated_low_confidence(0.07)	MODERATE
M122308	PDE4DIP	17	57340621	57340621	chr1:149017837-149017837	Missense_Mutation	G	G	A	0.567	p.E2105K	37/49	tolerated(0.1)	MODERATE
M73441	PDE4DIP	17	57136025	57136025	chr1:120197205-120197205	Missense_Mutation	C	C	G	0.25	p.Q99E	1/1	tolerated_low_confidence(0.44)	MODERATE
M73441	PDE4DIP	17	57136076	57136076	chr1:120197256-120197256	Missense_Mutation	G	G	T	0.25	p.G116C	1/1	deleterious_low_confidence(0.02)	MODERATE
M99876	PDE4DIP	17	57330396	57330396	chr1:149007328-149007328	Missense_Mutation	G	G	T	0.054	p.D1750Y	31/49	deleterious(0)	MODERATE

M99876	PDE4DIP	17	57332774	57332774	chr1:149009633-149009633	Missense_Mutation	G	G	T	0.053	p.R1825L	33/49	deleterious(0)	MODERATE
M99876	PDE4DIP	17	57333677	57333677	chr1:149010538-149010538	Missense_Mutation	C	C	A	0.072	p.P1910T	34/49	tolerated(0.07)	MODERATE
L53739	PDGFB	10	25809081	25809081	chr22:39233918-39233918	Missense_Mutation	C	C	A	0.4	p.P12Q	1/4		MODERATE
M52097	PDGFB	10	25809140	25809140	chr22:39233859-39233859	Missense_Mutation	C	C	A	0.329	p.L32I	1/4		MODERATE
M73441	PDGFB	10	25809111	25809111	chr22:39233888-39233888	Missense_Mutation	G	G	T	0.25	p.R22L	1/4		MODERATE
M99876	PDGFB	10	25798994	25798994	chr22:39243907-39243907	Missense_Mutation	C	C	A	0.103	p.S19R	1/7	tolerated(0.31)	MODERATE

M99876	PDGFB	10	25809099	25809099	chr22:39233900-39233900	Missense_Mutation	G	G	T	0.4	p.G18V	1/4		MODERATE
M99876	PDGFB	10	25809130	25809130	chr22:39233869-39233869	Missense_Mutation	G	G	T	0.414	p.W28C	1/4		MODERATE
L53739	PDGFRA	13	46732149	46732149	chr4:54231404-54231404	Missense_Mutation	G	G	T	0.333	p.A64S	1/23		MODERATE
L53739	PDGFRA	13	46732165	46732165	chr4:54231418-54231418	Missense_Mutation	G	G	T	0.286	p.S69I	1/23		MODERATE
M120655	PDGFRA	13	46732231	46732231	chr4:54231472-54231472	Missense_Mutation	G	G	T	0.4	p.G91V	1/23		MODERATE
M99876	PDGFRA	13	46732467	46732467	chr4:54231686-54231686	Missense_Mutation	C	C	T	0.25	p.R170C	1/23	deleterious_low_confidence(0)	MODERATE

M106053	PER1	5	32961201	32961201	chr17:81444263-81444263	Missense_Mutation	C	C	T	0.4	p.A840T	19/24	tolerated(0.65)	MODERATE
M73441	PER1	5	32961180	32961180	chr17:81444242-81444242	Nonsense_Mutation	C	C	A	0.4	p.G847*	19/24		HIGH
M114677	PHF6	X	1.05E+08	1.05E+08	chrX:134415094-134415094	Nonsense_Mutation	C	C	T	0.957	p.Q271*	8/10		HIGH
M121064	PIM1	12	6213181	6213181	chr6:37170256-37170256	Missense_Mutation	A	A	G	0.061	p.H186R	1/5	deleterious_low_confidence(0)	MODERATE
M99876	PIM1	12	6213412	6213413	chr6:37170484-37170485	Missense_Mutation	GC	GC	TT	0.025	p.S263I	1/5	deleterious_low_confidence(0)	MODERATE
M99876	PLAG1	29	7565665	7565665	chr8:56167315-56167315	Missense_Mutation	G	G	A	0.07	p.A144V	4/4	deleterious(0)	MODERATE

M99876	PLCG1	24	29202658	29202658	chr20:41163797-41163797	Missense_Mutation	C	C	A	0.067	p.P213H	9/1	deleterious(0)	MODERATE
M99876	PMS2	6	11434445	11434445	chr7:60025500-60025550	Missense_Mutation	G	G	T	0.124	p.T147N	5/31	deleterious_low_confidence(0.01)	MODERATE
M99876	POLD1	1	1.06E+08	1.06E+08	chr19:50407372-50407372	Missense_Mutation	C	C	A	0.15	p.G578C	14/27	deleterious(0)	MODERATE
M99876	POLD1	1	1.06E+08	1.06E+08	chr19:50398846-50398846	Splice_Site	T	T	C	0.2				HIGH
L52744	POLG	3	52405502	52405502	chr15:89362686-89362686	Missense_Mutation	G	G	T	0.286	p.A54E	1/23		MODERATE
M120486	POLG	3	52405391	52405391	chr15:89362575-	Missense_Mutation	G	G	A	0.395	p.A91V	1/23		MODERATE

					89362575									
M73441	POLG	3	52405503	52405503	chr15:89362687-89362687	Missense_Mutation	C	C	A	0.25	p.A54S	1/23		MODERATE
M99876	POLG	3	52405636	52405636	chr15:89362833-89362833	Missense_Mutation	C	C	A	0.25	p.Q9H	1/23		MODERATE
L114148	POLQ	33	24714859	24714859	chr3:121432932-121432932	Missense_Mutation	C	C	T	0.545	p.E2663K	30/31	deleterious(0.02)	MODERATE
M108735	POLQ	33	24837033	24837033	chr3:121545903-121545903	Missense_Mutation	G	G	T	0.286	p.S112Y	2/1	deleterious_low_confidence(0.02)	MODERATE
M120655	POLQ	33	24837240	24837240	chr3:121546108-121546108	Missense_Mutation	C	C	A	0.396	p.A55S	1/31		MODERATE

M73441	POLQ	33	24763669	24763669	chr3:121481686-121481686	Missense_Mutation	C	C	A	0.049	p.G2146W	20/31	deleterious(0)	MODERATE
M99876	POLQ	33	24836952	24836952	chr3:121545822-121545822	Missense_Mutation	G	G	A	0.4	p.S139F	2/1	deleterious_low_confidence(0.02)	MODERATE
M121010	PPFIBP1	27	20055928	20055929	chr12:27667259-27667260	Missense_Mutation	CA	CA	TG	0.458	p.L393S	12/29	tolerated(0.8)	MODERATE
M101740	PPM1D	9	35857127	35857127	chr17:60663320-60663320	Missense_Mutation	G	G	T	0.373	p.T529N	6/6	deleterious_low_confidence(0.01)	MODERATE
M71679	PPM1D	9	35857396	35857397	chr17:60663050-60663051	Frame_Shift_Del	AA	AA	-	0.541	p.L439Rfs*3	6/6		HIGH
M99876	PPM1D	9	35868961	35868961	chr17:60648067-	Missense_	C	C	A	0.079	p.E334D	4/6	tolerated(0.1)	MODERATE

					60648067	Mutation								
M58697	PRDM1	12	63490198	63490199	chr6:106105525-106105526	Frame_Shift_Ins	-	-	GGCGGCGG	0.227	p.L455Gfs*53	5/7		HIGH
U69959	PRDM1	12	63490198	63490199	chr6:106105525-106105526	Frame_Shift_Ins	-	-	GGCGGCGG	0.218	p.L455Gfs*53	5/7		HIGH
M99876	PRDM16	5	57994900	57994900	chr1:34124006-34124006	Missense_Mutation	C	C	A	0.028	p.L724I	9/17	tolerated(0.05)	MODERATE
M103733	PREX2	29	17529712	17529712	chr8:68017859-68017859	Missense_Mutation	G	G	T	0.25	p.R52L	2/1	deleterious(0)	MODERATE
M58697	PRF1	4	21500862	21500862	chr10:70600993-70600993	Translation_Start_Site	C	C	A	0.222	p.M1?	1/2		HIGH

M121064	PRKCB	6	22064779	22064779	chr16:23837092-23837092	Missense_Mutation	G	G	T	0.286	p.P121H	1/17	deleterious_low_confidence(0)	MODERATE
M99876	PRKCB	6	22064770	22064770	chr16:23837101-23837101	Missense_Mutation	C	C	A	0.246	p.C124F	1/17	deleterious_low_confidence(0)	MODERATE
M58698	PRKD1	8	9027775	9027775	chr14:29597730-29597730	Missense_Mutation	C	C	T	0.146	p.R689Q	18/20	deleterious(0)	MODERATE
M99876	PRPF40B	27	5031239	5031239	chr12:49631480-49631480	Missense_Mutation	G	G	T	0.059	p.P157Q	2/24	deleterious(0.04)	MODERATE
M99876	PSIP1	11	35761479	35761479	chr9:15479661-15479661	Missense_Mutation	C	C	A	0.079	p.E161D	6/15	tolerated(0.36)	MODERATE
M99876	PTCH1	1	71296212	71296212	chr9:95456386-95456386	Nonsense_Mutation	G	G	T	0.049	p.E1063*	21/25		HIGH

L110446	PTPN11	26	10014644	10014644	chr12:112450395-112450395	Missense_Mutation	C	C	T	0.298	p.A72V	3/15	deleterious(0.02)	MODERATE
L114148	PTPN11	26	10014608	10014608	chr12:112450359-112450359	Missense_Mutation	G	G	T	0.251	p.G60V	3/15	deleterious(0)	MODERATE
L114182	PTPN11	26	10014644	10014644	chr12:112450395-112450395	Missense_Mutation	C	C	T	0.333	p.A72V	3/15	deleterious(0.02)	MODERATE
M101740	PTPN11	26	10014656	10014656	chr12:112450407-112450407	Missense_Mutation	A	A	C	0.459	p.E76A	3/15	deleterious(0)	MODERATE
M120378	PTPN11	26	10014644	10014644	chr12:112450395-112450395	Missense_Mutation	C	C	T	0.408	p.A72V	3/15	deleterious(0.02)	MODERATE
M120398	PTPN11	26	10014640	10014640	chr12:112450391-112450391	Missense_Mutation	T	T	C	0.138	p.F71L	3/15	deleterious(0)	MODERATE

M120399	PTPN11	26	10014655	10014655	chr12:112450406-112450406	Missense_Mutation	G	G	A	0.406	p.E76K	3/15	deleterious(0.01)	MODERATE
U69959	PTPN11	26	10007439	10007439	chr12:112446385-112446385	Missense_Mutation	A	A	G	0.317	p.T42A	2/15	tolerated(0.05)	MODERATE
L105735	PTPN13	32	10255337	10255337	chr4:86732431-86732431	Missense_Mutation	C	C	A	0.286	p.T548K	11/1	deleterious(0.01)	MODERATE
M108089	PTPN13	32	10255319	10255319	chr4:86732413-86732413	Missense_Mutation	C	C	A	0.329	p.P542H	11/1	deleterious(0)	MODERATE
L107858	PTPRB	10	12286320	12286320	NA	Missense_Mutation	C	C	A	0.4	p.G2154V	28/28		MODERATE
L110446	PTPRB	10	12286237	12286237	NA	Missense_Mutation	G	G	A	0.397	p.R2182C	28/28		MODERATE

M73441	PTPRB	10	12286170	12286170	NA	Missense_Mutation	G	G	T	0.286	p.P2204Q	28/28		MODERATE
M73441	PTPRB	10	12286299	12286299	NA	Missense_Mutation	C	C	A	0.333	p.C2161F	28/28		MODERATE
M73441	PTPRC	7	4214422	4214422	NA	Missense_Mutation	G	G	T	0.282	p.S103Y	1/28	deleterious_low_confidence(0)	MODERATE
M73441	PTPRC	7	4214645	4214645	NA	Missense_Mutation	G	G	C	0.333	p.H29D	1/28		MODERATE
M99876	PTPRC	7	4214596	4214596	NA	Missense_Mutation	G	G	A	0.25	p.A45V	1/28		MODERATE
M71679	PTPRD	11	29115327	29115327	chr9:8341250-8341250	Missense_Mutation	C	C	T	0.531	p.A1667T	30/35	tolerated(0.12)	MODERATE
M73441	PTPRD	11	29115326	29115326	chr9:8341249-	Missense_	G	G	T	0.088	p.A1667D	30/35	deleterious(0)	MODERATE

					8341249	Mutation								
M99876	PTPRD	11	29270371	29270371	chr9:85010200-85010120	Missense_Mutation	G	G	T	0.071	p.P618Q	12/1	tolerated(0.57)	MODERATE
M58697	PTPRK	1	66628471	66628472	chr6:127996943-127996944	Frame_Shift_Ins	-	-	T	0.331	p.D1018Rfs*4	20/34		HIGH
M71593	PTPRT	24	30045002	30045002	chr20:42116043-42116043	Missense_Mutation	C	C	A	0.4	p.G1037V	23/33	tolerated_low_confidence(0.06)	MODERATE
M99876	RABEP1	5	31432080	31432080	chr17:53352779-53352779	Missense_Mutation	C	C	G	0.086	p.A200P	4/18	tolerated(0.09)	MODERATE
L105585	RAC1	6	11732828	11732828	chr7:63745785-63745785	Missense_Mutation	C	C	T	0.4	p.S105F	1/7	deleterious_low_confidence(0)	MODERATE

M115951	RAC1	6	11732848	11732848	chr7:637460 5-63746 05	Missense_Mutation	G	G	T	0.286	p.G112C	1/7	deleterious_low_confidence(0)	MODERATE
M120655	RAC1	6	11732735	11732735	chr7:637449 3-63744 93	Missense_Mutation	A	A	G	0.222	p.E74G	1/7	deleterious_low_confidence(0)	MODERATE
M69965	RAC1	6	11732621	11732621	chr7:637436 4-63743 64	Missense_Mutation	G	G	A	0.333	p.S36N	1/7	deleterious_low_confidence(0)	MODERATE
M73441	RAD21	13	16348326	16348326	chr8:116857456-116857456	Missense_Mutation	C	C	G	0.25	p.D167H	6/14	tolerated(0.08)	MODERATE
M121064	RANBP2	10	35109833	35109833	chr2:108765695-108765695	Missense_Mutation	C	C	T	0.447	p.G1718E	20/30	tolerated(0.16)	MODERATE
M121064	RANBP2	10	35127511	35127511	chr2:108749114-108749114	Missense_Mutation	C	C	T	0.44	p.A420T	9/30	tolerated(0.25)	MODERATE

M99876	RAP1GDS1	32	20635996	20635996	chr4:98379157-98379157	Nonsense_Mutation	G	G	T	0.088	p.E168*	6/16		HIGH
M99876	RAP1GDS1	32	20669630	20669630	chr4:98417430-98417430	Missense_Mutation	G	G	T	0.286	p.W324L	10/16	tolerated(0.08)	MODERATE
M69965	RARA	9	22262910	22262910	chr17:40348378-40348378	Missense_Mutation	G	G	A	0.569	p.L81F	3/9	tolerated(0.15)	MODERATE
L105585	RB1	22	3073920	3073920	chr13:48465007-48465007	Missense_Mutation	G	G	A	0.333	p.R733C	21/26	tolerated(0.09)	MODERATE
M99876	REL	10	61023652	61023652	chr2:60922530-60922530	Missense_Mutation	G	G	T	0.094	p.G596C	10/10	tolerated_low_confidence(0.19)	MODERATE
L107858	RET	28	3949668	3949668	chr10:43126591-	Missense_Mutation	G	G	A	0.553	p.A1105V	19/20	deleterious(0.02)	MODERATE

					43126591									
M99876	RFWD3	5	75964806	75964806	chr16:74661142-74661142	Missense_Mutation	G	G	T	0.25	p.S142I	2/13	tolerated_low_confidence(0.1)	MODERATE
M99876	RFWD3	5	75995411	75995411	chr16:74628661-74628661	Missense_Mutation	C	C	A	0.333	p.P623Q	11/13	deleterious(0)	MODERATE
M52097	RHOA	20	39824745	39824745	chr3:49411818-49411818	Splice_Site	T	T	C	0.286				HIGH
M101740	ROBO2	31	9507204	9507204	chr3:77565037-77565037	Missense_Mutation	G	G	A	0.529	p.T589M	12/27	deleterious(0)	MODERATE
M99876	RPL5	6	56213160	56213160	chr1:92834840-92834840	Missense_Mutation	G	G	T	0.13	p.P87Q	4/8	deleterious(0)	MODERATE

M122308	RSPO2	13	8660557	8660557	chr8:107957883-107957883	Missense_Mutation	A	A	G	0.158	p.F265L	4/4		MODERATE
L105735	RUNX1	31	30178051	30178051	chr21:34799419-34799419	Frame_Shift_Del	T	T	-	0.421	p.Q283Hfs*28	8/9		HIGH
L110446	RUNX1	31	30210024	30210025	chr21:34834466-34834467	Frame_Shift_Ins	-	-	T	0.301	p.R250Qfs*11	7/9		HIGH
M119591	RUNX1	31	30254169	30254170	chr21:34880686-34880687	Frame_Shift_Ins	-	-	T	0.365	p.G127Rfs*11	5/9		HIGH
M69860	SALL4	24	37949140	37949140	chr20:51792326-51792326	Missense_Mutation	C	C	T	0.449	p.G53S	2/4	tolerated(0.09)	MODERATE
M99876	SALL4	24	37947949	37947949	chr20:51791129-51791129	Missense_Mutation	C	C	A	0.202	p.G450C	2/4	tolerated(0.22)	MODERATE

M108089	SBDS	6	12634 54	12634 54	chr7:72828452-72828452	Missense_Mutation	T	T	C	0.333	p.K5R	1/6		MODERATE
M122308	SDHAF2	18	54987040	54987040	chr11:61429684-61429684	Missense_Mutation	G	G	A	0.614	p.R119W	1/4		MODERATE
M58697	SDHAF2	18	54987040	54987040	chr11:61429684-61429684	Missense_Mutation	G	G	A	0.558	p.R119W	1/4		MODERATE
M58698	SDHAF2	18	54986706	54986706	chr11:61430019-61430019	Missense_Mutation	G	G	A	0.286	p.A230V	1/4		MODERATE
U69959	SDHAF2	18	54986680	54986680	chr11:61430045-61430045	Missense_Mutation	A	A	G	0.333	p.S239P	1/4		MODERATE
L107858	SDHC	38	21200065	21200065	chr1:161314643-161314643	Missense_Mutation	C	C	T	0.25	p.R70Q	1/6	deleterious_low_confidence(0)	MODERATE

M58698	SDHC	38	21200267	21200267	chr1:161314440-161314440	Missense_Mutation	C	C	T	0.4	p.A3T	1/6		MODERATE
M71609	SDHC	38	21200252	21200252	chr1:161314455-161314455	Missense_Mutation	G	G	A	0.25	p.P8S	1/6		MODERATE
M99876	SDHC	38	21199948	21199948	chr1:161314754-161314754	Missense_Mutation	C	C	A	0.286	p.R109I	1/6	deleterious(0)	MODERATE
M71679	SETBP1	7	46121201	46121201	chr18:44951954-44951954	Missense_Mutation	C	C	T	0.973	p.G872R	4/6	deleterious(0)	MODERATE
L107858	SETD1B	26	7466639	7466639	chr12:121805154-121805154	Missense_Mutation	G	G	A	0.387	p.P71S	2/17	deleterious(0)	MODERATE
M99876	SETD1B	26	7456166	7456166	chr12:121817400-121817400	Missense_Mutation	G	G	A	0.27	p.A1006V	8/17	tolerated(0.09)	MODERATE

M101740	SFPQ	15	68806620	68806620	chr1:351925534-35192534	Missense_Mutation	C	C	A	0.333	p.S169R	3/12	deleterious_low_confidence(0.01)	MODERATE
M73441	SFPQ	15	68805995	68805995	chr1:351925559-35192559	Missense_Mutation	C	C	A	0.2	p.A161E	3/12	deleterious_low_confidence(0.01)	MODERATE
M99876	SFPQ	15	68847007	68847007	chr1:351880067-35188067	Missense_Mutation	G	G	T	0.219	p.R569M	9/12	deleterious(0)	MODERATE
M99876	SFPQ	15	68878447	68878447	chr1:351845584-35184584	Missense_Mutation	C	C	A	0.091	p.R661S	12/12	deleterious_low_confidence(0)	MODERATE
M69965	SGK1	1	27089647	27089647	chr6:134172224-134172224	Missense_Mutation	C	C	T	0.286	p.G347D	10/14	tolerated(0.87)	MODERATE
L107858	SH2B3	26	90685776	90685776	chr12:111446826-	Missense_	C	C	T	0.416	p.P287L	3/8	deleterious(0)	MODERATE

					111446826	Mutation								
M73441	SH3GL1	20	55311139	55311139	chr19:43607772-43607772	Missense_Mutation	G	G	T	0.119	p.C383F	11/11		MODERATE
M99876	SH3GL1	20	55305986	55305986	chr19:43669441-43669441	Missense_Mutation	C	C	A	0.087	p.F33L	2/11	deleterious(0.01)	MODERATE
L114148	SLC34A2	3	84717536	84717536	NA	Missense_Mutation	C	C	G	0.333	p.R24T	2/14	tolerated_low_confidence(0.2)	MODERATE
M99876	SMAD4	1	23882555	23882555	chr18:51078400-51078400	Missense_Mutation	C	C	A	0.073	p.R531L	12/12	deleterious(0)	MODERATE
M99876	SMAD4	1	23884331	23884331	chr18:51076659-51076659	Missense_Mutation	G	G	T	0.096	p.H444N	11/12	deleterious(0.02)	MODERATE

M120486	SMARCA4	20	50245796	50245797	chr19:10986932-10986933	Frame_Shift_Ins	-	-	G	0.312	p.G264Rfs*23	5/1		HIGH
M73441	SMARCA4	20	50241852	50241852	chr19:10989397-10989397	Missense_Mutation	G	G	T	0.075	p.A400E	7/1	deleterious(0)	MODERATE
M99876	SMARCA4	20	50209148	50209148	chr19:11024385-11024385	Missense_Mutation	G	G	T	0.075	p.H1010N	21/35	deleterious(0)	MODERATE
M99876	SMARCE1	9	22032657	22032657	chr17:40630858-40630858	Nonsense_Mutation	C	C	T	0.25	p.Q260*	9/10		HIGH
M99876	SMARCE1	9	22035203	22035203	chr17:40628952-40628952	Missense_Mutation	G	G	T	0.4	p.G322C	10/10	tolerated(0.16)	MODERATE
M99876	SMC1A	X	45116164	45116165	chrX:53380689-53380690	Missense_Mutation	CT	CT	AA	0.059	p.Q1183L	24/25	deleterious(0)	MODERATE

M99876	SMC1A	X	45137601	45137601	chrX:53405930-53405930	Missense_Mutation	C	C	A	0.13	p.Q524H	10/25	tolerated(0.9)	MODERATE
L110446	SMO	14	7527914	7527914	NA	Missense_Mutation	C	C	G	0.286	p.E40D	1/12	tolerated_low_confidence(0.05)	MODERATE
M108089	SNX29	6	30414081	30414081	chr16:12477780-12477780	Missense_Mutation	C	C	A	0.36	p.S730I	18/20	tolerated(0.14)	MODERATE
L114182	SPECC1	5	40137543	40137543	chr17:20096712-20096712	Missense_Mutation	G	G	C	0.66	p.R21G	1/14	deleterious(0.04)	MODERATE
M99876	SRC	24	26017548	26017548	chr20:37403199-37403199	Missense_Mutation	G	G	T	0.086	p.Q494H	13/13	deleterious(0.03)	MODERATE
M99876	STAG1	23	32954065	32954065	chr3:136521386-	Missense_Mutation	C	C	A	0.073	p.G168V	6/1	deleterious(0)	MODERATE

					136521386									
M73441	STAG2	X	95477869	95477869	chrX:124045167-124045167	Missense_Mutation	A	A	G	0.25	p.S156G	7/1	deleterious(0.02)	MODERATE
M99876	STAT3	9	20584599	20584599	chr17:42345640-42345640	Missense_Mutation	G	G	T	0.088	p.K97N	4/23	tolerated(0.74)	MODERATE
M70848	STAT5B	9	20700870	20700870	chr17:42219355-42219355	Missense_Mutation	A	A	G	0.4	p.N264D	6/18	deleterious(0.04)	MODERATE
L107858	STAT6	10	12433398	12433398	chr12:57108521-57108521	Missense_Mutation	A	A	G	0.333	p.L46P	1/20		MODERATE
M70848	STAT6	10	12434366	12434366	chr12:57108589-57108589	Missense_Mutation	T	T	A	0.4	p.Q23H	1/20		MODERATE

M99876	STRN	17	29274009	29274009	chr2:36849487-36849487	Missense_Mutation	C	C	A	0.083	p.G670V	18/18	deleterious(0)	MODERATE
M120486	SUZ12	9	41015311	41015311	chr17:31975710-31975710	Missense_Mutation	T	T	C	0.333	p.I274V	7/16	tolerated(0.24)	MODERATE
M99876	SYK	1	95912187	95912187	chr9:90887769-90887769	Missense_Mutation	C	C	A	0.222	p.W559C	12/15	deleterious(0)	MODERATE
L114182	TAF15	9	37844660	37844683	chr17:35844712-35844735	In_Frame_Del	TAGCCGCCTCCTCGGTCTCCCCCG	TAGCCGCCTCCTCGGTCTCCCCCG	-	0.58	p.G509_G516del	13/14		MODERATE
M108735	TAL1	15	13453717	13453717	chr1:47225055-47225055	Missense_Mutation	G	G	T	0.286	p.A262S	2/4	deleterious_low_confidence(0.04)	MODERATE

M70848	TAL1	15	13453220	13453220	chr1:47225552-47225552	Missense_Mutation	C	C	A	0.4	p.A96D	2/4		MODERATE
M73441	TAL1	15	13453653	13453653	chr1:47225120-47225120	Missense_Mutation	G	G	C	0.4	p.W240C	2/4		MODERATE
M99876	TBL1XR1	34	40587081	40587081	chr3:177038173-177038173	Splice_Site	C	C	A	0.043	p.X350_splice			HIGH
M73441	TCEA1	29	5665811	5665811	chr8:54051143-54051143	Missense_Mutation	G	G	T	0.124	p.H161N	8/17	deleterious_low_confidence(0)	MODERATE
M73441	TCF12	30	22247659	22247659	chr15:57063816-57063816	Nonsense_Mutation	C	C	A	0.058	p.S72*	3/20		HIGH
M99876	TCF12	30	22387929	22387929	chr15:57192197-57192197	Missense_Mutation	G	G	T	0.083	p.A144S	6/20	tolerated(0.31)	MODERATE

M108735	TCF3	20	57280917	57280917	chr19:16154 91-16154 91	Missense_Mutation	C	C	A	0.333	p.P592H	17/17	deleterious(0.01)	MODERATE
M120486	TCF7L2	28	24162640	24162645	chr10:11316 5929-11316 5934	In_Frame_Del	CCCAGC	CCCAGC	-	0.572	p.Q555_P556del	13/13		MODERATE
M120486	TCF7L2	28	24162678	24162695	NA	In_Frame_Del	CAGCCCCAGCCCCAGCC	CAGCCCCAGCCCCAGCC	-	0.571	p.Q551_P556del	13/13		MODERATE
M121047	TCF7L2	28	24091961	24091961	chr10:11308 9440-11308 9440	Missense_Mutation	A	A	G	0.4	p.H93R	4/13	deleterious_low_confidence(0.01)	MODERATE
M70848	TCF7L2	28	24162694	24162695	NA	Frame_Shift_Ins	-	-	G	0.376	p.Q553Pfs*60	13/13		HIGH
M99876	TENT5C	17	54967213	54967213	chr1:117622860-117622860	Missense_Mutation	C	C	A	0.083	p.P42Q	1/1	tolerated_low_confidence(0.1)	MODERATE

M73441	TERT	34	11306872	11306872	chr5:1253901-1253901	Missense_Mutation	G	G	T	0.049	p.R1228L	15/15		MODERATE
M99876	TERT	34	11288850	11288850	chr5:1294808-1294808	Missense_Mutation	G	G	T	0.286	p.G61V	1/15	deleterious(0.02)	MODERATE
M99876	TERT	34	11293009	11293009	chr5:1282604-1282604	Missense_Mutation	G	G	T	0.099	p.A521S	3/15	tolerated(1)	MODERATE
M71593	TET1	4	19839169	19839169	chr10:68645608-68645608	Missense_Mutation	A	A	G	0.639	p.E961G	3/11	deleterious(0.03)	MODERATE
L114182	TET2	32	26139881	26139881	chr4:105272843-105272843	Nonsense_Mutation	A	A	T	0.364	p.K1498*	10/11		HIGH
M108089	TET2	32	26105091	26105092	chr4:105234382-105234383	Frame_Shift_Del	AG	AG	-	0.427	p.E151Ifs*12	3/11		HIGH

M108089	TET2	32	26108086	26108086	chr4:105237353-105237353	Splice_Site	T	T	C	0.25	p.X1147_splice			HIGH
M99876	TET2	32	26105333	26105334	chr4:105234621-105234622	Frame_Shift_Ins	-	-	A	0.386	p.T232Nfs*25	3/11		HIGH
M99876	TET2	32	26106613	26106613	chr4:105235919-105235919	Missense_Mutation	G	G	T	0.07	p.Q656H	3/11	deleterious(0.02)	MODERATE
M99876	TET2	32	26108065	26108065	chr4:105237332-105237332	Missense_Mutation	C	C	A	0.2	p.F1140L	3/11	tolerated(0.14)	MODERATE
M114677	TFEB	12	10393400	10393400	chr6:41710719-41710719	Missense_Mutation	C	C	A	0.286	p.G81W	1/9	deleterious_low_confidence(0)	MODERATE
M121047	TFEB	12	10418357	10418357	chr6:41730744-41730744	Missense_Mutation	T	T	A	0.4	p.R18W	1/9	deleterious_low_confide	MODERATE

													nce(0.01)	
M99876	TFEB	12	10418377	10418377	chr6:41730764-41730764	Missense_Mutation	G	G	T	0.4	p.P11H	1/9	tolerated_low_confidence(0.05)	MODERATE
M99876	TFPT	1	1.03E+08	1.03E+08	chr19:54108191-54108191	Missense_Mutation	G	G	T	0.103	p.E159D	5/6	tolerated(0.06)	MODERATE
L52744	TFRC	33	29237184	29237184	chr3:196082116-196082116	Missense_Mutation	C	C	T	0.68	p.G115R	1/19	deleterious_low_confidence(0)	MODERATE
M113164	TFRC	33	29237184	29237184	chr3:196082116-196082116	Missense_Mutation	C	C	T	0.384	p.G115R	1/19	deleterious_low_confidence(0)	MODERATE
M114337	TFRC	33	29237184	29237184	chr3:196082116-196082116	Missense_Mutation	C	C	T	0.538	p.G115R	1/19	deleterious_low_confidence(0)	MODERATE

M71593	TFRC	33	29237184	29237184	chr3:196082116-196082116	Missense_Mutation	C	C	T	0.778	p.G115R	1/19	deleterious_low_confidence(0)	MODERATE
M99876	TFRC	33	29210018	29210018	chr3:196053421-196053421	Missense_Mutation	C	C	G	0.219	p.M837I	18/19	deleterious(0.01)	MODERATE
M99876	TFRC	33	29218564	29218564	chr3:196062903-196062903	Missense_Mutation	C	C	A	0.111	p.S610I	12/19	deleterious(0)	MODERATE
M99876	TFRC	33	29237264	29237264	chr3:196082195-196082195	Missense_Mutation	C	C	A	0.222	p.W88L	1/19	deleterious_low_confidence(0)	MODERATE
L114182	THRAP3	15	5958971	5958973	chr1:36301614-36301616	In_Frame_Del	TGT	TGT	-	0.56	p.N858del	11/12		MODERATE
M99876	THRAP3	15	5970135	5970135	chr1:36286937-36286937	Missense_Mutation	G	G	T	0.4	p.A237D	4/12	tolerated(0.12)	MODERATE

M114337	TNC	11	69135427	69135427	chr9:115084260-115084260	Missense_Mutation	C	C	T	0.423	p.A694T	4/30	deleterious(0)	MODERATE
M58698	TNFAIP3	1	30258145	30258145	chr6:137878513-137878513	Missense_Mutation	G	G	T	0.38	p.W356C	6/8	deleterious(0)	MODERATE
M99876	TNFAIP3	1	30258965	30258965	chr6:137879333-137879333	Nonsense_Mutation	G	G	T	0.071	p.E630*	6/8		HIGH
M101740	TP53	5	32563362	32563362	chr17:7674191-7674191	Missense_Mutation	C	C	T	0.946	p.E310K	7/11	deleterious(0)	MODERATE
M120398	TP53	5	32563400	32563400	chr17:7674229-7674229	Missense_Mutation	C	C	T	0.125	p.G297D	7/11	deleterious(0)	MODERATE
M120486	TP53	5	32563026	32563026	chr17:7673773-7673773	Missense_Mutation	G	G	A	0.433	p.R335W	8/11	deleterious(0)	MODERATE

M71593	TP53	5	32563423	32563423	chr17:7674252-7674252	Missense_Mutation	C	C	A	0.872	p.M289I	7/11	deleterious(0)	MODERATE
L105585	TPM3	7	43051147	43051147	chr1:154176142-154176142	Missense_Mutation	C	C	T	0.337	p.A117V	3/9	deleterious(0.04)	MODERATE
L52744	TPM3	7	43052657	43052657	chr1:154173167-154173167	Missense_Mutation	G	G	T	0.333	p.D138Y	4/9	deleterious(0)	MODERATE
M120486	TPM3	7	43051120	43051120	chr1:154176169-154176169	Missense_Mutation	C	C	T	0.329	p.A108V	3/9	deleterious(0.04)	MODERATE
M119591	TPR	7	19418017	19418017	chr1:186345596-186345596	Missense_Mutation	C	C	T	0.57	p.R1064H	25/52	deleterious(0.02)	MODERATE
M121064	TRAF7	6	38960593	38960593	chr16:1974418-1974418	Missense_Mutation	C	C	T	0.428	p.D91N	2/20	tolerated(0.42)	MODERATE

M99876	TRIM27	35	25918623	25918623	chr6:28920240-28920240	Missense_Mutation	G	G	T	0.088	p.S124R	3/7	tolerated(0.55)	MODERATE
M99876	TRIM33	17	52138890	52138890	chr1:114421464-114421464	Missense_Mutation	G	G	T	0.088	p.P648Q	12/21	deleterious(0.01)	MODERATE
M99876	TRIM33	17	52230400	52230400	chr1:114511250-114511250	Missense_Mutation	G	G	A	0.141	p.A44V	1/21	tolerated_low_confidence(0.08)	MODERATE
M99876	TRIM33	17	52230418	52230418	chr1:114511268-114511268	Missense_Mutation	C	C	A	0.25	p.G38V	1/21		MODERATE
M99876	TRIP11	8	12778000	12778000	chr14:91999392-91999392	Missense_Mutation	C	C	A	0.06	p.E1669D	15/23	tolerated(0.09)	MODERATE
M99876	TRIP11	8	13494009	13494011	chr14:92096759-	In_Frame_Del	GAA	GAA	-	0.067	p.S35del	2/11		MODERATE

					92096761									
M70848	TRRAP	6	10597812	10597812	chr7:98925166-98925166	Missense_Mutation	G	G	A	0.243	p.R959W	21/72	tolerated(0.05)	MODERATE
M73441	TRRAP	6	10574733	10574733	chr7:98955247-98955247	Missense_Mutation	C	C	A	0.082	p.E1959D	40/72	tolerated(0.06)	MODERATE
M99876	TRRAP	6	10541193	10541193	chr7:98988793-98988793	Missense_Mutation	C	C	A	0.073	p.A3139S	62/72	tolerated(0.12)	MODERATE
M99876	TSC1	9	51447220	51447220	chr9:132903693-132903693	Missense_Mutation	G	G	T	0.102	p.K722N	15/21	deleterious(0)	MODERATE
M99876	TSC1	9	51454589	51454589	chr9:132896317-132896317	Missense_Mutation	C	C	A	0.091	p.P1141Q	21/21	tolerated(0.14)	MODERATE
M120486	UBR5	13	39274241	39274241	chr8:102297589-	Nonsense_	C	C	A	0.176	p.E1148*	27/59		HIGH

					10229 7589	Mutati on								
M121 064	UBR5	13	39095 82	39095 82	chr8:1 02278 876-10227 8876	Misse nse_ Mutati on	T	T	C	0.391	p.S20 80G	44/59	tolerat ed(0.5 8)	MOD ERAT E
M715 93	UBR5	13	39795 79	39795 79	chr8:1 02361 619-10236 1619	Nonse nse_ Mutati on	C	C	A	0.25	p.E24 *	2/1		HIGH
M998 76	UBR5	13	39369 43	39369 46	chr8:1 02305 082-10230 5085	Splice _Site	CAC C	CAC C	-	0.143	p.X94 3_spli ce	21/59		HIGH
M998 76	USP4 4	15	35409 532	35409 533	chr12: 95528 811-95528 812	Frame _Shift _Del	AC	AC	-	0.124	p.C53 9*	2/5		HIGH
M998 76	USP4 4	15	35409 534	35409 534	chr12: 95528 813-95528 813	Misse nse_ Mutati on	A	A	T	0.124	p.C53 9S	2/5	delete rious(0)	MOD ERAT E

M99876	VHL	20	8211232	8211232	chr3:10141898-10141898	Missense_Mutation	C	C	A	0.049	p.E17D	1/3	deleterious_low_confidence(0.03)	MODERATE
M121064	WAS	X	41887752	41887752	chrX:48688813-48688813	Nonsense_Mutation	C	C	A	0.333	p.S333*	9/10		HIGH
M70848	WIF1	10	7670331	7670331	chr12:65062549-65062549	Missense_Mutation	C	C	A	0.091	p.G253V	7/12	deleterious(0)	MODERATE
M121010	WRN	16	33198653	33198653	chr8:31143586-31143586	Missense_Mutation	C	C	A	0.15	p.D1208Y	27/35	deleterious(0.03)	MODERATE
M99876	WRN	16	33200329	33200329	chr8:31141777-31141777	Splice_Site	A	A	G	0.079	p.X1170_splice			HIGH
M99876	WRN	16	33233690	33233690	chr8:31100890-	Nonsense_Mutation	C	C	A	0.042	p.E765*	17/35		HIGH

					31100890									
U69959	WRN	16	33184109	33184109	chr8:31154712-31154712	Missense_Mutation	G	G	A	0.134	p.A1351V	31/35	tolerated(0.51)	MODERATE
M73441	WWTR1	23	44302803	44302803	chr3:149542357-149542357	Missense_Mutation	C	C	T	0.072	p.R250H	3/6	deleterious(0.01)	MODERATE
M73441	XPC	20	4302937	4302937	chr3:14148617-14148617	Missense_Mutation	C	C	A	0.086	p.D799Y	13/16	deleterious(0)	MODERATE
M99876	XPC	20	4309394	4309394	chr3:141586661-141586661	Nonsense_Mutation	C	C	A	0.064	p.G416*	9/16		HIGH
M120486	XPO1	10	61560181	61560182	chr2:61502041-61502042	Splice_Site	-	-	T	0.573	p.X122_splice			HIGH

M99876	XPO1	10	61558165	61558165	chr2:61499712-61499712	Splice_Site	C	C	A	0.111	p.X197_splice			HIGH
M71335	ZCCHC8	26	6902909	6902910	chr12:122492753-122492754	Frame_Shift_Ins	-	-	TT	0.457	p.L94Ffs*8	3/14		HIGH
L71592	ZFHX3	5	78608288	78608288	chr16:72958440-72958440	Missense_Mutation	C	C	A	0.145	p.R567L	1/9	tolerated_low_confidence(0.14)	MODERATE
M120486	ZFHX3	5	78609959	78609959	chr16:72960117-72960117	Missense_Mutation	G	G	A	0.579	p.S10L	1/9	tolerated_low_confidence(0.14)	MODERATE
M73441	ZFHX3	5	78464723	78464723	chr16:72797270-72797270	Missense_Mutation	G	G	T	0.028	p.S1820R	8/9	deleterious(0)	MODERATE
M99876	ZFHX3	5	78461923	78461923	chr16:72794473-	Nonsense_	C	C	A	0.021	p.E2754*	8/9		HIGH

					72794473	Mutation								
M99876	ZFHX3	5	78466180	78466180	chr16:72798703-72798703	Missense_Mutation	C	C	A	0.141	p.D1335Y	8/9	deleterious(0)	MODERATE
M99876	ZFHX3	5	78609580	78609580	chr16:72959738-72959738	Missense_Mutation	C	C	A	0.056	p.Q136H	1/9	deleterious(0)	MODERATE
U69959	ZFHX3	5	78461123	78461125	chr16:72793673-72793675	In_Frame_Del	CTT	CTT	-	0.166	p.K3020del	8/9		MODERATE
M99876	ZMYM2	25	18054376	18054376	chr13:20082807-20082807	Missense_Mutation	C	C	A	0.119	p.D1199Y	22/24	deleterious(0)	MODERATE
M99876	ZMYM3	X	55594730	55594730	chrX:71245685-71245685	Missense_Mutation	G	G	T	0.103	p.A1001D	16/24	deleterious(0.02)	MODERATE

M99876	ZMYM3	X	55602055	55602055	chrX:71252615-71252615	Missense_Mutation	C	C	G	0.05	p.S214T	2/24	tolerated_low_confidence(0.39)	MODERATE
M119591	ZNRF3	26	22391622	22391622	chr22:29050456-29050456	Missense_Mutation	T	T	C	0.676	p.Y651H	7/8	tolerated_low_confidence(0.1)	MODERATE
M58698	ZNRF3	26	22391050	22391050	chr22:29049860-29049860	Missense_Mutation	G	G	A	0.548	p.C460Y	7/8	deleterious(0)	MODERATE
M99876	ZNRF3	26	22387828	22387828	chr22:29046792-29046792	Missense_Mutation	G	G	A	0.389	p.R174H	5/8	tolerated(0.18)	MODERATE

Supplemental Table 21: Overview of genes with variants identified and their gene family

Gene Family	Genes
Cytokines and growth factors	NRG1, PDGFB, PDGFRA, RABEP1, SBDS, TNC
Transcription factors	ACVR2A, AFDN, AFF1, AFF3, ARHGAP35, ARID1B, ATRX, BAZ1A, BCL11B, BCL3, BCLAF1, BRD3, CBFA2T3, CHD4, CIC, CIITA, CNBP, CNOT3, CREB1, CREBBP, CTCF, EBF1, ELF4, EP300, ERCC2, ETV4, ETV5, EZH2, FLI1, FOXA1, FOXP1, GATA2, GATA3, GLI1, HIF1A, HNF1A, HOXA13, IKZF1, KAT6A, KDM5C, KEAP1, KLF4, KMT2A, KMT2D, LEF1, MAF, MAFB, MECOM, MED12, MYB, NAB2, NCOA1, NCOR2, NFATC2, NFIB, NSD2, PAX3, PAX5, PER1, PLAG1, PRDM1, PRDM16, PSIP1, RARA, RB1, REL, RUNX1, SALL4, SETBP1, SMAD4, SMARCA4, SMARCE1, STAT3, STAT5B, STAT6, TAF15, TAL1, TCF12, TCF3, TCF7L2, TFEB, THRAP3, TP53, TRIM27, TRIM33, TRIP11, ZFHX3, ZMYM3
Homoeodomain proteins	HNF1A, HOXA13, PAX3, PAX5, ZFHX3
Cell differentiation markers	BMPR1A, CDH1, DDR2, ERBB2, FAS, FGFR3, FLT3, ITGAV, KIT, MPL, MUC1, PDGFRA, PTPRC, TFRC
Protein kinases	ABL1, ACVR2A, AKT2, ATM, ATR, BMPR1A, BRD3, BTK, BUB1B, DDR2, ERBB2, ERBB3, ERBB4, FES, FGFR3, FLT3, FLT4, IKBKB, KIT, LATS2, LCK, MAP2K2, MAP3K1, MTOR, NTRK3, PDGFRA, PIM1, PRKCB, PRKD1, RET, SGK1, SRC, SYK, TRIM33, TRRAP

Oncogenes	ABL1, ACSL3, AFDN, AFF1, AFF3, AKAP9, AKT2, ARHGAP26, ARHGEF12, ASPSCR1, ATIC, BCL11B, BCL3, BIRC3, BRD3, CARD11, CBFA2T3, CCND1, CCND3, CIC, CIITA, CLTC, CLTCL1, CNBP, CNTRL, COL1A1, CREB1, CREBBP, CRTC1, CRTC3, DDX10, EIF4A2, ELF4, ELL, ELN, EML4, EPS15, ERBB2, ETV4, ETV5, EWSR1, FCRL4, FGFR3, FIP1L1, FLI1, FLT3, FOXP1, FSTL3, GAS7, GATA2, GMPS, GNAS, GOLGA5, GPHN, HIP1, HOXA13, HSP90AA1, HSP90AB1, IDH1, IDH2, IKZF1, IL21R, JAK2, KAT6A, KDM5A, KIAA1549, KIT, KLK2, KMT2A, KRAS, KTN1, LCK, LCP1, LHFPL6, MAF, MAFB, MALT1, MAML2, MECOM, MN1, MPL, MUC1, MYB, MYH11, MYH9, NCOA1, NFIB, NIN, NOTCH1, NRAS, NSD1, NSD2, NSD3, NTRK3, NUMA1, NUP214, PAFAH1B2, PAX3, PAX5, PCM1, PDE4DIP, PDGFB, PDGFRA, PER1, PIM1, PLAG1, PRDM16, PSIP1, PTPN11, RABEP1, RAP1GDS1, RARA, REL, RET, RUNX1, SFPQ, SH3GL1, SMO, SPECC1, SUZ12, SYK, TAF15, TAL1, TCEA1, TCF12, TCF3, TET1, TFEB, TFPT, TFRC, THRAP3, TPM3, TPR, TRIM27, TRIM33, TRIP11, ZMYM2
Tumor suppressors	APC, ASXL1, ATM, BMPR1A, BRCA1, BRCA2, BRIP1, BUB1B, CBLB, CDC73, CDH1, CYLD, DICER1, EP300, ERCC2, FANCA, FANCF, FANCG, FAS, FBXW7, GATA3, HNF1A, KDM5C, KDM6A, MUTYH, NBN, NF1, PALB2, PMS2, PRF1, PTCH1, RB1, SBDS, SDHAF2, SDHC, SMAD4, SMARCA4, TET2, TNFAIP3, TP53, TSC1, VHL, WRN, XPC

Supplemental Table 22: Epigenetic factors				
Gene_Symbol	Function/Modification_1	Function/Modification_2	Function/Modification_3	Function/Modification_4
DAXX	#			
TBL1XR1	#			
NBN	Chromatin remodeling			
IKZF1	Chromatin remodeling	TF		
ATRX	Chromatin remodeling			
FOXA1	Chromatin remodeling	TF		
CHD4	Chromatin remodeling			
KEAP1	Chromatin remodeling			
PSIP1	Chromatin remodeling			
ARID2	Chromatin remodeling cofactor			
SMARCE1	Chromatin remodeling cofactor			
TET2	DNA modification/DNA hydroxymethylation			
TET1	DNA modification/DNA hydroxymethylation			
TFPT	DNA modification/DNA hydroxymethylation	Chromatin remodeling cofactor		
DNMT3A	DNA modification/DNA methylation			

CREBBP	Histone modification write/Histone acetylation			
BRCA2	Histone modification write/Histone acetylation			
TP53	Histone modification write/Histone acetylation	TF/TF activator, TF repressor		
EP300	Histone modification write/Histone acetylation			
KAT6A	Histone modification write/Histone acetylation			
TRRAP	Histone modification write cofactor/Histone acetylation			
BRCA1	Histone modification write cofactor/Histone acetylation, Histone methylation, Histone ubiquitination	TF/TF activator, TF repressor		
NCOA1	Histone modification write/Histone acetylation			
NCOR2	Histone modification erase cofactor/Histone acetylation			

TRIM27	Histone modification erase cofactor/Histone acetylation			
ZMYM2	Histone modification erase cofactor/Histone acetylation	TF		
ZMYM3	Histone modification erase cofactor/Histone acetylation			
BAZ1A	Histone chaperone			
BCORL1	Histone modification erase cofactor/Histone deacetylation			
ASXL1	Histone modification erase/Histone deubiquitination	Polycomb group (PcG) protein		
KMT2D	Histone modification write/Histone methylation			
EZH2	Histone modification write/Histone methylation	Polycomb group (PcG) protein		
KDM6A	Histone modification erase/Histone methylation			
SETD1B	Histone modification write/Histone methylation			

KMT2A	Histone modification write/Histone methylation			
KDM5C	Histone modification erase/Histone methylation			
CDC73	Histone modification write cofactor/Histone methylation			
KDM5A	Histone modification erase/Histone methylation			
SUZ12	Histone modification write cofactor/Histone methylation	Histone modification write cofactor/Histone ubiquitination	Polycomb group (PcG) protein	TF/TF repressor
PRKCB	Histone modification write/Histone methylation			
NSD1	Histone modification write/Histone methylation			
RARA	Histone modification write/Histone methylation	TF/TF activator, TF repressor		
PRDM16	Histone modification write/Histone methylation	TF/TF repressor		
ERBB4	Histone modification cofactor			
BRD3	Histone modification read			
ASXL2	Histone modification read			

PRDM1	Histone modification write cofactor/Histone methylation			
PBRM1	Histone modification read			
TRIM33	Histone modification read			
ATM	Histone modification write/Histone phosphorylation			
JAK2	Histone modification write/Histone phosphorylation			
ATR	Histone modification write/Histone phosphorylation			
RB1	Chromatin remodeling	Histone modification write/Histone ubiquitination		
CUL3	Histone modification write/Histone ubiquitination			
UBR5	Chromatin remodeling	Histone modification write cofactor/Histone ubiquitination		

ARID1B	Histone modification write/Histone ubiquitination			
BARD1	Histone modification write/Histone ubiquitination			
USP44	Histone modification erase/Histone ubiquitination			
BCOR	Polycomb group (PcG) protein			
THRAP3	RNA modification/RNA degradation			
FOXP1	TF			
CTCF	TF/TF activator	Chromatin remodeling		
SMARCA4	Histone modification read	TF/ TF activator		
SFPQ	Chromatin remodeling cofactor	RNA modification	TF/ TF repressor	

Supplemental Table 23: Positional clustering enrichment analysis results

Gene_symbol	total	MutatedSamples	AlteredSamples	clusters	muts_in_clusters	clusterScores	protLen	zscore	pval	fdr	fract_muts_in_clusters
NRAS	21	19	19	2	21	0.878559	189	4.611995	1.99E-06	2.39E-05	1
KRAS	9	9	9	1	7	0.680147	189	3.085744	0.001015	0.006091	0.777778
KIT	6	5	5	1	4	0.617851	976	2.606547	0.004573	0.018292	0.666667
GATA2	7	7	7	1	4	0.571429	480	2.249451	0.012242	0.029381	0.571429
TFRC	7	5	5	1	4	0.571429	760	2.249451	0.012242	0.029381	0.571429
PTPN11	8	8	8	1	6	0.525888	593	1.899141	0.028773	0.057546	0.75
CBL	7	6	6	1	3	0.428571	906	1.150549	0.124959	0.214215	0.428571

IKZF1	17	14	14	2	10	0.399548	519	0.927292	0.176888	0.265331	0.588235
MED12	26	23	23	3	7	0.35	2177	0.546154	0.29248	0.389973	0.269231
BCL11B	12	11	11	1	4	0.318182	894	0.301399	0.381555	0.457866	0.333333
BCORL1	8	4	4	1	2	0.25	1711	-0.22308	0.588262	0.641741	0.25
FBXW7	9	7	7	1	2	0.222222	707	-0.43675	0.668854	0.668854	0.222222

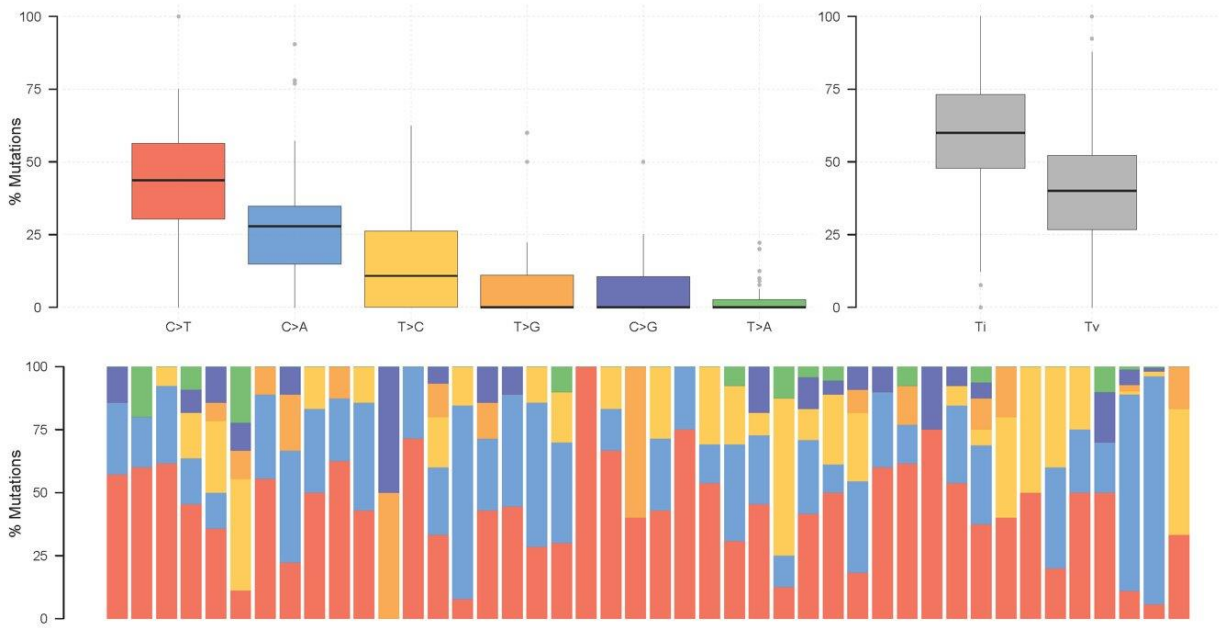

Supplemental Figure 16: Overview of SNV transitions and transversions that were identified in the prioritized variants: Top row represents the box plots of the proportion of mutations and their associated nucleotide variant change. The bottom row is a stacked bar plot of the distribution of SNV changes associated with each sample.

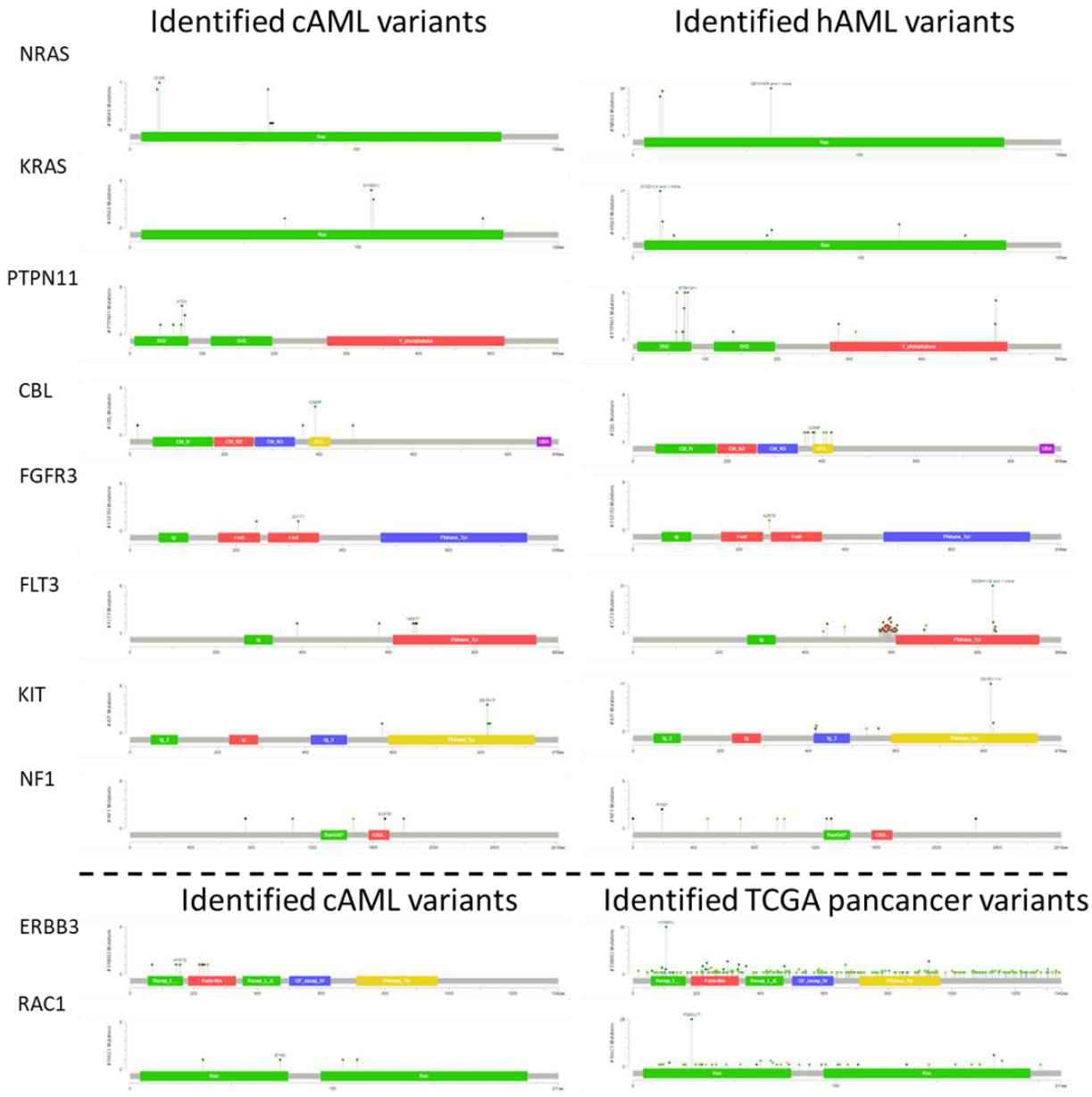

Supplemental Figure 17: Comparative features between cAML samples and reported hAML and pan cancer variants in the top 10 genes identified in the RTK-RAS pathway: The left column represents the variants identified in cAML samples and the right column represents variants identified in hAML samples (both pediatric and adult AML). Variants in ERBB3 and RAC1 were not readily identified in hAML samples. Therefore, we referenced the TCGA pancancer studies (below dashed line) to highlight comparative features with other human neoplasms.